

AD _____

Grant Number DAMD17-96-1-6189

TITLE: Biology of Somatostatin and Somatostatin Receptors in
Breast Cancer

PRINCIPAL INVESTIGATOR: Yogesh C. Patel, M.D., Ph.D.

CONTRACTING ORGANIZATION: McGill University
Montreal, Quebec, Canada H3A1A1

REPORT DATE: September 1999

TYPE OF REPORT: Annual

PREPARED FOR: U.S. Army Medical Research and Materiel Command
Fort Detrick, Maryland 21702-5012

DISTRIBUTION STATEMENT: Approved for public release;
distribution unlimited

The views, opinions and/or findings contained in this report are
those of the author(s) and should not be construed as an official
Department of the Army position, policy or decision unless so
designated by other documentation.

20000710 146

DMIC QUALITY INSPECTED 4

REPORT DOCUMENTATION PAGE

Form Approved
OMB No. 0704-0188

Public reporting burden for this collection of information is estimated to average 1 hour per response, including the time for reviewing instructions, searching existing data sources, gathering and maintaining the data needed, and completing and reviewing the collection of information. Send comments regarding this burden estimate or any other aspect of this collection of information, including suggestions for reducing this burden, to Washington Headquarters Services, Directorate for Information Operations and Reports, 1215 Jefferson Davis Highway, Suite 1204, Arlington, VA 22202-4302, and to the Office of Management and Budget, Paperwork Reduction Project (0704-0188), Washington, DC 20503.

1. AGENCY USE ONLY (Leave blank)		2. REPORT DATE September 1999		3. REPORT TYPE AND DATES COVERED Annual (12 Aug 98 - 11 Aug 99)	
4. TITLE AND SUBTITLE Biology of Somatostatin and Somatostatin Receptors in Breast Cancer				5. FUNDING NUMBERS DAMD17-96-1-6189	
6. AUTHOR(S) Yogesh C. Patel, M.D., Ph.D.					
7. PERFORMING ORGANIZATION NAME(S) AND ADDRESS(ES) McGill University Montreal, Quebec, Canada H3A1A1				8. PERFORMING ORGANIZATION REPORT NUMBER	
9. SPONSORING/MONITORING AGENCY NAME(S) AND ADDRESS(ES) U.S. Army Medical Research and Materiel Command Fort Detrick, Maryland 21702-5012				10. SPONSORING/MONITORING AGENCY REPORT NUMBER	
11. SUPPLEMENTARY NOTES This report contains colored photographs					
12a. DISTRIBUTION / AVAILABILITY STATEMENT Approved for public release; distribution unlimited				12b. DISTRIBUTION CODE	
13. ABSTRACT (Maximum 200) Analysis of SSTR1-5 mRNA expression by semiquantitative RT-PCR in two separate batches of primary ductal NOS breast cancer (n, N 48 and 50) has revealed a strong positive correlation (p , 0.001) between SSTR3 expression and tumor grade suggesting that SSTR3 induction in high grade tumors may represent a compensatory mechanism for regulating proliferative activity through apoptosis. Expression of SSTR1, 2, and 4 strongly correlates with estrogen receptor levels and SSTR2 expression additionally correlates positively with progesterone receptor levels. Tamoxifen exhibits a dose-dependent biphasic effect on SSTR1 and SSTR5 mRNA, low doses being inhibitory and high doses being stimulatory. SST induces apoptosis selectively through the SSTR3 subtype. This effect is dependent on activation of SHP-1 and caspase-8-mediated decrease in intracellular pH. SST induced apoptosis is not dependent on disruption of mitochondrial function and caspase-9 activation and is inhibited by cAMP-mediated prevention of acidification. Acting via subtypes 1, 2, 4, 5, SST exerts cytostatic action by SHP-mediated induction of the hypophosphorylated form of the retinoblastoma protein Rb and p21. These signalling events are dependent on regulatory domains in the receptor C-tail. Antisense knockout of endogenous SSTRs in MCF-7 cells has demonstrated a relatively higher potency of SSTR3 and SSTR5 compared to SSTR1 and SSTR2 for inducing antiproliferation.					
14. SUBJECT TERMS Breast Cancer				15. NUMBER OF PAGES 139	
				16. PRICE CODE	
17. SECURITY CLASSIFICATION OF REPORT Unclassified	18. SECURITY CLASSIFICATION OF THIS PAGE Unclassified	19. SECURITY CLASSIFICATION OF ABSTRACT Unclassified	20. LIMITATION OF ABSTRACT Unlimited		

FOREWORD

Opinions, interpretations, conclusions and recommendations are those of the author and are not necessarily endorsed by the U.S. Army.

 Where copyrighted material is quoted, permission has been obtained to use such material.

 Where material from documents designated for limited distribution is quoted, permission has been obtained to use the material.

 Citations of commercial organizations and trade names in this report do not constitute an official Department of Army endorsement or approval of the products or services of these organizations.

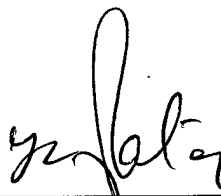
✓ In conducting research using animals, the investigator(s) adhered to the "Guide for the Care and Use of Laboratory Animals," prepared by the Committee on Care and use of Laboratory Animals of the Institute of Laboratory Resources, national Research Council (NIH Publication No. 86-23, Revised 1985).

✓ For the protection of human subjects, the investigator(s) adhered to policies of applicable Federal Law 45 CFR 46.

 In conducting research utilizing recombinant DNA technology, the investigator(s) adhered to current guidelines promulgated by the National Institutes of Health.

 In the conduct of research utilizing recombinant DNA, the investigator(s) adhered to the NIH Guidelines for Research Involving Recombinant DNA Molecules.

 In the conduct of research involving hazardous organisms, the investigator(s) adhered to the CDC-NIH Guide for Biosafety in Microbiological and Biomedical Laboratories.



PI - Signature

9/10/99

Date

TABLE OF CONTENTS

Front Cover	Page 1
Report Documentation Page SF 298	Page 2
Foreword	Page 3
Table of Contents	Page 4
Introduction	Page 5
Longterm Objectives	Page 6
Details of Progress	Pages 7-17
Summary and Conclusions	Pages 17-20
Tables	Pages 21-26
Figure Legends	Pages 27
Appendix	Page 28

INTRODUCTION

Somatostatin (SST) a regulatory peptide, is produced by neuroendocrine, inflammatory and immune cells, and acts as an endogenous inhibitory regulator of the secretory and proliferative responses of target cells that are widely distributed throughout the body (1). These actions are mediated by a family of seven transmembrane domain G protein coupled receptors that comprise five distinct subtypes (termed SSTR1-5) that are encoded by separate genes segregated on different chromosomes (1, 2). SST blocks regulated secretion from many different cells by inhibiting intracellular Ca^{2+} , cAMP, as well as the distal steps of exocytosis, and additionally inhibits the release of constitutively secreted proteins such as growth factors and cytokines by unknown mechanisms (1). In contrast to the antisecretory properties of SST, its antiproliferative effects were relatively late in being recognized and came about largely through use of longacting SST analogs such as Octreotide in the early 1980's for the treatment of hormone hypersecretion from pancreatic intestinal and pituitary tumors (3). It was noted that SST not only blocked hormones hypersecretion from these tumors but also caused variable tumor shrinkage through an additional antiproliferative effect. The antiproliferative effects of SST have since been demonstrated in normal dividing cells, e.g. intestinal mucosal cells, activated lymphocytes, and inflammatory cells as well as *in vivo* in solid tumors, e.g. DMBA-induced or transplanted rat mammary carcinomas, and cultured cells derived from both endocrine and epithelial tumors (pituitary, thyroid, breast, prostate, colon, pancreas, lung, and brain) (1). These effects involve cytostatic (growth arrest) and cytotoxic (apoptotic) actions and are mediated (1) directly by SSTRs present on tumor cells, and (2) indirectly via SSTRs present on nontumor cell targets to inhibit the secretion of hormones and growth factors that promote tumor growth and to inhibit angiogenesis, promote vasoconstriction, and modulate immune cell function (1, 4-6). All five SSTR subtypes acting via several different signal transduction pathways have been implicated. Most interest is focused on protein phosphatases that dephosphorylate receptor tyrosine kinases or that modulate the MAPK signalling cascade, thereby attenuating mitogenic signal transduction (reviewed in 1). A SST-sensitive PTP was first described in 1985 in human pancreatic cancer cells and has since been demonstrated in normal pancreatic acinar cells, human coronary smooth muscle cells, human breast and prostate cancer cells, and rat pancreatic and thyroid tumor cells (1, 7). All five SSTR subtypes have been shown to stimulate PTP activity in various transfected cells (1). SSTR-induced activation of PTP is sensitive to pertussis toxin and orthovanadate (8). The PTP activity associated with SST action has been attributed to the SH2 domain containing cytosolic PTPs whose members include SHP-1 (SHPTP1/PTP1C) and SHP-2 (SHPTP2/PTP1D/syp) (9). The relative importance of the two PTPs is unclear although direct evidence has shown an important role of SHP-1 in SSTR-mediated PTP activation and antiproliferative signalling. Like PTP, all of the SSTRs have been shown to modulate the MAPK pathway either positively or negatively in a PTP-dependent manner to effect cell growth inhibition (1). The precise steps linking the ligand activated receptor to PTP stimulation and mitogenic signalling remain to be determined. Recent evidence based on the β -adrenergic receptor suggests that *c-src* which associates with and may be a direct substrate of SHP-2 could provide the link between the receptor, PTP, and the MAPK signalling cascade (10). Four of the receptors (SSTR1,2,4,5) induce cell cycle arrest via PTP-dependent modulation of MAPK,

associated with induction of the retinoblastoma tumor suppressor protein and p21 (1, 5). The maximal effect is exerted by SSTR5 followed by SSTR2, 4, and 1 (5). In contrast, SSTR3 uniquely triggers PTP-dependent apoptosis accompanied by activation of p53 and the pro-apoptotic protein Bax (4, 11). Furthermore, SSTR3 induced apoptotic signalling involves the activation of a cation insensitive acidic endonuclease and intracellular acidification (12).

From the above description it is clear that major strides have been made in our laboratory and elsewhere towards understanding the subtype selectivity and signalling mechanisms underlying the antiproliferative actions of SST. Despite this experimental success, SST analogs such as Octreotide (which bind SSTR2, 3, 5 but not SSTR1 and 4) have so far produced variable clinical effects on tumor growth due to a number of reasons such as patient selection (e.g. early vs end stage disease), the absence of appropriate SSTRs in the tumors being treated (e.g. tumors expressing SSTR1 and SSTR4 will not respond to Octreotide; SSTR3 expression is required for inducing apoptosis), the presence of mutated p53 gene which abrogates the apoptotic effect of SST, and the dose and duration of treatment. Future work will need to address these issues to optimize the oncological utility of SST analogs.

LONGTERM OBJECTIVES

The longterm goal of our work will be **to elicit the pattern of expression of the five individual SSTR subtypes in breast tumor, to determine whether their pattern of expression can provide an independent prognostic marker, and whether the SSTRs are modulated by estrogens and antiestrogens.** In addition, we wish to determine the subtype selectivity for the antiproliferative effects of SST, as well as the role of PTP, p53, and other downstream effectors in mediating the cytostatic and cytotoxic effects of SST.

SPECIFIC TASKS PROPOSED FOR YEAR 3

Dr. Y.C. Patel

- 1) Completion of RT-PCR analysis of SSTR1-5 in breast tumor
- 2) Immunocytochemical analysis of SSTR1-5 in tumor samples.
- 3) Antireceptor blockade experiments
- 4) Antisense knockout experiments
- 5) Regulation of SSTR1-5 by estrogens/tamoxifen

Dr. C.B. Srikant

- 1) Studies correlating SSTR binding with PTP-1c regulation and growth inhibition
- 2) Studies of subtype selectivity for PTP-1c association in CHO-K1 and COS-7 cells
- 3) Studies of subtype selectivity for apoptosis in CHO-K1 and COS-7 cells
- 4) PTP-1c involvement in apoptosis
- 5) Overexpression and antisense blockade of SSTRs to see effect on apoptosis

DETAILS OF PROGRESS

General Comments

Whilst our broad objectives remain unchanged from those proposed in the original application, we have had to make a number of directional changes as a result of new leads or progress from other laboratories in the field. This has resulted in the de-emphasis of some specific tasks at the expense of others, and the development of some new experiments. For instance, quantitative RT-PCR analysis of all five SSTRs in 150 samples proved to be a much larger task than originally calculated and had to be extended to year 3. It proved to be a worthwhile investment since we now have the most complete description of SSTR subtype expression in human breast cancer together with histological correlations seen for the first time. Given our success with SSTR1-5 immunocytochemistry, it seemed pointless to do both immunocytochemistry as well as *in situ* hybridization to look at the cellular pattern of expression of SSTRs in tumor sections. Accordingly, the *in situ* hybridization studies were cancelled as explained in last year's report. Because CHO-K1 cells generally express low levels of PTP, we had initially proposed studying SST-induction of PTP in COS cells as well. This, however, could be delayed since we were able to show sufficient PTP induction by the key antiproliferative subtypes (SSTR3, SSTR5) in CHO-K1 cells. Finally, a strategic decision was made to undertake in depth studies of the mechanism of antiproliferative signalling by two of the subtypes that we had identified, SSTR3 (the only subtype capable of inducing apoptosis) and SSTR5 (the most potent of the four SSTRs shown to induce cytostasis) rather than to tackle the more proximal receptor-PTP interactions for all five subtypes as originally proposed. This has led to new structure-function studies of these two receptors and to elucidation of the role of intracellular acidification and caspase activation on SSTR3-induced PTP-dependent apoptosis. The review of our last annual report found that "a very large amount of research has been completed". Several key personnel engaged on this project (R. Sasi, K. Sharma, B. Allard, B. Al-Atassi) left during the year thereby interrupting some tasks. Nonetheless, we have maintained steady progress during the third year covered by this report. A revised statement of work (SOW) including the new experiments is included as recommended by the reviewer.

TASK 1. Expression of SSTR1-5 mRNA in Human Breast Tumor Tissue

We have used a semiquantitative RT-PCR method for measuring SSTR1-5 mRNA in primary breast tumors obtained as frozen sections from the Manitoba Breast Tumor Bank. The method is based on modifications of techniques that we have reported previously (13). 5 µg DNA free RNA was reverse transcribed and the resulting cDNA samples were amplified by PCR as previously described (13) using the following primers.

hSSTR1	sense	5'-TAT CTG CCT GTG CTA CGT GC-3'
	antisense	5'- GAT GAC CGA CAG CTG ACT CA-3'
hSSTR2	sense	5'- ATC TGG GGC TTG GTA CAC AG-3'
	antisense	5'- CTT CTT CCT CTT AGA GGA GG-3'

hSSTR3	sense	5'- GG CCC TCCC GCC GTGT-3'
	antisense	5'- CTCC TGC CCG CT GGT-3'
hSSTR4	sense	5'- CGC TCG GAG AAG AAAA TCAC-3'
	antisense	5'- CCC ACC TTT GCT CTT GA GAG-3'
hSSTR5	sense	5'- CGT CTT CAT CAT CTA CAC G-3'
	antisense	5'- CCA GGT TGA CGA TGT TGA-3'
β -actin	sense	5'- ATC ATG AAG TGT GAC GTG GAC-3'
	antisense	5'- AA CCGACTGCT GTC ACC TTCA-3'

The PCR products were separated by electrophoresis, hybridized with ^{32}P labelled SSTR1-5 probes and processed for autoradiography. β -actin signals were used as controls. The hybridization signals were quantitated with a Java Video Analysis Software Package and used as an index of SSTR and actin mRNA. To ensure that the hybridization bands were quantitated in the linear range, each blot was exposed to x-ray film for various intervals of time. Only bands that did not reach saturation density of exposure were subjected to quantitative analysis. The units derived from the Java Analysis were arbitrarily assigned a pixel density corrected for background. Values of SSTR1-5 mRNA expression were normalized to those of actin mRNA on the same gels.

In year 1 we analysed 90 samples in several different batches as previously reported. Because our method for quantitating SSTR mRNA was still being optimized and because of possible mRNA degradation during shipment as well as interassay variability, the results obtained from these different analyses were somewhat variable. In year 2, we analysed a second batch of 50 samples all processed together (Study 1). The data were analysed statistically by Dr. Michael Edwards, Department of Epidemiology and Biostatistics, McGill University for possible association between SSTR subtype expression, tumor histology, and estrogen (ER) and progesterone (PR) receptor levels and showed several potential pairwise Pearson correlations that were described in the last annual report. We have now completed the quantitative analysis of SSTR1-5 mRNA in a further 50 samples that were also processed as a single batch (Study 2) (Table 1). To improve statistical power, data from the two study sets were analysed separately and then pooled, thereby confirming and strengthening several of the associations.

The tumors analysed were all ductal NOS cancers of different grades (Table 1). As in our previous analyses, all of the tumors expressed at least one SSTR subtype and frequently featured more than one SSTR isoform. In the pooled data (Study1 and 2) SSTR1, 2, and 3 were the most frequently expressed subtypes occurring in 91%, 96%, and 98% of the tumors analysed (Table 2). SSTR4 occurred in 76% of samples whereas SSTR5 was present in approximately half the samples. Statistical analyses (14) of the pooled data showed the following correlations (Table 3):

- (1) a strong positive correlation between SSTR1 and ER levels (r 0.356, $P < 0.0003$)
- (2) positive correlation between SSTR4 and ER levels (r 0.228, $P < 0.019$)
- (3) a strong positive correlation between SSTR2 and ER levels (r 0.264, $P < 0.007$)

- (4) a positive correlation between SSTR2 and PR levels (r 0.262, $P < 0.03$)
- (5) a very strong positive correlation between SSTR3 and tumor grade (r 0.415, $P < 0.00002$)

The association between SSTR1, SSTR2, SSTR4, and ER levels and between SSTR2 and PR levels (items 1-4 above) was seen in both studies and accounted for the significant correlations observed in the pooled data. Likewise, the strong correlation between SSTR3 and tumor grade was maintained in both studies (item 5). In contrast, SSTR1 correlated negatively with tumor grade and SSTR2 and 4 individually showed a negative trend with tumor grade that was not significant statistically. When SSTR1, 2, and 4 levels were pooled, however, there was a very significant negative correlation with tumor grade. The trend towards a negative correlation between SSTR1 and lymph node status and of SSTR2 vs tumor size noted in Study 1 cancelled out in Study 2.

Our results represent the first finding of statistically significant correlations between SSTR subtype expression and various tumor markers in human breast cancer. There have been several earlier reports of SSTR mRNA expression in breast tumor that have failed to find any correlation between receptor expression, tumor histology, and ER/PR status probably because of relatively small sample sizes and the use of qualitative rather than quantitative methods for SSTR mRNA analysis (6, 15, 16). In addition to providing tumor markers, the pattern of SSTR subtype expression that we have found may help in the understanding of the biology of breast cancer cell growth. The question of why tumors overexpress SSTRs, what the underlying stimulus is, and what biological role is served by tumor SSTRs remain largely unanswered. We suspect that SST and SSTRs are activated by growth factors and serve as an endogenous paracrine/autocrine growth inhibitory system for modulating cell proliferation. The finding of a strong positive correlation between SSTR3 levels and tumor grade is of considerable interest in view of the apoptotic properties of this receptor (1, 4). Presumably SSTR3 expression is induced in response to increasing malignancy perhaps as a compensatory mechanism to regulate proliferative activity through apoptosis. Induction of SSTR3 appears to occur differentially at the expense of the other (cytostatic) subtypes (SSTR1, 2, 4) whose expression decreases with higher grade malignancy. The biological significance of an association between three of the SSTR subtypes and ER levels is less clear. SSTR1 and SSTR2, two key subtypes expressed in breast cancer, are both induced by estrogens (1, 17-19). A practical implication of these findings is that tumors that have low or absent levels of ER will be expected to display weak SSTR expression and may not be amenable to therapy with SST analogs.

This task has now been completed. Data are being prepared for publication in combination with the immunocytochemical data (see Task 3 below).

TASK 2. In Situ Hybridization Analysis

This task was cancelled as explained in the last annual report.

TASK 3. Immunocytochemistry

We have developed a panel of antipeptide rabbit polyclonal antibodies against all five human

and rat SSTR isoforms (13, 20, 21). The antibodies were affinity purified, characterized by Western blots, and by immunocytochemistry of stable CHO-K1 cells individually transfected with hSSTR1-5 (21). The specificity of the antibodies using these methods has been reported in several recent publications from our laboratory and was included in the last annual report (13, 20, 21). The antibodies have been successfully used for immunocytochemical localization of all five SSTR antigens in normal rat pituitary, normal human islets, normal rat aorta, and human medullary thyroid carcinoma, and brain tumors by both immunoperoxidase and fluorescence immunocytochemistry (22, 23). Our objective with this task is to (i) correlate SSTR1-5 mRNA expression as determined by RT-PCR with receptor protein expression by immunocytochemistry in a subset of samples, and (ii) to determine the cellular pattern of expression of SSTR1-5 in tumor cells and peritumoral structures such as blood vessels and stroma. We selected 16 samples from Study 1 and obtained histological sections of these from the Manitoba Breast Tumor Bank. The samples were fixed in 4% paraformaldehyde and processed for peroxidase immunocytochemistry using SSTR1-5 primary antibodies (diluted 1:200 to 1:500) and goat antirabbit secondary antibody followed by exposure to avidin-biotinylated horse radish peroxidase complex (Vectastain Elite ABC Kit). The slides were sent coded to Dr. P. Watson, our pathology collaborator at the University of Manitoba. The sections were assessed with respect to the presence or absence of SSTR1-5 immunoreactivity and the results are compared with SSTR1-5 mRNA in the same samples (graded + to ++++ based on their mRNA concentration by RT-PCR) in Table 4. Receptor analyses exhibiting a match between mRNA and immunocytochemistry are indicated by the shaded boxes. Whilst there is a good overall correlation, there are frequent mismatches. Some are due to the quality of the tissues or of the sections producing a so-called "edge effect". A more real problem has been the distant collaboration whereby it has not been possible for our immunocytochemistry expert, Dr. U. Kumar, to sit with Dr. Watson and to review and discuss each section in an attempt to identify and allow for any sample or histological artifacts. Certainly, our own review of some independent sections by in-house pathologists has shown excellent localization of SSTR antigens in both tumor cells as well as peritumoral blood vessels (detailed sections of 4 such tumors analysed for SSTR1-5 were included in the last annual report). We are now processing an additional 20 samples from Study 2 for SSTR1-5 immunocytochemistry. To facilitate the comparative analysis, we are engaging the services of Dr. Leslie Alpert, a pathologist at the Jewish General Hospital, McGill University, who is willing to make a time commitment towards this project and will work closely with us. We will also have her re-examine sections from the 16 tumor samples from Study 1 (Table 4). Analysis of these remaining samples will complete this task over the coming months. It is our plan to combine the SSTR mRNA data with immunocytochemistry and report our findings of receptor subtype expression in breast tumor at both gene and protein levels in a single major publication.

TASK 4. Analysis of SSTR Expression in Breast Tumor Cell Lines

This task was completed as described in the last annual report.

TASKS 5&6. Antireceptor Blockade of SSTR1-5 and Antisense Knockout of SSTR1-5

These two tasks share a common objective and are based on similar experimental protocols

and will be described together. Just as we have characterized the antiproliferative activity of each SSTR subtype by isolating them individually in stably transfected CHO-K1 cells, these are complementary experiments designed to block or eliminate the expression of individual endogenous SSTRs to see what effect it has on cell proliferation. We have carried out a complete antisense experiment of all relevant SSTRs in MCF7 cells. These cells were found by RT-PCR to express mRNA for several SSTRs with the following relative abundance (compared to actin mRNA): SSTR1 (+++), SSTR2 (+), SSTR3 (+/-), SSTR4 (-), and SSTR5 (+++) (24). Confocal fluorescence immunocytochemistry (Fig. 1) confirmed the protein expression of SSTR1, 2, 3, 5 (but not SSTR4) in these cells. Cells were grown to confluence in culture medium containing 10% heat inactivated fetal calf serum. Cultures were then treated for 4 days with 2 µg/ml sense or antisense oligonucleotides (ODN) directed against hSSTR1, 2, 3, 5. Phosphorothioate modified ODNs against the first 6 codons of the SSTRs were synthesized as follows:

SSTR1	sense	5'-ATG TTC CCC AAT GGC ACC-3'
	antisense	5'-GGT GCC ATT GGG GAA CAT-3'
SSTR2	sense	5'-ATG GAC ATG GCG GAT GAG-3'
	antisense	5'-CTC ATC CGC CAT GTC CAT-3'
SSTR3	sense	5'-ATG CTT CAT CCA TCA TCG-3'
	antisense	5'-CGA TGA TGG ATG AAG CAT-3'
SSTR5	sense	5'-ATG GAG CCC CTG TTC CCA-3'
	antisense	5'-TGG GAA GAC GGG CTC CAT-3'

50% of the medium was replenished at day 2. At the end of the four day period of treatment with ODN, medium was replaced with regular culture medium for two days and the total number of cells per well analysed by cell count. The results are summarized in Fig. 1 (upper panel) and show a significant increase in the proliferative activity of cells treated with antisense ODNs to SSTR3 and SSTR5 compared to sense ODNs. Blockade of SSTR1 and SSTR2 showed small, nonsignificant increases in cell numbers. These experiments confirm the relatively high potency of SSTR3 and SSTR5 in inducing antiproliferation similar to our findings in transfected CHO-K1 cells. The pronounced SSTR3 effect in these cells is interesting given the relatively low level expression of this receptor subtype in these cells. As we have shown previously these cells also undergo apoptosis presumably via the type 3 receptor when treated with Octreotide. We have carried out some initial studies of the immunoblockade of SSTRs with our polyclonal antireceptor antibodies. SSTR2, the best of our immunoneutralizing antibodies, has not shown a very convincing effect on MCF-7 cell proliferation similar to the results obtained with antisense SSTR2 ODNs. The two neutralizing antibodies of particular interest, those against SSTR3 and SSTR5 are unfortunately of much lower grade than our antiSSTR2 antibody. For this reason and because our antisense experiments are now working, we have assigned a somewhat low priority to these additional immunoneutralization experiments. Another important development has been the recent identification of a series of nonpeptide agonists from combinatorial libraries by the Merck Research Group (1, 25). Three of the compounds identified from this screen L-797591, L-779976, and L-803087 display low nanomolar affinity for hSSTR1 (1.4 nM), hSSTR2 (0.05 nM), and hSSTR4 (0.7 nM), representing 120-6200, and 285 fold selectivity respectively for

these subtypes. A fourth compound L-796778 shows 50 fold selectivity for hSSTR3 and L-817818 binds to both hSSTR5 and hSSTR1 with high selectivity. These compounds represent powerful new probes for dissecting subtype selective receptor functions in cells such as MCF-7 which express multiple SSTR subtypes. We have obtained four of the compounds (the fifth is pending) and will test them alone and in combination in MCF-7 cells to delineate subtype selective cytostatic and cytotoxic effects. Finally, a major observation made in our laboratory during the past year has an important bearing on understanding the function of multiple receptor subtypes coexisting in the same cell. We have demonstrated that upon activation by ligand, SSTRs form dimers, both homodimers or heterodimers, with other members of the SSTR family and that dimerization alters the functional properties of the receptor such as ligand binding affinity, signalling, and agonist-induced regulation (24). This means that endogenous SSTRs in normal or tumor cells which commonly occur as multiple isoforms in the same cell, operate in concert with other members of the family and that elucidation of individual receptor effects such as with antisense experiment or subtype-selective analogs will have to take these interactions into account. Overall, we have made good progress with the experiments underlying these tasks which will continue into year 4 as originally proposed.

TASK 7. Regulation of SSTR1-5 by Estrogens/Tamoxifen

As described in our last annual report, there are now several studies of the effects of estrogens on SSTRs. Estrogen induces SST binding sites in cultured rat prolactinoma cells due to upregulation of SSTR2 and SSTR3 (26). Estrogen similarly induces mRNA for SSTR2 and SSTR3 in primary cultures of rat pituitary cells in which it additionally inhibits SSTR1 mRNA levels (17). The *in vivo* effects of estrogen on pituitary SSTR expression in the rat also show induction of SSTR2 and SSTR3 mRNA (18). In addition, SSTR1 mRNA was also upregulated and SSTR5 mRNA inhibited in the *in vivo* experiments (18). Finally in MCF-7 breast cancer cells, estrogen has been reported to stimulate SSTR2 mRNA expression (19). Overall, there is general agreement among these studies for a positive effect of estrogen on SSTR2 and SSTR3 expression and variable or minimal effects on the remaining three subtypes. We have studied the dose response of estradiol (E) on SSTR subtype mRNA expression in MCF-7 cells by quantitative RT-PCR and compared the effects with those of tamoxifen (T) (Fig. 2). E induced dose-dependent stimulation of SSTR1 mRNA from 10^{-12} - 10^{-8} M with inhibition at higher (10^{-7} M) concentrations. Estrogen also stimulated SSTR5 mRNA at 10^{-12} - 10^{-7} M with a biphasic dose response curve. SSTR3 and SSTR2 showed no effect, and SSTR4 remained undetectable in this cell line. The absent SSTR2 and SSTR3 responses in our hands differs from those described by others based on qualitative PCR changes only. The effects of tamoxifen are quite interesting and show a dose-dependent biphasic response with SSTR1 and SSTR5 mRNA, low doses (10^{-12} M) being inhibitory and higher doses (10^{-10} - 10^{-7} M) being stimulatory. This presumably reflects both the anti-estrogenic as well as the estrogenic effects of tamoxifen. SSTR3 and SSTR2 mRNA also showed small but distinct increases in mRNA levels at high tamoxifen concentrations. Our attempts to correlate estrogen and tamoxifen-induced changes in SSTR mRNA levels with SSTR Western blots proved futile since the Western signals in MCF-7 cells could not be quantitated and our *in vivo* studies of estrogen treatment in the rat produced multiple tissue-specific bands on Western blots which were difficult to interpret. An interesting new lead

to emerge from these studies was the regulation of somatostatin itself from MCF-7 cells. Two previous studies have shown that MCF-7 cells produce small quantities of somatostatin peptide as measured by radioimmunoassay (27, 28). We were able to confirm this and additionally showed that estrogen treatment inhibited SST production whereas tamoxifen at 10^{-8} - 10^{-10} M (but not higher or lower concentrations) stimulated SST. Since many different tumor cells have now been shown to produce SST, probably as a paracrine/autocrine inhibitory regulator, the finding that tamoxifen can induce the endogenous SST system is exciting since it points to a potential novel mechanism of action of this drug. We are pursuing this lead with additional experiments to test a direct effect of tamoxifen on SST expression at both protein and mRNA levels in other cell lines as well as in some normal SST producing tissues such as cultured hypothalamic cells.

TASK 8. Correlation Between SSTR Subtype Selective Binding, PTP Activation and Growth Inhibition

We have demonstrated that Octreotide which binds to SSTR2, 3, and 5 is a potent inducer of antiproliferative signalling (4). SSTR3 mediated action was cytotoxic whereas SSTR2 and 5 mediated signalling was cytostatic (4,11). Since Octreotide does not bind to SSTR1 and 4, we used D-Trp⁸ SST-14 to investigate the nature of antiproliferative signalling, transduced through these two subtypes. SSTRs 1 and 4 were found to promote weak cytostasis, significantly less than SSTR2 and 5. In our Mol. Endocrinology paper (5) which was appended with our report last year and which has since been revised and finalized, we compared the cytostatic properties of hSSTR1, 2, 4, and 5, all expressed in CHO-K1 cells and found that the relative efficacy of these receptors to initiate cytostatic signalling was hSSTR5 > hSSTR2 > hSSTR4 = hSSTR1. Inhibition of cell growth in each case was due to cell cycle arrest in G₁ and not due to apoptosis. By Western blot analysis, we correlated cytostasis with subtype-selective inductive effects on Rb and p21. Because of its high potency, hSSTR5 was then selected for detailed studies of SSTR induced cytostatic signalling. hSSTR5 initiated cytostatic signalling was G protein dependent and PTP-mediated (5). Octreotide treatment induced a translocation of cytosolic PTP to the membrane whereas it did not stimulate PTP activity when added directly to the cell membrane (5). Western blot analysis revealed concentration-dependent Octreotide-induced increase in hypophosphorylated Rb. C-tail truncation mutants of hSSTR5 displayed progressive loss of antiproliferative signalling proportional to the length of deletion as reflected by the marked decrease in the effects of Octreotide on membrane translocation of cytosolic PTP and induction of Rb and G₁ arrest. The last 16 residues were critical since their deletion resulted in 75% loss of SSTR5 initiated Rb induction and PTP activity. Based on this, we are planning a detailed mutational analysis of this segment to identify critical residues that confer cytostatic signalling ability as a new experiment (to be included as a separate SOW for year 4). In previous studies, we have also shown that hSSTR3-induced apoptosis by SSTR3 correlates with receptor binding potency and is PTP-dependent (4). Other laboratories have now fully characterized PTP-dependent signalling by SSTR1, SSTR2, and SSTR4, and accordingly we do not plan to duplicate studies with these receptors (reviewed in 1).

In addition to the use of SSTR1-5 individually transfected in host cells for characterizing

subtype -selective growth inhibition, another approach has been the use of subtype-selective analogs. In pilot experiments, we found that synthetic octapeptide SST analogs NC8-12, EC-521, and DC23-60 (all SSTR2 preferring) and BIM23056, and BIM23060 (SSTR5 preferring) exerted antiproliferative effects at much lower concentrations (< 100 pM compared to < 25 nM for Octreotide). However, the magnitude of growth inhibition did not increase indicating that the finite levels of cell cycle regulatory proteins limit the extent of the response. The recent availability of nonpeptide receptor monoselective analogs (described in Tasks 5, 6) will make it possible to test these compounds in cell lines such as MCF7 cells expressing multiple SSTR isoforms. We have obtained these analogs from Merck and will use them to further characterize the subtype selective SSTR-mediated antiproliferative signalling. We will also look at the possible involvement of p27 kip1 in SSTR5 mediated growth inhibition in view of recent reports of its involvement in SSTR2 signalled growth inhibition (27).

Overall, we would consider this task to be almost completed. It has generated new leads which we intend to pursue in year 4.

TASKS 9 & 11. Studies of SSTR Subtype Selectivity For PTP Association and Involvement in Apoptosis

These two tasks form a continuum and will be reported together. We have shown that in tumor cells there is a robust regulation of SHP1 as a result of SSTR activation. In CHO-K1 cells, we found that the level of expression of SHP1 was much lower and as a result could not characterize its association with the receptor. We have nonetheless confirmed the obligatory involvement of SHP1 in antiproliferative signalling in CHO-K1-hSSTR3 and CHO-K1-hSSTR5 cells by overexpressing the wild type and catalytically inactive SHP1 proteins. However, overexpression of SHP1 induces constitutive association of SHP1 to membrane constituents. While the increased presence of SHP1 at the membrane was itself incapable of inhibiting cell growth (via hSSTR5) or inducing apoptosis (via hSSTR3) it amplified the antiproliferative signalling of SST in these cells compared to that seen in mock transfected cells. We have now developed HEK293 cells overexpressing hSSTR1-5 for studies in task 12 (see below). SHP1 is more abundant in HEK293 cells compared to CHO-K1 cells and will allow us to undertake coimmunoprecipitation studies to look at receptor SHP1 association. This remaining work will continue into year 4.

TASK 10. Studies of Subtype Selectivity For SSTR-Induced Apoptosis

Early in our program we demonstrated that SST-induced apoptosis occurs uniquely via the hSSTR3 subtype (4). This essentially completed this task. However, we have gone well beyond our original objective and characterized the sequence of molecular events involved in SSTR apoptotic signalling since this is central to any understanding or future application of SST-based antitumor therapy. We have completed a study in MCF7 cells (J. Biol. Chem. submitted - manuscript appended) in which we demonstrate that SSTR signalled SHP1 mediated acidification requires caspase 8 activation. We investigated the temporal sequence of apoptotic events linking caspase activation, acidification, and mitochondrial dysfunction and show that (1) SHP1 mediated caspase 8 activation is required for SST-induced decrease in pH_i , (2) effector caspases are induced

only when there is concomitant acidification, (3) decrease in pH_i is necessary to induce reduction in mitochondrial membrane potential, cytochrome C release, and caspase 9 activation, and (4) depletion of ATP ablates SST-induced cytochrome C release and caspase 9 activation but not its ability to induce apoptosis. These data reveal that SHP-1-/caspase-8-mediated acidification occurs at a site other than the mitochondrion and that SST-induced apoptosis is not dependent on disruption of mitochondrial function and caspase 9 activation.

Somatostatin regulates other signalling pathways in addition to PTP. Principal amongst these is inhibition of stimulated (but not basal) adenylyl cyclase-cAMP signalling. We have investigated the interaction between SST-induced apoptosis and the cAMP signalling pathway and shown that apoptosis is inhibited by cAMP-mediated prevention of acidification (Fig. 4). Increasing intracellular cAMP with dbcAMP or forskolin before and during SST treatment attenuated SST-induced acidification and prevented apoptosis in MCF-7 cells. Addition of dbcAMP to cells during SST treatment, however, showed that once acidification sets in, cAMP is ineffective in preventing apoptosis. Since cAMP is known to phosphorylate and inactivate the Na^+/H^+ exchanger (NHE), these findings suggest the involvement of NHE in SST-induced acidification. Our results also suggest that cAMP is effective in phosphorylating the resting but not inhibited NHE.

TASK 12. Overexpression and Antisense Blockade of SSTRs to See Effect on Apoptosis

This task has become somewhat simplistic with our finding that SSTR3 is the sole receptor that signals SST-dependent apoptosis. Accordingly, we have expanded our objectives to include the following:

- 1) overexpression of all five hSSTRs to look at the effect on both apoptosis and cytostasis.
- 2) antisense blockade of hSSTR3 in MCF7 cells
- 3) structural studies of the regulation and apoptotic signalling via the C-tail of SSTR3

We have produced and pharmacologically characterized stably transfected HEK293 cells expressing hSSTR1, 2, 3, 4 (hSSTR5 is pending). By saturation binding analysis, the total number of receptors (B_{max}) in HEK293 cells is 5-15 fold greater than in CHO-K1 cells that we have studied up until now.

<u>Receptor</u>	<u>B_{max} (fmol/mg protein)</u>	<u>B_{max} (fmol/mg protein)</u>
	CHO-K1 cells	HEK293 cells
hSSTR1	174 \pm 40	800
hSSTR2	260 \pm 61	3200
hSSTR3	294 \pm 44	1200
hSSTR4	256 \pm 37	3800

In pilot studies we have carried out cell growth assays comparing nontransfected HEK293 cells with hSSTR3 transfected cells before and during treatment with SST-14 (10^{-6} M). Cells were

cultured in 96 microwell plate at two different concentrations, 10,000 and 20,000 cells/well. Cell numbers were determined at 0, 2, 4, and 6 days by the MTT assay. Compared to control HEK cells which showed a 2.6 fold increase in viable cells at 6 days, cells expressing hSSTR3 showed a 20% decrease in proliferative activity over the same time interval. Treatment of the hSSTR3 cells with SST-14 abolished all growth and indeed led to a virtual loss of all cells through cell death by day 6. We are characterizing apoptosis in these cells and will be embarking on similar studies with the other receptors overexpressed in HEK293 cells. Additionally, as explained in our last annual report, we have begun a series of new experiments (to be covered under a new SOW) on structure-function and regulation of SSTR3 that were not originally proposed but which we felt were important to our longterm objectives. They arose from our observation that SSTR3 is prominently expressed in breast tumor samples and that it is the only subtype which mediates apoptosis. To get a handle on the regulation of SSTR3, we sequenced 5 Kb of the DNA sequence 5' to the ATG codon and identified a number of potential cis regulatory elements (described in the last annual report). We have now carried out primer extension analysis and mapped the start site to 73 bp upstream of the ATG (Fig. 3). Based on this the promoter sequence has been revised and updated and shows 2 sterol response elements (SREBP-1) in addition to consensus sites for SP1, NF-1/L, E-Box, NFKappa E2, IRF-2, AP-2 as well as a distal 5' CRE element. Despite evidence for estrogen induction of SSTR3, there is no estrogen response element in the promoter suggesting a post transcriptional effect. To investigate the role of the cytoplasmic C-tail of hSSTR3 in inducing apoptosis, we embarked on a mutational study and created the following mutants:

- 1) deletion of hSSTR3 C-tail at the 7th transmembrane (TM) junction to see if it blocks apoptosis
- 2) introduction of a palmitoylation motif in the hSSTR3 C-tail to see whether it attenuates apoptosis (SSTR3 is the only member of this family whose cytoplasmic tail does not possess a palmitoylation anchor shown in other receptors to be important in receptor function) (1)
- 3) chimeric hSSTR3/hSSTR5 receptors substituting the C-tail, TM domains VI and VII and the third intracellular loop of hSSTR3 with the corresponding region of hSSTR5 to see if such a swap will abrogate the cytotoxic property of hSSTR3 (loss of function chimera).

The three mutants were expressed in HEK cells and characterized pharmacologically. Deletion of the C-tail of hSSTR3 produced an inactive mutant with total loss of binding. This is likely because the C-tail was deleted at the junction of the VIIth TM and may have disrupted the ligand binding pocket. We then created a slightly modified mutant with a small overhanging C-tail which produced a binding competent mutant. The palmitoylation mutant and the hSSTR5/hSSTR3 chimeric receptors both displayed high affinity ligand binding and will be suitable for further studies. We have also created the reverse hSSTR5/hSSTR3 chimeric receptor substituting the C-tail TM domains VI and VII, and the third intracellular loop of hSSTR5 with the corresponding region of hSSTR3 to see if such a swap will confer the ability to induce apoptosis by hSSTR5 (gain of function chimera). Finally, our finding that SST induced apoptosis in MCF7 cells and in CHO-K1 cells expressing hSSTR3 is acidification-dependent, whereas the

cytostatic action of SST elicited via the other hSSTRs does not affect intracellular pH, has raised the possibility that the unique ability of hSSTR3 to initiate a pH regulatory signal may lie in its C-tail where it displays the greatest divergence from the C-tails of the other hSSTRs. Of particular interest is the presence within the C-tail of hSSTR3 of a putative PDZ-interacting domain capable of binding to Na⁺/H⁺ exchanger regulatory factor (NHERF) to modulate proton extrusion through Na⁺/H⁺ exchanger (NHE). We plan to delineate the importance of the putative PDZ binding domain and the potential involvement of NHE in SST-induced acidification through additional mutational studies of the C-tail. With the last exception, all of the hSSTR3 mutants and chimeric receptors described above have been constructed and expressed, some partly characterized pharmacologically, and all will be systematically investigated in year 4 for apoptosis and apoptotic signalling. Finally, the antisense experiment to block hSSTR3 induced apoptosis in MCF7 cells will continue in year 4 as originally proposed.

REVISED STATEMENT OF WORK FOR YEAR 4

- Task 3 - Immunocytochemistry - to be completed
- Task 5 - Antireceptor blockade of SSTR1-5
- Task 6 - Antisense knockout of SSTR1-5
- Task 9 - Studies of subtype selectivity for PT1C association
- Task 10 - Already completed in year 3
- Task 11 - PTP1C involvement in apoptosis
- Task 12 - overexpression and antisense blockade of SSTRs to see effect on apoptosis

NEW TASKS PROPOSED FOR YEAR 4

- Task 13 - Mutational analysis of the C-tail of hSSTR3
- Task 14 - Mutational analysis of the C-tail of hSSTR5
- Task 15 - Completion of studies of cAMP effects on SSTR-mediated apoptosis

SUMMARY AND CONCLUSIONS

- 1) Analysis of SSTR1-5 expression in two separate batches of 48 and 50 samples respectively of primary ductal NOS breast cancer by semiquantitative RT-PCR has confirmed expression of all five subtypes. SSTR1, 2, and 3 are the most frequently expressed isoforms occurring in 91%, 96%, and 98% of the tumors. SSTR4 occurs in 76% of samples whereas SSTR5 is present in approximately half the samples. Receptor expression at the mRNA level generally matches receptor protein expression by immunocytochemistry.
- 2) Statistical analysis of the pooled data shows a very strong positive correlation between SSTR3 expression and tumor grade. Induction of SSTR3 in high grade tumors may represent a compensatory mechanism for regulating proliferative activity through apoptosis and is offset by a decrease in SSTR1, 2, and 4 expression. Expression of SSTR1, 2, and 4

strongly correlates with estrogen receptor levels and SSTR2 expression additionally correlates positively with progesterone receptor levels.

- 3) Antisense knockout of SSTR expression in MCF-7 cells has revealed a relatively high potency of SSTR3 and SSTR5 compared to SSTR1 and SSTR2 in inducing antiproliferation in these cells expressing multiple endogenous SSTRs similar to our earlier findings in transfected CHO-K1 cells individually expressing the SSTR subtypes.
- 4) Tamoxifen exhibits a dose-dependent biphasic effect on SSTR1 and SSTR5 mRNA in MCF-7 cells, low levels (10^{-12} M) being inhibitory and high doses (10^{-10} - 10^{-7} M) being stimulatory.
- 5) SST induces apoptosis selectively through the SSTR3 subtype. This effect is dependent on activation of SHP-1 and caspase-8 mediated decrease in intracellular pH (pH_i) to 6.5. Since SHP-1-mediated caspase-8 activation is required for SST-induced decrease in pH_i , since effector caspases are induced only when there is concomitant acidification, and since a decrease in pH_i is necessary to induce reduction in mitochondrial membrane potential, cytochrome c release and caspase 9 activation, our findings suggest that SHP-1/caspase-8 mediated acidification occurs at a site other than the mitochondrion, and that SST induced apoptosis is not dependent on disruption of mitochondrion function and caspase-9 activation.
- 6) SST induced apoptosis is inhibited by cAMP-mediated prevention of acidification.
- 7) Acting via subtypes 1, 2, 4, 5, SST exerts cytostatic action by SHP-mediated induction of the hypophosphorylated form of the retinoblastoma protein Rb and the CDK inhibitor p21. In cells expressing these subtypes, SST inhibits cell cycle progression. The C-tail of hSSTR5 (the subtype which displays the most potent cytostatic effect) is required for its antiproliferative signalling.

REFERENCES

- 1) Patel, Y.C. Somatostatin and its receptor family. *Frontiers in Neuroendocrinology* 20:157-198, 1999.
- 2) Patel, Y.C. and C.B. Srikant. Somatostatin receptors. *Trends in Endocrinology & Metabolism* 8:398-405, 1997.
- 3) Lamberts, S.W.J., Van Der Lely, A-J, Deherder, W.W. et al. Drug therapy: Octreotide. *New Eng. J. Med.* 334:246-254, 1996.
- 4) Sharma, K., Patel, Y.C., Srikant, C.B. Subtype-selective induction of p53-dependent apoptosis but not cell cycle arrest by human somatostatin receptor 3. *Mol. Endocrinol.* 10:1688-1696, 1996.
- 5) Sharma, K., Patel, Y.C., Srikant, C.B. C-terminal region of human somatostatin receptor 5 is required for induction of Rb and Gi cell cycle arrest. *Mol. Endocrinol.* 13:82-90, 1999.

- 6) Patel, Y.C., M.T. Greenwood, R. Panetta, N. Hukovic, S. Grigorakis, L-A Robertson and C.B. Srikant. *Metabolism* 45 (8):31-38, 1996.
- 7) Hierowski, M.T., Liebow, C., Dusapin, K., Schally, A.V. Stimulation by somatostatin of dephosphorylation of membrane proteins in pancreatic cancer Mia PaCA-2 cell line. *FEBS Lett* 179:252-256, 1985.
- 8) Pan, M.G., Florio, T., Stork, P.J.S. G protein activation of a hormone-stimulated phosphatase in human tumor cells. *Science* 256:1215-1217, 1992.
- 9) Neel, B. Structure and function of SH2-domain containing tyrosine phosphatase. *Semin Cell Biol.* 4:419-432, 1993.
- 10) Luttrell, L.M., S.S.G. Ferguson, Y. Daaka et al. β -arrestin-dependent formation of β 2-adrenergic receptor-src protein kinase complexes. *Science* 283:655-660, 1999.
- 11) Sharma, K., Srikant, C.B. Induction of wild type p53 Bax and acidic endonuclease during somatostatin signalled apoptosis in MCF-7 human breast cancer cells. *Int. J. Cancer* 76:259-266, 1998.
- 12) Sharma, K., C.B. Srikant. G protein coupled receptor signalled apoptosis is associated with activation of a cation insensitive acidic endonuclease and intracellular acidification. *Biochem. Biophys. Res. Commun.* 242:134-140, 1998.
- 13) Khare, S., U. Kumar, R. Sasi, L. Puebla, L. Calderon, K. Lemstrom, P. Hayry, and Y.C. Patel. Differential regulation of somatostatin receptor types 1-5 in rat aorta after angioplasty. *Faseb J.* 13:387-394, 1999.
- 14) Rice, W.R. A consensus combined p-value test and the family wide significance of component tests. *Biometrics* 46:303-308, 1990.
- 15) Vikić-Topić, S., K.P. Raisch, L.K. Kovols, and S. Vuk-Pavlovic. Expression of somatostatin receptor subtypes in breast carcinoma, carcinoid tumor, and renal cell carcinoma. *J. Clin. Endocrinol. Metab.* 80:2974-2979, 1995.
- 16) Evans, A.A., T. Crook, S.A.M. Laws, A.C. Gough, G.T. Royle, and J.N. Primrose. Analysis of somatostatin receptor subtype mRNA expression in human breast cancer. *Br. J. Cancer* 75 (6):798-803, 1997.
- 17) Djordjijević, D., J. Zhang, M. Priam, C. Viollet, D. Gourdj, C. Kordon, and J. Epelbaum. Effect of 17- β -estradiol on somatostatin receptor expression and inhibitory effects on growth hormone and prolactin release in rat pituitary cell cultures. *Endocrinology* 139:2272-2277, 1998.
- 18) Kimura, N., S. Tomizawa, K.N. Arai, and N. Kimura. Chronic treatment with estrogen upregulates expression of SST2 messenger ribonucleic acid (mRNA) but downregulates expression of SST5 mRNA in rat pituitaries. *Endocrinology* 139:1573-1580, 1998.
- 19) Xu, Y., J. Song, M. Berelowitz, and J.F. Bruno. Estrogen regulates somatostatin receptor subtype 2 messenger ribonucleic acid expression in human breast cancer cells. *Endocrinology* 137:5634-5640, 1996.
- 20) Kumar, U., D. Laird, C.B. Srikant, E. Escher, and Y.C. Patel. Expression of the five somatostatin receptor (SSTR1-5) subtypes in rat pituitary somatotrophs: quantitative analysis by double-label immunofluorescence confocal microscopy. *Endocrinology* 138:4473-4476, 1997.
- 21) Kumar, U., R. Sasi, S. Suresh, A. Patel, M. Thangaraju, P. Metrakos, S.C. Patel, and Y.C.

- Patel. Subtype selective expression of the five somatostatin receptors (hSSTR1-5) in human pancreatic islet cells: a quantitative double-label immunohistochemical analysis. *Diabetes* 48:77-85, 1999.
- 22) Dutour, A., U. Kumar, R. Panetta, L'H Ouafik, F. Fina, R. Sasi, and Y.C. Patel. Expression of somatostatin receptor subtypes in human brain tumors. *Int. J. Cancer* 76:620-627, 1998.
 - 23) Papotti, M., U. Kumar, M. Volante, C. Pecchioni, and Y.C. Patel. Immunohistochemical detection of somatostatin receptor types 1-5 in medullary carcinoma of the thyroid. *J. Clin. Endocrinol. Metab.* (Submitted).
 - 24) Rocheville, M., D. Lange, U. Kumar, R. Sasi, R.C. Patel, and Y.C. Patel. Subtypes of the somatostatin receptor assemble as functional homo- and heterodimers. *Proc. Natl. Acad. Sci. (USA)* (submitted).
 - 25) Rohrer, S.P., Birzin, E.T., Mosley, R. T. Rapid identification of subtype-selective agonists of the somatostatin receptor through combinatorial chemistry. *Science* 282:737-740, 1998.
 - 26) Visser-Visselaar, H.A., C.J.C. van Uffelen, P.M. van Koesveld et al. 17- β -estradiol-dependent regulation of somatostatin receptor subtype expression in the 7315b prolactin secreting rat pituitary tumor *in vitro* and *in vivo*. *Endocrinology* 138:1180-1189, 1997.
 - 27) Ciocca, D.R., L.A. Puy, L.C. Fasoli, O. Tello, J.C. Aznar, F.E. Gago, S.I. Papa, and R. Sonego. Corticotropin releasing hormone, leutinizing hormone releasing hormone, growth hormone releasing hormone, and somatostatin-like immunoreactivities in biopsies from breast cancer patients. *Breast Cancer Res. Treat.* 15:175-184, 1990.
 - 28) Nelson, J., M. Cremin, and R.F. Murphy. Synthesis of somatostatin by breast cancer cells and their inhibition by exogenous somatostatin and sandostatin. *Br. J. Cancer* 59 (5):739-742, 1989.
 - 29) Pages, P., Benali, N., Saint-Laurent, N. et al. SST2 somatostatin receptor mediates cell cycle arrest and induction of p27^{kip1}. Evidence for the role of SHP-1. *J. Biol. Chem.* 274:15186-15193, 1999.

TABLE 1

**QUANTITATIVE ANALYSIS OF SSTR1-5 MRNA IN PRIMARY DUCTAL NOS BREAST CANCER SAMPLES IN
RELATION TO TUMOR HISTOLOGY AND ER/PR STATUS**

TB#	sstr1	sstr2	sstr3	sstr4	sstr5	GR	IV	STR	FAT	ER	PR	SIZE	LN	LN+
10817	1.43	0.59	0.1	0.57	0	8	80	20	0	69	123	>4.5	6	2
12868	1.15	0.22	0.07	0.22	0.13	9	70	30	0	93	141	3.5	98	0
11601	1.01	0.26	0.13	0.5	0.16	7	40	0	0	1.3	5.8	1.5	31	29
11603	0.89	0.79	0.2	0.86	0.46	8	35	50	10	69	17.9	>2.5	8	2
12475	1.83	0.35	0.09	0.6	0	9	20	60	10	28	35	4.2	18	1
11238	0.57	0.09	0.11	0.53	0	7	60	0	0	0	9.1	3.5	11	2
12804	0.75	0.01	0.08	0.35	0.03	9	40	30	30	9.2	5.8	1.6	19	3
12723	1.94	0.67	0.2	0.29	0.55	8	40	40	30	63	10.7	5.5	13	13
11279	0.66	1.2	0.32	0.27	0.21	8	60	10	30	0	16.5	2.8	8	3
11600	2.12	0.04	0.08	0.26	0.15	8	70	30	0	60	10.8	1.5	17	15
11657	1.71	0.01	0.07	0.26	0.03	9	45	40	10	0	8	4	10	15
11418	0.6	0.04	0.14	0.6	0	9	40	30	20	0	12	2.2	12	0
12715	0.22	0.01	0.11	0.21	0.08	7	40	60	0	1.5	16	3	98	0
12831	0.29	0.25	0.13	0.41	0.28	9	30	40	20	5.6	16.5	3	10	3
12805	0.46	0.47	0.13	0.3	0.36	6	70	25	0	22	226	3.5	10	0
10820	1.56	0.22	0.11	0.5	0.09	5	75	0	0	247	56	4.7	9	5
12687	1.44	0.76	0.11	0.34	0.22	6	50	40	10	2.3	4.5	1.5	7	0
12291	1.52	0	0.38	0.72	0.23	8	25	65	10	0.4	6.1	1.2	18	2
12845	0.16	0.12	0.09	0.2	0	8	30	60	10	0.2	11.9	2.5	17	0
11361	0.93	0.53	0.07	1.08	0.01	6	50	40	10	104	466	3	2	1
13195	1	0.34	0.1	0.46	0	5	40	40	20	59	172	2	15	1
12924	1.22	0.23	0.09	0.77	0.6	5	25	25	50	17.3	42	2	15	0
13175	0.61	0	0.06	0.32	0.26	6	50	40	5	1.8	15.3	2	7	7
11301	1.26	0.06	0.06	0.24	0.07	7	75	0	0	0	6.3	4	14	14
13150	0.83	0.06	0.19	0.66	0	5	35	65	0	18.3	23	1.8	12	10
11154	0.36	0	0.11	0.22	0	8	30	50	20	0	4.7	2.2	14	0

11298	2.12	0.01	0.09	0.33	0	6	50	0	0	3.3	5.2	2.7	12	1
12866	0.74	0	0.05	0.13	0	6	30	55	5	104	10.7	1.8	10	0
13410	0.57	0.04	0.04	0.2	0	6	30	30	40	3.9	12.2	3.5	15	8
12780	1.36	0.09	0.07	0.73	0	5	20	30	40	57	147	2.5	10	0
12710	1.01	0.65	0.02	0.67	0	5	20	80	0	7.8	4.7	11.5	4	4
11459	1.13	0.48	0.05	0.41	0	5	50	50	0	3.6	98	4.7	16	4
11339	0.24	0.14	0.09	0.31	0	9	80	20	0	5.5	11.5	2.5	98	0
10795	1.59	0.22	0.06	0.89	0.27	5	25	25	50	50	57	2.6	14	0
12179	1.21	0.33	0.04	0.36	0	6	50	0	0	262	250	2.5	13	2
13360	0.95	0.74	0.05	0.29	0	5	35	50	5	31	12.8	2.5	27	0
13302	2.18	0.14	0.06	0.31	0.17	9	20	40	40	7.9	12.6	>3	12	0
12472	2.59	0.23	0.1	0.46	0	7	50	0	0	1.5	8.3	1.8	13	0
13239	1.95	0.29	0.05	0.54	0.18	5	40	60	0	80	82	3	17	1
11827	0.96	0.26	0.09	0.49	0	7	70	0	0	1.3	3.6	6.5	11	8
11350	0.4	0.34	0.23	0.48	0.2	9	50	15	35	0	8	2.5	7	1
13019	1.35	0.82	0.11	0.37	0	6	20	65	5	15.2	12.8	1.5	11	0
13408	1.15	0.44	0.05	0.45	0	5	30	60	10	32	15.3	1.8	11	0
13094	1.27	0.71	0.03	0.48	0	5	40	40	10	6.3	19	3	7	0
11937	1.05	0.25	0.04	0.14	0	7	20	0	0	1.2	6.3	4	16	3
12999	0.7	0.83	0.03	0.39	0.17	5	30	30	30	85	138	1.7	5	1
13087	0.66	0.58	0.07	0.1	0.31	8	50	40	0	0	7.2	11.8	49	49
11612	0.97	0.64	0.03	0.37	0	6	75	0	0	32	92	2.5	22	0
11753	0.43			0.03	0	5	40	40	15	36	157	1.5	18	0

TB# = Tumor Bank Number. All are primary ductal NOS cancers

SSTR1-5 = SSTR1-5 mRNA expressed as fold increase compared to actin mRNA

GR = tumor grade (Nottingham scale)

IV = % invasiveness (% of section occupied by invasive epithelial cells)

STR = % stroma (% of section occupied by collagenous stroma)

Fat = % fat (% of section occupied by fat)

ER = estrogen receptor levels (fmol/mg protein)

PR = progesterone receptor levels (fmol/mg protein)

Size = tumor size in centimeters, 99.9, size unknown; 99.8, multi-focal

LN = total no. of nodes assessed

LN+ = number of positive axillary lymph nodes

TABLE 2***INCIDENCE OF SSTR1-5 MRNA IN PRIMARY DUCTAL NOS BREAST CANCER SAMPLES***

	<u>STUDY 1</u>		<u>STUDY 2</u>		<u>POOLED DATA</u>	
	No.	% Positive	No.	% Positive	No.	% Positive
SSTR1	48	81%	50	100%	98	91%
SSTR2	42	100%	50	92%	92	96%
SSTR3	48	92%	50	100%	98	98%
SSTR4	48	50%	50	100%	98	76%
SSTR5	48	58%	50	50%	98	54%

TABLE 3

**STATISTICAL CORRELATIONS BETWEEN SSTR EXPRESSION, TUMOR HISTOLOGY,
AND ER/PR STATUS IN PRIMARY DUCTAL NOS BREAST CANCER SAMPLES**

TABLE 3A.

Pooled Data From Study 1 and Study 2

	r	P
SSTR1 vs ER	+ 0.356	0.0003
SSTR4 vs ER	+ 0.228	0.019
SSTR2 vs ER	+ 0.264	0.017
SSTR2 vs PR	+ 0.262	0.03
 SSTR3 vs grade	 + 0.415	 0.00002
 SSTR1 vs grade	 - 0.204	 0.017
SSTR2 vs grade	- 0.167	0.123
SSTR4 vs grade	- 0.167	0.4

TABLE 3B.

Separate Analysis of Study 1 and Study 2

	<u>Study 1</u>		<u>Study 2</u>	
	r	P	r	P
SSTR1 vs ER	+ 0.26	0.08	+ 0.28	0.05
SSTR2 vs ER	+ 0.31	0.05	+ 0.17	0.24
SSTR2 vs PR	+ 0.28	0.07	+ 0.21	0.15
SSTR3 vs grade	+ 0.24	0.1	+ 0.45	0.001
SSTR2 vs size	- 0.33	0.04	+ 0.295	0.04
SSTR1 vs lymph node status	- 0.27	0.07	+ 0.02	0.9
 SSTR4 vs ER	 + 0.2	 0.17	 + 0.25	 0.09
SSTR1 vs grade	- 0.216	0.14	- 0.193	0.185
SSTR2 vs grade	- 0.108	0.496	- 0.227	0.122
SSTR4 vs grade	- 0.07	0.65	- 0.118	0.42

TABLE 4

COMPARISON OF SSTR1-5 mRNA EXPRESSION WITH SSTR1-5 IMMUNOCYTOCHEMISTRY IN
HUMAN BREAST TUMOR SAMPLES (STUDY 1)

CASE #	SSTR1	SSTR2	SSTR3	SSTR4	SSTR5
11894	+ 1	+ 1	+/- 1	- 1	- 0
11833	++++ 1	++ 0	++++ 1	++++ 1	++++ 0
11806	+/- 1	++++ 1	++++ 1	- 1	++ 0
11756	++++ 1	++ 1	+ 1	- 1	+ 1
11644	+ 1	+ 0	++ 1	- 1	- 1
11629	++++ 1	+++ 0	+++ 0	- 1	- 0
11522	++++ 1	++++ 0	++++ 1	++ 1	+ 1
11332	- 1	- 0	- 1	+/- 1	- 0
11287	+ 1	+ 1	+++ 1	+ 1	+ 0
11280	- 1	+++ 1	- 1	+++ 1	- 0
11110	- 1	++ 1	++++ 0	+/- 1	- 0
11051	+/- 1	++ 1	++++ 0	- 1	- 0
10969	- 1	++ 1	- 1	+ 1	+/- 0

10963	++++ 1	++ 1	++++ 0	+++ 1	++++ 0
10937	- 1	++ 0	- 0	- 1	+++ 0
10870	++ 1	+++ 1	+ 0	- 0	+ 0

In each paired analysis, SSTR mRNA expression is shown as + to ++++ based on quantitative RT-PCR. Absence of SSTR mRNA is indicated by -. The presence or absence of SSTR immunoreactivity by peroxidase immunocytochemistry in the matching samples is shown as 1 or 0 respectively. A match between SSTR mRNA and protein expression by immunocytochemistry is indicated by the shaded boxes.

FIGURE LEGENDS

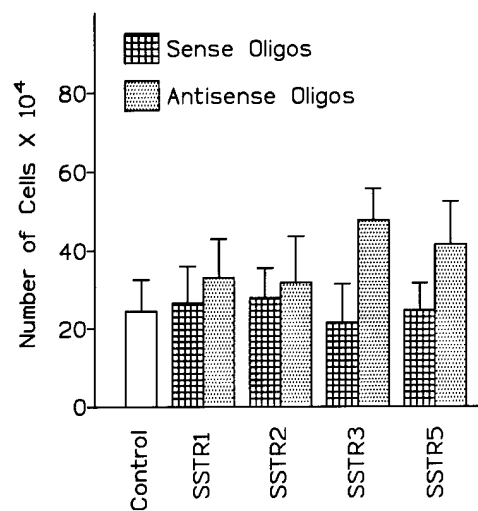
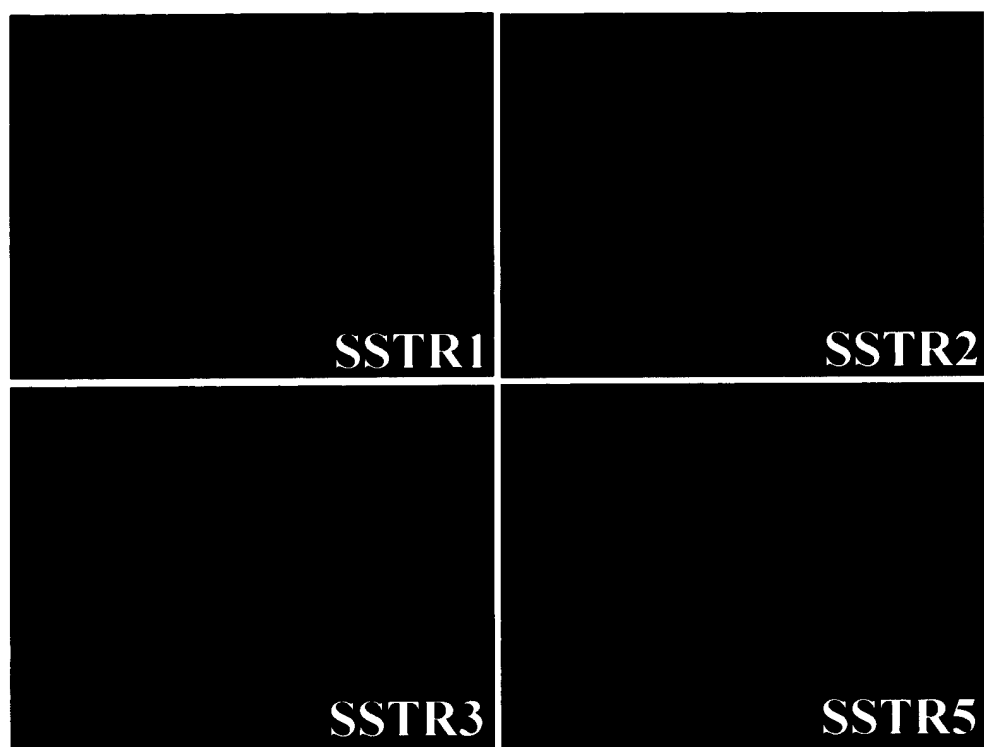
FIGURE 1 A. Effect of antisense knockout of SSTR1, SSTR2, SSTR3, and SSTR5 on MCF-7 cell growth. Cultured MCF-7 cells were exposed for 4 days with 2 $\mu\text{g/ml}$ of antisense or sense oligonucleotides (ODNs). Cell counts were determined at the end of treatment. Cells incubated with medium alone (without ODNs) served as absolute control. Antisense knockout of SSTR3 and SSTR5 significantly increased cell growth rate. Knockout of SSTR1 and SSTR2 produced a small nonsignificant increase in the number of proliferating cells (mean \pm SE, $n=4$). **B.** Localization of SSTRs in MCF-7 cells by confocal fluorescence immunocytochemistry. Note the strong expression of SSTR1, SSTR2, and SSTR5 in these cells, localized to both plasma membrane and cytoplasmic structures. SSTR3 is clearly present in these cells but exhibits a relatively weak labelling. The immunofluorescence was specific and was inhibited in control cells treated with antigen absorbed antibody or by treatment with preimmune serum (not shown).

FIGURE 2. Dose-dependent alterations in SSTR1, 2, 3, 5 mRNA in MCF-7 cells treated with estradiol (E, 10^{-12} - 10^{-7} M), or tamoxifen (T, 10^{-12} - 10^{-7} M). SSTR mRNA was analysed by semiquantitative RT-PCR and expressed as a fold increase compared to β -actin.

FIGURE 4. Cytotoxic signalling of SST is inhibited by cyclic AMP (cAMP) upstream of acidification in MCF-7 cells. The effect of increase in cellular cAMP on the ability of D-Trp⁸ SST-14 to signal cellular acidification and apoptosis was investigated. Increase in cAMP was achieved by addition of dibutyryl cAMP (dbcAMP), by stimulating adenylyl cyclase with forskolin (FSK) or by activating the VIP receptor (details not shown). **A.** SST-induced oligonucleosomal DNA fragmentation is inhibited by dbcAMP. **B.** Elevation of endogenous cAMP by FSK and VIP prevents SST-induced apoptosis. **C.** dbcAMP does not prevent SST-induced membrane-association of SHP-1. **D.** Cells incubated with dbcAMP, FSK and VIP displayed an increase in the resting intracellular pH (pHi) and became resistant to SST-induced acidification. **E.** dbcAMP prevents SST-induced apoptosis only when added before the onset of acidification. SST-induced acidification could be detected after 2 h (not shown). Addition of dbcAMP after this time point failed to inhibit the cytotoxic signalling of SST.

APPENDIX

- 1) Patel, Y.C. Somatostatin and its receptor family. *Frontiers in Neuroendocrinology*. 20:157-198, 1999.
- 2) Kumar, U., R. Sasi, S. Suresh, A. Patel, M. Thangaraju, P. Metrakos, S.C. Patel, and Y.C. Patel. Subtype-selective expression of the five somatostatin receptors (hSSTR1-5) in human pancreatic islet cells. *Diabetes* 48:88-85, 1999.
- 3) Khare, S., U. Kumar, R. Sasi, L. Puebla, L. Calderon, K. Lemstrom, P. Hayry, and Y.C. Patel. Differential regulation of somatostatin receptor types 1-5 in rat aorta after angioplasty. *FASEB Journal* 13:387-394, 1999.
- 4) Hukovic, N., M. Rocheville, U. Kumar, R. Sasi, S. Khare, and Y.C. Patel. Agonist-dependent upregulation of human somatostatin receptor type 1 requires molecular signals in the cytoplasmic C-tail. *J. Biol. Chem.* 274:24550-24558, 1999.
- 5) Sharma, K., Y.C. Patel, and C.B. Srikant. C-terminal region of human somatostatin receptor 5 is required for induction of Rb and G1 cell cycle arrest. *Molecular Endocrinology* 13:82-90, 1999.
- 6) Liu, D., G. Martino, M. Thangaraju, M. Sharma, F. Halwani, S-H Shen, Y.C. Patel, and C.B. Srikant. Caspase-8-mediated intracellular acidification precedes mitochondrial dysfunction in somatostatin-induced apoptosis. *J. Biol. Chem.* 1999 (submitted).
- 7) Liu, D., M. Thangaraju, S-H Shen, and C.B. Srikant. Activation of caspase-8 precedes intracellular acidification that is necessary to induce caspase 3 during G protein-coupled receptor signalled apoptosis. Program Annual Meeting of the U.S. Endocrine Society, San Diego, CA., June 1999 (Abstr. P-2346).

A**B****FIGURE 1.**

Effect of estrogen and tamoxifen on SSTR1-5 expression in MCF-7 cells

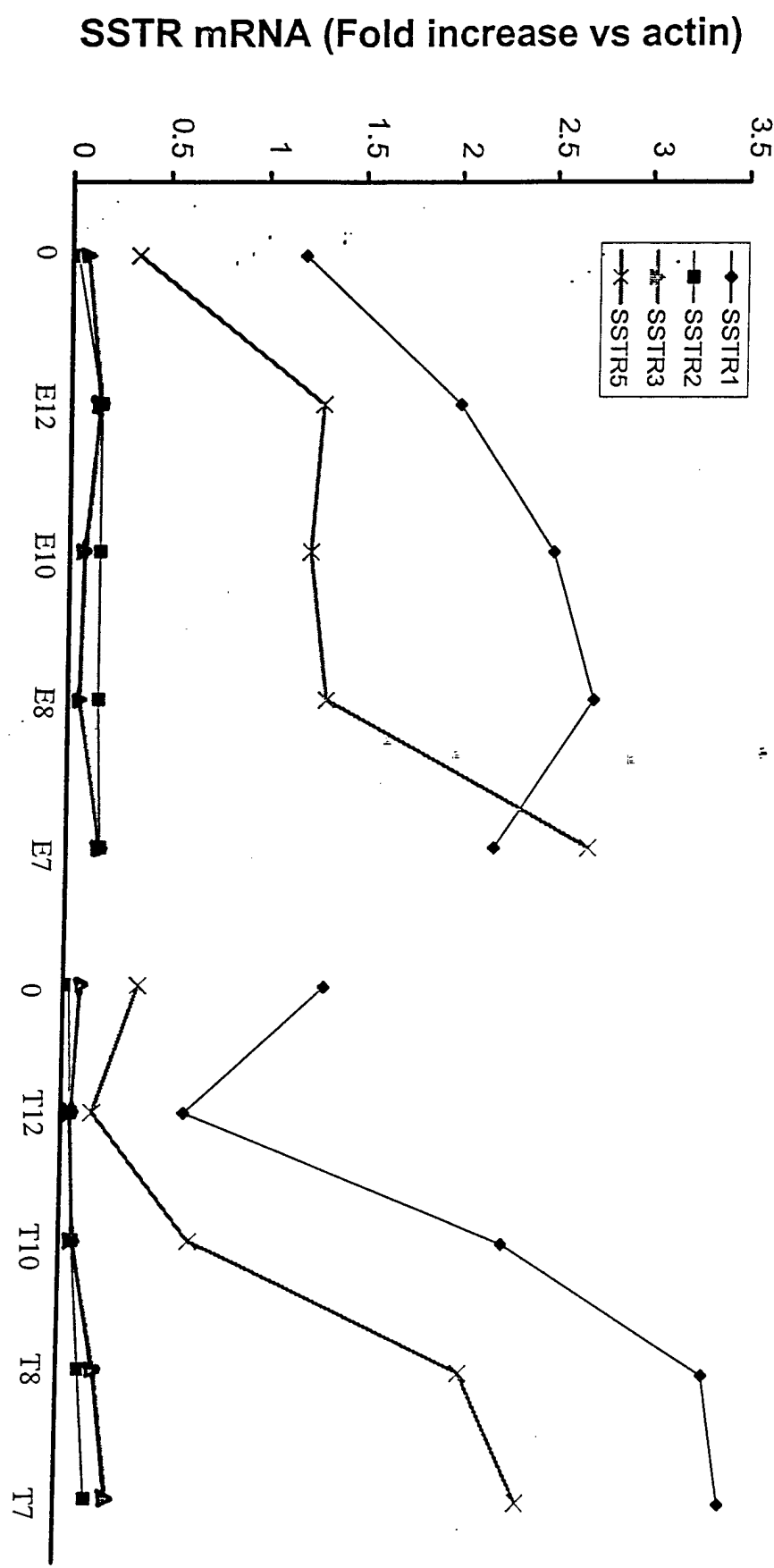


FIGURE 2.

```

GGAGGCTCCT GCATCCAGCC TGGCTCTGCC TGGGCCTCCT CCTGAGCGTG GCTTTCCTCA -1128
                NF-1/L
GTGGGGCCTG ACATTACCCC CTTGGCACTG GGCTTGGTCC ACTGAAGGCT TCTCTGGTTC -1068
                IRF-2
ATTTGATGCC TGACACTGAG GCAGAGCTCG TGCCTGTGCG GAAGTGATGG GGCAGAAAGC -1008
    AP-2
AATGGGGAGG GTCCAAAGCT GGCTGGAGAC TCCACAGGGG AGGGGATCAG AGTCTCGCAG -948

GGGAGCCAG AGGAGCCCCA GCTTCTTCTG CGCAGGCATG GGATGAGAAA GACACTAAGA -888

AAGCACCTGG AGTGCGGGGG GGCTCTTGCT TATGCTGCAA ATCCCTTCTG AAAATGTCCC -828

CTTTTCCAGG CAGCTGGCCC CTCCAGCCAG GGGGAGGGAC TACTCTTGA TAGCATCTGC -768
    IRF-2                AP-2                NF-
TAAGTGAATT GTAAAGTTCT CCAACCCAG CCGGCCTCTG GGGAGAAGGG GCCTCAGCCA -708
kappaE2
CCTGCCCCC AGGTTACAG CCAACCTTCC TGGGCAGGGC CTTTGGGAGG GGCACAGTGG -648

GATGGCCAG GCTGAGGGGG CACCTAAGGA CTCTGACTCC CAGGGGAGGG GACACCCCAA -588

GCCTGTGGTT CTTAACTCCA TTTGGAACCT GAAGAATCTG ATAACAGATC TGACATTAAC -528

CTTCACCTGG AGTTTAGGGC GTTCATGGAT CCTCTGAAGT TCATCTAGGG AGCAGGTTTC -468
                E-box
CAGGTGAAGG TCCTGTGATA TGAAGCAGTG TTTTTCAGAT GTGAGGGCGA GACCTGTTGG -408
NF-1/L
TGGCAATGCA ACCCACTTCA CAGGGCCCTG CCAGCTGGGG CCTCACATGT AGAAAGGAAG -348
                SREBP-1
GGCAGGTATT TGTTGGTGAA ACAGTATGAC TTCATGCCAC ACACCACACC CTCACTCCAC -288
    SREBP-1
GATGGAGAAT GATCACCTCA CCTCCCTGAG CCTCAGTTTC CTCATCTGAG AAAAGGGGAT -228

AACACGACTC AGCCTTGCGG GGCTGTGCGG GGTGAATGAG ATGGTGCGTG CTAAGCACCT -168
                SP1
CCCATCTTCT GAAATCTCTC AGACGATGGG AGGATGGGCG TGCAGCAGGT CCCAGGTTTC -108
    SP1                |→
GGCATGATGG GAGGGGGCAG CACAGAGAAA GCCATTCTCT GCTGTGACCG AGCTGTTTTT -48

CCTTCCCCCA GGCAAATAGC TGA CTGCTGA CCACCCTCCC CTCAGCCATG GACATGCTTC +13

```

Figure 3. Sequence analysis of 1.1kb of hSSTR3 promoter region. The first base pair of the translation start site (ATG) is defined as +1. The putative transcription start site is indicated by an arrow and the first base pair of the transcript is underlined and shown in bold. Relevant promoter elements are underlined, with the names indicated above.

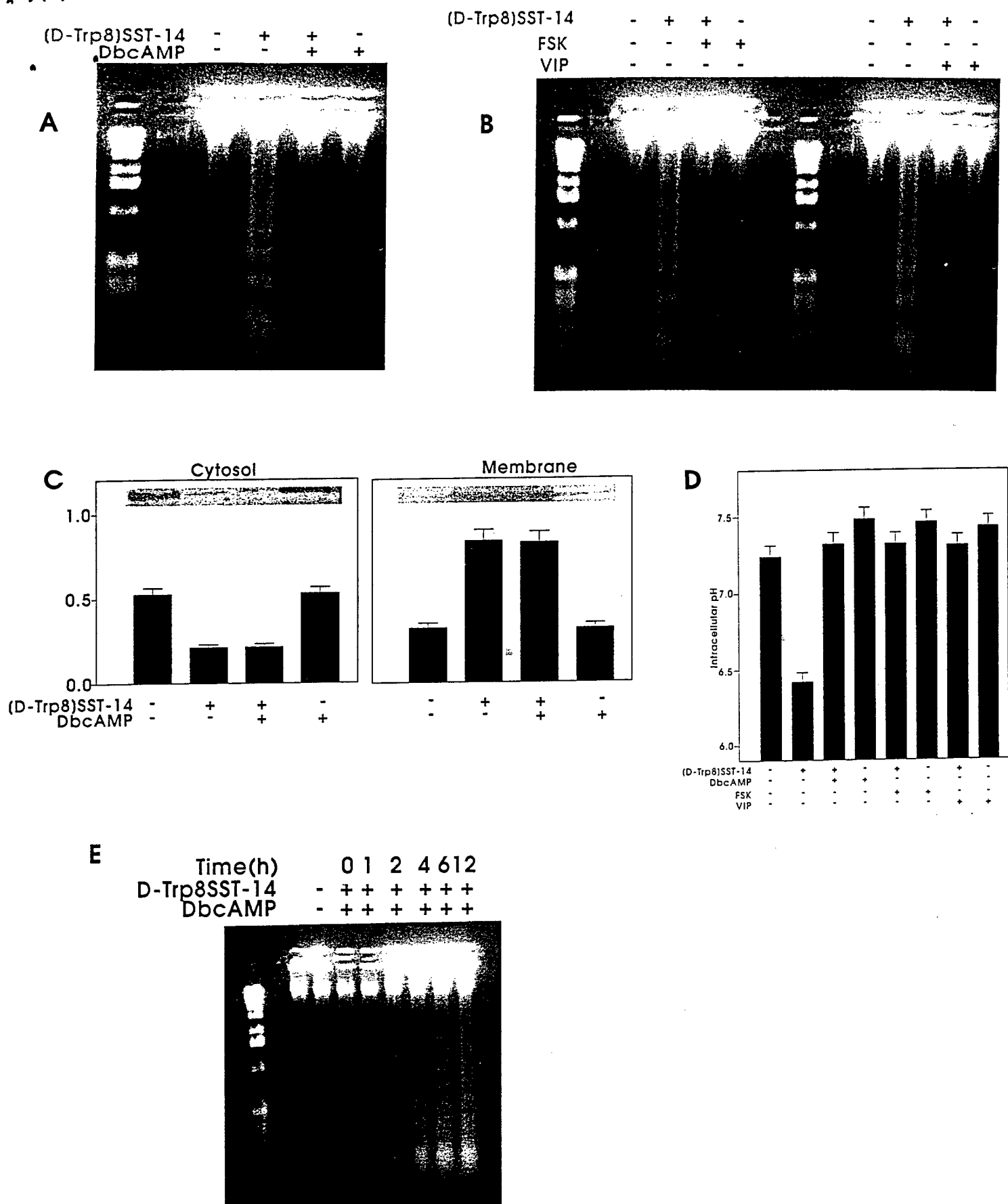


FIGURE 4.
32

Somatostatin and Its Receptor Family

Yogesh C. Patel

*Fraser Laboratories, Department of Medicine, Department of Neurology and Neurosurgery,
and Department of Pharmacology and Therapeutics, Royal Victoria Hospital and Montreal
Neurological Institute, Montreal, Quebec, Canada H3A 1A1*

Somatostatin (SST), a regulatory peptide, is produced by neuroendocrine, inflammatory, and immune cells in response to ions, nutrients, neuropeptides, neurotransmitters, thyroid and steroid hormones, growth factors, and cytokines. The peptide is released in large amounts from storage pools of secretory cells, or in small amounts from activated immune and inflammatory cells, and acts as an endogenous inhibitory regulator of the secretory and proliferative responses of target cells that are widely distributed in the brain and periphery. These actions are mediated by a family of seven transmembrane (TM) domain G-protein-coupled receptors that comprise five distinct subtypes (termed SSTR1-5) that are encoded by separate genes segregated on different chromosomes. The five receptor subtypes bind the natural SST peptides, SST-14 and SST-28, with low nanomolar affinity. Short synthetic octapeptide and hexapeptide analogs bind well to only three of the subtypes, 2, 3, and 5. Selective nonpeptide agonists with nanomolar affinity have been developed for four of the subtypes (SSTR1, 2, 3, and 4) and putative peptide antagonists for SSTR2 and SSTR5 have been identified. The ligand binding domain for SST ligands is made up of residues in TMs III-VII with a potential contribution by the second extracellular loop. SSTRs are widely expressed in many tissues, frequently as multiple subtypes that coexist in the same cell. The five receptors share common signaling pathways such as the inhibition of adenylyl cyclase, activation of phosphotyrosine phosphatase (PTP), and modulation of mitogen-activated protein kinase (MAPK) through G-protein-dependent mechanisms. Some of the subtypes are also coupled to inward rectifying K⁺ channels (SSTR2, 3, 4, 5), to voltage-dependent Ca²⁺ channels (SSTR1, 2), a Na⁺/H⁺ exchanger (SSTR1), AMPA/kainate glutamate channels (SSTR1, 2), phospholipase C (SSTR2, 5), and phospholipase A₂ (SSTR4). SSTRs block cell secretion by inhibiting intracellular cAMP and Ca²⁺ and by a receptor-linked distal effect on exocytosis. Four of the receptors (SSTR1, 2, 4, and 5) induce cell cycle arrest via PTP-dependent modulation of MAPK, associated with induction of the retinoblastoma tumor suppressor protein and p21. In contrast, SSTR3 uniquely triggers PTP-dependent apoptosis accompanied by activation of p53 and the pro-apoptotic protein Bax. SSTR1, 2, 3, and 5 display acute desensitization of adenylyl cyclase coupling. Four of the subtypes (SSTR2, 3, 4, and 5) undergo rapid agonist-dependent endocytosis. SSTR1 fails to be internalized but is instead upregulated at the membrane in response to continued agonist exposure. Among the wide spectrum of SST effects, several biological responses have been identified that display absolute or relative subtype selectivity. These include GH secretion (SSTR2 and 5), insulin secretion (SSTR5), glucagon secretion (SSTR2), and immune responses (SSTR2). **KEY WORDS:** somatostatin; receptors; expression; signal transduction; secretion; cell proliferation. © 1999 Academic Press

Over a quarter century has now elapsed since somatostatin (SST) was first identified in the hypothalamus as a tetradecapeptide that inhibited the release of growth hormone (17). Momentous as it was, this discovery turned out to be

only the first glimpse of the many faces of this intriguing peptide that have become slowly revealed over the subsequent years. SST is produced not only in the hypothalamus but throughout the central nervous system and in most major peripheral organs (75, 154, 166). SST-like immunoreactivity has been found in all vertebrates as well as in some invertebrate species and in the plant kingdom (145, 166). Along with its wide anatomical distribution, SST acts on multiple targets via a family of five receptors to produce a broad spectrum of biological effects (145, 166). Several genes encoding SST-like peptides have been identified (reviewed in 150). Today, SST is best regarded as a phylogenetically ancient multigene family of peptides with two important bioactive products, SST-14, the form originally identified in the hypothalamus, and SST-28, a congener of SST-14 extended at the N-terminus that was discovered subsequently (157). The two peptides are produced in various proportions by different SST cells and act as a neurotransmitter or paracrine/autocrine regulator or more widely through the circulation to regulate such diverse physiological processes as cell secretion, neuromodulation, smooth muscle contractility, nutrient absorption, and cell growth (145, 166). The physiological role of hypothalamic SST on GH and thyroid stimulating hormone secretion is well established (145, 166). The peptide also appears to be a physiological regulator of islet cells, gastrointestinal cell functions, and immune cell functions and may be of considerable importance in the pathophysiology of disease, e.g., neoplasia, inflammation, diabetes mellitus, epilepsy, Alzheimer's disease, Huntington's disease, and AIDS (reviewed in 46, 150, 156). This article will focus on somatostatin and its receptors as a major biological system, with particular emphasis on the molecular biology and pharmacology of the recently cloned receptor family.

PRODUCTION AND ACTIONS OF SOMATOSTATIN

SST-producing cells occur at high densities throughout the central and peripheral nervous systems, in the endocrine pancreas, and in the gut and in small numbers in the thyroid, adrenals, submandibular glands, kidneys, prostate, and placenta (145, 150, 166). The typical morphological appearance of a SST cell is that of a neuron with multiple branching processes or of a secretory cell often having short cytoplasmic extensions (δ cells) (49, 110). SST-positive neurons and fibers are abundantly dotted throughout the CNS with the notable exception of the cerebellum (49, 85). Brain regions rich in SST include the hypothalamus, the deeper layers of the cortex, all limbic structures, the striatum, the periaqueductal central gray, and all levels of the major sensory pathways. Within the hypothalamus, the anterior periventricular nucleus with its axonal projections to the median eminence comprises the principal somatostatinergic tract that accounts for ~80% of hypothalamic SST immunoreactivity. SST perikarya in low to moderate densities occur in the paraventricular, arcuate, and ventromedial nuclei (49, 85). Gastrointestinal (GI) SST cells are of

two types: δ cells in the mucosa and neurons that are intrinsic to the submucous and myenteric plexuses (75, 110). SST cells in the pancreas are confined to the islet where they occur as δ cells in close proximity to the insulin, glucagon, and pancreatic polypeptide-producing cells (43). Within the thyroid, SST coexists with calcitonin in a subpopulation of C cells (166). In addition to these typical SST-producing neuroendocrine cells that secrete large amounts of the peptide, many tumor cells as well as inflammatory and immune cells (lymphocytes, macrophages, thymic epithelial cells, synovial cells) also produce SST, usually in small amounts upon activation (2, 44, 48, 57, 88, 163, 198). In the rat, the gut accounts for ~65% of total body SST-like immunoreactivity, the brain for ~25% the pancreas for ~5%, and the remaining organs for ~5% (154).

SST functions as a neurotransmitter in the brain with effects on cognitive, locomotor, sensory, and autonomic functions (these and other actions listed below are reviewed in 46, 145, 166). It inhibits the release of dopamine from the midbrain and of norepinephrine, TRH, CRH, and endogenous SST from the hypothalamus. It inhibits both the basal and the stimulated secretion of GH, TSH, and islet hormones but has no effect on LH, FSH, prolactin, or ACTH in normal subjects. It does, however, suppress elevated ACTH levels in Addison's disease and in ACTH-producing tumors. In addition, it inhibits the basal and the TRH-stimulated release of prolactin *in vitro* and diminishes elevated prolactin levels in acromegaly. In the GI tract, SST inhibits the release of virtually every gut hormone that has been tested. It has a generalized inhibitory effect on gut exocrine secretion (gastric acid, pepsin, bile, colonic fluid) and suppresses motor activity generally as well as through inhibition of gastric emptying, gallbladder contraction, and small intestinal segmentation. SST, however, stimulates migrating motor complex activity. The effects of SST on the thyroid include the inhibition of the TSH-stimulated release of T4 and T3 and of calcitonin from thyroid parafollicular cells. The adrenal effects consist of the inhibition of angiotensin II stimulated aldosterone secretion and the inhibition of acetylcholine stimulated medullary catecholamine secretion. In the kidneys, SST inhibits the release of renin stimulated by hypovolemia and inhibits ADH-mediated water absorption. SST also blocks the release of growth factors (IGF1, EGF, PDGF) and of cytokines (IL6, IFN- γ) (15, 44, 65). Other effects of SST include vasoconstriction, especially in the splanchnic circulation, and inhibition of proliferation of lymphocytes and inflammatory, intestinal mucosal, and cartilage and bone precursor cells (3, 87, 145, 166, 198, 218). All of these diverse effects of SST can be explained by the inhibitory effects of the peptide on two key cellular processes, secretion and cell proliferation.

SOMATOSTATIN, GENES, AND GENE PRODUCTS

Like other protein hormones, SST is synthesized from a large preprosomatostatin (preproSST) precursor molecule that is processed enzymatically to yield several mature products (reviewed in 150). cDNAs for several preproSST molecules were first identified in 1980 followed by the elucidation of the

structure of the rat and human SST genes in 1984 (130, 188). The human gene maps to the long arm of chromosome 3. Mammalian proSST consists of a 92-amino-acid protein that is processed predominantly at the C-terminal segment to generate two bioactive forms, SST-14 and SST-28 (150). The two peptides are synthesized in variable amounts by different SST-producing cells due to differential precursor processing. SST-14 predominates in pancreatic islets, stomach, and neural tissues and is virtually the only form in retina, peripheral nerves, and enteric neurons. SST-28 accounts for 20–30% of total immunoreactive SST in brain but it is not clear whether it is cosynthesized with SST-14 or whether it is produced in separate neurons (150). SST-28 is synthesized as a terminal product of proSST processing in intestinal mucosal cells that constitute the largest peripheral source of the peptide. Several genes encoding SST-like peptides have been identified (72, 130, 150, 188, 206). The various forms of SST observed in mammals are all derived from differential processing of a common precursor preproSST-I. In fish, however, there are two separate genes, one corresponding to mammalian preproSST-I, which gives rise to only SST-14, and another preproSST-II, which generates NH₂-terminally extended forms of SST such as anglerfish-28 (a homologue of mammalian SST-28) and catfish-22. The SST-14 sequence is totally conserved between fish and mammals, whereas mammalian SST-28 shares only 40–66% homology with its fish counterparts. Interestingly, expression of the SST-28 encoding genes in fish is restricted to the pancreatic islets, whereas the SST-14 encoding gene, like its mammalian counterpart, is widely expressed in many body cells including the pancreas (125, 206). Recently, a novel second SST-like gene called cortistatin (CST) that gives rise to two cleavage products comparable to SST-14 and SST-28 was described in human and rat (36, 160). These cleavage products consist of human CST-17 and its rat homologue CST-14 and human and rat CST-29. Unlike the broad distribution of the preproSST-I gene, gene expression of CST is restricted to the cerebral cortex (36). The human CST gene is distinct from the preproSST-II gene and appears to be the homologue of a recently described novel SST-like gene in the frog whose expression is also restricted to the brain (206). Based on nucleotide sequence homologies, the picture that emerges suggests that the preproSST-I gene of the fish is the common ancestral gene that has evolved into the human preproSST gene. The preproSST-II gene of teleosts arose from a gene duplication event. A separate duplication event in the tetrapod lineage ~400 million years ago gave rise to the CST gene, which has been carried through from amphibians to human (206).

REGULATION OF SOMATOSTATIN SECRETION AND GENE EXPRESSION

Secretion of SST can be influenced by a broad array of secretagogues ranging from ions and nutrients, to neuropeptides, neurotransmitters, classical hormones, growth factors, and cytokines (reviewed in 145, 150, 166). Some of these agents exert common effects on SST cells in different locations presumably by direct action; others tend to be tissue-selective, a fact that can be explained by

tissue-specific expression of receptors for the secretagogues on SST cells or by indirect effects through the release of other peptides or transmitters. Membrane depolarization activates SST release from both neurons and peripheral SST-secreting cells (D cells), suggesting that this mode of release is a fundamental property of all SST cells (145, 150). Nutrients exert tissue-specific effects on SST release most prominently in islet D cells stimulated by glucose, amino acids, and lipids. Hypothalamic SST secretion is inhibited by glucose and is insensitive to aminogenic stimuli, whereas gut SST secretion is triggered by luminal but not circulating nutrients (145, 150). Virtually every neurotransmitter or neuropeptide tested has been shown to exert some effect on SST secretion with varying degrees of potency and tissue selectivity. Within this group, glucagon, GH-releasing hormone, neurotensin, corticotrophin-releasing hormone, calcitonin gene-related peptide, and bombesin are potent stimulators of SST release from several tissue sites, and opiates and GABA generally inhibit SST secretion (46, 145, 150). Of the various hormones studied, GH and thyroid hormones enhance SST secretion from the hypothalamus; their effect in other tissues has not been adequately investigated (145, 150). Glucocorticoids exert a dose-dependent biphasic effect on SST secretion, with low doses being stimulatory and high doses inhibitory. Insulin stimulates hypothalamic SST release but has an inhibitory effect on the release of islet and gut SST. Members of the growth factor-cytokine family appear to be an important group of compounds that have been shown to regulate SST synthesis and secretion from brain and immune cells. For instance, GH and IGF-I induce SST secretion and synthesis from the rat cerebral cortex and hypothalamus (12, 13). The inflammatory cytokines IL-1, TNF- α , and IL-6 stimulate SST secretion and mRNA levels from cultured rat brain cells (179). The IL-1 effect is seen with doses as low as 10^{-11} M and is dose-dependent up to a maximally effective dose of 10^{-9} M. TNF- α has a slightly lower potency but shows synergism with IL-1 β . Basic fibroblast growth factor, which shares sequence homology with IL-1, also stimulates SST function (179). IFN- γ and IL-10 activate SST expression in macrophages and splenocytes (44). In contrast to these stimulatory cytokines, leptin and TGF- β both inhibit SST secretion and mRNA levels in cultured rat hypothalamic cells (161, 162).

The transcriptional unit of the rat SST gene consists of exons of 238 and 367 bp separated by an intron of 621 bp (130, 150) (Fig. 1). The 5' upstream region contains a number of regulatory elements: a variant of the TATA box at -26 bp, a cAMP response element (CRE) at -48 to -41 bp, two nonconsensus glucocorticoid response elements (GREs) at -167 and -219 bp, and a consensus insulin response element CGGA activated by an ETS-related transcription factor in the 5' UT at +43 to +46 bp. In addition, tissue-specific promoter elements consisting of TAAT motifs that operate in concert with CRE to provide high-level constitutive activity are reiterated three times over a 500-nucleotide region (150). Many of the agents that influence SST secretion are also capable of altering SST gene expression (Table 1). Steady state SST mRNA levels are stimulated by various members of the growth factor-cytokine family (GH, IGF-I, IGF-II, IL-1, TNF- α , IL-6, IFN- γ , and IL-10), glucocorticoids, testoster-

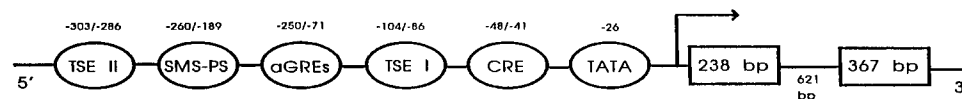


FIG. 1. Schematic depiction of the rat SST gene and its regulatory domains. The messenger RNA coding region consists of two exons of 238 and 367 bp separated by an intron of 621 bp. Located upstream (i.e., 5' end) from the start site of mRNA transcription (arrow) are the regulatory elements TATA (-26 bp), cAMP response element, CRE (-48/-41 bp), atypical glucocorticoid response element GRE (-250/-71 bp), and a somatostatin promoter silencer element, SMS-PS (-260/-189 bp). Tissue-specific elements (TSE) consisting of TAAT motifs that operate in concert with CRE to provide high-level constitutive activity are located within the TSE 1 (-104/-86 bp) and TSE II (-303/-286 bp) regions.

one, estradiol, and NMDA receptor agonists and inhibited by glucocorticoids, insulin, leptin, and TGF- β (44, 150, 179) (Table 1). Among the intracellular mediators known to modulate SST gene expression are Ca^{2+} , cAMP, cGMP, and nitric oxide (NO) (1, 131, 153, 205). cAMP is a potent activator of both gene transcription and secretion of SST and has emerged as the most prominent signaling pathway for regulating SST function. cAMP induces transcription of the SST gene via CRE, which binds a 43-kDa nuclear protein, CREB (cAMP

TABLE 1

Regulation of Gene Expression of Somatostatin and Its Receptors

Class of agent	Effect on mRNA						References
	SST	SSTR1	SSTR2	SSTR3	SSTR4	SSTR5	
Intracellular mediators							
cAMP	↑		↑			↑	61, 99, 129, 131, 147, 153
Ca^{2+}	↑						205
cGMP	↑						1
NO	↑						1
Thyroid/steroid hormones							
Glucocorticoids	↑↓	↑↓	↑↓				50, 88, 145, 222
Testosterone	↑						145, 150
Estrogens	↑		↑	↑		↓	39, 91, 145, 150, 214, 215
Thyroid hormone		↑				↑	84
Insulin	↓						150
Growth factors/cytokines							
GH	↑						145, 150
IGF-I	↑						150
IGF-II	↑						150
IL-1	↑						179
TNF- α	↑						179
IL-6	↑						179
IFN- γ	↑						44
IL-10	↑						44
TGF- β	↓						161
leptin	↓						162
NMDA receptor agonists	↑						145, 150

response element binding protein), whose transcriptional efficacy is regulated through phosphorylation by the cAMP-dependent protein kinase A (129). cAMP-inducible transcriptional activation in turn requires the recruitment of a 265-kDa CREB binding protein (CBP) that acts as an adapter molecule linking CREB to the polymerase II complex (98, 129). Ca^{2+} -dependent induction of the SST gene occurs through phosphorylation of CREB by Ca^{2+} -dependent protein kinase I and II. Induction of the SST gene by GH is transcriptionally induced through promoter interaction at the -71 to -44 bp region (150). IGF-I and IGF-II also stimulate SST gene transcription in promoter transfection studies although the nature of the promoter interaction remains unknown. Likewise, the molecular mechanisms underlying the potent stimulation of SST mRNA levels by cytokines remain to be clarified. The inhibitory effect of TGF- β on SST mRNA levels appears to be induced posttranscriptionally via accelerated mRNA degradation (161). Glucocorticoids exert a dual effect on the SST gene involving transcriptional activation through interaction between the glucocorticoid receptor and SST promoter elements between -250 and -71 bp, as well as through accelerated SST mRNA degradation (150). Finally, estrogens, testosterone, cGMP, and NO all augment steady state SST mRNA levels but the direct or indirect bases as well as the molecular mechanisms underlying the effects of these agents remain to be determined.

IDENTIFICATION OF SOMATOSTATIN RECEPTORS

Somatostatin acts through high-affinity plasma membrane receptors (termed SST receptors, SSTRs), which were first described in the pituitary GH_4C_1 cell line by whole-cell binding analysis (180). Subsequent studies using a variety of other techniques such as membrane binding analyses, *in vivo* and *in vitro* autoradiography, covalent crosslinking, and purification of a solubilized receptor showed SSTR expression in various densities in brain, gut, pituitary, endocrine and exocrine pancreas, adrenals, thyroid, kidneys, and immune cells (reviewed in 146, 148, 151, 156, 168, 170). Many other tumor cell lines have also been shown to be a rich source of membrane SSTRs, e.g., AtT-20 pituitary tumor cells, hamster insulinoma and Rin m5F islet tumor cells, AR42J and Mia PaCa pancreatic tumor cells, and human breast cancer, neuroblastoma, glioma, and leukemic and myeloma cell lines (reviewed in 146, 148, 156, 168). The existence of more than one SSTR subclass was first proposed based on differential receptor binding potencies and actions of SST-14 and SST-28 in brain, pituitary, and islet cells (122, 193). Subsequent studies confirmed and extended these observations toward the realization that not only were there distinct SST-14 and SST-28 selective receptors but that the SST-14 binding site itself was heterogeneous and could be further distinguished into two subclasses that are differentially sensitive to the octapeptide SST analog SMS201-995 or Octreotide (207). Identical findings were reported with the hexapeptide SST analog MK678 and led to the recognition of two pharmacological subgroups of SSTRs, SRIF I, which bound octapeptide and hexapeptide analogs, and SRIF

II, which was insensitive to these compounds (168). Attempts to characterize the molecular properties of SSTRs by chemical crosslinking of receptor-bound radioligands have yielded widely divergent size estimates ranging from 21 to 228 kDa (148, 151, 168). Much of this discrepancy may be explained by differential glycosylation of the receptor proteins and by the use of different ligands, different crosslinking conditions, and possibly receptor degradation. Photoaffinity labeling and purification studies, which are much more specific, have provided evidence for the existence of several molecular species of SSTR proteins of 32–85 kDa that are expressed in a tissue-specific manner and some that exhibit selective agonism for SST-14 or SST-28. In the rat, these include a 58-kDa form that is found in most tissues and additional 32- and 80-kDa receptor proteins unique to the brain and pituitary, respectively (192). Photoaffinity labeled bands of 72, 75, 82, and 85 kDa have been identified in HIT insulinoma, AR42J pancreatic, and AtT-20 and GH₄C₁ pituitary tumor cells, respectively (20).

MOLECULAR CLONING OF SOMATOSTATIN RECEPTORS

Exactly 20 years after the discovery of SST, the structure of the first of its receptors was elucidated by molecular cloning (226). Five distinct SSTR genes were rapidly identified and revealed a more extensive receptor family than previously suspected from pharmacological and biochemical criteria (146, 148, 156, 168) (Table 2). The first two SSTRs termed (SSTR1 and SSTR2) were cloned from human islet RNA. The rat SSTR2 gene was identified simultaneously by Kluxen *et al.* (93) by expression cloning. The success of these two laboratories was rapidly followed by the cloning of rat SSTR1, bovine and porcine SSTR2, mouse, rat, and human SSTR3, rat, mouse, and human SSTR4, and rat, mouse, and human SSTR5 (22, 34, 37, 112, 127, 139, 142, 148, 156, 168, 173, 227, 229). Genes for SSTR1, 3, 4, and 5 lack classical introns. The SSTR2 gene displays a cryptic intron at the 3' end of the coding segment, which gives rise to two spliced variants, a long (SSTR2A) form and a short (SSTR2B) form (147, 209). In the human gene, the spliced exon encodes for 25 amino acid residues compared to 38 residues in the unspliced form (147). The 2A and 2B variants differ only in the length of the cytoplasmic tail. There are thus six putative SSTR subtypes of closely related size, each displaying seven α helical transmembrane (TM) segments typical of G-protein-coupled receptors (GPCR). The five human SSTR genes segregate on separate chromosomes (Table 2). The encoded receptor proteins range in size from 356 to 391 amino acid residues, show the greatest sequence similarity in the putative TMs (55–70% sequence identity), and diverge the most at their amino- and carboxy-terminal segments (148, 156, 168). Overall, there is 39–57% sequence identity among the various members of the SSTR family. All SSTR isoforms that have been cloned so far from humans as well as other species possess a highly conserved sequence motif, YANSCANPI/VLY, in the seventh TM, which serves as a signature sequence for this receptor family. The five hSSTRs display one to four sites for

TABLE 2

Characteristics of the Cloned Subtypes of Human Somatostatin Receptors

	SSTR1	SSTR2A	SSTR3	SSTR4	SSTR5	References
Chromosomal localization	14q13	17q24	22q13.1	20p11.2	16p13.3	146, 148, 168
Molecular size (kDa)	53-72	71-95	65-85	45	52-66	66
Amino acids	391	369	418	388	363	34, 142, 148, 168, 173, 226, 227
mRNA (kb)	4.8	8.5 (?)	5.0	4.0	4.0	34, 142, 148, 168, 173, 226, 227
G protein coupling	+	+	+	+	+	149
Effector coupling						
Adenylyl cyclase activity	↓	↓	↓	↓	↓	77, 149
Tyrosine phosphatase activity	↑	↑	↑	↑	↑	26, 27, 52-54, 164, 187
MAP kinase activity	↑	↓	↓↑	↑	↓	14, 30, 33, 54, 165, 230
K ⁺ channels (GIRK)		↑	↑	↑	↑	100
Ca ²⁺ channels	↓	↓				55, 175, 211
Na ⁺ /H ⁺ exchanger	↑					76
AMPA/kainate glutamate channels	↑	↓				109
Phospholipase C/IP ₃ activity		↑			↓↑	4, 14, 31
Phospholipase A2 activity				↑		182
Tissue distribution ^a	Brain, pituitary, islet, stomach, liver, kidneys	Brain, pituitary, islet, stomach, kidneys	Brain, pituitary, islet, stomach	Brain, stomach, islet, lungs, placenta	Brain, pituitary, islet, stomach	108, 146

^a Not all tissues have been tested simultaneously; IP₃, inositol, triphosphate, MAP kinase, mitogen-activated protein kinase.

N-linked glycosylation within the amino-terminal segment and second extracellular loop (ECL). All of the hSSTRs feature three to eight putative recognition motifs for protein phosphorylation by protein kinase A, protein kinase C, and calmodulin kinase II in the cytoplasmic C-terminal segment and within the second and third intracellular loops. hSSTR1, 2, 4, and 5 display a conserved cysteine residue 12 amino acids downstream from the seventh TM, which may be the site of a potential palmitoyl membrane anchor as observed in several other members of the GPCR superfamily. Covalent attachment of palmytic acid in this position likely creates a fourth cytoplasmic loop. Interestingly, hSSTR3, which uniquely lacks the cysteine palmitoylation membrane anchor, features a

much longer C-tail than the other four members of the family. The five SSTR subtypes display a remarkable degree of structural conservation across species (148, 168). For instance, there is 94–99% sequence identity among the human, rat, and mouse isoforms of SSTR1, 93–96% sequence identity among human, rat, mouse, porcine, and bovine isoforms of SSTR2, and 88% sequence identity between the rat and the human isoforms of SSTR4. SSTR3 and SSTR5 are somewhat less conserved, showing 82–83% sequence identity between the human and the rodent homologues. The nearest relatives of the SSTRs are the opioid receptors whose Δ subtype displays 37% sequence similarity to the mouse SSTR1 (47). It remains to be seen whether there are additional members of the SSTR family still waiting to be cloned. There is some evidence for a variant form of SSTR5 (152). Cortistatin, which is capable of interacting with the five known SSTR subtypes, nonetheless possesses unique neuronal depressant and sleep modulating properties that are not present in SST, suggesting a separate CST receptor that may be related to the SSTR family (36, 146). Several novel genes with sequence similarity to the SSTR family have been recently described. Two of these (SLC-1/GPR-24, and GPR-25) display 34–40% sequence homology with the TMs of SSTRs but do not contain the YANSCANPI/VLY motif (86, 95). These receptors do not bind SST or any other known ligand and therefore currently remain as orphan receptors that probably belong to a related family.

ANTIRECEPTOR ANTIBODIES

Antibody probes have now been developed against all five rat and human SSTR subtypes (42, 66, 82, 103, 106, 152). They consist of rabbit polyclonal antibodies directed against peptide sequences in the extracellular and intracellular receptor domains. The specificity of the antibodies has been validated by immunocytochemistry of tissue sections and cell lines expressing recombinant SSTR5, as well as by immunoblot analysis. Using these antibodies, Western blot analysis of the five hSSTR subtypes individually expressed in mammalian cell lines has revealed estimates of 53–72 kDa for hSSTR1, 71–95 kDa for hSSTR2, 65–85 kDa for hSSTR3, 45 kDa for hSSTR4, and 52–66 kDa for hSSTR5 (66) (Table 2). Enzymatic deglycosylation reduces the size of hSSTR1, 2, 3, and 5 to that of the core protein, confirming N-linked glycosylation of these four subtypes. hSSTR4, on the other hand, does not appear to be glycosylated at its single putative glycosylation site (66). The size of the native rat SSTR subtypes has been determined by immunoblot analysis of rat brain membranes (106). The molecular mass of brain rSSTR1 (53 kDa) is within the range reported for hSSTR1 (66). Likewise, the size of rSSTR3 and rSSTR4 is similar or virtually identical to that described for the human isoforms of these two subtypes. The molecular mass of brain rSSTR5 (58 kDa) is comparable to that of the recombinant human receptor although both are somewhat smaller than the receptor size described for endogenous pituitary rSSTR5 (128). The size of rSSTR2 remains controversial ranging from 57 to 72 kDa for rat brain and

mouse AtT-20 cells (106, 152) to 90 kDa by a different antibody in rat brain and pancreas (42, 82). These discrepancies may be due to variations in antibody specificity and differential glycosylation of the receptor protein in the different transfected cell lines and tissues studied.

SOMATOSTATIN AGONISTS AND ANTAGONISTS

The five hSSTR subtypes bind SST-14 and SST-28 with nanomolar affinity (Table 3). hSSTR1-4 bind SST-14 \geq SST-28, whereas hSSTR5 exhibits 10- to 15-fold selectivity for SST-28 compared to SST-14 (146, 148, 155). The putative cleavage products of CST processing, hCST-17 and rCST-14, display nanomolar affinity for the five hSSTRs (56, 146). Synthetic rCST-29 binds to hSSTR1, 3, and 4 with comparable affinity to SST-14. Its affinity for SSTR2 and SSTR5 is 5- to 100-fold lower than that of SST-14 and SST-28 (146). The specificity of endogenous SST derives from the fact that it is produced mainly at local sites of action and is rapidly inactivated following release by peptidases in tissue and blood, thereby minimizing unwanted systemic effects. Injections of synthetic SST, however, produce a wide array of effects due to simultaneous activation of

TABLE 3

Binding Selectivity of Endogenous SST-like Peptides, Short Peptide Analogs, and Nonpeptide Agonists for the Cloned Human Somatostatin Receptors

	IC ₅₀ (nM) ^a					References
	SSTR1	SSTR2	SSTR3	SSTR4	SSTR5	
Endogenous SST-like peptides						
SST-14	0.1–2.26	0.2–1.3	0.3–1.6	0.3–1.8	0.2–0.9	25, 155, 168, 189
SST-28	0.1–2.2	0.2–4.1	0.3–6.1	0.3–7.9	0.05–0.4	25, 155, 168, 189
hCST-17	7	0.6	0.6	0.5	0.4	56
rCST-29	2.8	7.1	0.2	3	13.7	146
Short synthetic peptides						
Octreotide	290–1140	0.4–2.1	4.4–34.5	>1000	5.6–32	25, 155, 168, 189
Lanreotide	500–2330	0.5–1.8	43–107	66–2100	0.6–14	25, 155, 168, 189
Vapreotide	>1000	5.4	31	45	0.7	155
Seglitide	>1000	0.1–1.5	27–36	127–>1000	2–23	25, 155, 168, 189
BIM23268	18.4	15.1	61.6	16.3	0.37	189
NC8-12	>1000	0.024	0.09	>1000	>1000	155
BIM23197	>1000	0.19	26.8	>1000	9.8	189
CH275	3.2–4.3	>1000	>1000	4.3–874	>1000	113, 146
Nonpeptide agonists						
L-797,591	1.4	1,875	2240	170	3600	174
L-779,976	2760	0.05	729	310	4260	174
L-796,778	1255	>10,000	24	8650	1200	174
L-803,087	199	4720	1280	0.7	3880	174
L-817,818	3.3	52	64	82	0.4	174

^a Data of Patel and Srikant (155) and Rohrer *et al.* (174) expressed as K_i.

	$\begin{array}{c} \text{Ser-Ala-Asn-Ser-Asn-Pro-Ala-Met-Ala-Pro-Arg} \\ \text{Glu-Arg-Lys-Ala-Gly-Cys-Lys-Asn-Phe-} \text{Phe-} \text{Trp} \\ \text{Cys-Ser-Thr-Phe-Thr} \text{ } \text{Lys} \end{array}$
SST-28	
	$\begin{array}{c} \text{Ala-Gly-Cys-Lys-Asn-Phe-} \text{Phe-} \text{Trp} \\ \text{Cys-Ser-Thr-Phe-Thr} \text{ } \text{Lys} \end{array}$
SST-14	
	$\begin{array}{c} \text{Asp-Arg-Met-Pro-Cys-Arg-Asn-Phe-} \text{Phe-} \text{Trp} \\ \text{Lys-Cys-Ser-Ser-Phe-Thr} \text{ } \text{Lys} \end{array}$
CST-17	
	$\begin{array}{c} \text{DPhe-Cys-Phe-} \text{DTrp} \\ \text{Thr(ol)-Cys-Thr} \text{ } \text{Lys} \end{array}$
SMS 201-995 <i>octreotide</i>	
	$\begin{array}{c} \text{D}\beta\text{Nal-Cys-Tyr-} \text{DTrp} \\ \text{Thr-Cys-Val} \text{ } \text{Lys} \end{array}$
BIM23014 <i>lanreotide</i>	
	$\begin{array}{c} \text{DPhe-Cys-Tyr-} \text{DTrp} \\ \text{Trp-Cys-Val} \text{ } \text{Lys} \end{array}$
RC-160 <i>vapreotide</i>	
	$\begin{array}{c} \text{(N-Me)-Ala-Tyr-} \text{DTrp} \\ \text{Phe-Val} \text{ } \text{Lys} \end{array}$
MK678 <i>seglitide</i>	
CH275	$\begin{array}{c} \text{Cys-Lys-Phe-Phe-} \text{DTrp} \\ \text{Cys-Ser-Thr-Phe-Thr} \text{ } \text{Lys} \end{array}$

FIG. 2. Natural and synthetic peptide agonists of the SST receptor family.

conserved residues (10, 201, 210). In this way, a library of short synthetic compounds has been synthesized, several of which show greater metabolic stability and subtype selectivity than SST-14 (Table 3). Using this approach, the first clinically useful compound to emerge was the octapeptide analog SMS201-995 (SMS, Octreotide), which was introduced into clinical practice in 1983 for treatment of hormone-producing pituitary, pancreatic, and intestinal tumors and has remained the mainstay of SST analog therapy (10, 107, 108). SMS, along with BIM23014 (Lanreotide, now also available for clinical use), the octapeptide RC160 (Vapreotide), and the hexapeptide MK678 (Seglitide), binds to only three of the five hSSTR subtypes, displaying high affinity for subtypes 2 and 5 and moderate affinity for subtype 3 (25, 146, 148, 155, 168, 189). It should be noted that the binding affinity of SMS, BIM23014, RC160, and MK678 for subtypes 2 and 5 is comparable to that of SST-14, indicating that they are neither selective for these subtypes nor more potent than the endogenous ligands (155). The striking low-affinity interaction of hSSTR1 and 4 with the conformationally restricted analogs, coupled with their high degree of amino acid identity, has led to the subdivision of these two receptors into a distinct SSTR subclass (78). SSTR2, 3, and 5 react with these analogs and fall into another subgroup. These two subclasses correspond to the previously described SRIF II and SRIF I binding sites, respectively. Other than SST-14 and SST-28 and some of their immediate structural derivatives, there are no current SST compounds capable of binding to all five subtypes (155). The analog Des-AA^{1,2,5} [D-Trp⁸ IAMP⁹] SST (CH275) has been recently described as a SSTR1-selective compound (113). We find that CH275 also binds to SSTR4 and appears to be a prototypic agonist for the SSTR1 and 4 subclass (146). Several other SST analogs have been similarly reported to be selective for one SSTR subtype, e.g., BIM23056 (SSTR3), and BIM23052, and L362-855 (SSTR5) (168). Due to methodological variations in the binding analyses, however, such claims of subtype selectivity of these and other analogs have not been confirmed by others and remain controversial (25, 155). To resolve this discrepancy several groups have analyzed these and other SST analogs under uniform binding conditions using only the human SSTR clones (25, 155, 189). These studies have identified BIM23268 with modest selectivity for hSSTR5. L362855 binds well to SSTR5 and SSTR2, being only weakly selective for SSTR5. NC812 displays modest 20- to 50-fold selectivity for SSTR2 and 3; DC2360, EC5-21, and BIM23197 exhibit 19- to 50-fold selectivity for hSSTR2 although these compounds also bind well to hSSTR5. Overall, then these results suggest that the binding selectivity of the present generation of peptide SST analogs for the human SSTR subtypes is relative rather than absolute, except for BIM23268, which displays some monospecificity for hSSTR5. Very recently, the Merck Research Group has identified a series of nonpeptide agonists for each of the five hSSTRs in combinatorial libraries constructed on the basis of molecular modeling of known peptide agonists (174, 228) (Table 3). Three of the compounds identified from this screen, L-797591, L-779976, and L-803087, display low nanomolar affinity for hSSTR1 (1.4 nM), hSSTR2 (0.05 nM), and hSSTR4 (0.7 nM), representing 120–6200-, and 285-fold selectivity, respectively, for

these subtypes (174). L-796778 binds to hSSTR3 with K_i 24 nM representing 50-fold selectivity and L-817818 displays selectivity for two of the subtypes hSSTR5 and hSSTR1 (K_i 0.4 and 3.3 nM, respectively) but also shows some binding to the other three subtypes. The availability of these high-affinity subtype-selective agonists for several of the SSTRs represents a major breakthrough in the field, which should now facilitate the direct probing of subtype-selective physiological functions as well as the development of orally active subtype-selective therapeutic compounds. Recently, the first potential SST peptide antagonists were also described (9). One such compound [AC-4-NO₂-Phe-c(d-Cys-Tyr-D-Trp-Lys-Thr-Cys)-D-Tyr-NH₂] binds to hSSTR2 and hSSTR5 with nanomolar affinity but antagonizes the normal receptor effector coupling to adenylyl cyclase (9). A second peptide, BIM23056, also blocks hSSTR5 signaling and appears to be an antagonist for this subtype (220).

LIGAND BINDING DOMAIN

It has not been possible as yet to crystallize any of the GPCRs and accordingly attempts to elucidate the ligand binding domain of these molecules have relied on indirect methods such as site-directed mutagenesis and receptor chimeras. These approaches in the case of other GPCR systems have suggested that the ligand binding domain is made of a number of noncontiguous amino acid residues that form a binding pocket within the folded 3-dimensional structure of the receptor (7, 195). An alternative view proposes that there is no performed binding cavity but that agonists interact with crucial residues in the extracellular and/or TM domains to stabilize spontaneous receptor conformations (181). In the case of very large protein ligands such as glycoprotein hormones, the interacting residues appear to be exclusively located in the amino-terminal segment. Biogenic amines interact with residues exclusively within the TMs. In contrast, the ligand binding site of peptide agonists comparable to SST typically involves residues in the ECLs or both the ECLs and the TMs (58, 71, 181). By taking advantage of the binding selectivity of ligands such as SMS for hSSTR2 but not hSSTR1, Kaupmann *et al.* (89) systematically mutated hSSTR1 to resemble hSSTR2. They identified two crucial residues, Gln²⁹¹ and Ser³⁰⁵, in TMs VI and VII, respectively, of hSSTR1, substitution of which for the corresponding residues Asn²⁷⁶ and Phe²⁹⁴ in hSSTR2 increased the affinity of hSSTR1 for SMS and other octapeptide analogs 1000-fold. By molecular modeling using these identified residues as well as the known structure of SMS, Kaupmann *et al.* have postulated a binding cavity for SMS involving hydrophobic and charged residues located exclusively within TMs III-VII. Their model predicts that the core residues Phe⁷, Trp⁸, Lys⁹, and Thr¹⁰ of SMS interact with Asn²⁷⁶ and Phe²⁹⁴ located at the outer end of TMs VI and VII, respectively (present in hSSTR2 but not in hSSTR1), which provide a hydrophobic environment for lipophilic interaction with Phe⁷, Trp⁸, and Thr¹⁰, whereas Asp¹³⁷ in TM III anchors the ligand by an electrostatic interaction with Lys⁹. SMS binds poorly to hSSTR1 because of the

presence of residues Gln²⁹¹ and Ser³⁰⁵ located close to the extracellular rims of TM helices VI and VII, which prevent the short peptide from reaching deep within the pocket, whereas the corresponding residues Asn²⁷⁶ and Phe²⁹⁴ in hSSTR2 provide for a stable interaction with the disulfide bridge of SMS. Because of their greater length and flexibility, the natural ligands, SST-14 and SST-28, can presumably adopt a conformation that allows their entry into the binding pocket of all five SSTRs. Such a model is consistent with mutational studies of the Asp residue in TM III, which abolishes ligand binding, although it is not known whether this is due to a direct interaction of the residue with SST ligands or to an allosteric alteration in receptor structure (135). Using chimeric mouse SSTR1/SSTR2 receptors, Fitz-Patrick and Vandlen have confirmed the importance of residues in the upper segments of TMs VI and VII for binding the hexapeptide MK678 (50). It should be noted that the residues identified by mutagenesis so far to be important in recognizing SMS and MK678 have not been shown directly to be critical for binding the natural ligands SST-14 and SST-28. Furthermore, the assumption that the hSSTR2 ligand binding pocket may be common for the other SSTR subtypes may not be valid since closely related GPCRs feature different sets of epitopes for binding of a common ligand. The involvement of the extracellular domains for binding SST ligands has been investigated by Greenwood *et al.* (60), whose results predict a potential contribution of ECL2 (but not of ECL1 or ECL3 or the amino-terminal segment) to binding of the natural SST ligands (SST-14, SST-28) as well as SMS. The overall model that emerges from these studies suggests a binding domain for SST ligands made up of residues within TMs III to VII, with a potential contribution by ECL2, and is consistent with other peptide binding GPCRs such as neurokinin I, angiotensin II, and GnRH receptors, which also interact with residues in both ECLs and TMs (51, 58, 71, 181).

EXPRESSION OF SSTR SUBTYPES

The cellular expression of SSTR subtypes has been characterized in rodent and human tissues as well as in various tumors and tumor cell lines by mRNA analysis using Northern blots, reverse transcriptase-PCR, ribonuclease protection assay, and *in situ* hybridization (18, 23, 97, 148, 168, 203, 204). The advent of subtype-selective SSTR antibodies has additionally opened the door to the direct localization of SSTR subtype proteins by immunohistochemistry. These studies have revealed an intricate pattern of SSTR subtype expression throughout the central nervous system and in the periphery with an overlapping but characteristic pattern that is subtype-selective, tissue-specific, and species-specific (reviewed in 146, 148, 168). In the rat, mRNA for SSTR1-5 has been localized in cerebral cortex, striatum, hippocampus, amygdala, olfactory bulb, and preoptic area (23). A comparison of the relative mRNA abundance suggests a high level of expression of SSTR1 mRNA throughout the neuraxis, whereas SSTR2 displays a high level of expression in cerebral cortex compared to subcortical brain structures (18, 97). SSTR5 mRNA is moderately well ex-

pressed throughout the rat brain (203). SSSTR3 mRNA is preferentially localized in the cerebellum (97, 127); SSSTR4 is the least well expressed subtype in brain compared to the other four isoforms (203). In contrast to the rat, there is negligible expression of SSSTR5 mRNA in the human brain (142, 204). By immunohistochemistry, three of the SSSTRs (types 1–3) have been mapped in the rat brain. A high density of SSSTR1-positive neurons has been identified in layers 2, 3, 5, and 6 of the cerebral cortex, in the CA2 area and dentate gyrus of the hippocampus, the hypothalamus, the midbrain, and the granular layer of the cerebellar cortex (68). The distribution of SSSTR2 in rat brain by immunohistochemistry shows a rich expression of receptors in the olfactory tubercle, the pyriform cortex, layers 2, 3, 5, and 6 of the cerebral cortex, the basal ganglia, the CA1-2 area but not the dentate gyrus of the hippocampal formation, the amygdala, pons, and medulla (42). SSSTR3 localizes predominantly to layers V and VI of the cerebral cortex and in the granular layer of the cerebellum (105). Furthermore, double-labeling studies have suggested that a subset of SSSTR2 receptors consist of autoreceptors on SST immunopositive neurons (41). All five SSSTRs have been studied by immunohistochemistry in the rat hypothalamus (67, 106). SSSTR1 is strongly localized in neuronal perikarya in all major hypothalamic nuclei as well as in nerve fibers in the zona externa of the median eminence and in the ependyma of the third ventricle (67, 68, 104). SSSTR2 is also expressed in these regions but with a relatively lower abundance. In contrast, SSSTR3 and 4 are localized primarily to the arcuate-ventromedial nucleus and the median eminence (104). SSSTR5 is the least expressed subtype, occurring only in the arcuate nucleus and the median eminence. The rostral hypothalamus thus preferentially expresses SSSTR1 and 2. Overall, SSSTR1 is the predominant hypothalamic subtype followed by SSSTR2, 3, 4, and 5 (104). SSSTR1 colocalizes with SST in the para- and periventricular nuclei, suggesting that as in the case of SSSTR2 in the cortex, this receptor may also act as an autoreceptor (67). Double-labeling studies have also colocalized SSSTR1 and SSSTR2 mRNA in GHRH-producing arcuate neurons (200). Analysis of SSSTR1 and SSSTR2 mRNA at the single-cell level by RT-PCR has shown simultaneous expression of both subtypes in 18% of cultured fetal hypothalamic neurons (109). Adult rat pituitary features all five SSSTR genes, whereas the adult human pituitary expresses four of the subtypes, 1, 2, 3, and 5 (23, 35, 138, 143). hSSSTR4 is transiently expressed during development but is absent in the adult (143). Colocalization of SSSTR mRNA in pituitary cell subsets in the rat has revealed expression of one or more subtypes in all of the major pituitary cell types including corticotrophes and gonadotrophes previously thought to be SSSTR negative (35, 138). SSSTR5 is the principal subtype expressed throughout the pituitary followed by SSSTR2 (35, 91). Immunohistochemical colocalization has confirmed SSSTR5 and SSSTR2 as the principal pituitary isoforms in the rat (103, 128). SSSTR5 is the predominant subtype in rat somatotrophes, being expressed in 86% of cells followed by SSSTR2 in 42% of GH-positive cells. SSSTR4 and 3 are modestly expressed, whereas SSSTR1 occurs in only 5% of somatotrophes (103). The preponderance of SSSTR, the only SST-28 preferring subtype, correlates with the reported higher potency of SST-28 than SST-14 for inhibiting GH

secretion in the rat (193). A proportion of somatotrophes colocalizes both SSTR5 and SSTR2, providing proof for the expression of more than one SSTR subtype in individual target cells (128). Although there are no direct data on the pattern of expression of SSTRs in human pituitary cells, SSTR5 and SSTR2 appear to be the principal subtypes mediating GH suppression based on pharmacological evidence correlating the preferential agonist binding properties of some SST analogs for SSTR2 and SSTR5 with their ability to regulate GH secretion from human fetal pituitary cultures (189).

Previous studies using autoradiography have described SST-14-selective binding sites on rat islet α cells and SST-28 preferring sites on β cells, which may account for the selective suppression of glucagon by SST-14 and of insulin by SST-28 in these species (5). Rat islets express all five SSTR mRNA species (148). In the case of human islets, immunohistochemical colocalization of SSTR1-5 with insulin, glucagon, and SST has revealed predominant expression of SSTR1, 2, and 5 (106). Like pituitary cells, human islet β , α , and δ cells express multiple SSTR isoforms, with β cells being rich in SSTR1 and SSTR5, α cells in SSTR2, and δ cells in SSTR5. Although there is no absolute specificity of any SSTR for an islet cell type, SSTR1 is preferentially expressed in β cells, SSTR2 in α cells, and SSTR5 in β and δ cells (106). Such selectivity could form the basis for preferential insulin suppression by SSTR1-specific ligands and of glucagon inhibition by SSTR2-selective compounds. mRNA for all five SSTRs has also been identified in the rat stomach, duodenum, jejunum, ileum, and colon by *in situ* hybridization (101). In all of these tissues SSTR1-5 occur in the epithelial and external muscle layers as well as in the submucosal plexus, whereas the enteric plexuses feature only SSTR1-3. All five SSTR mRNAs have also been identified in the human stomach (111). The adrenals, a known target of SST action, display a rich concentration of SSTR2 and modest levels of SSTR1 and 3 (23, 148). A number of peripheral organs exhibit a surprising level of expression of some SSTR subtypes, e.g., SSTR3 in the liver and spleen, SSTR4 in the lung, heart, and placenta, and SSTR1, 2, and 3 in spermatocytes and Sertoli cells in the testis (23, 29, 148, 173, 233). All five SSTRs are expressed in rat aorta, mainly in smooth muscle cells, both as mRNA and as protein (90). SSTR1, SSTR2A, and SSTR3 mRNAs are expressed in the normal human thymus (48). Finally, activated immune cells (macrophage, T cells, B cells) as well as mouse thymocytes preferentially express the SSTR2 subtype (44, 45).

In addition to normal tissues, many tumor cell lines of pituitary (AtT-20, GH₄C₁), islet (Rin m5f, HIT), pancreatic (AR42J), breast (MCF7), neural (LA-N-2 neuroblastoma), and hematopoietic (Jurkat, U266, ISK-B, MT-2T) origin are rich in SSTRs that are typically expressed as multiple SSTR mRNA subtypes (146, 148, 152, 168). Likewise, the majority of human tumors, either benign or malignant, are generally positive for SSTRs, featuring more than one isotype (reviewed in 146). These include functioning and nonfunctioning pituitary tumors, carcinoid tumors, insulinomas, glucagonomas, pheochromocytoma, breast carcinoma, renal carcinoma, prostate carcinoma, meningioma, and glioma. The general pattern of SSTR expression in these tumors suggests a

very high frequency of SSTR2 mRNA in all tumors. mRNA for SSTR1 is the next most common followed by SSTR3 and 4. SSTR5 expression appears to be tumor-specific, being positive in some tumors, e.g., breast, but absent in others, e.g., islet cell tumors (146). It should be noted that virtually all analyses of SSTR subtypes in tumors carried out so far have been based on mRNA expression, which may not necessarily reflect functional receptor levels. Future studies will need to correlate mRNA expression with receptor protein expression by immunocytochemistry or binding analyses with subtype selective analogs.

G PROTEIN COUPLING AND SIGNAL TRANSDUCTION

Somatostatin receptors elicit their cellular responses through G-protein-linked modulation of multiple second-messenger systems including adenylyl cyclase, Ca^{2+} and K^{+} ion channels, $\text{Na}^{+}/\text{H}^{+}$ antiporter, guanylate cyclase, phospholipase C, phospholipase A2, MAP kinase (MAPK), and serine, threonine, and phosphotyrosyl protein phosphatase (PTP) (146, 148, 168) (Table 2). SSTRs are potent inhibitors of adenylyl cyclase and cAMP formation. Based on the ability of antiserum to G_i or antisense G_i plasmids to block SSTR inhibition of adenylyl cyclase in AtT-20 and GH_4C_1 cells, all three $\text{G}\alpha_i$ subunits, $\text{G}\alpha_{i1}$, $\text{G}\alpha_{i2}$, and $\text{G}\alpha_{i3}$, have been implicated (63, 115, 183, 199). Native SSTRs are coupled to several subsets of K^{+} channels including delayed rectifier, inward rectifier, ATP-sensitive K^{+} channels, and large-conductance Ca^{2+} -activated BK channels (38, 190, 215, 219). $\text{G}\alpha_{i3}$ and $\beta\gamma$ dimers that associate with $\text{G}\alpha_{i3}$ appear to be responsible for transducing SSTR activation of the inward rectifying K^{+} current (197). G protein mediation of the other K^{+} channel subsets remains to be determined. Receptor activation of K^{+} channels induces hyperpolarization of the membrane, rendering it refractory to spontaneous action potential activity, leading to a secondary reduction in intracellular Ca^{2+} due to inhibition of the normal depolarization-induced Ca^{2+} influx via voltage-sensitive Ca^{2+} channels (94, 151, 190). In addition to this indirect effect on Ca^{2+} entry, SSTRs act directly on high-voltage-dependent Ca^{2+} channels via $\text{G}\alpha_{o2}$ protein to block Ca^{2+} currents (83, 92). Stimulation of both K^{+} and Ca^{2+} channels can additionally occur through dephosphorylation of the channel proteins secondary to SSTR activation of a serine-threonine phosphatase (219). Furthermore, SSTRs may inhibit Ca^{2+} currents through induction of cGMP, which activates cGMP protein kinase with further phosphorylation-dependent inhibition of Ca^{2+} channels (126). SSTRs activate a number of phosphatases such as serine-threonine phosphatase, the Ca^{2+} -dependent phosphatase calcineurin, and PTP (26, 27, 52, 53, 54, 164, 165, 169, 187, 194, 219). These actions are dependent on stimulation of pertussis toxin-sensitive G proteins. SSTRs in colon carcinoma cells are coupled to a $\text{Na}^{+}/\text{H}^{+}$ exchanger via a pertussis toxin-insensitive mechanism (8). Other less prominent signaling pathways for endogenous SSTRs that have been described include phospholipase A2-dependent stimulation of arachidonate production in hippocampal neurons and phospholipase

C-mediated stimulation of IP_3 formation in astrocytes and intestinal smooth muscle cells (123, 133, 182).

A key issue concerning the signaling specificity of a family of receptor isotypes such as the SSTRs is whether a given subtype activates only one or several G-protein-linked effector pathways. Several laboratories have begun to address this question using SSTR subtypes individually expressed in various host cells. A putative BBXB (where B is the basic residue) consensus sequence for G protein coupling exists in the third cytoplasmic loop of SSTR2, 3, 4, and 5 but not SSTR1. Nonetheless, SSTR1 is coupled to adenylyl cyclase via $G_{\alpha_{i3}}$ (102). SSTR2A purified from GH_4C_1 cells or expressed in CHO cells is capable of associating with $G_{\alpha_{i1}}$, $G_{\alpha_{i2}}$, $G_{\alpha_{i3}}$, and $G_{\alpha_{o2}}$ (63, 120). SSTR3 interacts with $G_{\alpha_{i1}}$, $G_{\alpha_{i2}}$, $G_{\alpha_{i4}}$, and $G_{\alpha_{i6}}$ (96). The specific G proteins that associate with the other SSTR subtypes have not been determined. Although initial studies of the coupling of SSTRs to adenylyl cyclase were contradictory, there is now general agreement that all five SSTR subtypes and especially the human isoforms are functionally coupled to inhibition of the adenylyl cyclase-cAMP pathway via pertussis toxin-sensitive G proteins (77, 146, 149) (Table 2). The five human SSTRs also stimulate PTP, once again through pertussis toxin-sensitive pathways (26, 27, 52–54, 141, 164, 165, 187, 231). However, the nature of the G proteins involved and whether they couple the receptor directly or indirectly to PTP remain unclear. Furthermore, there may be species-specific differences in the case of SSTR5 since the rat homologue has been found not to regulate PTP (33, 187). Three of the SSTR subtypes inhibit the MAPK signaling cascade: SSTR2 in SY-5Y neuroblastoma cells, SSTR3 in NIH3T3 cells and mouse insulinoma cells, and SSTR5 in transfected CHO-K1 cells (30, 33, 230). In contrast, SSTR1 and SSTR4 have been reported to stimulate MAPK in transfected CHO-K1 cells (14, 54). SSTR2–5, but not SSTR1, activate G-protein-gated inward rectifying K^+ channels in *Xenopus* oocytes, with coupling by SSTR2 being the most efficient (100). In rat insulinoma cells, endogenously expressed SSTR1 and SSTR2 inhibit voltage-operated Ca^{2+} channels, with the effect of SSTR1 being more pronounced than that of SSTR2 (55, 175). SSTRs with the pharmacological profile of the type 2 isoform have also been shown to inhibit voltage-dependent Ca^{2+} channels in rat amygdaloid neurons (211). SSTR1 stimulates a Na^+/H^+ exchanger via a pertussis-toxin-insensitive mechanism (76). SSTR2 does not activate the antiporter, and coupling of SSTR3, 4, and 5 to this pathway remains to be investigated. SSTRs also modulate the activity of glutamate receptor ion channels in a subtype-selective manner; in cultured mouse hypothalamic neurons, SSTR2 decreases and SSTR1 increases AMPA/kainate receptor-mediated glutamate currents (109). SSTR4 activates PLA-2-dependent arachidonate production via a pertussis toxin-sensitive G protein in transfected CHO-K1 cells (14). Although initial studies had ruled out an effect of SSTRs on PLC- IP_3 signaling, more recent evidence suggests SSTR modulation of this pathway in both normal and transfected cells (4, 123, 133, 220). Coupling, however, is generally weak, occurring at high agonist concentrations (220). The endogenous SSTR in intestinal smooth muscle cells, which signals through activation of PLC β_3 and Ca^{2+} mobilization, and SSTR2A and

SSTR5 stimulate PLC-dependent IP_3 production in transfected COS-7 and F4C1 pituitary cells (4, 31, 133). SSTR5 has also been reported to inhibit IP_3 -mediated Ca^{2+} mobilization in transfected CHO-K1 cells, whereas SSTR4 is without effect (14). These results clearly suggest that individual SSTR subtypes can activate more than one G protein and G-protein-linked signaling cascades. Since all five SSTRs bind the natural ligands SST-14 and SST-28 with nanomolar affinity and share common signaling pathways such as adenylyl cyclase, and since single cells express more than one SSTR subtype, the question arises whether multiple SSTRs in the same cell are redundant or whether they interact functionally for greater signaling diversity. There is some evidence to suggest that members of the SSTR family undergo homodimerization and heterodimerization and that dimeric association alters the functional properties of the receptor such as ligand binding affinity, signaling, and agonist-induced regulation (172). Such direct protein interaction between different members of the SSTR subfamily and possibly between the SSTR and related receptor families defines a new level of molecular crosstalk between G-protein-coupled receptors. Major voids still remain in our understanding of SSTR subtype selectivity for K^+ and Ca^{2+} channel coupling and of the molecular signals in the receptors responsible for activation of the various phosphatases and the MAPK pathway. Much of our current knowledge on subtype selectivity for signaling is based on transfected cells and should be interpreted with caution given the limitations of these systems. The arrival of highly selective agonists for each of the subtypes as well as the future development of subtype-selective antagonists should greatly facilitate the study of subtype-selective effector coupling of endogenous SSTRs in normal cells.

SSTR-MEDIATED INHIBITION OF SECRETION AND CELL PROLIFERATION

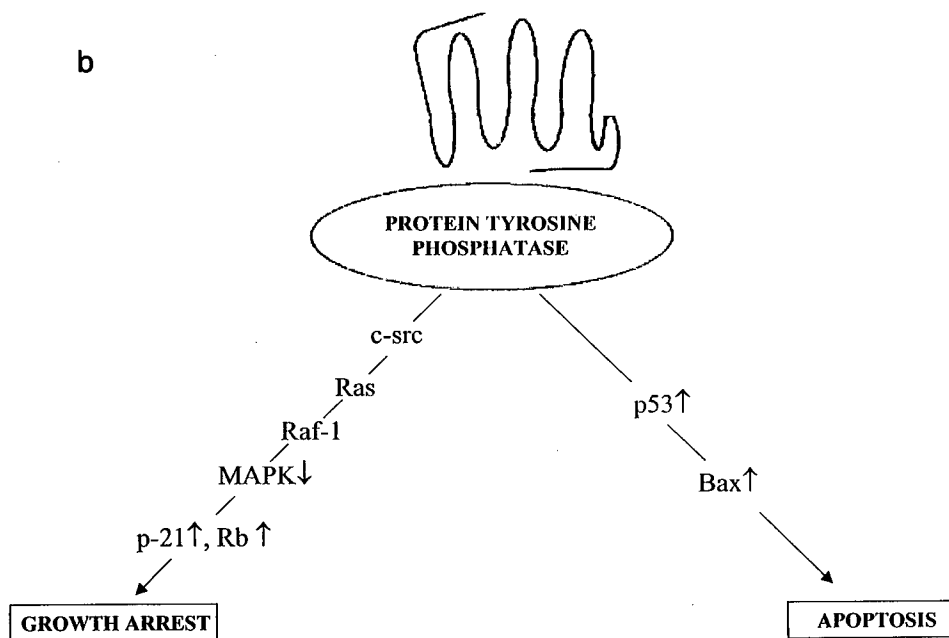
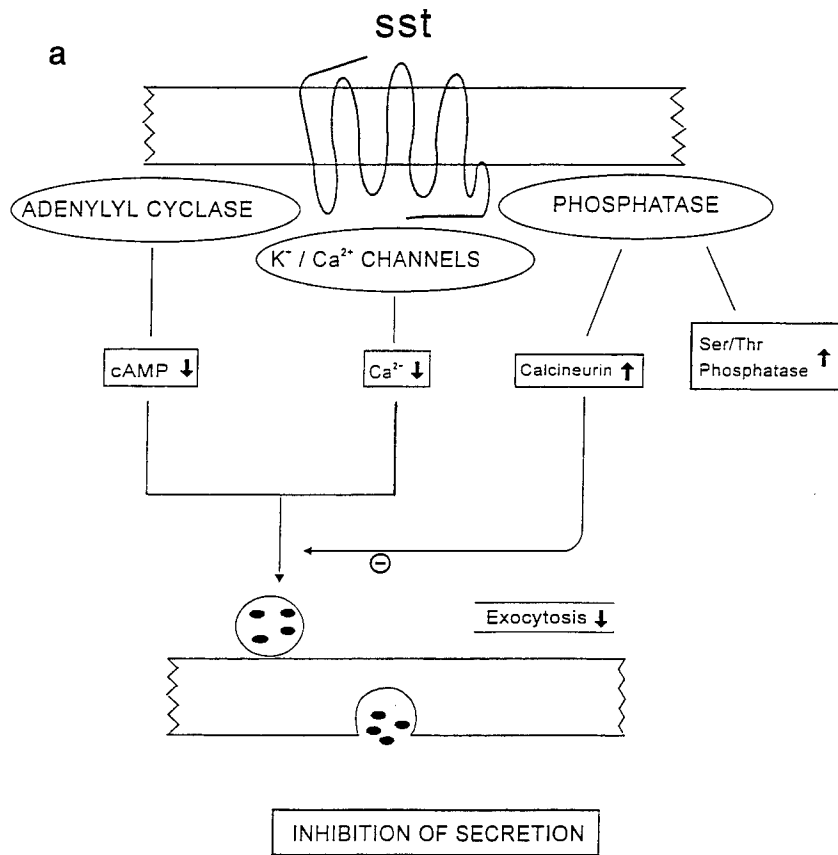
The pronounced ability of SST to block regulated secretion from many different cells is due in part to SSTR-induced inhibition of two key intracellular mediators, cAMP and Ca^{2+} . In addition to this so-called proximal effect, SST can inhibit secretion stimulated by cAMP, Ca^{2+} ionophores (A23187, ionomycin), the Ca^{2+} channel agonist BAYK8644 or by IP_3 , diacylglycerol, and extracellular Ca^{2+} in permeabilized cells (119, 145, 148, 151, 156, 169, 221). These observations clearly indicate that SST, independent of any effects on cAMP, Ca^{2+} , or indeed any other known second messenger, is able to inhibit secretion via this distal action. This effect appears to be mediated via a G-protein-dependent inhibition of exocytosis and is induced through SST-dependent activation of the protein phosphatase calcineurin (169). A similar distal effect on the secretory process has been shown for other inhibitory receptors, e.g., α -adrenergic and galanine receptors, and suggests that phosphorylation-dephosphorylation events rather than the Ca^{2+} signal play a key role in the distal steps of exocytosis. The specific SSTR subtypes that are coupled to exocytotic secretion as well as the signaling mechanisms leading to calcineurin activation remain to be determined. In addition to its effect on exocytotic

secretion, SST inhibits the release of constitutively secreted proteins such as growth factors and cytokines by unknown mechanisms. In contrast to the antisecretory properties of SST, its antiproliferative effects were relatively late in being recognized (218) and came about largely through use of long-acting analogs such as Octreotide in the early 1980s for the treatment of hormone hypersecretion from pancreatic, intestinal, and pituitary tumors (107, 108, 216). It was noted that SST not only blocked hormone hypersecretion from these tumors but also caused variable tumor shrinkage through an additional antiproliferative effect. The antiproliferative effects of SST have since been demonstrated in normal dividing cells, e.g., intestinal mucosal cells (166), activated lymphocytes (3), and inflammatory cells (87, 198), as well as *in vivo* in solid tumors, e.g., DMBA-induced or transplanted rat mammary carcinomas, and cultured cells derived from both endocrine and epithelial tumors (pituitary, thyroid, breast, prostate, colon, pancreas, lung, and brain) (216, 217). These effects involve cytostatic (growth arrest) and cytotoxic (apoptotic) actions and are mediated (i) directly by SSTRs present on tumor cells and (ii) indirectly via SSTRs present on nontumor cell targets to inhibit the secretion of hormones and growth factors that promote tumor growth and to inhibit angiogenesis, promote vasoconstriction, and modulate immune cell function (28, 32, 140, 144, 184–186, 191). Several SSTR subtypes and signal transduction pathways have been implicated (Fig. 3). Each of the three key second-messenger systems, cAMP, Ca^{2+} , and PTP modulated by SSTRs, could play a role (146, 216). Most interest is focused on protein phosphatases that dephosphorylate receptor tyrosine kinases or that modulate the MAPK signaling cascade, thereby attenuating mitogenic signal transduction. Several other GPCRs have been shown to regulate cell proliferation through modulation of PTP, e.g., dopamine 2, angiotensin II, and α and β adrenergic receptors. A SST-sensitive PTP was first described in 1985 (69) and shown to dephosphorylate and inactivate the EGF receptor kinase in MiaPaCa human pancreatic cancer cells and to antagonize additional tyrosine kinases such as the insulin and IGF-I receptor tyrosine kinases (16, 59, 114, 208). Induction of PTP by SST has now been confirmed in normal pancreatic acinar cells, human coronary smooth muscle cells, MiaPaCa human and AR42J rat pancreatic tumor cells, LNCaP human prostate cancer cells, MCF7 human breast cancer cells, and PCC13 and FRTL5 thyroid tumor cells (19, 59, 114, 194, 208, 213). Furthermore, all five SSTR subtypes have been shown to stimulate PTP activity in various transfected cells (26, 27, 33, 52, 53, 54, 165, 184, 187). SSTR-induced activation of PTP is sensitive to pertussis toxin and orthovanadate (141). The dose response for PTP activation parallels the concentration of SST ligand required for receptor activation. The PTP activity associated with SST action has been attributed to the *src* homology (SH2) domain containing cytosolic PTPs whose members include SHP1 (SHPTP-1, *syp*, PTP-1D) and SHP-2 (SHPTP-2, PTP-1C). SHP-1 is expressed mainly in hematopoietic cells, whereas SHP-2 occurs more widely in many different cell types including CHO cells (134). A 66-kDa PTP identified as SHP-1 copurifies with membrane SSTRs from AR42J pancreatic cells that are enriched in SSTR2 (231). Coimmunoprecipitation studies in CHO-K1 cells

coexpressing SSTR2 and SHP-1 have shown specific immunoprecipitation of $G_{i\alpha 3}$ by anti-SSTR2 and anti-SHP-1 antibodies, suggesting that $G_{i\alpha 3}$ may be involved in the SSTR2/SHP-1 complexes (117). Based on these findings, SHP-1 has been postulated as the PTP responsible for SSTR2-mediated inhibitory growth signaling. Other studies, however, have proposed that the more widely expressed SHP-2 is the principal component of SSTR-mediated antiproliferative signaling. For instance, Reardon *et al.* (164) showed that SHP-2 is the PTP involved in coupling SSTR2-, 3-, and 4 (but not SSTR1 or 5)-induced activation of PTP in membranes from Ras-transformed NIH3T3 cells by functional blockade of the PTP activity with the catalytically inactive SHP-2 mutant protein. Similar studies in CHO-K1 cells have also demonstrated the involvement of SHP-2 in SSTR1-dependent PTP activation (54). The question of whether PTP stimulation by SSTRs requires the intact cell remains controversial. Several reports have found evidence of PTP stimulation by SSTRs in membrane preparations. Others, however, have found that SSTR activation promotes translocation of cytosolic PTP to the membrane with little direct stimulation of PTP by SST ligands in membrane preparations (187, 194).

Like PTP, all of the SSTRs have now been reported to modulate MAPK activity (14, 30, 33, 54, 165, 230). Acting through a putative SSTR2 in SY-5Y neuroblastoma cells, SST inhibits MAPK activity and cell proliferation induced by receptor tyrosine kinases (30). This effect is blocked by orthovanadate, suggesting dephosphorylation-dependent inactivation of MAPK through SST activation of PTP. Likewise, SSTR3 also inhibits MAPK activity via PTP-dependent inactivation of *Raf-1* in transfected NIH3T3 cells (165). In Min-6 mouse insulinoma cells, SSTR3 exerts a dual effect on MAPK activity characterized by a transient increase followed by a decrease (230). SSTR5 inhibits MAPK activity through inhibition of guanylate cyclase and cGMP formation (33). In contrast, SSTR1 and SSTR4 activate MAPK in CHO-K1 cells (14, 54). Activation of MAPK via SSTR1 required a *c-src* like cytoplasmic tyrosine kinase, *Ras*, *Raf-1*, and SHP-2. Despite the positive coupling of SSTR1 to the MAPK signaling cascade, SSTR1 in these cells inhibited cell proliferation due to MAPK-dependent increase in the expression of the cyclin-dependent protein kinase inhibitor $p^{21\text{ cip1/WAF1}}$ (54). These results suggest that the MAPK signal-

FIG. 3. Schematic depiction of SSTR signaling pathways leading to inhibition of secretion (a) and cell proliferation and induction of apoptosis (a). Receptor activation leads to a fall in intracellular cAMP (due to inhibition of adenylyl cyclase), a fall in Ca^{2+} influx (due to activation of K^+ and Ca^{2+} ion channels), and stimulation of phosphatases such as calcineurin (which inhibits exocytosis) and serine threonine phosphatases (which dephosphorylate and activate Ca^{2+} and K^+ channel proteins). Blockade of secretion by SST is in part mediated through inhibition of Ca^{2+} and cAMP (proximal effect) and through a more potent distant effect involving direct inhibition of exocytosis via SST-dependent activation of calcineurin (b). Induction of protein tyrosine phosphatase by SST plays a key role in mediating cell growth arrest (via SSTRs 1, 2, 4, 5) or apoptosis (via SSTR3). Cell growth arrest is dependent on activation of the MAPK pathway and induction of Rb (retinoblastoma tumor suppressor protein) and p21 (cyclin-dependent kinase inhibitor). *c-sac*, which associates with both the activated receptor and PTP (e.g., SHP-2), may provide the link between the receptor, PTP, and the mitogenic signaling complex. Induction of apoptosis is associated with dephosphorylation-dependent activation of p53 and of Bax.



ing pathway is modulated either positively or negatively by each of the five SSTR subtypes in a PTP-dependent manner to effect cell growth inhibition. The precise steps linking the ligand-activated receptor to PTP stimulation remain to be determined. Recent work with the β -adrenergic receptor suggests a pivotal role for β -arrestin, which binds to the ligand-activated, phosphorylated receptor and triggers the assembly of clathrin and *c-src* on β -arrestin molecules to initiate internalization of the receptor complex as a necessary step for effecting MAPK activation (121). Based on this model, *c-src*, which associates with and may be a direct substrate of SHP-2, could provide the link between the receptor, PTP, and the MAPK signaling cascade.

In addition to its cytostatic effect, SST induces apoptosis as first demonstrated in AtT-20 and MCF7 cells treated with Octreotide (140, 186, 191). Apoptosis occurs in a dose-dependent manner over the concentration range 10^{-10} to 10^{-5} M in cells progressing through cell cycle division but not under cell cycle block (191). In MCF7 cells, Octreotide induces marked apoptosis that can be blocked by orthovanadate, implicating PTP activation as a necessary step in SSTR-mediated apoptotic signaling (186). Since AtT-20 and MCF7 cells both express more than one Octreotide-sensitive SSTR subtype, it is not possible to determine subtype selectivity for signaling apoptosis in these cells. In CHO-K1 cells individually expressing the five recombinant SSTRs, apoptosis is triggered uniquely via the hSSTR3 subtype (184). hSSTR3-induced apoptosis is blocked by pretreatment with pertussis toxin or orthovanadate, suggesting the mediation of pertussis toxin-sensitive G proteins and PTP (184). hSSTR3-promoted apoptosis is associated with activation of wild-type (wt) tumor suppressor protein p53 and the pro-apoptotic protein Bax (184). p53 induction occurs rapidly in a time-dependent manner and precedes the activation of Bax and the onset of apoptosis. wt p53 is believed to be in an inactive phosphorylated form and is activated by dephosphorylation of serine residues. In control CHO-K1 cells expressing hSSTR3, p53 displays a distinct perinuclear localization by immunofluorescence (184). Treatment with SST agonist leads to nuclear localization of p53 concomitant with nuclear shrinkage, a characteristic feature of cells undergoing apoptosis (184). The increase in p53 induced by activation of hSSTR3 occurs in all phases of the cell cycle and does not require G_i cell cycle arrest as suggested by the lack of induction of the cyclin-dependent kinase inhibitor p21, which typifies cells undergoing G_i arrest. More recently, hSSTR3-induced apoptotic signaling has been shown to involve the activation of a cation-insensitive acidic endonuclease and intracellular acidification (185). In contrast to hSSTR3-mediated apoptosis, the remaining four subtypes undergo G_i cell cycle arrest in CHO-K1 cells (187). SST-induced G_i cell cycle arrest in these cells is associated with marked induction of Rb (retinoblastoma tumor suppressor protein) and of p21. The maximal effect is exerted by hSSTR5 followed by hSSTR2, 4, and 1 (187). Furthermore, residues in the cytoplasmic C-tail of the receptor appear to be critical for signaling cell cycle arrest presumably through disruption of ligand-induced activation of receptor phosphorylation, clathrin binding, and MAPK activation (121, 187).

REGULATION OF SSTRs

Agonist-Dependent Regulation

Although the acute administration of SST produces a large number of inhibitory effects, the initial response diminishes with continued exposure to the peptide (108, 146, 148, 168). The ability to regulate their responsiveness to continued agonist exposure is a common property of many GPCRs. Such agonist-specific regulation typically involves receptor desensitization due to uncoupling from G proteins as well as receptor internalization and receptor degradation (40, 195). Phosphorylation of the C-tail and intracellular loops of the agonist-occupied receptor by a second-messenger-activated or G-protein-coupled receptor kinase plays a crucial role in the desensitization and internalization processes. Agonist-induced uncoupling of SSTRs from G proteins has been shown in AtT-20 cells (167). Agonist-dependent internalization of SSTRs has been demonstrated in rat anterior pituitary cells, in rat islet cells, and in AtT-20 mouse and human pituitary and islet tumor cells (6, 73, 74, 132). Prolonged agonist exposure for 24–48 h has been shown to upregulate SSTRs in GH₄C₁ and Rin m5f cells (158, 196). Since normal pituitary and islet cells or their tumor cell derivatives express multiple SSTR subtypes, it has been necessary to study host cells stably transfected with each SSTR subtype in order to characterize the response of individual receptor isoforms. SSTR1, 2, 3, and 5 display acute desensitization of adenylyl cyclase coupling (70, 80, 81, 176). hSSTR2, 3, 4, and 5 undergo rapid internalization in a time- and temperature-dependent manner over 60 min in CHO-K1 cells upon agonist activation (81). Maximum internalization occurs with SSTR3 (78%) followed by SSTR5 (66%), SSTR4 (29%), and SSTR2 (20%). In contrast, hSSTR1 fails to be internalized. Similar results have been reported for hSSTR1 and mouse SSTR2 in transfected COS7 cells and for rat SSTR2 overexpressed in GH₄C₁ cells (GH-R2 cells) (70, 137). A different pattern of internalization has been described for the five rSSTR subtypes in human embryonic kidney cells in which SSTR1–3 are rapidly internalized in the presence of SST-14 or SST-28, whereas SSTR5 is internalized only in the presence of SST-28, and SSTR4 is not internalized by either SST ligand (177). The reason for this discrepancy is unclear but may be due in part to structural differences between the rodent and the human SSTR isoforms as well as the cell lines used for transfecting the SSTRs. Mutational analysis of the receptor C-tail and direct phosphorylation studies have demonstrated that phosphorylation of cytoplasmic residues, especially in the carboxyl terminus, plays an important role in agonist-induced desensitization and internalization of SSTR2A, SSTR3, and SSTR5 subtypes (70, 80, 177). Prolonged exposure of SSTRs to agonist for 22 h upregulates hSSTR1 levels at the membrane by 110% and hSSTR2 and hSSTR4 by 26 and 22%, respectively, whereas hSSTR3 and 5 show no change (81). Upregulation of SSTRs by long-term agonist treatment was described 10 years ago in pituitary and islet tumor cells (158, 196) and has been recognized for a number of other GPCRs, e.g., β 3-adrenergic, 5HT_{2A}, GnRH, and the long form of dopamine 2

receptors (118, 136, 202). Since continuous exposure of receptors to agonists is unlikely to occur under normal physiological conditions, this type of response appears to be pharmacological and is observed during long-term drug therapy or in disease states. Unlike receptor downregulation, the underlying molecular mechanisms for upregulation are poorly understood. Upregulation of hSSTR1 occurs by a temperature-dependent, active process of ligand-induced receptor recruitment from a preexisting cytoplasmic pool. It does not require new protein synthesis or signal transduction and is critically dependent on molecular signals in the receptor C-tail (79). The nature of these molecular signals becomes very important in light of recent evidence postulating internalization as a necessary requirement for activation of the mitogenic signaling complex (121). Indeed, the finding that SSTR1 can activate MAPK without being internalized suggests that there may be alternative, non-arrestin-dependent pathways for coupling the receptor to MAPK signaling (54, 81).

Regulation of SSTR Gene Expression

SSTR genes are developmentally regulated in a time- and tissue-specific manner and are influenced by a variety of hormones and disease states in the adult (Table 1). Starvation or insulin deficiency diabetes is associated with decreased mRNA levels for SSTR1-3 in the pituitary and of SSTR5 in the hypothalamus (24). The underlying mechanisms remain to be elucidated. Steady state SSTR mRNA levels are augmented in response to treatment with cAMP, gastrin, or EGF, and SST itself (21, 147, 212). Estrogen induces SST binding sites in cultured rat prolactinoma cells due to upregulation of SSTR2 and SSTR3 (214). Estrogen similarly induces mRNA for SSTR2 and SSTR3 in primary cultures of rat pituitary cells in which it additionally inhibits SSTR1 mRNA levels (39). The *in vivo* effects of estrogen on pituitary SSTR expression in the rat also show induction of SSTR2 and 3 mRNA (91). In addition, SSTR1 mRNA was also upregulated and SSTR5 mRNA inhibited in the *in vivo* experiments (91). Finally, in MCF7 breast cancer cells, estrogen has been reported to stimulate SSTR2 mRNA expression (225). Overall, there is general agreement among these studies for a positive effect of estrogen on SSTR2 and SSTR3 expression and variable or minimal effects on the remaining three subtypes. Glucocorticoids regulate SSTR gene transcription in a time-dependent biphasic manner in GH₄C₁ cells (222). Short-term exposure to glucocorticoids induces SSTR1 and SSTR2 mRNA, whereas prolonged treatment inhibits transcription of both genes. Thyroid hormone induces mRNA for SSTR1 and SSTR5 in mouse thyrotrophe tumor cells (84). To gain a better understanding of extracellular and tissue-specific factors regulating SSTR genes, a number of laboratories have begun to analyze promoter sequences. rSSTR1, hSSTR2, rSSTR4, hSSTR5, and mSSTR5 feature TATA-less G+C-rich promoters typical of tissue-specific housekeeping promoters (11, 61, 62, 64, 223, 224). In the case of hSSTR2, a novel initiator element SSTR2 *inr* located close to the mRNA initiation site confers gene expression in the absence of the TATA

box by binding a helix-loop-helix transcription factor SEF-2, which interacts with the basal transcription machinery (159). The mSSTR2 gene features two previously unrecognized exons separated by introns larger than 25 kb and three tissue- and cell-specific alternative promoters (99). The four SSTR promoters that have been characterized contain consensus sequences for a number of common transcription factors. rSSTR1 showed AP-2 and Pit-1 binding sites as well as the consensus TRE between -97 and -81 bp downstream from Pit-1 (64). The second promoter of the mSSTR2 gene contains DNA elements for regulation by glucocorticoids, estradiol, and cAMP (99). An estrogen-responsive sequence has also been localized in the hSSTR2 promoter (223). rSSTR4 displays multiple AP-1 and AP-2 sites that may confer cAMP responsiveness (222). The hSSTR5 promoter is also cAMP-inducible and additionally displays marked polymorphism, which may influence the pattern of SSTR5 expression in different individuals as well as disease susceptibility (61, 178).

SUBTYPE-SELECTIVE BIOLOGICAL ACTIONS OF SSTRs

Since SST exerts its numerous biological effects through five receptors, the question arises whether a given response is selective for one subtype or whether multiple subtypes are involved. The marked overlap in the cellular pattern of expression of the different SSTR pathways, coupled with the finding that individual target cells typically express multiple SSTR subtypes, and often all five isoforms in the same cell, suggests that SSTRs may operate in concert, rather than as individual members. Nonetheless, there is evidence for relative subtype selectivity for some SSTR effects. At the level of cell secretion and cell proliferation, the two general cellular effects modulated by SST, four of the subtypes (SSTR1, 2, 4, and 5) are capable of arresting cell growth, whereas SSTR3 is uniquely cytotoxic (54, 184, 187). In contrast to cell proliferation, surprisingly little is known about subtype selectivity, if any, for cell secretion. Immune, inflammatory, and neoplastic cells are being increasingly recognized as important new targets for SST action (3, 15, 44, 45, 48, 87, 88, 107, 146, 163, 198). Unlike the classical SST-producing neuroendocrine cells, e.g., in hypothalamus or islets, which release large quantities of the peptide acutely from storage pools, SST and SSTRs in inflammatory cells such as macrophages and lymphocytes are coinduced probably by growth factors and cytokines as part of a general mechanism for activating the endogenous SST system for paracrine/autocrine modulation of the proliferative and hormonal responses associated with inflammatory and immune reactions. Such dual activation of SST and SSTRs has been shown in macrophages in granulomatous reactions, T lymphocytes, and splenocytes and in synovial fibroblasts in rheumatoid arthritis (44, 48, 198). SSTR2 is the main isotype expressed in lymphocytes and inflammatory cells and appears to be the functional SSTR responsible for modulating the proliferative and secretory responses of these cells (44, 198). Many tumor cells coexpress SST along with SSTRs (171). Transfection of NIH3T3 cells with the SSTR2 receptor has been shown to induce SST gene expression, suggesting

that as in the case of immune and inflammatory cells, the presence of a high density of SSTRs as well as SST may reflect an attempt by the tumor to activate the endogenous SST system for autocrine/paracrine modulation of the neoplastic response (163). Studies with selective nonpeptide agonists have shown that GH secretion from rat pituitary somatotrophes is preferentially blocked by SSTR2- and SSTR5-specific compounds (174) (Table 4). This correlates with the preferential expression of SSTR2 and SSTR5 in somatotrophes by immunohistochemistry and suggests that SSTR2 and SSTR5 are the subtypes involved in mediating GH secretion from the pituitary (103). Although the cellular pattern of SSTR subtype expression in the human pituitary has not been characterized, functional studies with subtype-selective peptide agonists have confirmed the mediation of SSTR2 and SSTR5 in regulating GH and TSH secretion from human pituitary (189). In the case of islet hormones, insulin release from mouse pancreatic islets appears to be specific for the SSTR5 subtype (174) (Table 4). This, however, differs from the predicted response in human β cells, which show a rich expression of not only SSTR5 but also SSTR1, suggesting that both subtypes are involved in regulating insulin response in humans (106). There is general agreement that SSTR2 is the islet α cell receptor both in rodents and in humans because of the preferential α cell expression of this subtype as well as the monoselectivity for glucagon suppression exhibited by SSTR2-specific nonpeptide agonists (82, 106, 174) (Table 4). The ideal approach

TABLE 4

Subtype Selectivity for GH, Insulin, and Glucagon Release: Correlation between the Functional Activity of SSTR-Selective Nonpeptide Agonists and SSTR Subtype Expression by Immunocytochemistry

Immunohistochemistry ^a				
	GH cells	β cells	α cells	
SSTR1	+	++++	+	
SSTR2	+++	+++	++++	
SSTR3	++	++	+	
SSTR4	++	+	-	
SSTR5	++++	++++	++	
Functional activity ^b				
Compound release	SSTR selectivity	GH release	Insulin release	Glucagon
L-797,591	SSTR1	>1000	>100	>100
L-779,976	SSTR2	0.025	>100	0.1
L-796,778	SSTR3	>1000	>100	>100
L-803,087	SSTR4	>1000	>100	>100
L-817,818	SSTR5	3.1	0.3	>30

^a Based on expression in rat somatotrophes (103) and human islets (106).

^b Based on results of Rohrer *et al.* (1974) using primary cultures of rat anterior pituitary cells and mouse islet preparations. Values given are IC₅₀ in nM.

for delineating subtype-selective biological responses is the creation of SSTR gene knockouts. Toward this goal, the first SSTR gene knockout, a SSTR2-deficient mouse, has been generated by Zheng *et al.* (232). These animals appear healthy up to 15 months of age excluding an essential role of SSTR2 in embryogenesis and development. Strangely, despite the pharmacological evidence for the involvement of SSTR2 in pituitary GH secretion, the only neuroendocrine abnormality in GH control identified is an absence of GH-induced feedback suppression of GH due to a loss of SSTR2 receptors in arcuate GHRH neurons (232). Despite this, the animals grow normally both *in utero* and postnatally, suggesting maintenance of overall GH secretion. These mice also display high basal gastric acid secretion in the face of normal gastrin levels, indicating that SSTR2 is the subtype responsible for SST suppression of endogenous gastric acid (116, 124). Further work with this model is required to test the requirement for SSTR2 in mediating other putative biological effects such as the regulation of islet glucagon or the inflammatory response. Finally, additional gene knockouts of the remaining four SSTR subtypes are required to shed further light on subtype selective biological responses, if any, attributable to the other members of the receptor family.

ACKNOWLEDGMENTS

The work cited from the author's laboratory was supported by grants from the Canadian Medical Research Council (MT10411, MT6011), the NIH (NS32160), the U.S. Department of Defense, and the National Cancer Institute of Canada. The expert secretarial help of Maria Correia is gratefully acknowledged.

REFERENCES

1. Aguila MC. Growth hormone-releasing factor increases somatostatin release and mRNA levels in the rat periventricular nucleus via nitric oxide by activation of guanylate cyclase. *Proc Natl Acad Sci USA* 1994; **91**: 782-786.
2. Aguila MC, Dees WL, Haensly WE, McCann SM. Evidence that somatostatin is localized and synthesized in lymphoid organs. *Proc Natl Acad Sci USA* 1991; **88**: 11485-11489.
3. Aguila MC, Rodriguez AM, Aguila-Mansilla HN, Lee WT. Somatostatin antisense oligodeoxynucleotide-mediated stimulation of lymphocyte proliferation in culture. *Endocrinology* 1996; **137**: 1585-1590.
4. Akbar M, Okajima F, Tomura H, Majid MA, Yamada Y, Seino S, Kondo Y. Phospholipase C activation and Ca^{2+} mobilization by cloned human somatostatin receptor subtypes 1-5 in transfected COS-7 cells. *FEBS Lett* 1994; **348**: 192-196.
5. Amherdt M, Patel YC, Orci L. Selective binding of somatostatin-14 and somatostatin-28 to islet cells revealed by quantitative electron microscopic autoradiography. *J Clin Invest* 1987; **80**: 1455-1458.
6. Amherdt M, Patel YC, Orci L. Binding and internalization of somatostatin, insulin, and glucagon by cultured rat islet cells. *J Clin Invest* 1989; **84**: 412-417.
7. Baldwin JM. Structure and function of receptors coupled to G proteins. *Curr Opin Cell Biol* 1994; **6**: 180-190.

8. Barber DL, McGuire ME, Ganz MB. Beta-adrenergic and somatostatin receptors regulate Na-H exchange independent of cAMP. *J Biol Chem* 1989; **264**: 21038-21042.
9. Bass RT, Buckwalter BL, Patel BP, Pausch MH, Price LA, Strnad J, Hadcock JR. Identification and characterization of novel somatostatin antagonists. *Mol Pharmacol* 1996; **50**: 709-715.
10. Bauer W, Briner U, Doepfner W, Halber R, Huguenin R, Marbach P, Petcher TJ, Pless J. SMS 201-995: A very potent and selective octapeptide analogue of somatostatin with prolonged action. *Life Sci* 1982; **31**: 1133-1140.
11. Baumeister H, Kreuzer OJ, Roosterman D, Schafer J, Meyerhof W. Cloning, expression, pharmacology and tissue distribution of the mouse somatostatin receptor subtype 5. *J Neuroendocrinol* 1998; **10**: 283-290.
12. Berelowitz M, Firestone S, Frohman LA. Effects of growth hormone excess and deficiency on hypothalamic somatostatin content and release and on tissue somatostatin distribution. *Endocrinology* 1981; **109**: 714-719.
13. Berelowitz M, Szabo M, Frohman LA, Firestone S, Chu L. Somatomedin-C mediates growth hormone negative feedback by effects on both the hypothalamus and the pituitary. *Science* 1981; **212**: 1279-1281.
14. Bito H, Mori M, Sakanaka C, Takano T, Honda Z, Gotoh Y, Nishida E, Shimizu T. Functional coupling of SSTR4, a major hippocampal somatostatin receptor, to adenylate cyclase inhibition, arachidonate release and activation of the mitogen-activated protein kinase cascade. *J Biol Chem* 1994; **269**: 12722-12730.
15. Blum AM, Metwali A, Matthew RC, Cook G, Elliott D, Weinstock JV. Granuloma T lymphocytes in murine schistosomiasis mansoni have somatostatin receptors and respond to somatostatin with decreased IFN- γ secretion. *J Immunol* 1992; **149**: 3621-3626.
16. Bousquet C, Delesque N, Lopez F, Saint-Laurent N, Esteve JP, Bedecs K, Buscail L, Vaysse N, Susini C. sst2 somatostatin receptor mediates negative regulation of insulin receptor signaling through the tyrosine phosphatase SHP-1. *J Biol Chem* 1998; **273**: 7099-7106.
17. Brazeau P, Vale WW, Burgus R, Ling N, Butcher M, Rivier J, Guillemin R. Hypothalamic peptide that inhibits the secretion of immunoreactive pituitary growth hormone. *Science* 1973; **179**: 77-79.
18. Breder CD, Yamada YY, Yasuda K, Seino S, Saper CB, Bell GI. Differential expression of somatostatin receptor subtypes in brain. *J Neurosci* 1992; **12**: 3920-3934.
19. Brevini TAL, Bianchi R, Motta M. Direct inhibitory effect of somatostatin on the growth of the human prostatic cancer cell line LNCaP: Possible mechanism of action. *J Clin Endocrinol Metab* 1993; **77**: 626-631.
20. Brown PJ, Lee AB, Norman MG, Presky DH, Schonbrunn A. Identification of somatostatin receptors by covalent labeling with a novel photoreactive somatostatin analog. *J Biol Chem* 1990; **265**: 17995-18004.
21. Bruno JF, Xu Y, Berelowitz M. Somatostatin regulates somatostatin receptor subtype mRNA expression in GH₃ cells. *Biochem Biophys Res Commun* 1994; **202**: 1738-1743.
22. Bruno JF, Xu Y, Song J, Berelowitz M. Molecular cloning and functional expression of a brain-specific somatostatin receptor. *Proc Natl Acad Sci USA* 1992; **89**: 11151-11155.
23. Bruno JF, Xu Y, Song J, Berelowitz M. Tissue distribution of somatostatin receptor subtype messenger ribonucleic acid in the rat. *Endocrinology* 1993; **133**: 2561-2567.
24. Bruno JF, Xu Y, Song J, Berelowitz M. Pituitary and hypothalamic somatostatin receptor subtype messenger ribonucleic acid expression in the food-deprived and diabetic rat. *Endocrinology* 1994; **135**: 1787-1792.
25. Bruns C, Raulf F, Hoyer D, Schloos J, Lubbert H, Weckbecker G. Binding properties of somatostatin receptor subtypes. *Metabolism* 1996; **45**(Suppl 1): 17-20.
26. Buscail L, Delesque N, Esteve J-P, Saint-Laurent N, Prats H, Clerc P, Robberecht P, Bell GI, Liebow C, Schally AV, Vaysse N, Susini C. Stimulation of tyrosine phosphatase and inhibi-

- tion of cell proliferation by somatostatin analogues: Mediation by human somatostatin receptor subtypes SSTR1 and SSTR2. *Proc Natl Acad Sci USA* 1994; **91**: 2315-2319.
27. Buscail L, Esteve J-P, Saint-Laurent N, Bertrand V, Reisine T, O'Carroll AM, Bell GI, Schally AV, Vaysse N, Susini C. Inhibition of cell proliferation by the somatostatin analogue RC-160 is mediated by somatostatin receptor subtypes SSTR2 and SSTR5 through different mechanisms. *Proc Natl Acad Sci USA* 1995; **92**: 1580-1584.
 28. Candi E, Melino G, de Laurant V, Piamonte M, Guerrei P, Spinedi A, Knight RA. Tamoxifen and somatostatin affect tumors by inducing apoptosis. *Cancer Lett* 1995; **96**: 141-145.
 29. Caron P, Buscail L, Beckers A, Esteve J-P, Igout A, Hennen G, Susini C. Expression of somatostatin receptor SST4 in human placenta and absence of octreotide effect on human placental growth hormone concentrations during pregnancy. *J Clin Endocr Metab* 1997; **82**: 3771-3776.
 30. Cattaneo MG, Amoroso D, Gussoni G, Sanguini AM, Vincenti LM. A somatostatin analogue inhibits MAP kinase activation and cell proliferation in human neuroblastoma and in human small cell lung carcinoma cell lines. *FEBS Lett* 1996; **397**: 164-168.
 31. Chen L, Fitzpatrick D, Vandlen RL, Tashjian AH. Both overlapping and distinct signalling pathways for somatostatin receptor subtype SSTR1 and SSTR2 in pituitary cells. *J Biol Chem* 1997; **272**: 18666-18672.
 32. Cheung NW, Boyages SC. Somatostatin-14 and its analog octreotide exert a cytostatic effect on GH₃ rat pituitary tumor cell proliferation via a transient G₀/G₁ cell cycle block. *Endocrinology* 1995; **136**: 4174-4181.
 33. Cordelier P, Esteve J-P, Bousquet C. Characterization of the antiproliferative signal mediated by the somatostatin receptor subtype sst5. *Proc Natl Acad Sci USA* 1997; **94**: 9343-9348.
 34. Corness JD, Demchyshyn LL, Seeman P, Van Tol HHM, Srikant CB, Kent G, Patel YC, Niznik HB. A human somatostatin receptor (SSTR3), located on chromosome 22, displays preferential affinity for somatostatin-14 like peptides. *FEBS Lett* 1993; **321**: 279-284.
 35. Day R, Dong W, Panetta R, Kraicer J, Greenwood MT, Patel YC. Expression of mRNA for somatostatin receptor (sstr) types 2 and 5 in individual rat pituitary cells. A double labeling in situ hybridization analysis. *Endocrinology* 1995; **136**: 5232-5235.
 36. De Lecea L, Criado JR, Prospero-Garcia O, Gautvik KM, Schweitzer P, Danielson PE, Dunlop CLM, Siggins GR, Henriksen SJ, Sutcliffe JG. A cortical neuropeptide with neuronal depressant and sleep-modulating properties. *Nature* 1996; **381**: 242-245.
 37. Demchyshyn LL, Srikant CB, Sunahara RK, Kent G, Seeman P, Van Tol HHM, Panetta R, Patel YC, Niznik HB. Cloning and expression of a human somatostatin-14 selective receptor variant (SSTR4) located on chromosome 20. *Mol Pharmacol* 1993; **43**: 894-901.
 38. De Wille JR, Schmid-Antomarchi H, Fosset M, Lazdunski M. Regulation of ATP-sensitive K⁺ channels in insulinoma cells: Activation by somatostatin and protein kinase C and the role of cAMP. *Proc Natl Acad Sci USA* 1989; **86**: 2971-2975.
 39. Djordjijevic D, Zhang J, Priam M, Viollet C, Gourdji D, Kordon C, Epelbaum J. Effect of 17 beta-estradiol on somatostatin receptor expression and inhibitory effects on growth hormone and prolactin release in rat pituitary cell cultures. *Endocrinology* 1998; **139**: 2272-2277.
 40. Dohlman HG, Thorner J, Caron MG, Lefkowitz RJ. Model systems for the study of seven transmembrane segment receptors. *J Biol Chem* 1991; **268**: 337-341.
 41. Dournaud P, Boudin H, Schonbrunn A, Tannenbaum GS, Beaudet A. Interrelationships between somatostatin SST2A receptors and somatostatin-containing axons in rat brain. Evidence for regulation of cell surface receptors by endogenous somatostatin. *J Neurosci* 1998; **18**: 1056-1071.
 42. Dournaud P, Gu YZ, Schonbrunn A, Mazella J, Tannenbaum GS, Beaudet A. Localization of the somatostatin receptor SST2A in rat brain using a specific antipeptide antibody. *J Neurosci* 1996; **16**: 4468-4478.

43. Dubois MP. Immunoreactive somatostatin is present in discrete cells of the endocrine pancreas. *Proc Natl Acad Sci USA* 1975; **72**: 1340–1343.
44. Elliott DE, Blum AM, Li J, Metwaki A, Weinstock JV. Preprosomatostatin messenger RNA is expressed by inflammatory cells and induced by inflammatory mediators and cytokines. *J Immunol* 1998; **160**: 3997–4003.
45. Elliott DE, Metwali A, Blum AM, Sandor M, Lynch R, Weinstock JV. T lymphocytes isolated from the hepatic granulomas of schistosome-infected mice express somatostatin receptor subtype II (SSTR2) messenger RNA. *J Immunol* 1994; **153**: 1180–1186.
46. Epelbaum J, Dournaud P, Fodor M, Viollet C. The neurobiology of somatostatin. *Crit Rev Neurobiol* 1994; **8**: 25–44.
47. Evans CJ, Keith DE Jr, Morrison H, Magendzo K, Edwards RH. Cloning of a delta opioid receptor by functional expression. *Science* 1992; **258**: 1952–1955.
48. Ferone D, Van Hagen PM, Van Koetsveld PM, Zuijderwijk J, Mooy DM, Lichtenauer-Kaligis EGR, Colao A, Bogers AJJC, Lombardi G, Lamberts SWJ, Hofland LJ. *In vitro* characterization of somatostatin receptors in the human thymus and effects of somatostatin and octreotide on cultured thymic epithelial cells. *Endocrinology* 1999; **140**: 373–380.
49. Finley JCW, Maderdrut JL, Roger LJ, Petrusz P. The immunocytochemical localization of somatostatin-containing neurons in the rat central nervous system. *Neurosci* 1981; **6**: 2173–2192.
50. Fitz-Patrick VD, Vandlen RL. Six agonist selectivity determinants in somatostatin receptor subtypes I and II. *J Biol Chem* 1994; **269**: 24621–24626.
51. Flanagan CA, Becker II, Davidson JS, Wakefield IK, Zhou W, Sealfon SC, Miller RP. Glutamate 301 of the mouse gonadotrophin releasing hormone receptor confers specificity for arginine 8 of mammalian gonadotrophin releasing hormone. *J Biol Chem* 1994; **269**: 22636–22641.
52. Florio T, Rim C, Hershberger RE, Loda M, Stork PJ. The somatostatin receptor SSTR1 is coupled to phosphotyrosine phosphatase activity in CHO-K1 cells. *Mol Endocrinol* 1994; **8**: 1289–1297.
53. Florio T, Scarziello A, Fattore M, Dalto V, Salzano S, Rossi G, Berlingieri MT, Fusco A, Schettini G. Somatostatin inhibits PC C13 thyroid cell proliferation through the modulation of phosphotyrosine phosphatase activity-impairment of the somatostatinergic effects by stable expression of EIA viral oncogene. *J Biol Chem* 1996; **271**: 6129–6136.
54. Florio T, Yao H, Carey KD, Dillon TJ, Stork PJS. Somatostatin activation of mitogen-activated protein kinase via somatostatin receptor 1 (SSTR1). *Mol Endocrinol* 1999; **13**: 24–37.
55. Fujii Y, Gono T, Yamada Y, Chihara K, Inagaki N, Seino S. Somatostatin receptor subtype SSTR2 mediates the inhibition of high voltage activated calcium channels by somatostatin and its analogue SMS201-995. *FEBS Lett* 1994; **355**: 117–120.
56. Fukusumi S, Kitada C, Takekawa S, Kizawa H, Sakamoto J, Miyamoto M, Hinuma S, Kitano K, Fujino M. Identification and characterization of a novel human corticostatin like peptide. *Biochem Biophys Res Commun* 1997; **232**: 157–163.
57. Fuller P, Verity K. Somatostatin gene expression in the thymus gland. *J Immunol* 1989; **143**: 1015–1017.
58. Gether U, Johansen TE, Snider RM, Lowe JA, Edmons-Alt X, Yokota Y, Nakamishi S, Schwartz TW. Binding epitopes for peptide and nonpeptide ligands on the NK1 (substance P) receptor. *Regul Pep* 1993; **46**: 49–58.
59. Grant MB, Wargovich TJ, Ellis EA, Caballero S, Mansour M, Pepine CJ. Localization of insulin-like growth factor I and inhibition of coronary smooth muscle cell growth by somatostatin analogues in human coronary smooth muscle cells. A potential treatment for restenosis. *Circulation* 1994; **89**: 1511–1517.

60. Greenwood MT, Hukovic N, Kumar U, Panetta R, Hjorth SA, Srikant CB, Patel YC. Ligand binding pocket of the human somatostatin receptor 5 (hsstr5): Mutational analysis of the extracellular domains. *Mol Pharmacol* 1997; **52**: 807-814.
61. Greenwood MT, Panetta R, Robertson LA, Liu J-L, Patel YC. Sequence analysis of the 5'-flanking promoter region of the human somatostatin receptor 5. *Biochem Biophys Res Commun* 1994; **205**: 1883-1890.
62. Greenwood MT, Robertson LA, Patel YC. Cloning of the gene encoding the human somatostatin receptor 2: Sequence analysis of the 5' flanking promoter region. *Gene* 1995; **159**: 291-292.
63. Gu Y-Z, Schonbrunn A. Coupling specificity between somatostatin receptor sst2A and G proteins: Isolation of the receptor-G protein complex with a receptor antibody. *Mol Endocrinol* 1997; **11**(5): 527-537.
64. Hauser F, Meyerhof W, Wulfsen I, Schonrock C, Richter D. Sequence analysis of the promoter region of the rat somatostatin receptor subtype 1 gene. *FEBS Lett* 1994; **345**: 225-228.
65. Hayry P, Raisanen A, Ustinov J, Mennander A, Paaavonen T. Somatostatin analog Lanreotide inhibits myocyte replication and several growth factors in allograft arteriosclerosis. *FASEB J* 1993; **7**: 1055-1060.
66. Helboe L, Moller M, Novregaard L, Schiodt M, Stidsen CE. Development of selective antibodies against the human somatostatin receptor subtypes SST1-SST5. *Mol Brain Res* 1997; **49**: 82-88.
67. Helboe L, Stidsen CE, Moller M. Immunohistochemical and cytochemical localization of the somatostatin receptor subtype sst₁ in the somatostatinergic parvocellular neuronal system of the rat hypothalamus. *J Neurosci* 1998; **18**: 4938-4945.
68. Hervieu G, Emson PC. The localization of somatostatin receptor 1 (sst₁) immunoreactivity in the rat brain using an N-terminal specific antibody. *Neuroscience* 1998; **85**: 1263-1284.
69. Hierowski MT, Liebow C, du Sapin K, Schally AV. Stimulation by somatostatin of dephosphorylation of membrane proteins in pancreatic cancer Mia PaCA-2 cell line. *FEBS Lett* 1985; **179**: 252-256.
70. Hipkin RW, Friedman J, Clark RB, et al. Agonist-induced desensitization, internalization and phosphorylation of the sst_{2A} somatostatin receptor. *J Biol Chem* 1997; **272**: 13869-13876.
71. Hjorth SA, Schambye HT, Greenlee WJ, Schwartz TW. Identification of peptide binding residues in the extracellular domains of the AT1 receptor. *J Biol Chem* 1994; **269**: 30953-30959.
72. Hobart P, Crawford R, Shen L-P, Pictet R, Rutter WJ. Cloning and sequencing analysis of cDNAs encoding two distinct somatostatin precursors found in endocrine pancreas of anglerfish. *Nature* 1980; **288**: 137-141.
73. Hofland LJ, Breeman WAP, Krenning EP, de Jong M, Waaijers M, Van Koetsveld PM, Macke HR, Lamberts SWJ. Internalization of [DOTA⁰, ¹²⁵I-Tyr³] octreotide by somatostatin receptor-positive cells *in vitro* and *in vivo*: Implications for somatostatin receptor-targeted radioguided surgery. *Proc Assoc Amer Phys* 1999; **111**: 63-69.
74. Hofland LJ, Van Koetsveld PM, Waaijers M, Zzuyderwijk J, Breeman WAP, Lamberts SWJ. Internalization of the radioiodinated somatostatin analog [¹²⁵I-Tyr³] octreotide by mouse and human pituitary tumor cells: Increase by unlabelled octreotide. *Endocrinology* 1995; **136**: 3698-3706.
75. Hokfelt T, Effendic S, Hellerstrom C, Johansson O, Luft R, Arimura A. Cellular localization of somatostatin in endocrine-like cells and neurons of the rat with special references to the A₁ cells of the pancreatic islets and to the hypothalamus. *Acta Endocrinol* 1975; **80**(Suppl. 200): 5-41.
76. Hou C, Gilbert RL, Barber DL. Subtype-specific signalling mechanisms of somatostatin receptors SSTR1 and SSTR2. *J Biol Chem* 1994; **269**: 10357-10362.
77. Hoyer D, Lubbert H, Bruns C. Molecular pharmacology of somatostatin receptors. *Arch Pharmacol* 1994; **350**: 441-453.

78. Hoyer D, Bell GI, Berelowitz M, Epelbaum J, Feniuk W, Humphrey PPA, O'Carroll AM, Patel YC, Schonbrunn A, Taylor JE, Reisine T. Classification and nomenclature of somatostatin receptors. *Trends Pharmacol Sci* 1995; **16**: 86–88.
79. Hukovic N, Kumar U, Sasi R, Khare S, Rocheville M, Patel YC. Agonist-dependent upregulation of human somatostatin receptor type 1 (hSSTR1) requires molecular signals in the cytoplasmic C-tail. Program Annual Meeting US Endocrine Society 1998; p 139. [Abstract P1–80].
80. Hukovic N, Panetta R, Kumar U, Rocheville M, Patel YC. The cytoplasmic tail of the human somatostatin receptor type 5 is crucial for interaction with adenylyl cyclase, and in mediating desensitization and internalization. *J Biol Chem* 1998; **273**: 21416–21422.
81. Hukovic N, Panetta R, Kumar U, Patel YC. Agonist-dependent regulation of cloned human somatostatin receptor types 1–5 (hSSTR1–5): Subtype selective internalization or upregulation. *Endocrinology* 1996; **137**: 4046–4049.
82. Hunyady B, Hipkin RW, Schonbrunn A, Mezey E. Immunohistochemical localization of somatostatin receptor SSTR2A in the rat pancreas. *Endocrinology* 1997; **138**: 2632–2635.
83. Ikeda SR, Schofield GG. Somatostatin blocks a calcium current in rat sympathetic ganglion neurons. *J Physiol* 1989; **409**: 221–240.
84. James RA, Sarapura VD, Bruns C, Raulf F, Dowding JM, Gordon DF, Wood WM, Ridgway EC. Thyroid hormone induced expression of specific somatostatin receptor subtypes correlates with involution of the TtT-97 murine thyrotrope tumor. *Endocrinology* 1997; **138**(2): 719–724.
85. Johansson O, Hokfelt T, Elde RP. Immunohistochemical distribution of somatostatin-like immunoreactivity in the central nervous system of the adult rat. *Neuroscience* 1984; **13**: 265–339.
86. Jung BP, Nguyen T, Kolakowski LF Jr, Lynch KR, Heng HHQ, George SR, O'Dowd BF. Discovery of a novel human G protein coupled receptor gene (GPR25) located on chromosome 1. *Biochem Biophys Res Commun* 1997; **230**: 69–72.
87. Karalis K, Mastrorakos G, Chrousos GP, Tolis G. Somatostatin analogues suppress the inflammatory reaction *in vivo*. *J Clin Invest* 1994; **93**: 2000–2006.
88. Karalis K, Mastrorakos G, Sano H, Wilder RL, Chrousos GP. Somatostatin may participate in the antiinflammatory actions of glucocorticoids. *Endocrinology* 1995; **136**: 4133–4138.
89. Kaupmann K, Bruns C, Raulf F, Weber HP, Mattes H, Lubbert H. Two amino acids, located in transmembrane domains VI and VII, determine the selectivity of the peptide agonist SMS201-995 for the SSTR2 somatostatin receptor. *EMBO J* 1995; **14**: 727–735.
90. Khare S, Kumar U, Sasi R, Puebla L, Calderon L, Lemstrom K, Hayry P, Patel YC. Differential regulation of somatostatin receptor types 1–5 in rat aorta after angioplasty. *FASEB J* 1999; **13**: 387–394.
91. Kimura N, Tomizawa S, Arai KN, Kimura N. Chronic treatment with estrogen up-regulates expression of sst2 messenger ribonucleic acid (mRNA) but down-regulates expression of sst5 mRNA in rat pituitaries. *Endocrinology* 1998; **139**: 1573–1580.
92. Kleuss C, Hescheler J, Ewel C, Rosenthal W, Schultz G, Wittig B. Assignment of G protein subtypes to specific receptors inducing inhibition of calcium currents. *Nature* 1991; **353**(3): 43–48.
93. Kluxen FW, Bruns CH, Lubbert H. Expression cloning of a rat brain somatostatin receptor cDNA. *Proc Natl Acad Sci USA* 1992; **89**: 4618–4622.
94. Koch BD, Schonbrunn A. Characterization of the cyclic AMP-independent actions of somatostatin in GH cells. *J Biol Chem* 1988; **263**: 226–234.
95. Kolakowski FL, Jung BP, Nguyen T, Johnson MP, Lynch KR, Cheng R, Heng HHQ, George SR, O'Dowd BF. Characterization of a human gene related to genes encoding somatostatin receptors. *FEBS Lett* 1996; **398**: 253–258.

96. Komatsuzaki K, Murayama Y, Giambarella U, Ogata E, Seino S, Nishimoto I. A novel system that reports the G-proteins linked to a given receptor: A study of type 3 somatostatin receptor. *FEBS Lett* 1997; **406**: 165–170.
97. Kong H, DePaoli AM, Breder CD, Yasuda K, Bell GI, Reisine T. Differential expression of messenger RNAs for somatostatin receptor subtypes SSTR1, SSTR2, and SSTR3 in adult rat brain: Analysis by RNA blotting and in situ hybridization histochemistry. *Neuroscience* 1994; **59**(1): 175–184.
98. Kowk RPS, Lundblad JR, Chrivia JC, Richards JP, Bachinger HP, Brennan RG, Roberts SGE, Green MR, Goodman RH. Nuclear protein CBP is a coactivator for the transcription factor CREB. *Nature* 1994; **370**: 223–226.
99. Kraus J, Woltje M, Schonwetter N, Holtt V. Alternative promoter usage and tissue specific expression of the mouse somatostatin receptor 2 gene. *FEBS Lett* 1998; **428**: 165–170.
100. Kreienkamp HJ, Honck HH, Richter D. Coupling of rat somatostatin receptor subtypes to a G-protein gated inwardly rectifying potassium channel (GIRK1). *FEBS Lett* 1997; **419**: 92–94.
101. Krempels K, Hunyady B, O'Carroll AM, Mezey E. Distribution of somatostatin receptor messenger RNAs in the rat gastrointestinal tract. *Gastroenterology* 1997; **112**: 1948–1960.
102. Kubota A, Yamada Y, Kagimoto S, Yasuda K, Someya Y, Ihara Y, Okamoto Y, Kozasa T, Seino S, Seino Y. Multiple effector coupling of somatostatin receptor subtype SSTR1. *Biochem Biophys Res Commun* 1994; **204**: 176–186.
103. Kumar U, Laird D, Srikant CB, Escher E, Patel YC. Expression of the five somatostatin receptor (SSTR1–5) subtypes in rat pituitary somatotrophes: Quantitative analysis by double-label immunofluorescence confocal microscopy. *Endocrinology* 1997; **138**: 4473–4476.
104. Kumar U, Ong W-Y, Patel SC, Patel YC. Cellular expression of the five somatostatin receptor subtypes (SSTR1–5) in rat hypothalamus: A comparative immunohistochemical analysis. Program Annual Meeting US Endocrine Society, San Diego, CA June 12–15, 1999. Submitted for publication.
105. Kumar U, Patel SC, Patel YC. Immunohistochemical distribution of the five somatostatin receptor (SSTR) subtypes in rat cerebral cortex. Program Annual Meeting Society For Neuroscience, November 16–21, 1996.
106. Kumar U, Sasi R, Suresh S, Patel A, Thangaraju M, Metrakos P, Patel SC, Patel YC. Subtype-selective expression of the five somatostatin receptors (hSSTR1–5) in human pancreatic islet cells: A quantitative double-label immunohistochemical analysis. *Diabetes* 1999; **48**: 77–85.
107. Lamberts SWJ, Krenning EP, Reubi J-C. The role of somatostatin and its analogs in the diagnosis and treatment of tumors. *Endocr Rev* 1991; **12**: 450–482.
108. Lamberts SWJ, Van Der Lely A-J, de Herder WW. Drug therapy: Octreotide. *N Eng J Med* 1996; **334**: 246–254.
109. Lanneau C, Viollet C, Faivre-Bauman A, Loudes C, Kordon C, Epelbaum J, Gardette R. Somatostatin receptor subtypes sst1 and sst2 elicit opposite effects on the response to glutamate of mouse hypothalamic neurones: An electrophysiological and single cell RT-PCR study. *Eur J Neurosci* 1998; **10**: 204–212.
110. Larsson LI, Golterman N, De Magistris L, Rehfeld JF, Schwartz TW. Somatostatin cell processes as pathways for paracrine secretion. *Science* 1979; **205**: 1393–1395.
111. Le Romancer M, Cherifi Y, Levasseur S, Laigneau JP, Peranzi G, Jois P, Lewin MJ, Reyl-Desmars F. Messenger RNA expression of somatostatin receptor subtypes in human and rat gastric mucosae. *Life Sci* 1996; **58**: 1091–1098.
112. Li X-J, Forte M, North RA, Ross CA, Snyder SH. Cloning and expression of a rat somatostatin receptor enriched in brain. *J Biol Chem* 1992; **267**: 21307–21312.
113. Liapakis G, Haeger C, Rivier J, Reisine T. Development of a selective agonist at the somatostatin receptor subtype SSTR1. *JPET* 1996; **276**: 1089–1094.

114. Liebow C, Reilly C, Serrano M, *et al.* Somatostatin analogues inhibit growth of pancreatic cancer by stimulating tyrosine phosphatase. *Proc Natl Acad Sci USA* 1989; **86**: 2003–2007.
115. Liu YF, Jacobs KH, Rosewick MM, Albert PR. G protein specificity in receptor–effector coupling: Analysis of the roles of Go and Gi in GH₄C₁ pituitary cells. *J Biol Chem* 1994; **269**: 13880–13886.
116. Lloyd KC, Amirmoazzami S, Friedrik F, Chew P, Walsh JH. Somatostatin inhibits gastrin release and acid secretion by activating sst2 in dogs. *Am J Physiol* 1997; **272**: G1481–G1488.
117. Lopez F, Esteve JP, Buscail L, Delesque N, Saint-Laurent N, Theveniau M, Nahmias C, Vaysse N, Susini C. The tyrosine phosphatase SHP-1 associates with the sst2 somatostatin receptor and is an essential component of sst2-mediated inhibitory growth signalling. *J Biol Chem* 1997; **272**: 24448–2454.
118. Loumaye E, Catt KJ. Agonist-induced regulation of pituitary receptors for gonadotrophin releasing hormone. *J Biol Chem* 1983; **258**: 12002–12009.
119. Luini A, de Matteis MA. Evidence that receptor-linked G protein inhibits exocytosis by a post-second messenger mechanism in AtT-20 cells. *J Neurochem* 1990; **54**: 30–38.
120. Luthin DR, Eppler CM, Linden J. Identification and quantification of Gi-type GTP-binding proteins that copurify with a pituitary somatostatin receptor. *J Biol Chem* 1993; **268**: 5990–5996.
121. Luttrell LM, Ferguson SSG, Daaka Y, Miller WE, Maudsley S, Rocca GJD, Lin F-T, Kawakatsu H, Owada K, Luttrell DK, Caron MG, Lefkowitz RJ. β -arrestin-dependent formation of β_2 adrenergic receptor–Src protein kinase complexes. *Science* 1999; **283**: 655–660.
122. Mandarino L, Stenner D, Blanchard W, Nissen S, Gerich J, Ling N, Brazeau P, Bohlen P, Esch F, Guillemin R. Selective effects of somatostatin-14, -25, and -28 on in vitro insulin and glucagon secretion. *Nature* 1981; **291**: 76–77.
123. Marin P, Delumeau JC, Tence M, Cordier J, Glowinski J, Premont J. Somatostatin potentiates the α_1 -adrenergic activation of phospholipase C in striatal astrocytes through a mechanism involving arachidonic acid and glutamate. *Proc Natl Acad Sci USA* 1991; **88**: 9016–9020.
124. Martinez V, Curi AP, Torkian B, Schaeffer JM, Wilkinson HA, Walsh JH, Tache Y. High basal gastric acid secretion in somatostatin receptor subtype 2 knockout mice. *Gastroenterology* 1998; **114**: 1125–1132.
125. McDonald JK, Greiner F, Bauer GE, Elde RP, Noe BD. Separate cell types that express two different forms of somatostatin in anglerfish islets can be immunohistochemically differentiated. *J Histochem Cytochem* 1987; **35**: 155–162.
126. Meriney SD, Gray DB, Pilar GR. Somatostatin-induced inhibition of neuronal Ca²⁺ current modulated by cGMP-dependent protein kinase. *Nature* 1994; **369**: 336–339.
127. Meyerhof W, Wulfsen I, Schonrock C, Fehr S, Richter D. Molecular cloning of a somatostatin-28 receptor and comparison of its expression pattern with that of a somatostatin-14 receptor in rat brain. *Proc Natl Acad Sci USA* 1992; **89**: 10267–10271.
128. Mezey E, Hunyady B, Mitra S, Hayes E, Liu Q, Schaeffer J, Schonbrunn A. Cell specific expression of the SSTR2A and SSTR5 somatostatin receptors in the rat anterior pituitary. *Endocrinology* 1998; **139**: 414–419.
129. Montminy M, Brindle P, Arias J, Ferreri K, Armstrong R. Regulation of somatostatin gene transcription by cAMP. In: Somatostatin and Its Receptors, Ciba Foundation Symposium 190, West Sussex, UK: Wiley, 1995; pp. 7–20.
130. Montminy MR, Goodman RH, Horovitch SJ, Habener JF. Primary structure of the gene encoding rat preprosomatostatin. *Proc Natl Acad Sci USA* 1984; **81**: 3337–3340.
131. Montminy MR, Low MJ, Tapia-Arancibia L, Reichlin S, Mandel G, Goodman RH. Cyclic AMP regulates somatostatin mRNA accumulation in primary diencephalic cultures and in transfected fibroblast cells. *J Neurosci* 1985; **6**: 1171–1176.

132. Morel G, Leroux P, Pelletier G. Ultrastructural autoradiographic localization of somatostatin-28 in the rat pituitary gland. *Endocrinology* 1985; **116**: 1615-1620.
133. Murthy KS, Coy DH, Makhoul G. Somatostatin receptor-mediated signalling in smooth muscle. *J Biol Chem* 1996; **271**: 23458-23463.
134. Neel B. Structure and function of SH2-domain containing tyrosine phosphate. *Semin Cell Biol* 1993; **4**: 419-432.
135. Nehring RB, Meyerhof W, Richter D. Aspartic acid residue 124 in the third transmembrane domain of the somatostatin receptor subtype 3 is essential for somatostatin-14 binding. *DNA Cell Biol* 1995; **14**: 939-944.
136. Ng GYK, Varghese G, Chung HT, et al. Resistance of the dopamine D_{2L} receptor to desensitization accompanies the upregulation of receptors onto the surface of Sf9 cells. *Endocrinology* 1997; **138**: 4199-4206.
137. Nouel D, Gaudriault G, Houle M, Reisine T, Vincent J-P, Mazella J, Beaudet A. Differential internalization of somatostatin in COS-7 cells transfected with SST1 and SST2 receptor subtypes: A confocal microscopic study using novel fluorescent somatostatin derivatives. *Endocrinology* 1997; **138**: 296-306.
138. O'Carroll AM, Krempel K. Widespread distribution of somatostatin receptor messenger ribonucleic acids in rat pituitary. *Endocrinology* 1995; **136**: 5224-5227.
139. O'Carroll AM, Lolait SJ, Konig M, Mahan LC. Molecular cloning and expression of a pituitary somatostatin receptor with preferential affinity for somatostatin-28. *Mol Pharmacol* 1992; **42**: 939-946.
140. Pagliacci MC, Tognellin R, Grignani F, Nicoletti F. Inhibition of human breast cancer cell (MCF-7) growth in vitro by the somatostatin analog SMS201-995: Effects on cell cycle parameters and apoptotic cell death. *Endocrinology* 1991; **129**: 2555-2562.
141. Pan MG, Florio T, Stork PJS. G protein activation of a hormone-stimulated phosphatase in human tumor cells. *Science* 1992; **256**: 1215-1217.
142. Panetta R, Greenwood MT, Warszynska A, Demchyshyn LL, Day R, Niznik HB, Srikant CB, Patel YC. Molecular cloning, functional characterization, and chromosomal localization of a human somatostatin receptor (somatostatin receptor type 5) with preferential affinity for somatostatin-28. *Mol Pharmacol* 1994; **45**: 417-427.
143. Panetta R, Patel YC. Expression of mRNA for all 5 human somatostatin receptor (hSSTR1-5) in pituitary tumors. *Life Sci* 1994; **56**: 333-342.
144. Patel PC, Barrie R, Hill N, Landeck S, Kurozawa D, Woltering EA. Post receptor signal transduction mechanisms involved in octreotide induced inhibition of angiogenesis. *Surgery* 1994; **116**: 1148-1152.
145. Patel YC. General aspects of the biology and function of somatostatin. In: Weil C, Muller EE, Thorner MO, Eds. *Basic and Clinical Aspects of Neuroscience*. Berlin: Springer-Verlag, 1992; Vol. 4, 1-16.
146. Patel YC. Molecular pharmacology of somatostatin receptor subtypes. *J Endocrinol Invest* 1997; **20**: 348-367.
147. Patel YC, Greenwood MT, Kent G, Panetta R, Srikant CB. Multiple gene transcripts of the somatostatin receptor SSTR2: Tissue selective distribution and cAMP regulation. *Biochem Biophys Res Commun* 1993; **192**: 288-294.
148. Patel YC, Greenwood MT, Panetta R, Demchyshyn L, Niznik H, Srikant CB. The somatostatin receptor family: A mini review. *Life Sci* 1995; **57**: 1249-1265.
149. Patel YC, Greenwood MT, Warszynska A, Panetta R, Srikant CB. All five cloned human somatostatin receptors (hSSTR1-5) are functionally coupled to adenylyl cyclase. *Biochem Biophys Res Commun* 1994; **198**: 605-612.
150. Patel YC, Liu JL, Galanopoulou AS, Papachristou DN. Production, action, and degradation of somatostatin. In: Jefferson LS, Cherrington AD, Eds. *The Handbook of Physiology, The Endocrine Pancreas and Regulation of Metabolism*, New York: Oxford Univ. Press, 1999: in press.

151. Patel YC, Murthy KK, Escher E, Banville D, Spiess J, Srikant CB. Mechanism of action of somatostatin: An overview of receptor function and studies of the molecular characterization and purification of somatostatin receptor proteins. *Metabolism* 1990; **39**(Suppl. 2): 63-69.
152. Patel YC, Panetta R, Escher E, Greenwood M, Srikant CB. Expression of multiple somatostatin receptor genes in AtT-20 cells: Evidence for a novel somatostatin-28 selective receptor subtype. *J Biol Chem* 1994; **269**: 1506-1509.
153. Patel YC, Papachristou DN, Zingg HH, Farkas EM. Regulation of islet somatostatin secretion and gene expression: Selective effects of adenosine 3',5' monophosphate and phorbol esters in normal islets of Langerhans and in a somatostatin-producing rat islet clonal cell line 1027B₂. *Endocrinology* 1991; **128**: 1754-1762.
154. Patel YC, Reichlin S. Somatostatin in hypothalamus, extrahypothalamic brain and peripheral tissues of the rat. *Endocrinology* 1978; **102**: 523-530.
155. Patel YC, Srikant CB. Subtype selectivity of peptide analogs for all five cloned human somatostatin receptors (hsstr1-5). *Endocrinology* 1994; **135**: 2814-2817.
156. Patel YC, Srikant CB. Somatostatin receptors. *Trends Endocrinol Metab* 1997; **8**: 398-405.
157. Pradayrol L, Jornvall H, Mutt V, Ribet A. N-terminally extended somatostatin: The primary structure of somatostatin 28. *FEBS Lett* 1980; **109**: 55-8.
158. Presky DH, Schonbrunn A. Somatostatin pretreatment increases the number of somatostatin receptors in GH4C1 pituitary cells and does not reduce cellular responsiveness to somatostatin. *J Biol Chem* 1988; **263**: 714-721.
159. Pscherer A, Dorflinger U, Kirfel J, Gawlas K, Ruschoff J, Buettner R, Schule R. The helix-loop-helix transcription factor SEF2 regulates the activity of a novel initiator element in the promoter of the human somatostatin receptor II gene. *EMBO J* 1996; **15**: 6680-6690.
160. Puebla L, Khare S, Sasi R, Bennett HJP, James S, Mouchantaf R, Patel YC. Processing of rat preprocortistatin in mouse AtT-20 cells. Submitted for publication.
161. Quintela M, Senaris RM, Dieguez C. Transforming growth factor- β s inhibit somatostatin messenger ribonucleic acid levels and somatostatin secretion in hypothalamic cells in culture. *Endocrinology* 1997; **138**: 4401-4409.
162. Quintela M, Senaris R, Heiman ML, Casanueva FF, Dieguez C. Leptin inhibits *in vitro* hypothalamic somatostatin secretion and somatostatin mRNA levels. *Endocrinology* 1997; **138**: 5641-5644.
163. Raully I, Saint-Laurent N, Delesque N, Buscail L, Esteve J-P, Vaysse N, Susini C. Induction of a negative autocrine loop by expression of Sst2 somatostatin receptor in NIH 3T3 cells. *J Clin Invest* 1996; **97**: 1874-1883.
164. Reardon DB, Dent P, Wood SL, Kong T, Sturgill TW. Activation *in vitro* of somatostatin receptor subtypes 2, 3, or 4 stimulates protein tyrosine phosphatase activity in membranes from transfected Ras-transformed NIH 3T3 cells: Coexpression with catalytically inactive SHP-2 blocks responsiveness. *Mol Endocrinol* 1997; **11**: 1062-1069.
165. Reardon DB, Wood SL, Brautigan DL, Bell GI, Dent P, Sturgill TW. Activation of a protein tyrosine phosphate and inactivation of Raf-1 by somatostatin. *Biochem J* 1996; **31**: 401-404.
166. Reichlin S. Somatostatin. *N Engl J Med* 1983; **309**: 1495-1501, 1556-1563.
167. Reisine TD, Axelrod J. Prolonged somatostatin treatment desensitizes somatostatin's inhibition of receptor-mediated release of adrenocorticotropin hormone and sensitizes adenylate cyclase. *Endocrinology* 1983; **113**: 811-813.
168. Reisine T, Bell GI. Molecular biology of somatostatin receptors. *Endocr Rev* 1995; **16**: 427-442.
169. Renstrom E, Ding WG, Bokvist K, Rorsman P. Neurotransmitter-induced inhibition of exocytosis in insulin-secreting β cells by activation of calcineurin. *Neuron* 1996; **17**: 513-522.
170. Reubi JC, Horisberger U, Kappeler A, Laissue JA. Localization of receptors for vasoactive intestinal peptide, somatostatin, and substance P in distinct compartments of human lymphoid organs. *Blood* 1998; **92**: 191-197.

171. Reubi JC, Waser B, Lamberts SWJ, Mengod G. Somatostatin (SRIH) messenger ribonucleic acid expression in human neuroendocrine and brain tumors using *in situ* hybridization histochemistry: Comparison with SRIH receptor content. *J Clin Endocrinol Metab* 1993; **76**: 642–647.
172. Rocheville M, Hukovic N, Patel YC. Functional dimerization of the human somatostatin receptor subtype 5 (hSSTR5). Program Annual Meeting US Endocrine Society, New Orleans, 1998; 115. [Abstract OR46-6].
173. Rohrer L, Raulf F, Bruns C, Buettner R, Hofstaedter F, Schule R. Cloning and characterization of a fourth human somatostatin receptor. *Proc Natl Acad Sci USA* 1993; **90**: 4196–4200.
174. Rohrer SP, Birzin ET, Mosley RT, Berk SC, Hutchins SM, Shen D-M, Xiong Y, Hayes EC, Parmar RM, Foor F, Mitra SW, Degrado SJ, Shu M, Klopp JM, Cai SJ, Blake A, Chan WWS, Pasternak A, Yang L, Patchett AA, Smith RG, Chapman KT, Schaeffer JM. Rapid identification of subtype-selective agonists of the somatostatin receptor through combinatorial chemistry. *Science* 1998; **282**: 737–740.
175. Roosterman D, Glassmeier G, Baumeister H, Scherubl H, Meyerhof W. A somatostatin receptor 1 selective ligand inhibits Ca^{2+} currents in rat insulinoma 1046-38 cells. *FEBS Lett* 1998; **425**: 137–140.
176. Roth A, Kreienkamp HJ, Meyerhof W, *et al.* Phosphorylation of four amino acid residues in the carboxyl terminus of the rat somatostatin receptor subtype 3 is crucial for its desensitization and internalization. *J Biol Chem* 1997; **38**: 23769–23774.
177. Roth A, Kreienkamp HJ, Nehring RB, Roosterman D, Meyerhof W, Richter D. Endocytosis of the rat somatostatin receptors—Subtype discrimination, ligand specificity and delineation of carboxyterminal positive and negative sequence motifs. *DNA Cell Biol* 1997; **16**: 111–119.
178. Sasi R, Puebla L, Khare S, Patel YC. Polymorphism in the 5' flanking region of the human somatostatin receptor subtype 5 (hSSTR5). *Gene* 1998; **214**: 45–49.
179. Scarborough DE, Lee SL, Dinarello CA, Reichlin S. Interleukin-1 β stimulates somatostatin biosynthesis in primary cultures of fetal rat brain. *Endocrinology* 1989; **124**: 549–551.
180. Schonbrunn A, Tashjian AH Jr. Characterization of functional receptors for somatostatin in rat pituitary cells in culture. *J Biol Chem* 1978; **253**: 6473–6483.
181. Schwartz TW, Rosenkilde MM. Is there a lock for all agonist keys in 7 TM receptors. *TIPS* 1996; **17**: 213–216.
182. Schweitzer R, Madamba S, Siggins GR. Arachidonic acid metabolites as mediators of somatostatin-induced increase of neuronal M-current. *Nature* 1990; **346**: 464–466.
183. Senogles SE. The D2 dopamine receptor isoforms signal through distinct Gi alpha proteins to inhibit adenylyl cyclase. A study with site-directed mutant Gi alpha proteins. *J Biol Chem* 1994; **269**(37): 23120–23127.
184. Sharma K, Patel YC, Srikant CB. Subtype selective induction of p53-dependent apoptosis but not cell cycle arrest by human somatostatin receptor 3. *Mol Endocrinol* 1996; **10**: 1688–1696.
185. Sharma K, Srikant CB. G protein coupled receptor signaled apoptosis is associated with activation of a cation insensitive acidic endonuclease and intracellular acidification. *Biochem Biophys Res Commun* 1998; **242**: 134–140.
186. Sharma K, Srikant CB. Induction of wild type p53, bax and acidic endonuclease during somatostatin signaled apoptosis in MCF-7 human breast cancer cells. *Int J Cancer* 1998; **76**: 259–266.
187. Sharma K, Patel YC, Srikant CB. C-terminal region of human somatostatin receptor 5 is required for induction of Rb and Gi cell cycle arrest. *Mol Endocrinol* 1999; **13**: 82–90.
188. Shen LP, Rutter WJ. Sequence of the human somatostatin I gene. *Science* 1984; **224**: 168–171.
189. Shimon I, Taylor JE, Dong JZ, Bitonte RA, Kim S, Morgan B, Coy DH, Culler MD, Melmed S. Somatostatin receptor subtype specificity in human fetal pituitary culture. *J Clin Invest* 1997; **99**: 789–798.

190. Sims SM, Lussier BT, Kraicer J. Somatostatin activates an inwardly rectifying K⁺ conductance in freshly dispersed rat somatotrophs. *J Physiol* 1991; **441**: 615–637.
191. Srikant CB. Cell cycle dependent induction of apoptosis by somatostatin analog SMS201-995 in AtT-20 mouse pituitary tumor cells. *Biochem Biophys Res Commun* 1995; **209**: 400–407.
192. Srikant CB, Murthy KK, Escher E, Patel YC. Photoaffinity labelling of the somatostatin receptor: Identification of molecular subtypes. *Endocrinology* 1992; **130**: 2937–2946.
193. Srikant CB, Patel YC. Receptor binding of somatostatin-28 is tissue specific. *Nature* 1981; **294**: 259–260.
194. Srikant CB, Shen SH. Octapeptide somatostatin analog SMS 201-995 induces translocation of intracellular PTP1C to membranes in MCF-7 human breast cancer adenocarcinoma cells. *Endocrinology* 1996; **137**: 3461–3468.
195. Strader CD, Fong TM, Graziano MP, Tota MR. The family of G protein coupled receptors. *FASEB J* 1995; **9**: 745–754.
196. Sullivan SJ, Schonbrunn A. Distribution of somatostatin receptors in RINm5F insulinoma cells. *Endocrinology* 1988; **122**: 1137–1145.
197. Takano K, Yasufuku-Takano J, Teramoto A, Fujita T. G₁₃ mediates somatostatin-induced activation of an inwardly rectifying K⁺ current in human growth hormone-secreting adenoma cells. *Endocrinology* 1997; **138**: 2405–2409.
198. Takeba Y, Suzuki N, Takeno M, Asai T, Tsuboi S, Hoshino T, Sakane T. Modulation of synovial cell function by somatostatin in patients with rheumatoid arthritis. *Arthritis Rheumatism* 1997; **40**: 2128–2138.
199. Tallent M, Reisine T. Gi alpha 1 selectively couples somatostatin receptors to adenylyl cyclase in pituitary-derived AtT-20 cells. *Mol Pharmacol* 1992; **41**: 452–455.
200. Tannenbaum GS, Zhang W-H, Lapointe M, Zeitler P, Beaudet A. Growth hormone-releasing hormone neurons in the arcuate nucleus express both Sst1 and Sst2 somatostatin receptor genes. *Endocrinology* 1998; **139**: 1450–1453.
201. Taylor JE, Coy DH. The receptor pharmacology of somatostatin agonists and antagonists: Implications for clinical utility. *J Endocrinol Invest* 1997; **20**(Suppl. 7): 8–10.
202. Thomas RF, Holt BD, Schwinn DA, Liggett SB. Longterm agonist exposure induces upregulation of β 3-adrenergic receptor expression via multiple cAMP response elements. *Proc Natl Acad Sci USA* 1992; **89**: 4490–4494.
203. Thoss VS, Perez J, Duc D, Hoyer D. Embryonic and postnatal mRNA distribution of five somatostatin receptor subtypes in the rat brain. *Neuropharmacology* 1995; **34**: 1673–1688.
204. Thoss VS, Perez J, Probat A, Hoyer D. Expression of five somatostatin receptor mRNAs in the human brain and pituitary. *Arch Pharmacol* 1996; **354**: 411–419.
205. Tolon RM, Sanchez FF, de los Frailes MT, Lorenzo MJ, Cacicedo L. Effect of potassium-induced depolarization on somatostatin gene expression in cultured fetal rat cerebrocortical cells. *J Neurosci* 1994; **14**: 1053–1059.
206. Tostivini H, Likrmann I, Bucharles C, Vieau D, Coulouarn Y, Fournier A, Conlon JM, Vaudry H. Occurrence of two somatostatin variants in the frog brain: Characterization of the cDNAs, distribution of the mRNAs, and receptor-binding affinities of the peptides. *Proc Natl Acad Sci USA* 1996; **93**: 12605–12610.
207. Tran VT, Beal MF, Martin JB. Two types of somatostatin receptors differentiated by cyclic somatostatin analogs. *Science* 1985; **228**: 492–495.
208. Tsuzaki S, Moses AC. Somatostatin inhibits deoxyribonucleic acid synthesis induced by both thyrotropin and insulin-like growth factor I in FRTL5 cells. *Endocrinology* 1990; **126**: 3131–3138.
209. Vanetti M, Kouba M, Wang X, Vogt G, Holtt V. Cloning and expression of a novel mouse somatostatin receptor (SSTR2B). *FEBS Lett* 1992; **311**: 290–294.
210. Veber D, Saperstein R, Nutt R, Friedinger R, Brady S, Curley P, Perlow D, Palveda W, Colton C, Zacchei A, Tocco D, Hoff D, Vandlen R, Gerich J, Hall L, Mandarin L, Cordes E, Anderson

- P, Hirschmann R. A superactive cyclic hexapeptide analog of somatostatin. *Life Sci* 1984; **34**: 1371-1378.
211. Viana F, Hille B. Modulation of high voltage-activated calcium channels by somatostatin in acutely isolated rat amygdaloid neurons. *J Neurosci* 1996; **16**: 6000-6011.
212. Vidal C, Raully I, Zeggari M, Delesque N, Esteve JP, Saint-Laurent N, Vaysse N, Susini C. Up-regulation of somatostatin receptors by epidermal growth factor and gastrin in pancreatic cancer cells. *Mol Pharmacol* 1994; **46**: 97-104.
213. Viguerie N, Tahiri-Jouti N, Ayral AM, Cambillau C, Scemama JL, Bastie MJ, Knuhtsen S, Esteve JP, Pradayrol L, Susini C, Vaysse N. Direct inhibitory effects of a somatostatin analog, SMS 201-995, on AR4-2J cell proliferation via pertussis toxin-sensitive guanosine triphosphate-binding protein-independent mechanism. *Endocrinology* 1989; **124**: 1017-1025.
214. Visser-Wisselaar HA, Van Uffelen CJC, Van Koetsveld PM, Lichtenauer-Kaligis EGR, Waaijers AM, Uitterlinden P, Movy DM, Lamberts SWJ, Hofland LJ. 17 estradiol dependent regulation of somatostatin receptor subtype expression in the 7315 b prolactin secreting rat pituitary tumor *in vitro* and *in vivo*. *Endocrinology* 1997; **138**: 1180-1189.
215. Wang HL, Bogen C, Reisine T, Dichter M. Somatostatin-14 and somatostatin-28 induce opposite effects on potassium currents in rat neocortical neurons. *Proc Natl Acad Sci USA* 1989; **86**: 9616-9620.
216. Weckbecker G, Raulf F, Stolz B, Bruns C. Somatostatin analogs for diagnosis and treatment of cancer. *Pharmac Ther* 1993; **60**: 245-264.
217. Weckbecker G, Tolcsvai L, Stolz B, Pollack M, Bruns C. Somatostatin analogue octreotide enhances the antineoplastic effect of tamoxifen and ovariectomy on 7, 12-dimethylbenz(a)anthracene-induced rat mammary carcinomas. *Cancer Res* 1994; **54**: 6334-6337.
218. Weiss RE, Reddi AH, Nimni ME. Somatostatin can locally inhibit proliferation and differentiation of cartilage and bone precursor cells. *Calcif Tissue Int* 1981; **33**: 425-430.
219. White RE, Schonbrunn A, Armstrong DL. Somatostatin stimulates Ca^{2+} -activated K^{+} channels through protein dephosphorylation. *Nature* 1991; **351**: 570-573.
220. Wilkinson GF, Feniuk W, Humphrey PPA. Characterization of human recombinant somatostatin sst5 receptors mediating activation of phosphoinositide metabolism. *Br J Pharmacol* 1997; **121**: 91-96.
221. Wollheim CB, Winiger BP, Ullrich S, *et al.* Somatostatin inhibition of hormone release: Effects on cytosolic Ca^{2+} and interference with distal secretory events. *Metabolism* 1990; **39**(Suppl 11): 101-104.
222. Xu Y, Berelowitz M, Bruno JF. Dexamethasone regulates somatostatin receptor subtype messenger ribonucleic acid expression in rat pituitary GH₄C₁ cells. *Endocrinology* 1995; **136**: 5070-5075.
223. Xu Y, Berelowitz M, Bruno JF. Characterization of the promoter region of the human somatostatin receptor subtype 2 gene and localization of sequences required for estrogen-responsiveness. *Mol Cell Endocrinol* 1998; **139**: 71-77.
224. Xu Y, Bruno JF, Berelowitz M. Characterization of the proximal region of the rat somatostatin receptor gene, SSTR4. *Biochem Biophys Res Commun* 1995; **206**: 935-941.
225. Xu Y, Song J, Berelowitz M, Bruno JF. Estrogen regulates somatostatin receptor subtype 2 messenger ribonucleic acid expression in human breast cancer cells. *Endocrinology* 1996; **137**: 5634-5640.
226. Yamada Y, Post SR, Wang K, Tager HS, Bell GI, Sein S. Cloning and functional characterization of a family of human and mouse somatostatin receptors expressed in brain, gastrointestinal tract, and kidney. *Proc Natl Acad Sci USA* 1992; **89**: 251-255.
227. Yamada Y, Reisine T, Law SF, Ihara Y, Kubota A, Kagimoto S, Seino M, Seino Y, Bell GI, Sein S. Somatostatin receptors, an expanding gene family: Cloning and functional characterization of human SSTR3, a protein coupled to adenylate cyclase. *Mol Endocrinol* 1993; **6**: 2136-2142.

228. Yang L, Berk SC, Rohrer SP, Mosley RT, Guo L, Underwood DJ, Arison BH, Birzin ET, Hayes EC, Mitra SW, Parmar RM, Cheng K, Wu TJ, Butler BS, Foor F, Pasternak A, Pan Y, Silva M, Freidinger RM, Smith RG, Chapman K, Schaeffer JM, Patchett AA. Synthesis and biological activities of potent peptidomimetics selective for somatostatin receptor subtype 2. *Proc Natl Acad Sci USA* 1998; **95**: 10836-10841.
229. Yasuda K, Rens-Domiano S, Breder CD, Law SF, Saper CB, Reisine T, Bell GI. Cloning of a novel somatostatin receptor, SSTR3, coupled to adenylyl cyclase. *J Biol Chem* 1992; **267**: 20422-20428.
230. Yoshitomi H, Fujii Y, Miyazaki M, Nakajima M, Inagaki N, Seino S. Involvement of MAP kinase and cfos signalling in the inhibition of cell growth by somatostatin. *Am J Physiol Endocrinol Metab* 1997; **35**: E769-E774.
231. Zeggari M, Esteve JP, Raully I, Cambillau C, Mazarguil H, Dufresne M, Pradayrol L, Chayvialle JA, Vaaysse N, Susini C. Copurification of a protein tyrosine phosphatase with activated somatostatin receptors from rat pancreatic acinar membranes. *Biochem J* 1994; **303**: 441-448.
232. Zheng H, Bailey A, Jiang MH, et al. Somatostatin receptor subtype 2 knock out mice are refractory to growth hormone, negative feedback on arcuate neurons. *Mol Endocrinol* 1997; **11**: 1709-1717.
233. Zhu LJ, Krempels K, Bardin CW, O'Carroll AM, Mezey E. The localization of messenger ribonucleic acids for somatostatin receptors 1, 2, and 3 in rat testes. *Endocrinology* 1998; **139**: 350-357.

Subtype-Selective Expression of the Five Somatostatin Receptors (hSSTR1-5) in Human Pancreatic Islet Cells

A Quantitative Double-Label Immunohistochemical Analysis

Ujendra Kumar, Ramakrishnan Sasi, Sundar Suresh, Amit Patel, Muthusamy Thangaraju, Peter Metrakos, Shutish C. Patel, and Yogesh C. Patel

We have developed a panel of rabbit polyclonal antipeptide antibodies against the five human somatostatin receptor subtypes (hSSTR1-5) and used them to analyze the pattern of expression of hSSTR1-5 in normal human islet cells by quantitative double-label confocal fluorescence immunocytochemistry. All five hSSTR subtypes were variably expressed in islets. The number of SSTR immunopositive cells showed a rank order of SSTR1 > SSTR5 > SSTR2 > SSTR3 > SSTR4. SSTR1 was strongly colocalized with insulin in all β -cells. SSTR5 was also an abundant isotype, being colocalized in 87% of β -cells. SSTR2 was found in 46% of β -cells, whereas SSTR3 and SSTR4 were relatively poorly expressed. SSTR2 was strongly colocalized with glucagon in 89% of α -cells, whereas SSTR5 and SSTR1 colocalized with glucagon in 35 and 26% of α -cells, respectively. SSTR3 was detected in occasional α -cells, and SSTR4 was absent. SSTR5 was preferentially expressed in 75% of SST-positive cells and was the principal δ -cell SSTR subtype, whereas SSTR1-3 were colocalized in only a few δ -cells, and SSTR4 was absent. These studies reveal predominant expression of SSTR1, SSTR2, and SSTR5 in human islets. β -Cells, α -cells, and δ -cells each express multiple SSTR isoforms, β -cells being rich in SSTR1 and SSTR5, α -cells in SSTR2, and δ -cells in SSTR5. Although there is no absolute specificity of any SSTR for an islet cell type, SSTR1 is β -cell selective, and SSTR2 is α -cell selective. SSTR5 is well expressed in β -cells and δ -cells and moderately well expressed in α -cells, and thereby it lacks the islet cell selectivity displayed by SSTR1 and SSTR2. Subtype-selective SSTR expression in islet cells could be the basis for preferential insulin suppression by SSTR1-specific ligands and of glucagon inhibition by SSTR2-selective compounds. *Diabetes* 48:77-85, 1999

From Fraser Laboratories, Departments of Medicine and Neurology and Neurosurgery (Y.C.P., U.K., R.S., M.T.), and Surgery (P.M.), McGill University, Royal Victoria Hospital, and the Montreal Neurological Institute, Montreal, Quebec, Canada, and Neurobiology Research Laboratory (S.S., A.P., S.C.P.), VA Connecticut Health Care System, Newington, Connecticut.

Address correspondence and reprint requests to Dr. Yogesh C. Patel, Room M3-15, Royal Victoria Hospital, 687 Pine Ave. West, Montreal, Quebec H3A 1A1, Canada. E-mail: patel@rvhmed.lan.mcgill.ca.

Received for publication 24 April 1998 and accepted in revised form 31 August 1998.

BSA, bovine serum albumin; ECL, extracellular loop; FITC, fluorescein isothiocyanate; hSSTR, human somatostatin receptor; ICL, intracellular loop; IgG, immunoglobulin G; rSSTR, rat somatostatin receptor; SST, somatostatin; SSTR, somatostatin receptor; TBS, Tris-buffered saline.

Somatostatin (SST), a multifunctional peptide, is produced in many cells throughout the body, most notably in the brain, gastrointestinal tract, and pancreas (1,2). There are two endogenous bioactive forms of SST, i.e., SST-14 and SST-28, that act on a diverse array of endocrine, exocrine, neuronal, and immune cell targets to inhibit secretion, modulate neurotransmission, and regulate cell division (1-4). These actions are mediated by a family of G-protein-coupled receptors with five known subtypes, termed SSTR1-5, that are widely expressed in the brain and periphery in a tissue- and subtype-selective manner (3,4). All five SSTRs are functionally coupled to inhibition of adenylyl cyclase (3). Some of the receptor subtypes also signal through other effectors, such as phosphotyrosine phosphatase, K^+ , and voltage-dependent Ca^{2+} ion channels, a Na^+/H^+ exchanger, phospholipase C, phospholipase A_2 , and mitogen-activated protein kinase (3). SST-14 and SST-28 bind to all five human SSTR (hSSTR) subtypes with nanomolar affinity (5). SSTR1-4 bind the two peptides approximately equally, whereas SSTR5 displays weak selectivity for SST-28 (5). This is in contrast to the current generation of clinically used SST analogs, the octapeptides octreotide and lanreotide, which bind to only three SSTRs displaying high affinity for SSTR2 and SSTR5 and moderate affinity for SSTR3 (3-5). SSTRs are dynamically regulated at the membrane in a time-dependent manner by agonist treatment (6-9). SSTR2, SSTR3, SSTR4, and SSTR5 undergo acute desensitization and are variably internalized, whereas SSTR1 is resistant to internalization (6-9). Furthermore, during long-term agonist treatment, SSTR1 and to a lesser extent SSTR2 and SSTR4 are upregulated at the membrane, whereas there is no effect on SSTR3 and SSTR5 (6).

The pancreas is an important target of SST action, and with increasing use of SST analogs for treating neuroendocrine tumors and various digestive disorders, a great deal of interest is currently focused on the effects of long-term SST pharmacotherapy on islet cell function and the nature of the SSTR subtypes expressed in islet cells (1,2,10,11). SST is produced in the pancreas in islet δ -cells and acts directly on β -cells and α -cells to inhibit both the synthesis and secretion of insulin and glucagon (12-15). SST also inhibits pancreatic polypeptide as well as endogenous SST secretion from δ -cells through an autocrine feedback mechanism (2,16,17). Specific

high-affinity binding sites for SST have been demonstrated in isolated rat islets, cultured islet cells, and hamster (HIT) and rat (Rin M5f) insulinoma cells (2,18–24). By quantitative electron microscopic autoradiography, binding sites for SST have been identified in β -cells, α -cells, and δ -cells in cultured rat islet preparations (18,21,22). Furthermore, using SST-14-selective and SST-28-selective radioligands, SS-28-preferring sites have been shown to predominate on β -cells and SST-14 sites on α -cells (21). At a molecular level, little progress has been made in characterizing the pattern of expression of the five cloned SSTR subtypes in individual islet cell subpopulations. Preliminary evidence based on reverse transcriptase polymerase chain reaction has shown expression of mRNA for each of the five SSTR subtypes in whole rat islets (25). By immunohistochemistry, SSTR2 has been recently reported to be localized in α -cells and PP-cells but not in β -cells of rat islets (26). In contrast to the rat, nothing is currently known about the expression of SSTRs in human islets. Furthermore, because of known species-specific variations in SSTR expression, the results of rat islet SSTRs may not apply to human islets (2–4). Accordingly, in the present study, we have developed and characterized a panel of SSTR1–5-selective polyclonal antibodies and applied them to study the immunohistochemical colocalization of the receptor isotypes in human islet cells as a necessary step toward elucidating differential islet cell SSTR expression and subtype-specific regulation of individual pancreatic hormones.

RESEARCH DESIGN AND METHODS

Reagents and cell lines expressing SSTRs. Porcine monocomponent insulin and porcine glucagon were obtained from Novo Nordisk (Copenhagen, Denmark). Synthetic SST-14 was purchased from Bachem (Torrance, CA). Antisera to islet hormones were obtained as gifts as follows: guinea pig anti-insulin serum (P. Wright, Indianapolis, IN); sheep ant glucagon serum (R.A. Donald, Christchurch, New Zealand); and mouse monoclonal anti-SST-14 (J.C. Brown, Vancouver, British Columbia). Rhodamine-conjugated goat anti-rabbit secondary antibody as well as anti-guinea pig, anti-sheep, and anti-mouse fluorescein isothiocyanate (FITC)-conjugated secondary antibodies were obtained from Jackson Laboratory (Bar Harbor, ME). Stable CHO-K1 transfectants individually expressing hSSTR1–5 were prepared as described previously and cultured in Ham's F12 medium containing 10% fetal calf serum and 400 μ g/ml G418 (27).

Production and characterization of SSTR antibodies. Rabbit polyclonal antibodies were raised against synthetic oligopeptides of 13–22 mer corresponding to sequences in the C-tail, the third intracellular loop (ICL), or the second extracellular loop (ECL) of human or rat SSTR (rSSTR) as shown below. The sequences selected were identical in the case of human and rat SSTR1 and SSTR2 or differed by a single amino acid residue in the case of SSTR4 (4). The

rSSTR3 and rSSTR5 oligopeptides showed 50 and 70% sequence identity with the corresponding regions of the human receptors (4).

hSSTR1-C-tail	LKSRAYSVEDFQPENL
hSSTR2-C-tail	DGERSDSKQDKSRLNETTETQR
rSSTR3-3rd ICL	RAPSCQWVQAPACQRRR
rSSTR4-2nd ECL	DTRPARGGEAVAC
rSSTR5-C-tail	RRGYGMEDADAIEPRP

Peptides were conjugated to keyhole limpet hemocyanin and the complexes used for rabbit immunization (27). Anti-SSTR activity in rabbit sera was screened by dot-blot analysis against the peptide antigens. Antibodies identified in this way were purified from whole serum by immunoaffinity chromatography using the immunizing peptides cross-linked to activated agarose beads. Immunoaffinity-purified SSTR antibodies were characterized by Western blot analysis and immunocytochemistry using CHO-K1 cells individually transfected with hSSTR1–5.

Western blot analysis. Brain membranes were prepared from cerebrocortical tissue freshly obtained from male Sprague-Dawley rats for analysis of SSTR proteins. Membrane protein (35- μ g) was solubilized in sample buffer containing 62.5 mmol/l Tris-HCl, pH 6.8, 2% SDS, 10% glycerol, and 50 mmol/l dithiothreitol and fractionated by electrophoresis on 10% SDS polyacrylamide gels as described by Laemmli (28). The fractionated proteins were transferred by electrophoresis to 0.2 μ m nitrocellulose membranes (Protran BA83; Schleicher & Schuell, Keene, NH) in a transfer buffer containing 0.025 mol/l Tris, 0.192 mol/l glycine, and 15% methanol. The membranes were blocked with 5% bovine serum albumin (BSA) in Tris-buffered saline (TBS) (50 mmol/l Tris-HCl, pH 7.4, 1.5% NaCl) containing 0.2% Tween 20 for 3 h at 20°C and subsequently incubated overnight at 4°C with affinity-purified SSTR1–5 antisera or antigen-preabsorbed antisera (2 μ g/ μ l), each diluted 1:400 in TBS containing 0.2% Tween 20. Immunoreactive bands were detected by exposure to X-ray films processed for chemiluminescent detection (CSPD; Boehringer Mannheim, Indianapolis, IN). For molecular weight estimates, the 10 kDa protein ladder standard (Life Technologies, Bethesda, MD) was used.

Immunocytochemistry. CHO-K1 cells were fixed in 4% paraformaldehyde and processed for immunocytochemistry as previously described (27). Pancreases were freshly obtained from three accidentally deceased individuals (2 men, 1 woman, age range 34–56 years) through the McGill Pancreas Transplantation Program. Pancreases were removed by dissection, perfused with University of Wisconsin solution, and stored at 48°C for 8–12 h (cold ischemia time) before fixation in 4% formaldehyde for 2 h at room temperature and embedding in paraffin. Sections (5 μ m) were deparaffinized and incubated in 1% BSA and 5% normal goat serum in TBS for 1 h at room temperature. Sections were then incubated with SSTR antibodies (affinity-purified and diluted 1:500–1:700 in TBS) at 48°C overnight in a humid atmosphere. After three successive washes in TBS, sections were incubated with rhodamine-conjugated goat anti-rabbit immunoglobulin G (IgG) (diluted 1:100 in TBS) for 60 min at room temperature, and after several additional washes in TBS, they were mounted in Immunofluor mounting medium for visualization under a confocal microscope. For double immunofluorescence localization of SSTR1–5 with insulin, glucagon, and SST, sections were first immunostained for SSTR1–5 and then processed for islet hormone localization using a similar protocol to that for SSTR immunohistochemistry. Sections were incubated overnight at 48°C with guinea pig anti-insulin serum (1:800), sheep anti-glucagon serum (1:1,000), or anti-mouse monoclonal SST-14 (1:100) antibodies. After three washes in TBS, sections were incubated with

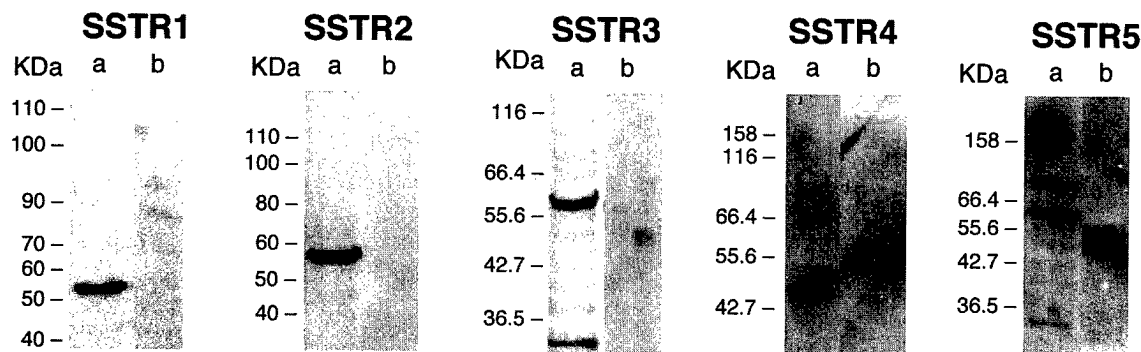


FIG. 1. Western blot analysis of SSTR1–5 in rat brain membranes. Membrane protein (35- μ g) was fractionated by SDS-PAGE and probed with immunoaffinity-purified SSTR antisera (lane a of each pair) or antigen-preabsorbed antibody (lane b of each pair). Major protein bands of 53 (SSTR1), 57 (SSTR2), 60 (SSTR3), 44 (SSTR4), and 58 kDa (SSTR5) were obtained. The bands were specific and were inhibited in the presence of antigen-absorbed antibody. Note that 10-kDa protein ladder standards were used for molecular weight estimates. Data are representative of three experiments.

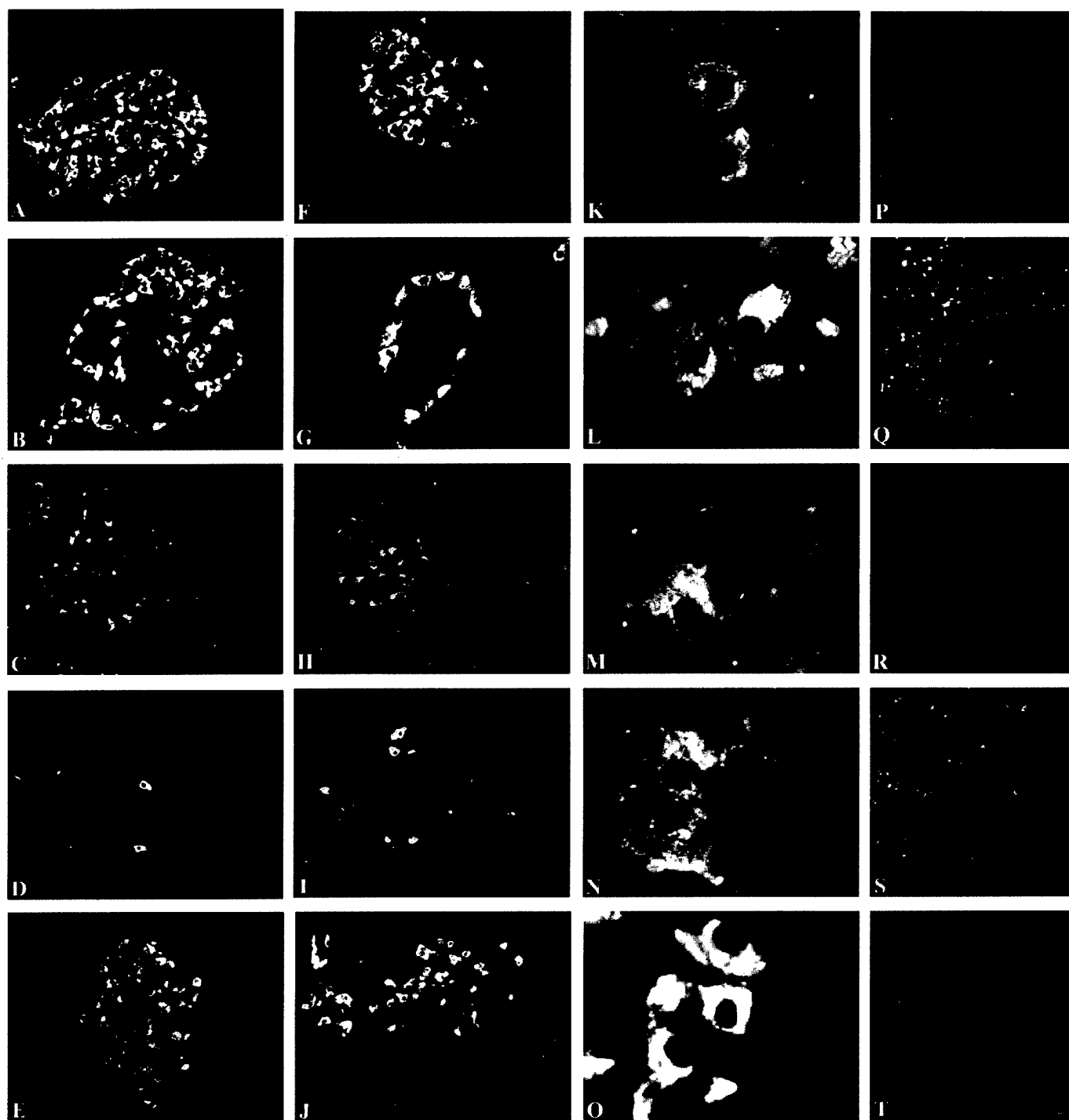


FIG. 2. A–J: Confocal images depicting the immunohistochemical localization of SSTR1–5 in representative islet sections. Sections were immunolabeled with anti-rabbit SSTR antibodies followed by rhodamine-conjugated goat anti-rabbit IgG. All five SSTRs are localized in islet cells with a rich expression of subtypes 1, 2, and 5 and relatively weak expression of subtypes 3 and 4. Note the differential expression of SSTR2 in large islets (many cells labeled) and small islets (only peripheral cells labeled). **K–O:** High-powered images showing SSTR immunoreactivity both as surface membrane and cytosolic immunofluorescence. Control sections in which the SSTR primary antibodies were replaced with antigen-preabsorbed serum show no immunoreactivity (**P–T**). Scale bar represents 10 μ m for panel G, 5 μ m for panels K–O, and 25 μ m for the remaining panels.

FITC-conjugated goat anti-guinea pig, goat anti-sheep, and goat anti-mouse secondary antibody to visualize insulin, glucagon, and SST, respectively. Sections were then washed again in TBS and mounted in Immunofluor.

All fluorescent images were visualized on a Zeiss LSM 410 inverted confocal microscope (Carl Zeiss, Inc., Thornwood, NY) equipped with an argon-krypton laser. Rhodamine signals for SSTR1–5 were imaged by exciting samples with a helium/neon (543 nmol/l) laser. Fluorescein signals for insulin, glucagon, and SST in the same field were obtained by excitation with a 488 nmol/l line from an argon/krypton laser. The images were overlapped for colo-

calization of SSTRs in insulin, glucagon, and SST immunoreactive cells. Images were obtained as single optical sections taken from the tissue and averaged over 32 scans per frame. All images were archived on Iomega Jaz disk (Iomega, Roy, UT) and printed on a Kodak XLS8300 high resolution (300 dpi) color printer. To validate the specificity of SSTR immunoreactivity, the following controls were included: 1) preimmune serum in place of primary antibody; 2) primary antibody absorbed with excess antigen; and 3) nontransfected CHO-K1 cells. Antigen-absorbed antibody was used as a control for insulin, glucagon, and SST immunofluorescence.

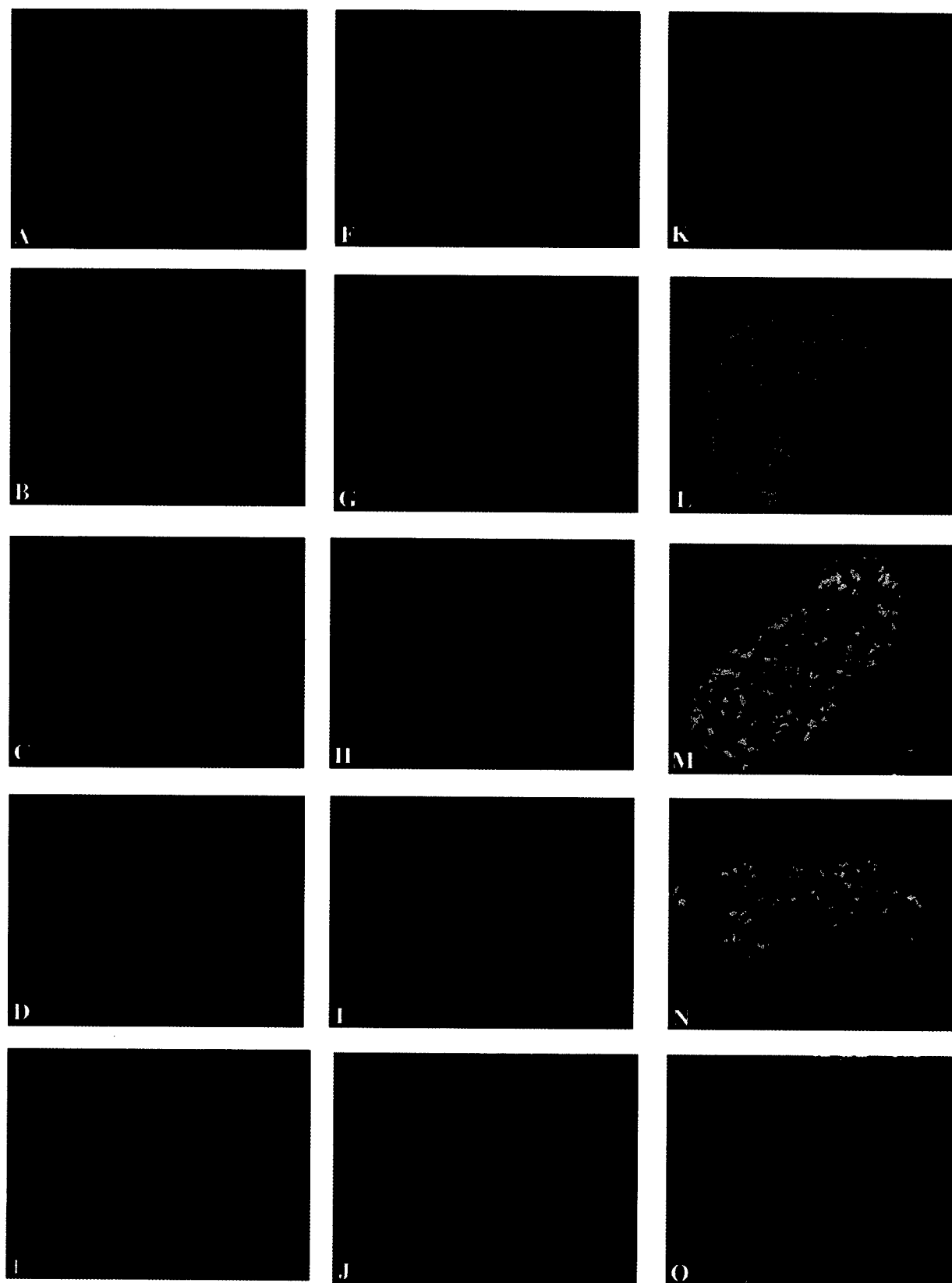


FIG. 3. Confocal images of representative islets double-labeled for immunofluorescence for SSTR1–5 and insulin. SSTR immunoreactivity is localized by rhodamine (red) fluorescence in *A–E*. Insulin-positive cells are identified by green immunofluorescence in the same sections (*F–J*). Coexpression of SSTRs with insulin is indicated by a yellow-orange color (*K–O*). These $1,100 \times 800$ pixel images constructed in a single composite do not fully reflect the quality of the fields viewed through the microscope. Please refer to the *METHODS* section for details of the primary antibodies and controls used for colocalization. Scale bar = 25 μ m.

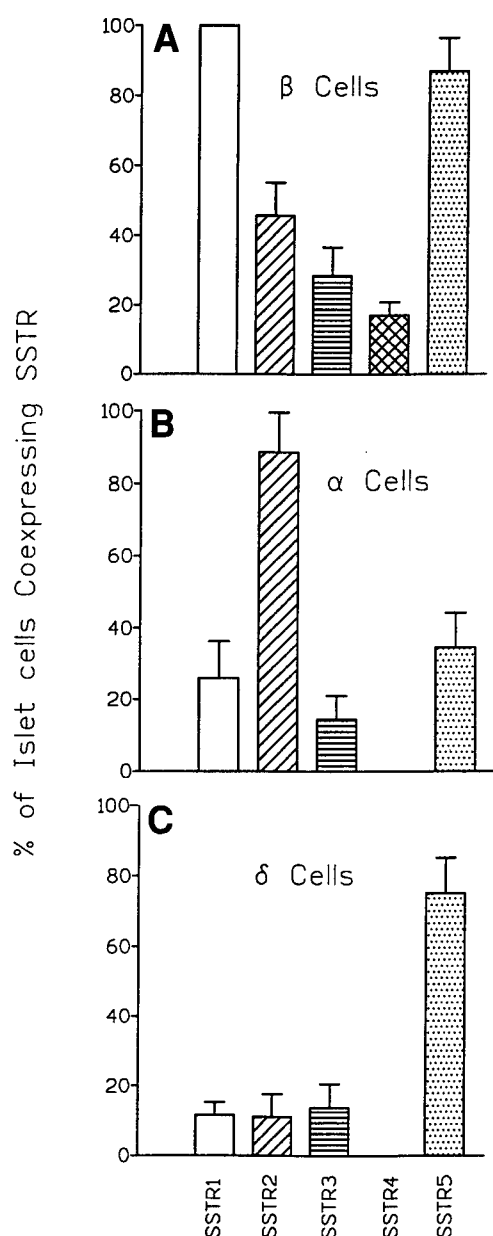


FIG. 4. Quantitative analysis of the expression of SSTR1–5 in β -cells, α -cells, and δ -cells. Bars represent the mean \pm SE ($n = 3$) percent of cells positive for a given SSTR subtype in 8–20 islets from each of the three pancreases. A mean of $1,081 \pm 80$ β -cells, 432 ± 28 α -cells, and 221 ± 12 δ -cells were analyzed.

Quantitative analysis. The three pancreases were subjected to quantitative analysis to determine the percent of insulin-, glucagon-, and SST-positive cells that colocalized SSTR1–5. The mean percent of β -cells, α -cells, and δ -cells coexpressing a given SSTR subtype was determined in 8–20 islets from each pancreas, and the results are presented as means \pm SE ($n = 3$). Because islets in a given section varied in size, they were randomly selected to include both large and small islets. There were $1,081 \pm 80$ insulin-positive cells, 432 ± 28 glucagon-positive cells, and 221 ± 12 SST-positive cells analyzed for colocalization of each of the five SSTRs.

RESULTS

Specificity of SSTR1–5 antibodies. Figure 1 illustrates Western blots of SSTR1–5 in rat brain membranes probed with immunoaffinity-purified SSTR antisera. Major protein bands of 53 kDa (SSTR1), 57 kDa (SSTR2), 60 kDa (SSTR3), 44 kDa (SSTR4), and 58 kDa (SSTR5) were obtained. Additional

minor bands of 43 kDa (SSTR1), 90 kDa (SSTR3), and 75 kDa (SSTR5) were observed in the case of three of the SSTRs. The bands were specific and were inhibited in the presence of antigen-absorbed antibody. CHO-K1 cells stably transfected with individual hSSTR1–5 displayed positive fluorescence only when reacted with the corresponding SSTR primary antibody (data not shown). There was no cross-reactivity of any of the five SSTR antisera with another (nonhomologous) subtype.

Distribution of SSTR1–5 in pancreatic islets. Figure 2 shows representative islets from different parts of the pancreas single-stained with SSTR1–5. The five SSTRs were variably expressed in all islets examined (Fig. 2A–J). Rhodamine immunofluorescence was confined mainly to islet endocrine cells and to occasional nonislet cells and was distributed both on the cell surface and in cytoplasmic vesicular structures (Fig. 2K–O). All islets displayed intense SSTR1 immunofluorescence in the majority of cells. In the case of SSTR2, two populations of islets of large and small size were identified with different patterns of expression of this subtype (Fig. 2B and G). Large islets expressed SSTR2 in many cells in the center as well as the periphery, whereas in smaller islets, SSTR2-positive cells were confined to the peripheral mantle zone. SSTR3 and SSTR4 were expressed in only a few islet cells, whereas SSTR5 was localized in the majority of islet cells. Quantitative analysis of the total number of SSTR immunopositive islet cells showed a rank order of SSTR1 > SSTR5 > SSTR2 > SSTR3 > SSTR4. Outside the islet, SSTR2 was readily identified in the walls of many small and medium arterioles; scattered nonislet cells with a neuronal appearance were positive for SSTR1, SSTR2, and SSTR3 (not shown).

Colocalization of SSTR1–5 with insulin in islet β -cells.

To determine the pattern of expression of SSTR1–5 in individual islet cell subpopulations, we undertook a quantitative analysis by double-label immunofluorescence confocal microscopy of SSTR antigens with insulin, glucagon, and SST. Figure 3A–E shows rhodamine immunofluorescent localization of SSTR1–5 (in red) in representative islet samples. β -cells were identified in the same sections by fluorescein immunofluorescence with insulin antibody (in green) and accounted for ~80% of the islet endocrine cells (Fig. 3F–J). Overlapping the SSTR and insulin immunofluorescent images revealed colocalization of SSTR1–5 with insulin (yellow-orange color) (Fig. 3K–O). By quantitative analysis, SSTR1 colocalized strongly with all insulin-positive cells and was the predominant β -cell SSTR (Fig. 4A). SSTR2 colocalized with $46 \pm 9\%$ of insulin-producing cells, whereas SSTR3 and SSTR4 were relatively poorly expressed in $28 \pm 8\%$ and $17 \pm 4\%$ of β -cells, respectively. SSTR5 was also a β -cell-abundant isotype, being colocalized in $87 \pm 10\%$ of cells. Overall, the relative frequency of SSTR expression in β -cells was SSTR1 > SSTR5 > SSTR2 > SSTR3 > SSTR4.

Colocalization of SSTR1–5 with glucagon in islet α -cells.

Figure 5 depicts representative islet sections processed for colocalization of SSTR1–5 (rhodamine fluorescence, red) with glucagon (fluorescein immunofluorescence, green). As expected, glucagon-producing α -cells were much less numerous than β -cells and were scattered both within the core region of the islet as well as around the islet mantle (Fig. 5F–J). Colocalization of SSTR1–5 with glucagon (Fig. 5K–O) showed a different profile of SSTR expression compared with β -cells. SSTR1-positive cells colocalized with only $26 \pm 10\%$ of glucagon-positive cells

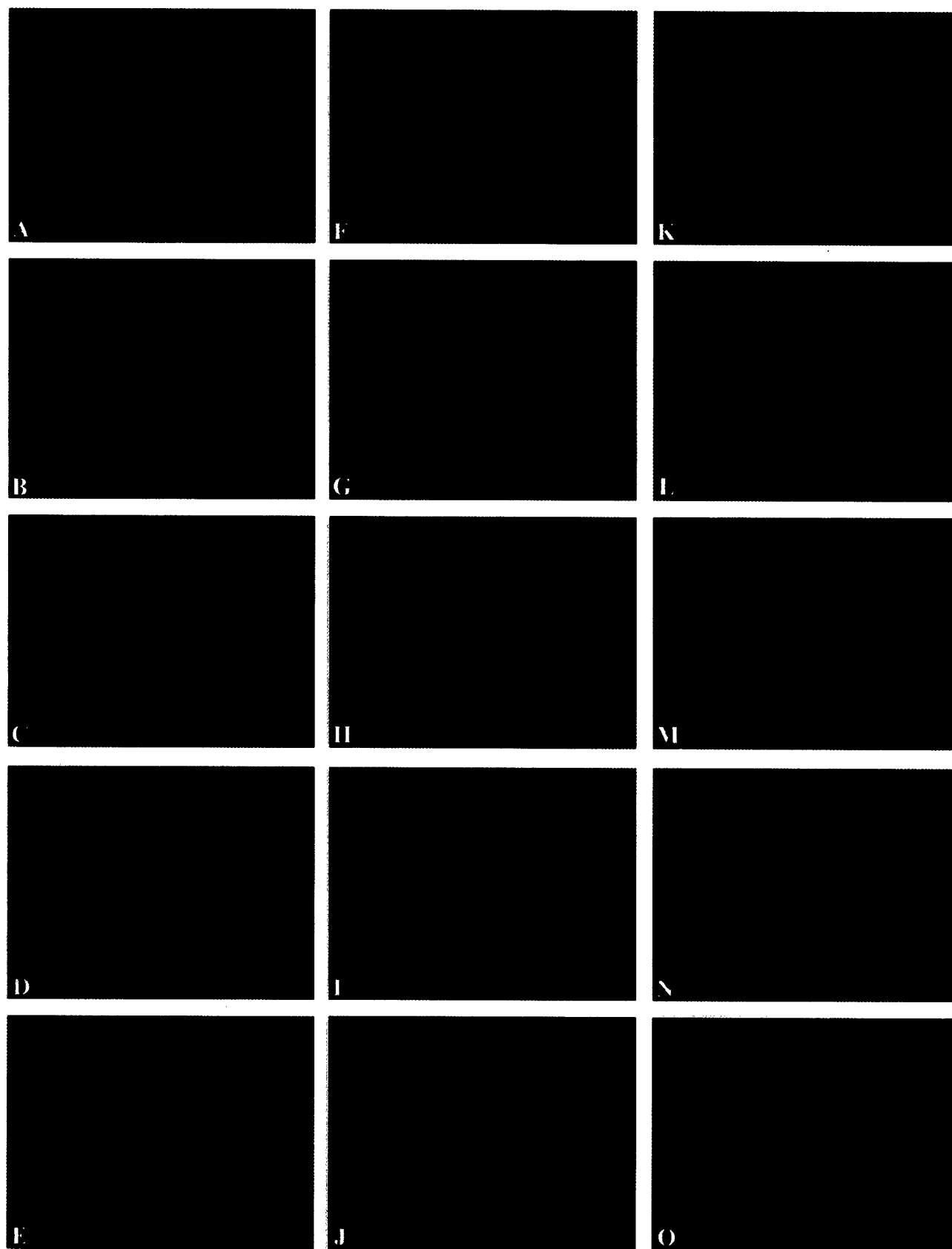


FIG. 5. Confocal images of pancreatic islet cells double-labeled for immunofluorescence for SSTR1-5 and glucagon. SSTR immunoreactivity is localized by rhodamine (red) fluorescence in A-E. Glucagon-positive cells are identified by green immunofluorescence in the same sections (F-J). Coexpression of SSTRs with glucagon is indicated by a yellow-orange color (K-O). For details of the primary antibodies and controls used for colocalization, refer to the METHODS section. See also legend to Fig. 3. Scale bar = 25 μ m.

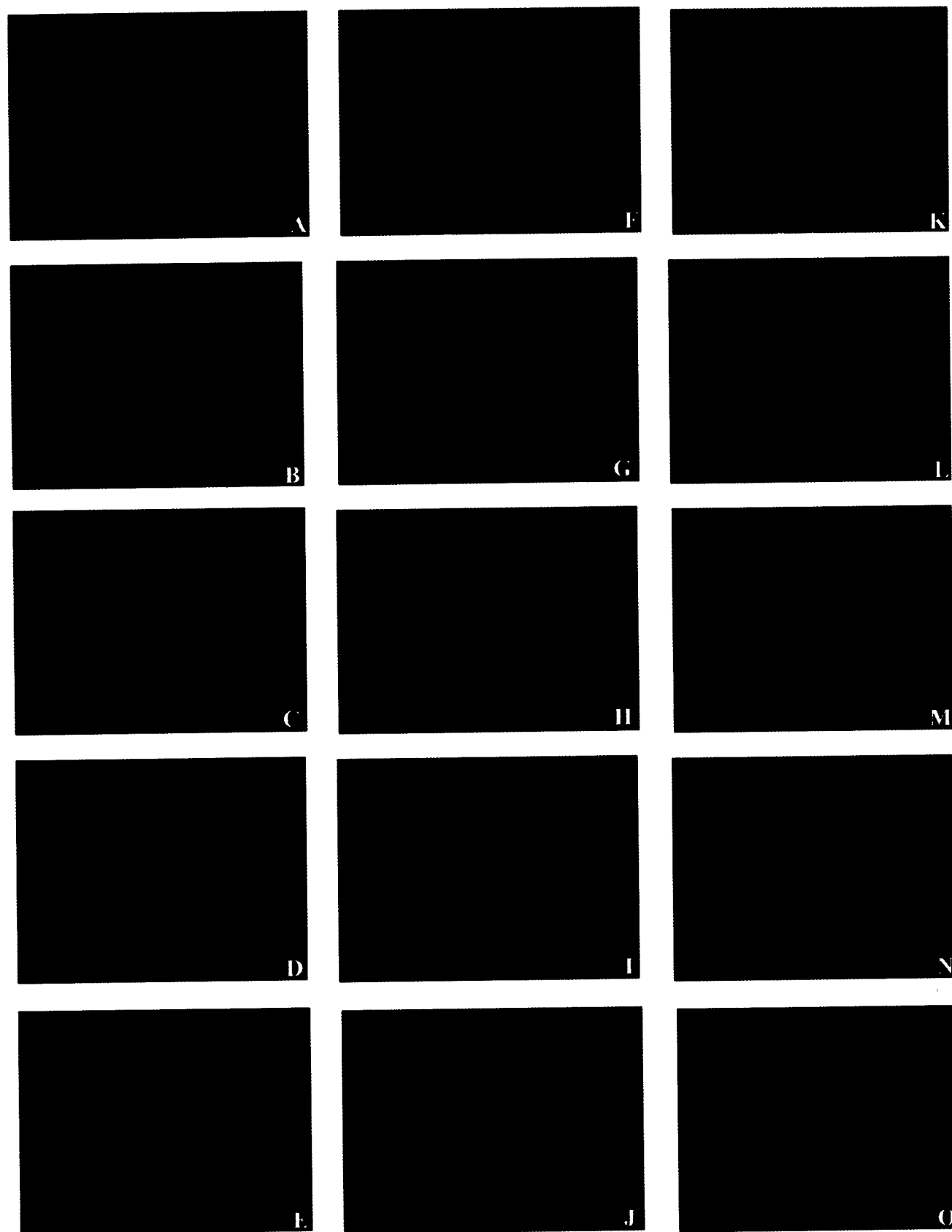


FIG. 6. Confocal images of pancreatic islet cells double-labeled for immunofluorescence for SSTR1-5 and SST. SSTR immunoreactivity is localized by rhodamine (red) fluorescence in A-E. SST-positive cells are identified by green immunofluorescence in the same sections (F-J). Coexpression of SSTRs with SST is indicated by a yellow-orange color (K-O). For details of the primary antibodies and controls used for colocalization, refer to the METHODS section. See also legend to Fig. 3. Scale bar = 25 μ m.

(Fig. 4B). SSTR2 was the predominant α -cell subtype, being colocalized in $89 \pm 11\%$ of glucagon-positive cells. SSTR3 immunofluorescence was confined to a small subset ($14 \pm 6\%$ of glucagon-positive cells), whereas SSTR4 was absent in α -cells (Fig. 5M–N). SSTR5 was moderately well colocalized with glucagon, being detected in $35 \pm 10\%$ of the α -cells (Figs. 5O and 4B).

Colocalization of SSTR1–5 with SST in δ -cells. Figure 6 shows the results of SSTR1–5 colocalization with SST in representative islet sections. SST-producing cells were identified as a sparse population of cells distributed within both the center and peripheral regions of the islet (Fig. 6F–J). A distinctive pattern of SSTR1–5 expression in δ -cells was observed that differed from that in β - and α -cells (Fig. 6K–O). SSTR5 was preferentially expressed in $75 \pm 10\%$ of SST-positive cells and was the predominant δ -cell SSTR subtype (Figs. 6O and 4C). In contrast, SSTR1–3 antigens were colocalized in only a few δ -cells, comprising 12 ± 4 , 11 ± 6 , and $14 \pm 6\%$ of the total SST-positive cells, respectively (Figs. 6K–M and 4C). As in the case of α -cells, SSTR4 was also absent from δ -cells (Fig. 6N). **SSTR subtype selectivity for β -cell, α -cell, and δ -cell expression.** A comparison of SSTR subtype selectivity for islet cell expression showed preferential expression of SSTR1 in β -cells and of SSTR2 in α -cells (Fig. 4). Such selectivity in the case of SSTR2 was relative rather than absolute, since approximately half the β -cells also expressed SSTR2. SSTR5 was well expressed in β -cells and δ -cells and moderately well expressed in α -cells, and thereby, it did not display the same degree of selectivity as SSTR1 and SSTR2. SSTR4, a weakly expressed islet subtype, was nonetheless only found in β -cells. SSTR3 was the least distinctive subtype, being constitutively expressed in 10–20% of all islet cells examined.

DISCUSSION

The present study represents the first description of the pattern of expression of the five SSTRs in normal human pancreas. All five SSTRs were detected in islets, with a rich expression of subtypes 1, 2, and 5 and relatively weak expression of subtypes 3 and 4. The five SSTRs displayed a cell-specific and subtype-specific pattern of expression in β -cells, α -cells, and δ -cells. All β -cells expressed SSTR1, and the majority coexpressed SSTR5, making these two isoforms the predominant β -cell SSTRs. α -cells preferentially expressed SSTR2, and δ -cells were selective for SSTR5. SSTR1 is thus β -cell-selective and SSTR2 α -cell-selective. SSTR5 was well expressed in β -cells and δ -cells and moderately well expressed in α -cells, thereby lacking the islet cell selectivity displayed by SSTR1 and SSTR2.

Because there are no monospecific agonists or antagonists currently available for any of the individual SSTR subtypes (3), we developed a panel of rabbit polyclonal antipeptide SST antibodies as tools for studying the cellular distribution of each individual SSTR protein. The specificity of our antibodies for the human receptors was validated by confocal immunofluorescence analysis of CHO-K1 cells individually transfected with hSSTR1–5. In addition, to reduce background immunoreactivity, we used only affinity-purified antibodies for Western blot analysis and immunocytochemistry, and we confirmed specific labeling in each case by using optimally titrated antibody concentrations and by inhibition with antigen-preabsorbed antibody controls. For colocalization experiments, we used primary antibodies against

the SSTRs and islet hormones that were raised in different species. Antibodies were directed against both rat and human receptor sequences and by immunoblot analysis of rat brain membranes reacted in each case with a single predominant protein species. The size of rSSTR1 (53 kDa) is within the range reported for hSSTR1 expressed in BHK-cells (53–72 kDa) (29). Likewise, the sizes of our rSSTR3 and rSSTR4 were similar or virtually identical to those described for the human isoforms of these two subtypes (29). Our estimate of the molecular mass of rSSTR5 (58 kDa) is comparable to that of the human receptor (52–66 kDa), although both are somewhat smaller than the receptor size recently described for pituitary rSSTR5 (29,30). In the case of SSTR2, our protein band of 57 kDa is within the range described previously for this subtype in rat brain and mouse AtT-20 cells and for hSSTR2 in transfected HEK-293 cells (29,31). Others, however, have found a somewhat larger SSTR2 protein of 90 kDa by immunoblot analysis in rat brain and pancreas (26,32). These differences may be explained by variations in antibody specificity, the presence of multiple bands, and differential glycosylation of the receptor protein in the different transfected cell lines and tissues studied.

Human islets were rich in SSTRs, expressing all five subtypes. Islets thus join other tissues, such as the rat brain and pituitary, which also have been shown to coexpress the full SSTR family (2–4,26,33). SSTR1 was a major islet cell receptor and was expressed in all β -cells. This contrasts with the poor expression of SSTR1 in the pituitary, especially in rat somatotrophs, which are virtually devoid of this subtype (27). Most β -cells also expressed SSTR5 and half expressed SSTR2, which means that individual β -cells coexpress SSTR1 with SSTR5 and that a small subpopulation features some of the remaining subtypes. Increasing evidence points to the occurrence of multiple SSTR subtypes in many different types of tumor cells as well as in normal cells, such as the pituitary, that have been characterized in detail (27,30,31,33). Because all five SSTR isoforms bind the natural ligands SST-14 and SST-28 with nanomolar affinity and share common signaling pathways, such as the inhibition of adenylyl cyclase, the functional significance of more than one SSTR subtype in the same cell remains unclear at the moment (3,4). Whether the different SSTRs subserve different biological roles in the same cell or cooperate through, e.g., dimerization, to create greater signaling diversity remains to be determined (34,35).

Our findings suggest that SST regulation of β -cell function is mediated via SSTR1 and SSTR5, the two predominant subtypes expressed in this cell. Binding studies using quantitative autoradiography have suggested a preponderance of SST-28 compared with SST-14 sites in rat β -cells, presumably reflecting preferential expression of the SST-28-selective SSTR5 subtype, but whether this applies also to human islets will require additional quantitative studies with subtype-selective ligands (21). The pattern of expression of SSTRs in α -cells was much more selective than that in β -cells. Virtually all of these cells expressed SSTR2, whereas coexpression of the remaining subtypes was restricted to 15–30% of cells. Our finding of the preferential expression of SSTR2 with glucagon is in agreement with similar results obtained by immunohistochemistry with SSTR2 antibody in the rat pancreas, and along with earlier autoradiographic data showing preferential labeling of α -cells with SST-14 compared with SST-28-selective ligands, it suggests that SSTR2

is the likely mediator of SST action in α -cells (21,26). Like α -cells, δ -cells also displayed a subtype-selective pattern of SSTR expression with virtually exclusive expression of SSTR5. The presence of specific SSTRs on δ -cells is consistent with the well-known ability of synthetic analogs of SST to inhibit endogenous SST secretion by autocrine feedback (17). Furthermore, the finding of SSTR5 as the δ -cell SSTR corroborates our earlier autoradiographic finding of mainly SST-28-selective binding sites on this cell type (20).

The present results have important functional and therapeutic implications. The predominant expression of SSTR1 and SSTR5 in β -cells and of SSTR2 in α -cells helps to explain the differential sensitivity of human and monkey islets to insulin suppression by SST-14 and to glucagon inhibition by octreotide (36,37). It may also explain the relatively benign effect of octapeptide SST analogs, like octreotide, on carbohydrate tolerance during long-term therapy. This is because SSTR1, a major β -cell SSTR, does not bind octreotide and SSTR5 in β -cells would likely desensitize with time, whereas the α -cell SSTR2 subtype would upregulate with continued SST treatment and remain responsive (5,6). Our finding of subtype-selective expression of SSTRs in islet cells now provides a rational basis for the development of SSTR1-specific ligands for preferential insulin suppression and of SSTR2-selective compounds for glucagon inhibition.

ACKNOWLEDGMENTS

This work was supported by grants from the Canadian Medical Research Council, the National Institutes of Health, and the U.S. Department of Defense. Y.C.P. is a Distinguished Scientist of the Canadian Medical Research Council.

We thank M. Correia for secretarial help.

REFERENCES

- Reichlin S: Somatostatin. *N Engl J Med* 309:1495-1501, 1556, 1563, 1983
- Patel YC, Liu J-L, Galanopoulou AS, Papachristou DN: Production, action, and degradation of somatostatin. In *The Handbook of Physiology: The Endocrine Pancreas and Regulation of Metabolism*. Jefferson LS, Cherrington AD, Eds. New York, Oxford University Press. In press
- Patel YC, Srikant CB: Somatostatin receptors. *Trends Endocrinol Metab* 8:398-405, 1997
- Reisine T, Bell GI: Molecular biology of somatostatin receptors. *Endocr Rev* 16:427-442, 1995
- Patel YC, Srikant CB: Subtype selectivity of peptide analogs for all five cloned human somatostatin receptors (hSSTR1-5). *Endocrinology* 135:2814-2817, 1994
- Hukovic N, Panetta R, Kumar U, Patel YC: Agonist-dependent regulation of cloned human somatostatin receptor types 1-5 (hSSTR1-5): subtype selective internalization or upregulation. *Endocrinology* 137:4046-4049, 1996
- Nouel D, Gaudriault G, Houle M, Reisine T, Vincent JP, Mazella J, Beaudet A: Differential internalization of somatostatin in COS-7 cells transfected with SSTR1 and SSTR2 receptor subtypes: a confocal microscopic study using novel fluorescent somatostatin derivatives. *Endocrinology* 138:296-306, 1997
- Hipkin RW, Friedman J, Clark RB, Eppler CM, Schonbrunn A: Agonist-induced desensitization, internalization, and phosphorylation of the SST_{2A} somatostatin receptor. *J Biol Chem* 271:13869-13876, 1997
- Roth A, Kreienkamp HJ, Meyerhoff W, Richter D: Phosphorylation of four amino acid residues in the carboxyl terminus of the rat somatostatin receptor subtype 3 is crucial for its desensitization and internalization. *J Biol Chem* 272:23769-23774, 1997
- Lamberts SWJ, Van Der Lely AJ, de Herder WW: Drug therapy: octreotide. *N Engl J Med* 334:246-254, 1996
- Koerker DJ, Ruch W, Chideckel E, Palmer J, Goodner CJ, Ensink J, Gale CC: Somatostatin: hypothalamic inhibitor of the endocrine pancreas. *Science* 184:482-483, 1974
- Dubois MP: Immunoreactive somatostatin is present in discrete cells of the endocrine pancreas. *Proc Natl Acad Sci U S A* 72:1340-1343, 1975
- Mandarino L, Stenner D, Blanchard W, Nissen S, Gerich J, Ling N, Brazeau P, Bohlen P, Esch F, Guillemin R: Selective effects of somatostatin-14, -25, and -28 on *in vitro* insulin and glucagon secretion. *Nature* 291:76-77, 1981
- Philippe J: Somatostatin inhibits insulin-gene expression through a post-transcriptional mechanism in a hamster islet cell line. *Diabetes* 42:244-249, 1993
- Kendall DM, Poutout V, Olson LK, Sorenson RL, Robertson RP: Somatostatin coordinately regulates glucagon gene expression and exocytosis in HIT-15 cells. *J Clin Invest* 96:2496-2502, 1995
- Williams G, Fuessl H, Kraenzlin M, Bloom SR: Postprandial effects of SMS201-995 on gut hormones and glucose tolerance. *Scand J Gastroenterol* 21 (Suppl. 119):73-83, 1985
- Ipp E, Rivier J, Dobbs RE, Brown M, Vale W, Unger RH: Somatostatin analog inhibits somatostatin release. *Endocrinology* 104:1270-1273, 1979
- Patel YC, Amherdt M, Orci L: Quantitative electron microscopic autoradiography of insulin-, glucagon-, and somatostatin-binding sites on islets. *Science* 217:1155-1156, 1982
- Reubi JC, Rivier J, Perrin M, Brown M, Vale W: Specific high-affinity binding sites for somatostatin-28 on pancreatic B-cells: differences with brain somatostatin receptors. *Endocrinology* 110:1049-1051, 1982
- Sullivan SJ, Schonbrunn A: Distribution of somatostatin receptors in RINm5F cells. *Endocrinology* 122:1137-1145, 1988
- Amherdt M, Patel YC, Orci L: Selective binding of somatostatin-14 and somatostatin-28 to islet cells revealed by quantitative electron microscopic autoradiography. *J Clin Invest* 80:1455-1458, 1987
- Amherdt M, Patel YC, Orci L: Binding and internalization of somatostatin, insulin, and glucagon by cultured rat islet cells. *J Clin Invest* 84:412-417, 1989
- Thermos K, Meglasson MD, Nelson J, Lounsbury KM, Reisine T: Pancreatic β -cell somatostatin receptors. *Am J Physiol* 259:E216-E224, 1990
- Maletti M, Andersson M, Marie JC, Rosselin G, Mutt V: Solubilization and partial purification of somatostatin-28-preferring receptors from hamster pancreatic beta cells. *J Biol Chem* 267:15620-15625, 1992
- Grigorakis SI, Panetta R, Patel YC: Expression of mRNA for somatostatin receptor (SSTR) subtypes 1-5 in islets and differential downregulation of SSTR2 mRNA by SST agonists (Abstract). *Diabetes* 44 (Suppl. 1):132A, 1995
- Hunyady B, Hipkin RW, Schonbrunn A, Mezey E: Immunohistochemical localization of somatostatin receptor SST2A in the rat pancreas. *Endocrinology* 138:2632-2635, 1997
- Kumar U, Laird D, Srikant CB, Escher E, Patel YC: Expression of the five somatostatin receptor (SSTR1-5) subtypes in rat pituitary somatotrophs: quantitative analysis by double-label immunofluorescence confocal microscopy. *Endocrinology* 138:4473-4476, 1997
- Laemmli UK: Cleavage of structural proteins during the assembly of the head of bacteriophage T4. *Nature* 227:680-685, 1970
- Helboe L, Moller M, Novregaard L, Schiodt M, Stidsen CE: Development of selective antibodies against the human somatostatin receptor subtypes SSTR1-SSTR5. *Mol Br Res* 49:82-88, 1997
- Mezey E, Hunyady B, Mitra S, Hayes E, Liu Q, Schaeffer J, Schonbrunn A: Cell-specific expression of the SSTR2A and SSTR5 somatostatin receptors in the rat anterior pituitary. *Endocrinology* 139:414-419, 1998
- Patel YC, Panetta R, Escher E, Greenwood MT, Srikant CB: Expression of multiple somatostatin receptor genes in AIT-20 cells: evidence for a novel somatostatin-28-selective receptor subtype. *J Biol Chem* 269:1506-1509, 1994
- Dournaud P, Gu YZ, Schonbrunn A, Marinella J, Tannenbaum GS, Beaudet A: Localization of the somatostatin receptor SST2A in rat brain using a specific antipeptide antibody. *J Neurosci* 16:4468-4478, 1996
- O'Carroll A, Krempel K: Widespread distribution of somatostatin receptor messenger ribonucleic acids in rat pituitary. *Endocrinology* 136:5224-5227, 1995
- Gouldson PR, Reynolds CA: Simulations on dimeric peptides: evidence for domain swapping in G-protein-coupled receptors? *Biochem Soc Trans* 25:1066-1071, 1997
- Rocheville M, Hukovic N, Patel YC: Functional dimerization of the human somatostatin receptor subtype 5 (hSSTR5) (Abstract). *Program of the 80th Annual Meeting of the U.S. Endocrine Society, New Orleans, LA, 24-27 June 1998*, p. 113
- Skamene A, Patel YC: Infusions of graded concentrations of somatostatin-14 in man: pharmacokinetics and differential inhibitory effects on pituitary and islet hormones. *Clin Endocrinol* 20:555-564, 1984
- Bauer W, Briner U, Doepfner W, Haller R, Huguenin R, Marbach P, Petcher IP, Pless J: SMS 201-995: a very potent and selective octapeptide analogue of somatostatin with prolonged action. *Life Sci* 31:1133-1140, 1982

Differential regulation of somatostatin receptor types 1-5 in rat aorta after angioplasty

**S. KHARE,* U. KUMAR,* R. SASI,* L. PUEBLA,* LAZARO CALDERON,[†]
KARL LEMSTROM,[†] PEKKA HAYRY,[†] AND YOGESH C. PATEL***

*Fraser Laboratories, Department of Medicine, McGill University, Royal Victoria Hospital, Montreal, Quebec, H3A 1A1 Canada; and [†]Transplantation Laboratory, The Haartman Institute, University of Helsinki, Finland 00014

Differential regulation of somatostatin receptor types 1-5 in rat aorta after angioplasty

S. KHARE,^{*,1} U. KUMAR,^{*,1} R. SASI,^{*} L. PUEBLA,^{*} LAZARO CALDERON,[†] KARL LEMSTROM,[†] PEKKA HAYRY,[†] AND YOGESH C. PATEL^{*,2}

^{*}Fraser Laboratories, Department of Medicine, McGill University, Royal Victoria Hospital, Montreal, Quebec, H3A 1A1 Canada; and [†]Transplantation Laboratory, The Haartman Institute, University of Helsinki, Finland 00014

ABSTRACT Treatment of restenosis after angioplasty with octapeptide somatostatin (SST) analogs has met with variable success. These analogs bind with high affinity to only two SST receptor (SSTR) subtypes (2 and 5), display moderate affinity for SSTR3, and low affinity for SSTR1 and 4. To optimize the vasculoprotective effect of SST, we have investigated the pattern of expression of all five SSTRs in rat thoracic aorta in the resting state and at 15 min, 3, 7, and 14 days after balloon endothelial denudation. SSTR1-5 were analyzed as mRNA by semiquantitative reverse transcriptase-polymerase chain reaction and as protein by immunocytochemistry. All five SSTRs were expressed in rat aorta both as mRNA and protein and displayed a time-dependent, subtype-selective response to endothelial denudation. mRNA for SSTR1 and 2 increased acutely (SSTR1 > SSTR2) on days 3 and 7, coincident with smooth muscle cell (SMC) proliferation, and declined to basal levels by day 14. SSTR3 and 4 displayed a different pattern with a delayed, more gradual increase in mRNA beginning at days 3-7 and continued to increase thereafter. SSTR5 mRNA was constitutively expressed at a low level and showed no change during the 2 wk postinjury period. By immunohistochemistry, SSTR1-5 antigens were localized predominantly in SMC that were present in the media or had migrated into the intima; antigen expression correlated with receptor mRNA expression. Notably, only SSTR1,3,4 were expressed in the intima: SSTR1 and 4 during the proliferative burst and SSTR3 and 4 after proliferation, when SMC migration into the intima continues. These results demonstrate dynamic changes in SSTR1-5 expression after vascular trauma localized to areas of vascular SMC migration and replication. In view of their early and prominent induction, SSTR1 may be the optimal subtype to target for inhibition of myointimal proliferation, and SSTR3 and 4 for migration and remodeling.—Khare, S., Kumar, U., Sasi, R., Puebla, L., Calderon, L., Lemstrom, K., Hayry, P., Patel, Y. C. Differential regulation of somatostatin receptor types 1-5 in rat aorta after angioplasty. *FASEB J.* 13, 387-394 (1999)

Key Words: receptor subtypes • smooth muscle cell • SST • leukocyte • MAPK • macrophage

VASCULAR INTIMAL DYSPLASIA and remodeling are characteristic features of reinjury after balloon angioplasty, coronary bypass surgery, and chronic allograft rejection (1-4). The initial response to vascular injury is inflammatory and involves the attraction of lymphocytes, macrophages, and thrombocytes to the site of injury as well as the secretion of cytokines, eicosanoids, and growth factors (5). Under the influence of growth factors and cytokines, smooth muscle cells (SMC)³ proliferate and migrate from the media into the intima and contribute to intimal hyperplasia and stenosis. The key mediators of SMC proliferation, migration and vascular remodeling are interleukin 1, tumor necrosis factor α , platelet-derived growth factor (PDGF), insulin-like growth factor 1 (IGF1), basic fibroblast growth factor, epidermal growth factor (EGF), transforming growth factor α , and vascular endothelial growth factor (5) as well as the matrix metalloproteinases that facilitate smooth muscle cell locomotion through the extracellular matrix (6, 7). In view of the central role of SMC proliferation, therapeutic strategies designed to prevent stenosis have attempted to suppress SMC proliferation and migration by blocking the production and action of growth factors and cytokines with receptor antagonists and antibodies, antisense oligonucleotides directed against cell cycle regulatory molecules, and peptide inhibitors of mitogenic signaling such as somatostatin (SST) (8-13).

¹ S.K. and U.K. contributed equally to this paper.

² Correspondence: Room M3-15, Royal Victoria Hospital, 687 Pine Ave. West, Montreal, Quebec H3A 1A1, Canada. E-mail: patel@rvhmed.lan.mcgill.ca

³ Abbreviations: H/E, Mayer's hematoxylin and eosin; SST, somatostatin; SSTR, somatostatin receptor; SMC, smooth muscle cell; PDGF, platelet-derived growth factor; EGF, epidermal growth factor; IGF1, insulin-like growth factor 1; MAPK, mitogen-activated protein kinase; RT-PCR, reverse transcriptase-polymerase chain reaction; LCA, leukocyte common antigen.

SST, a neurohormone, is produced widely in the body and acts both systemically via the circulation, as well as locally to inhibit cell proliferation as well as the secretion of various hormones, growth factors, and neurotransmitter substances (14, 15). SST and its metabolically stable synthetic analogs like the octapeptides SMS201-995 (octreotide), and BIM23014 (lanreotide, angiopeptin) exert a number of vascular effects such as vasoconstriction in the gut and inhibition of angiogenesis (16, 17). A family of five G-protein-coupled receptors with seven α helical transmembrane segments termed SSTR1-5 mediates the actions of SST (18). All five SSTRs are functionally coupled to inhibition of adenylyl cyclase (18). Some of the receptor isotypes also modulate other effectors such as phosphotyrosine phosphatase, K^+ , and voltage-dependent Ca^{2+} ion channels, a Na^+/H^+ exchanger, phospholipase C, phospholipase A_2 , and mitogen-activated protein kinase (MAPK) (18). Based on structural similarity and the ability to react with octapeptide and hexapeptide SST analogs, the receptor family can be subdivided into two subclasses: the SSTR2,3,5 subclass that reacts with these analogs, and the SSTR1,4 subfamily, which reacts poorly with these compounds (18).

SST can inhibit cell proliferation both directly via SSTRs that activate antimitogenic signaling as well as indirectly by blocking the production of growth factors such as EGF, IGF1, and PDGF (18–20). Furthermore, SST is capable of suppressing the immune cell response by inhibiting lymphocyte proliferation and the expression of lymphocyte and endothelial cell adhesion molecules (21, 22). These findings led to the use of SST analogs as potential therapeutic agents to minimize myointimal proliferation. In animal experiments using arterial, venous, and vascular transplant models, the administration of octreotide or lanreotide prevents the formation of dysplastic lesions (11–13, 22–24). These results, however, have been inconsistent in different experimental models. In randomized placebo controlled trials, lanreotide in some studies was found to prevent restenosis after subcutaneous transluminal angioplasty as quantitated by angiography or as clinical events (25, 26), whereas the same success has not been achieved with octreotide (27). Differences in the binding specificity of the SST analogs for the five SSTRs as well as the dose and duration of SSTR administration may contribute in part to the variable results obtained in these studies (18). For instance, octreotide and lanreotide both bind with high affinity to SSTR2 and 5, but display species-specific variability in binding to SSTR3; octreotide binds well to human SSTR3 but shows only moderate affinity for the rodent receptor, whereas the opposite is true for lanreotide (18). To optimize the vasculoprotective effect of SST, the ideal approach would be to characterize the pattern

of expression of SSTRs in the vascular wall after, trauma and to target the subtypes involved with appropriate agonists. Toward this objective, we have determined the time course of expression of mRNA for SSTR1-5 in rat aorta after endothelial denudation (balloon injury) by reverse transcriptase-polymerase chain reaction (RT-PCR) and localized receptors in the aortic wall directly by immunocytochemistry with rabbit polyclonal antibodies to receptor subtype-specific peptides.

MATERIALS AND METHODS

Aortic denudations

Male Wistar rats weighing 200–300 g were anesthetized with chloral hydrate (240 mg/kg i.p.). The thoracic aorta was denuded of endothelium using a 2F Fogarty arterial embolectomy catheter (Baxter Healthcare Corporation, Santa Ana, Calif.). The catheter was introduced into the thoracic aorta via the left iliac artery, inflated with 0.2 ml air, and passed five times to remove the endothelium. The iliac artery was ligated and the animals allowed to recover. Buprenorphine (Temgesic, Reckitt Coleman, Hull, England) was administered for peri- and postoperative pain relief. Groups of three to five rats were killed at 15 min, 3 days, 7 days, and 14 days; aortic tissue was removed in order to evaluate SSTR expression.

All animals received humane care in compliance with guidelines established by the National Institutes of Health (Bethesda, Md.). Three separate experiments were performed. In the first experiment, 12 rats were denuded in Helsinki and 15 coded specimens of thoracic vascular tissue (3 control, 12 denuded; 3 specimens/time point) were sent to Montreal for RNA isolation and RT-PCR. In the second experiment, 20 rats were denuded and 25 coded specimens were sent to Montreal (5 specimens/time point). Four of these were used for RNA isolation and RT-PCR; the fifth specimen was used for routine histology, quantitation of cell replication, and SSTR immunocytochemistry. In the third experiment, frozen sections of 20 aortas (4 control, 16 denuded) were processed for immunocytochemistry for SSTR1-5. The results described here derive from experiments 2 and 3.

For RNA isolation, aortic tissue specimens were flash frozen in liquid nitrogen and stored at -80°C . To evaluate morphological changes, aortic cross sections from the mid segment of the denuded area were fixed in 3% paraformaldehyde (pH 7.4), embedded in paraffin for sectioning, and stained with Mayer's hematoxylin and eosin (H/E). For immunocytochemistry, aortic specimens were embedded in Tissue-Tek (Miles Inc., Elkhart, Ind.) and snap frozen in liquid nitrogen. Serial frozen sections (4–6 μM) were air dried on silane coated slides, fixed in acetone at -20°C for 20 min, and stored at -20°C until use.

RT-PCR

Weighed vascular tissue samples were pulverized in liquid nitrogen using a mortar and pestle, and total RNA was isolated by guanidinium isothiocyanate-phenol-chloroform extraction (28). For reverse transcription, 20 μg total RNA was treated with 10 units/mg RQ1 RNase-free DNase I (Promega, Madison, Wis.) in 40 mM Tris-buffered HCl, pH 7.9, 10 mM NaCl, 6 mM MgCl_2 , and 10 mM CaCl_2 for 30 min at 37°C . The DNase I was inactivated and removed by phenol

chloroform extraction, followed by ethanol precipitation. The exact concentration and purity of DNA-free RNA were determined by UV absorbance of RNA solutions in quartz microcuvettes before reverse transcription. The absorbance ratio A260:280 of RNA preparations was consistently ≥ 2.0 . To estimate the concentration of RNA, we assumed an absorbance at 260 nm of 1 for a 40 $\mu\text{g}/\text{ml}$ RNA solution. Five micrograms of DNA-free RNA were then incubated in a 20 μl reaction containing 20 mM Tris-HCl, pH 8.4, 50 mM KCl, 5 mM MgCl_2 , 1 mM dNTPs, 20 units of RNasin (Promega), 100 pmol of random hexanucleotides (Pharmacia, Piscataway, N.J.), and 200 units of Moloney murine leukemia virus reverse transcriptase (Gibco BRL, Paisley, U.K.) at 42°C for 30 min. Four microliters of the resulting cDNA samples were denatured at 94°C in 20 mM Tris HCl, pH 8.4, 50 mM KCl, 1.5 mM MgCl_2 , 200 μM dNTPs, and 20 pmol each of SSTR1-5 primers in 50 μl reaction volume for 10 min. The following primers were used for the PCR amplification.

rSSTR1: Sense: 5' ATGTTCCCAATGGCACC 3' (nt 1-18)
Antisense: 5' CAGATTCTCAGGCTGGAAGTCCTC 3' (nt 1093-1115)

rSSTR2: Sense: 5' AGCAACGCGGTCTCTACGTT 3' (nt 124-143)
Antisense: 5' GGAGGTCTCCATTGAGGAGG 3' (nt 1077-1196)

rSSTR3: Sense: 5' ATGAGCACGTGCCACATGCAG 3' (nt 565-585)

Antisense: 5' ACAGATGGCTCAGCGTGCTG 3' (nt 1266-1286)
rSSTR4: Sense: 5' ATGGTAACTATCCAGTGCAT 3' (nt 127-147)
Antisense: 5' GTGAGGCAGAAGACACTCGTGAACAT 3' (nt 376-401)

SSTR5: Sense: 5' TGGTCACTGGTGGGCTCAGC 3' (nt 70-89)
Antisense: 5' CCTGCTGGTCTGCATGAGCC 3' (nt 1067-1086)

β -actin: Sense: 5' ATCATGAAGTGTGACGTGGAC 3' (nt 90-110)
Antisense: 5' AACCGACTGCTGTCACCTTCA 3' (nt 529-549)

PCR reaction was initiated by the addition of 2.5 units of Taq polymerase (Gibco BRL) at 85°C (hot start). The following conditions were used: SSTR1,2,4, denaturation at 94°C for 1 min, annealing at 55°C for 30 s, and extension at 72°C for 90 s; SSTR3,5, denaturation at 94°C for 1 min, annealing at 64°C for 30 s, and extension at 72°C for 90 s. The receptors were coamplified with β -actin for 30 cycles, followed by final extension at 72°C for 10 min.

Southern transfer and hybridization

PCR products (10 μl) were separated by electrophoresis on 1.2% agarose gels, transferred to Genescreen Plus Membranes (Dupont, Wilmington, Del.), and hybridized with ^{32}P -labeled SSTR1-5; β -actin-specific cDNA probes were labeled to high specific activity by random hexanucleotide primers using a Life Technologies Kit. After hybridization for 20–22 h at 70°C, filters were washed and exposed to Kodak XAR film for various times. The hybridization signals were quantitated with a Java Video analysis software package (Jandel Scientific, Corte Madera, Calif.) and used as an index of SSTR and actin mRNA. To ensure that the hybridization bands were quantitated in the linear range, each blot was exposed to X-ray film for various intervals of time. Only bands that did not reach saturation density of exposure were subjected to quantitative analysis. The units derived from the Java analysis were arbitrarily assigned a pixel density corrected for background. Values of SSTR1-5 mRNA expression were normalized to those of actin mRNA on the same gels. All experiments were performed at least three times, and each mRNA quantitation represents the average of six measurements.

BrdU staining of proliferating cells

The method used was modified from the radioisotope method of Goldberg et al. (29). Bromodeoxyuridine labeling

(BrdU-Zymed Laboratories, San Francisco, Calif.) quantitated cell proliferation. Rats were injected with 0.3 ml BrdU labeling reagent 4 h before death and cellular incorporation was visualized by staining of paraffin cross sections using a mouse primary antibody (Bu20a, Dako, A/S, Denmark) and Vectastain Elite ABC Kit (Vector Laboratories, Burlingame, Calif.). Sections were deparaffinized and microwave-treated at 500 W for 2×5 min in 0.1 M citrate buffer, pH 6, followed by treatment in 95% formamide in 0.15 M tri-sodium citrate at 70°C for 45 min. Antibody dilutions were made according to the manufacturer's instructions. Sections were counterstained with H/E; positive cells in intimal, medial, and adventitial layers were counted separately and analyzed.

Antibodies to SSTR1-5 and immunohistochemistry of SSTR1-5 antigens

Antipeptide rabbit polyclonal antibodies specific to SSTR1-5 were produced and characterized as previously described (30–33). Synthetic oligopeptides corresponding to deduced sequences in the amino terminal segment or extracellular loop 3 or cytoplasmic tail of hSSTR1-5 were conjugated to keyhole limpet hemocyanin and used to immunize New Zealand white rabbits. The sequences selected were identical or nearly identical between the human and rat SSTR isoforms. Anti-SSTR activity in rabbit sera was screened by the ability to inhibit [^{125}I -LTT] SST-28 binding to membrane SSTRs, by immunocytochemistry of stable CHO-K1 cells individually transfected with hSSTR1-5, and by Western blot analysis (30–33). Before immunostaining, the slides were refixed with chloroform and air dried (3). After incubation with 1.5% normal goat serum, frozen sections were incubated with the panel of SSTR1-5 primary antibodies (diluted 1:200 to 1:500) at 4°C for 12 h. With intervening washes in Tris-buffered saline, the sections were incubated with goat anti-rabbit rat absorbed secondary antibody at room temperature for 30 min, followed by exposure to avidin-biotinylated horseradish peroxidase complex (Vectastatin Elite, ABC Kit) in phosphate-buffered saline at room temperature for 30 min. The reaction was revealed by chromogen 3-amino-9-ethylcarbazole (AEC Sigma, St. Louis, Mo.) containing 0.1% hydrogen peroxide, yielding a brown-red reaction product. Specimens were counterstained with hematoxylin and coverslips were mounted (Aquamount BDH). Eosin was not used so that the brown-red immunoreactive product could be contrasted against the blue nuclear stain and readily visualized. Controls used to validate the specificity of the SSTR immunoreactivity included preimmune serum in place of primary antibody and primary antibody absorbed with excess antigen.

Statistical analysis

Statistical significance at different time points after vessel injury was determined by analysis of variance, followed by the Bonferroni test. *P* values of <0.05 were considered statistically significant.

RESULTS

Vascular cell proliferation in response to denudation injury

To validate our model against previous reports, we tested the proliferation and intimal response of denuded aorta at the same time points as those

selected for determination of SSTR mRNA levels and protein expression. After denudation, the endothelial lining was completely removed (Table 1). Quiescent cells in the media were induced to proliferation beginning on day 3, followed by migration and further proliferation in the intima on days 7–14. Staining with antibody to β -SMC actin and β -leukocyte common antigen (β -LCA) demonstrated that virtually all cells in the media and >95% of cells in the intima expressed β -actin; <5% of the intimal cells were positive for β -LCA, which indicates that the cells migrating and proliferating in the intima were SMC (not shown).

Expression of SSTR1-5 mRNA in the vascular wall after trauma

Figure 1 depicts Southern blots of RT-PCR products showing the pattern of expression of mRNA for the five SSTR subtypes at different times in control and denuded aortic samples. In all RT-PCR, fixed amounts (5 μ g) of total RNA were coamplified for SSTR1-5 and actin, allowing a valid comparison of the relative changes in their mRNAs. The time course of the mean levels of expression of mRNA for the five SSTR subtypes after vascular injury is summarized in Fig. 2. Control aorta expressed readily detectable levels of SSTR3 mRNA, moderate levels of SSTR1 and SSTR4 mRNA, and barely detectable concentrations of SSTR5 and SSTR2 mRNA. After injury, SSTR1 mRNA displayed a dramatic twofold increase at day 3 ($P<0.01$) concomitant with the induction of SMC proliferation in the media. The mRNA level remained elevated at day 7 ($P<0.01$) concurrently with SMC proliferation in the intima but thereafter declined to baseline by day 14 when the proliferation was over. A parallel increase in SSTR2 mRNA was also observed at day 3 ($P<0.01$) although the magnitude of the change (~20%) was considerably smaller than that of SSTR1 mRNA. Unlike SSTR1 and SSTR2 mRNA, SSTR3 mRNA showed a more gradual increase with no change at day 3, followed by a significant increase by 35% at day 7 ($P<0.01$) and by 40% at day 14 ($P<0.001$).

TABLE 1. Number of cells (nuclei per aorta circumference) and number of cells incorporating BrdU (in parentheses)^a at different time points after injury

	Adventitia	Media	Intima
Control	220(0)	1400(0)	144(0) ^b
15 Min	200(0)	1115(0)	1(0)
3 Days	290(21)	1122(13)	20(8)
7 Days	310(4)	1155(2)	235(11)
14 Days	218(3)	1231(1)	950(21)

^a BrdU pulse was given at -3 h before death. ^b Nuclei of the endothelial lining.

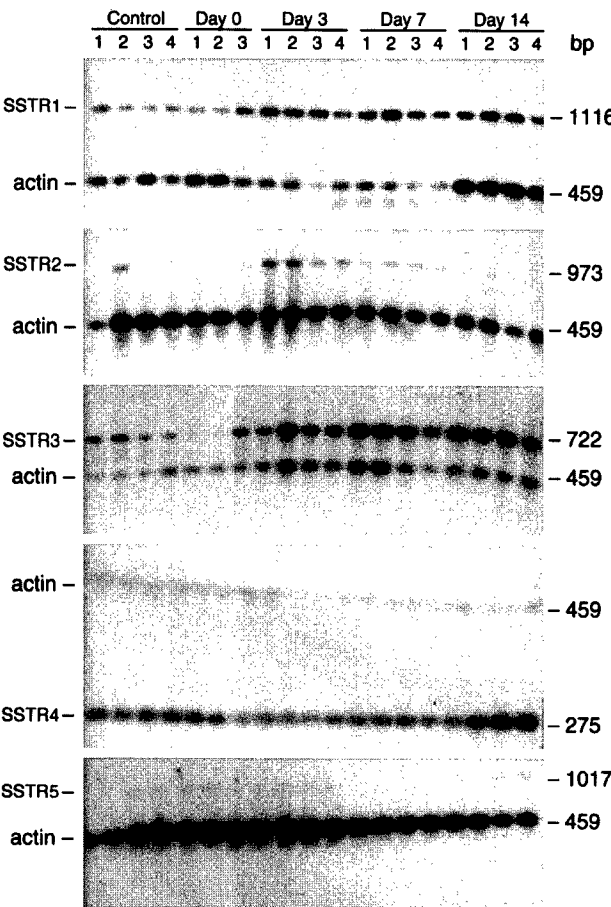


Figure 1. Analysis by RT-PCR of SSTR1-5 mRNA in aorta before and after balloon endothelial denudation. 5 μ g DNA-free total RNA was reverse transcribed and coamplified with primers specific for SSTR1-5 and β -actin. 10 μ l PCR products were fractionated on agarose gels, transferred to membranes, and hybridized simultaneously with ³²P-labeled SSTR1-5 and actin-specific cDNA probes. Control lanes represent Southern hybridization signals for nondenuded aortic samples. Day 0 represents results for samples obtained 15 min after denudation. The length of the PCR amplified fragments are indicated as base pairs (bp).

SSTR4 mRNA followed a similar pattern but the magnitude of the increase was smaller (20%) and statistically significant ($P<0.001$) only at day 14. In contrast to the other four subtypes, SSTR5 mRNA remained virtually undetectable and its expression pattern did not change after injury.

Expression of SSTR1-5 proteins by immunohistochemistry

Figure 3 illustrates the pattern of expression of the five SSTR proteins in control and injured aortic vessel wall at different times after endothelial denudation. The results confirm the mRNA expression analysis and localize the receptor proteins as a red-brown reaction product in the vascular wall. SSTR1,2,4 were expressed at low levels in the media of the nondenuded (control) aorta, but very little (if

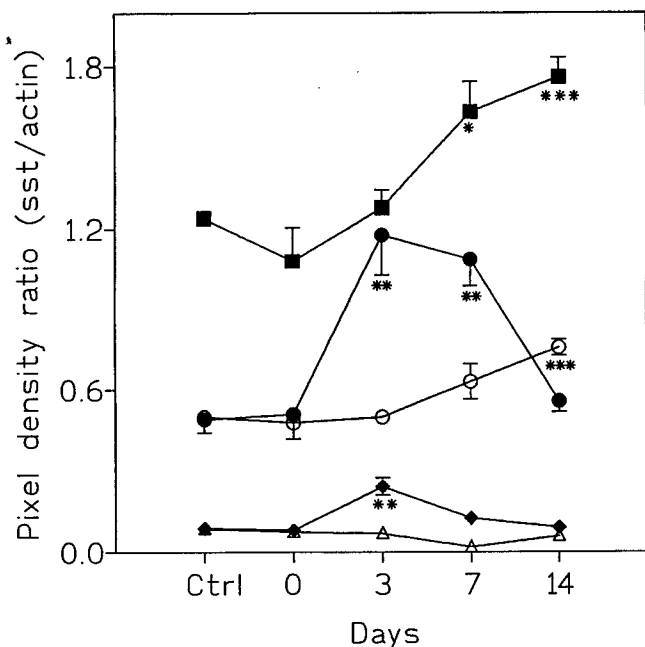


Figure 2. Time course of SSTR1-5 mRNA expression in vascular wall after trauma. SSTR1-5 mRNA was quantitated from Southern hybridization signals of RT-PCR products (Fig. 1) by densitometry using Java Video analysis. The arbitrary pixel density values were corrected for background and expressed as a ratio of actin mRNA. SSTR1 (●); SSTR2 (◆); SSTR3 (■); SSTR4 (○); SSTR5 (△). * $P < 0.05$; ** $P < 0.01$; *** $P < 0.001$ vs. control, nondenuded samples (CTRL). Time 0 represents samples collected 15 min after denudation. Mean \pm SE of at least six measurements of pixel densities of hybridization signals from three separate experiments.

any) SSTR3 and 5 was seen. After denudation, SSTR1 was expressed in the media on days 3, 7, and 14, when media proliferation occurred, and strongly in the intima on days 7 and 14 at the time of intimal SMC proliferation and migration. SSTR4 immunoreactivity was faintly visible in the media on days 3 and 7, but became readily detectable in the intima on day 14, correlating with increased intimal thickening and remodeling. SSTR3 was detected in the media on days 3 and 7, and was localized as a strong signal in the intima on day 14. SSTR2 was clearly detectable in the media on day 3, but did not localize in the intima subsequently. SSTR5 was seen as a weak immunopositive signal in the media and intima without a significant temporal change. Immunopositivity associated with all five SSTRs was blocked in control sections incubated with preimmune serum or antigen absorbed antibody in place of primary antibody (not shown).

DISCUSSION

The model used in this study to quantitate SMC replication and migration after endothelial injury of rat aorta has been well established (29, 34, 35).

Although the injury in this model is inflicted in a healthy rather than atheromatous vessel, as would be the case in coronary balloon dilatation in humans, the model is nonetheless valid for investigating SMC migratory and proliferative responses. Previous studies using the rat aortic model have shown that, after injury, cells in the media begin to proliferate on day 2, reach a peak on day 3, and decline to baseline on day 5 (8, 34–37). Migration of cells into the intima begins on day 4, peaks on day 7, and declines to baseline around day 14. Our results of SMC proliferative and intima responses were in complete agreement with results published previously; accordingly, changes in SSTR mRNA and protein expression at the time points selected (before denudation and at 15 min, 3 days, 7 days, and 14 days postdenudation) can be accurately related to the reported time course of myointimal proliferative and migratory responses (8, 34–37).

We found that all five SSTR mRNAs are expressed in rat aorta both as mRNA and protein. Aortic denudation induced a time-dependent, subtype-selective response in the pattern of SSTR expression. The earliest change occurred in the case of SSTR1 and SSTR2, whose mRNA increased after denudation, reached peak levels between days 3 and 7, and declined to basal levels by day 14. SSTR3 and 4 displayed a different pattern, with a delayed, more gradual increase in mRNA beginning at days 3–7, which remained elevated thereafter. SSTR5 was constitutively expressed with no change in the level of expression during the 2 wk postinjury. By immunohistochemistry, SSTR antigens were localized predominantly in SMC that were either present in the media or had migrated into the intima. In general, the level of expression of SSTR1-5 by mRNA measurement correlated with receptor protein expression by immunohistochemistry.

Our results provide the first evidence for the expression of all five SSTRs in the aorta and suggest that, like other tissues (e.g., brain, pituitary, and islet cells, which also express the five SSTR isoforms), the aorta is an important target of SST action (15, 18, 30). In previous studies, only SSTR2 mRNA has been detected in rat aorta (38, 39). By autoradiography, a rich concentration of SST binding sites has been described in peritumoral (but not normal) vessels, suggesting that SSTRs may be induced by a tumor product and/or by peritumoral inflammation, as also appears to be the case after denudation injury (40). We found a predominant cellular localization of SSTRs in SMC, although lower levels of expression in endothelial or inflammatory cells cannot be ruled out. Notably, no SSTR protein was observed in the vascular adventitia. Functional SSTRs have also been identified in glomerular mesangial cells and cultured intestinal SMC, which express SSTRs with

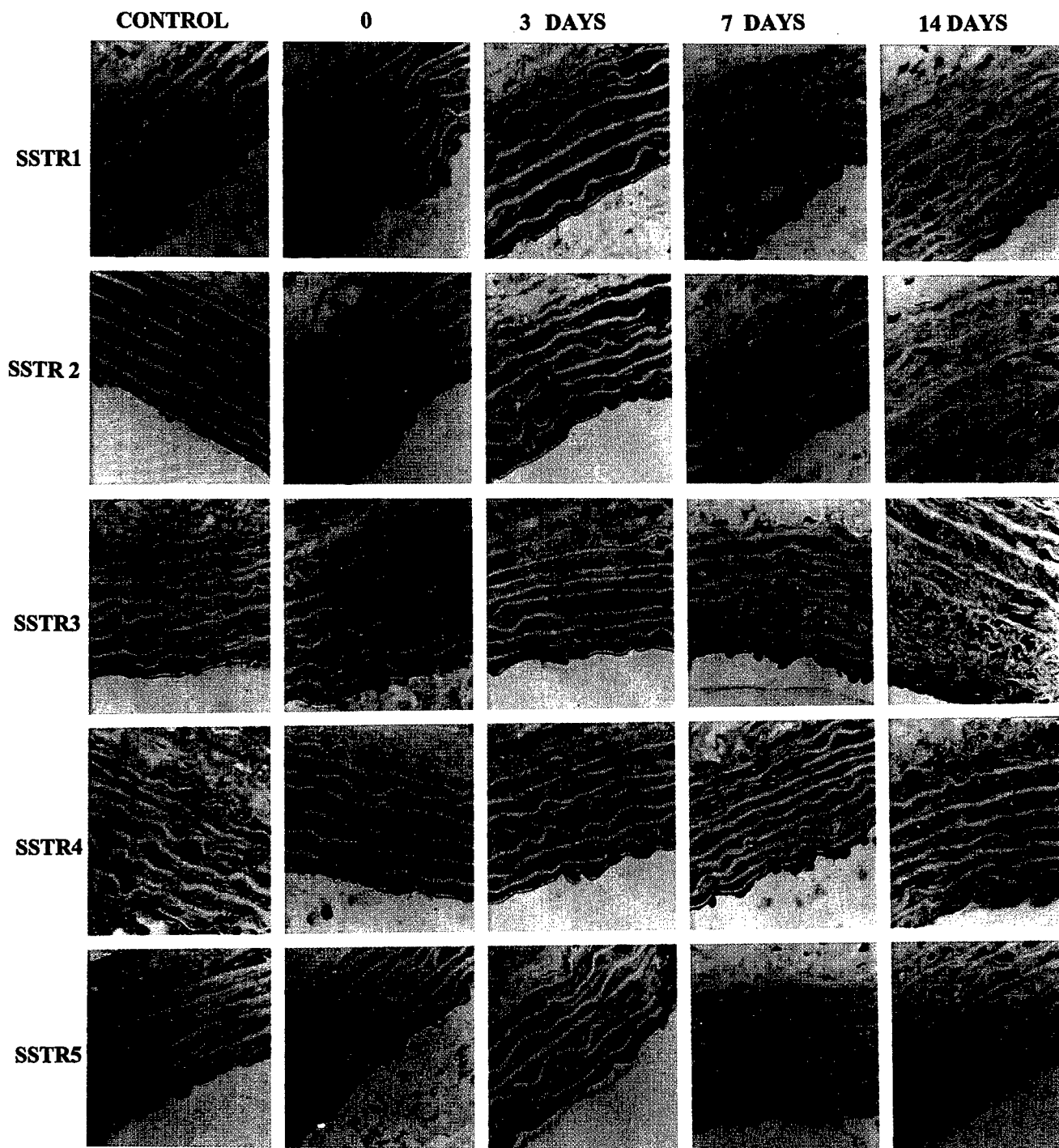


Figure 3. Photomicrographs illustrating immunohistochemical localization of SSTR1-5 antigen in aortic sections from control (nondenuded) or denuded specimens at different times postinjury. SSTR1-5 was visualized as a brown-red reaction product by peroxidase immunocytochemistry using SSTR1-5 subtype-specific rabbit antibodies. Representative sections ($\times 400$) counterstained with hematoxylin are shown. Eosin was not used in order to contrast the brown-red immunoreactive product against the blue nuclear stain. L, lumen; m, media; a, adventitia. SSTR1,2,4 are expressed at low levels in control media, but there is little expression of SSTR3 and 5. After denudation, strong SSTR1 immunoreactivity is seen in the media on day 3 and in the intima on days 7 and 14. SSTR4 immunoreactivity is localized in the media on days 3 and 7 and becomes readily detectable in the intima on day 14. SSTR3 is detectable in the media on days 3-7 and localizes as a strong signal in the intima on day 14. SSTR2 is readily detectable in the media on day 3 but not in the intima. SSTR5 is seen as a weak immunopositive signal in the media and intima, with little change over time. Immunoreactivity associated with all five SSTRs was blocked in control sections incubated with preimmune serum or antigen absorbed antibody in place of primary antibody (not shown).

the pharmacological profile of the type 3 receptor (41-42).

What is the mechanism of SSTR induction by

vascular injury? Steady-state SSTR mRNA levels are augmented by cAMP, gastrin, EGF, and SST itself (43-45). Glucocorticoids acutely induce SSTR1 and

SSTR2 mRNA, whereas estrogen induces SSTR2 and SSTR3 mRNA and thyroid hormone up-regulates SSTR1 and SSTR5 mRNA (46–48). The 5' upstream promoter regions of the four receptor genes that have been sequenced (SSTR1,2,4, and 5) display a number of consensus sequences that confer responsiveness to cAMP, AP1, AP2, Pit1, and thyroid hormone (49–53). The time course of the increase in SSTR3 and 4 mRNA in our study approximated the temporal profile of SMC hyperplasia, suggesting that induction of these two subtypes may simply reflect SMC replication. The earlier onset of induction of SSTR1 and SSTR2 suggests a different mediator, possibly a growth factor such as EGF. Induction of endogenous SSTRs in response to vascular injury may represent a compensatory attempt to modulate the proliferative response by SST produced locally by inflammatory cells.

The results of this study will be important in the rational design of SST agonists for inhibition of fibroproliferative myointimal hyperplasias. All five SSTRs are capable of inhibiting cell proliferation (18). SSTR1–4 act by stimulating PTP, which dephosphorylates receptor tyrosine kinases, thereby attenuating the mitogenic signal (18). SSTR5, on the other hand, inhibits guanylate cyclase, cGMP-dependent phosphorylation, and activation of MAPK (18). Since the five SSTRs are expressed in the arterial wall, they could all be potential targets for the direct antiproliferative effects of SST. To date, however, only the effects of octreotide and lanreotide on myointimal proliferation have been tested. Their reported actions are likely to be mediated via SSTR2,3,5, especially SSTR2 and 3, in view of the low-level constitutive expression of SSTR5. Our findings suggest that SSTR2 and 5 may not be the optimal targets for intervention. Their expression levels remained low after injury, and SSTR2 was never recorded in the intima. In view of their early and prominent induction, SSTR1,3 and 4 may be the optimal subtypes to target—SSTR1 for inhibition of myointimal proliferation and SSTR3 and 4 for migration and remodeling. FJ

We are grateful to M. Correia for secretarial help. This work was supported by grants to Y.C.P. from the Canadian Medical Research Council, the U.S. Department of Defence, and the Canadian National Cancer Institute, and to P.H. from Technology Development Center (TEKES), Academy of Finland Contract No. BMH-4CT95-1160 of Biomed 2, the European Union, and University of Helsinki Hospital Research Funds. Y.C.P. is a Distinguished Scientist of the Canadian Medical Research Council.

REFERENCES

- Holmes, D. R., Vlietstra, R. E., Smith, H. C., Vetrovec, G. W., Kent, K. M., Cowley, M. J., Faxon, D. P., Gruentzig, A. R., Kelsey, S. F., and Detre, K. M. (1984) Restenosis after percutaneous transluminal coronary angioplasty (PTCA): a report from the PTCA Registry of the National Heart, Lung, and Blood Institute. *Am. J. Cardiol.* 53, 77C–81C
- Holmes, D., Holubkov, R., and Vlietstra, R. (1988) Comparison of complications during percutaneous transluminal coronary angioplasty from 1977 to 1981 and from 1985 to 1986: the National Heart, Lung, and Blood Institute Percutaneous Transluminal Coronary Angioplasty Registry. *J. Am. Coll. Cardiol.* 22, 1149–1155
- Lemstrom, K. B., and Koskinen, P. K. (1997) Expression and localization of platelet-derived growth factor ligand and receptor protein during acute and chronic rejection of rat cardiac allografts. *Circulation* 96, 1240–1249
- Hayry, P., Isoniemi, H., Yilmaz, S., Mennander, A., Lenstrom, K., Raisanen-Sokolowski, A., Koskinen, P., Ustinov, J., Lautenschlager, I., and Taskinen, E. (1993) Chronic allograft rejection. *Immunol. Rev.* 134, 33–81
- Ross, R. (1993) The pathogenesis of atherosclerosis: a perspective for the 1990s. *Nature (London)* 362, 801–809
- Bendeck, M. P., Irvin, C., and Reidy, M. A. (1996) Inhibition of matrix metalloproteinase activity inhibits smooth muscle cell migration but not neointimal thickening after arterial injury. *Circ. Res.* 78, 38–43
- Galis, Z. S., Muszynski, M., Sukhova, G. K., Simon-Morrissey, E., and Libby, P. (1995) Thrombin promotes activation of matrix metalloproteinase-2 produced by cultured vascular smooth muscle cells. *Ann. N.Y. Acad. Sci.* 748, 501–507
- Hayry, P., Myllarniemi, M., Aavik, E., Alatalo, S., Aho, P., Yilmaz, S., Raisanen-Sokolowski, A., Cozzone, G., Jameson, B. A., and Baserga, R. (1995) Stable D-peptide analog of insulin-like growth factor-1 inhibits smooth muscle cell proliferation after carotid ballooning injury in the rat. *FASEB J.* 9, 1336–1344
- Sirois, M. G., Simons, M., and Edelman, E. R. (1997) Antisense oligonucleotide inhibition of PDGFR-beta receptor subunit expression directs suppression of intimal thickening. *Circulation* 95, 669–676
- Wrighton, C. J., Hofer-Warbinek, R., Moll, T., Eytner, R., Bach, F. H., and de Martin, R. (1996) Inhibition of endothelial cell activation by adenovirus-mediated expression of I kappa B alpha, an inhibitor of the transcription factor NF-kappa B. *J. Exp. Med.* 183, 1–10
- Grant, M. B., Wargovich, T. J., Ellis, E. A., Caballero, S., Mansour, M., and Pepine, C. J. (1994) Localization of insulin-like growth factor I and inhibition of coronary smooth muscle cell growth by somatostatin analogues in human coronary smooth muscle cells. A potential treatment for restenosis? *Circulation* 89, 1511–1517
- Hong, M. K., Bhatti, T., Matthews, B. J., Stark, K. S., Cathapermal, S. S., Foegh, M. L., Ramwell, P. W., and Kent, K. M. (1993) The effect of porous infusion balloon-delivered angioplasty on myointimal hyperplasia after balloon injury in the rabbit. *Circulation* 88, 638–648
- Lindner, V., and Reidy, M. A. (1991) Proliferation of smooth muscle cells after vascular injury is inhibited by an antibody against basic fibroblast growth factor. *Proc. Natl. Acad. Sci. USA* 88, 3739–3743
- Reichlin, S. (1983) Somatostatin. *N. Engl. J. Med.* 309, 1495–1501
- Patel, Y. C., Liu, J.-L., Galanopoulou, A. S., and Papachristou, D. N. (1999) In: *The Handbook of Physiology, The Endocrine Pancreas and Regulation of Metabolism* (Jefferson, L. S., and Cherrington, A. D., eds) Oxford University Press, New York In press
- Wahren, J. (1976) Influence of somatostatin on carbohydrate disposal and absorption in diabetes mellitus. *Lancet* 2, 1213–1215
- Waltering, E. A., Barrie, R., and O'Dorisio, T. M. (1991) Somatostatin analogues inhibit angiogenesis in the chick chorioallantoic membrane. *J. Surg. Res.* 50, 245–251
- Patel, Y. C., and Srikant, C. B. (1997) Somatostatin. *Trends Endocrinol. Metab.* 8, 398–405
- Hayry, P., Raisanen, A., Ustinov, J., Mennander, A., and Paavonen, T. (1993) Somatostatin analog lanreotide inhibits myocyte replication and several growth factors in allograft arteriosclerosis. *FASEB J.* 7, 1055–1060
- Yumi, K., Fagin, J. A., Fishbein, M. C., Shah, P. K., Kaul, S., Niu, W., Nilsson, J., Cercek, B., and Yamashita, M. (1997) Direct

- effects of somatostatin analog octreotide on insulin-like growth factor-I in the arterial wall. *Lab. Invest.* 76, 329–338
21. Aguila, M. C., Rodriguez, A. M., Aguila-Mansilla, H. N., and Lee, W. T. (1996) Somatostatin antisense oligodeoxynucleotide-mediated stimulation of lymphocyte proliferation in culture. *Endocrinology* 137, 1585–1590
22. Leszczynski, D., Josephs, M. D., Fournier, R. S., and Foegh, M. L. (1993) Angiopeptin, the octapeptide analogue of somatostatin, decreases rat heart endothelial cell adhesiveness for mononuclear cells. *Regul. Peptides* 43, 131–140
23. Foegh, M. L., Asotra, S., Conte, J. V., Howell, M., Kagan, E., Verma, K., and Ramwell, P. W. (1994) Early inhibition of myointimal proliferation by angiopeptin after balloon catheter injury in the rabbit. *J. Vasc. Surg.* 19, 1084–1091
24. Foegh, M. L., Lou, H., Chen, M. F., and Ramwell, P. W. (1997) Angiopeptin induces beneficial vascular remodeling after balloon injury. *Transplant. Proc.* 29, 2605–2608
25. Eriksen, U. H., Amtorp, O., Bagger, J. P., Emanuelsson, H., Foegh, H., Henningsen, P., Saunamaki, K. K., Schaeffer, M., Thayssen, P., and Orskov, H. (1995) Randomized double-blind Scandinavian trial of angiopeptin versus placebo for the prevention of clinical events and restenosis after coronary balloon angioplasty. *Am. Heart J.* 130, 1–8
26. Emanuelsson, H., Beatt, K. J., Bagger, J. P., Balcon, R., Heikkila, J., Piessens, J., Schaeffer, M., Suryapranata, H., and Foegh, M. (1995) Long-term effects of angiopeptin treatment in coronary angioplasty. Reduction of clinical events but not angiographic restenosis. *Circulation* 91, 1689–1696
27. von Essen, R., Ostermaier, R., Grube, E., Maurer, R., Tebbe, U., Erbel, R., Roth, M., Oel, W., Brom, J., and Weidinger, G. (1997) Effects of octreotide treatment on restenosis after coronary angioplasty: results of the VERAS study. *Circulation* 96, 1482–1487
28. Chomczynski, P., and Sacchi, N. (1987) Single-step method of RNA isolation by acid guanidium thiocyanate-phenol-chloroform extraction. *Anal. Biochem.* 162, 156–158
29. Goldberg, I., Stemerman, M. B., Schnipper, L. E., Ransil, B. J., Croocks, G. W., and Fuhro, R. L. (1979) Vascular smooth muscle cell kinetics: a new assay for studying patterns of cellular proliferation in vivo. *Science* 205, 920–921
30. Kumar, U., Laird, D., Srikant, C. B., Escher, E., and Patel, Y. C. (1997) Expression of the five somatostatin receptor (SSTR1-5) subtypes in rat pituitary somatotrophs: quantitative analysis by double-layer immunofluorescence confocal microscopy. *Endocrinology* 138, 4474–4476
31. Kumar, U., Sasi, S., Suresh, S., Patel, A., Thangaraju, M., Metrakos, P., Patel, S. C., and Patel, Y. C. (1999) Subtype selective expression of the five somatostatin receptors (hSSTR1-5) in human pancreatic islet cells: a quantitative double-labeled immunohistochemical analysis. *Diabetes* 48, 77–85
32. Patel, Y. C., Panetta, R., Esher, E., Greenwood, M., and Srikant, C. B. (1994) Expression of multiple somatostatin receptor genes in AtT-20 cells, evidence for a novel somatostatin-28 selective receptor subtype. *J. Biol. Chem.* 269, 1506–1509
33. Greenwood, M. T., Hukovic, N., Kumar, U., Panetta, R., Hjorth, S. A., Srikant, C. B., and Patel, Y. C. (1997) Ligand binding pocket of the human somatostatin receptor 5 (hSSTR5): mutational analysis of the extracellular domains. *Mol. Pharmacol.* 52, 807–814
34. Clowes, A., Reidy, M., and Clowes, M. (1983) Kinetics of cellular proliferation after arterial injury. *Lab. Invest.* 49, 327–333
35. Clowes, A. W., and Swartz, S. M. (1985) Significance of quiescent smooth muscle migration in the injured rat carotid artery. *Circ. Res.* 56, 139–145
36. Majesky, M. W., Reidy, M. A., Bowen-Pope, D. F., Hart, C. E., Wilcox, J. N., and Schwartz, S. M. (1990) PDGF ligand and receptor gene expression during repair of arterial injury. *J. Cell Biol.* 111, 2149–2158
37. Majesky, M. W., Giachelli, C. M., Reidy, M. A., and Schwartz, S. (1992) Rat carotid neointimal smooth muscle cells reexpress a developmentally regulated mRNA phenotype during repair of arterial injury. *Circ. Res.* 71, 759–768
38. Weckbecker, G., Pally, C., Raulf, C., Beckmann, N., Schuurman, J. H., Rudin, M., and Bruns, C. (1997) The somatostatin analog octreotide as potential treatment for re-stenosis and chronic rejection. *Transplant. Proc.* 29, 2599–2600
39. Chen, J. C., Hsiang, Y. N., and Buchan, A. M. (1997) Somatostatin receptor expression in rat iliac arteries after balloon injury. *J. Invest. Surg.* 10, 17–23
40. Reubi, J.-C., Horisberger, U., and Laissue, J. (1994) High density of somatostatin receptors in veins surrounding human cancer tissue: role in tumor-host interaction? *Int. J. Cancer* 56, 681–688
41. Dies-Marques, M. L., Garcia-Escribano, C., Medina, J., Boyano-Adanez, M. C., Arilla, E., Torrecilla, G., Rodriguez-Puyol, D., and Rodriguez-Puyol, M. (1995) Effects of somatostatin on cultures human mesangial cells. *Endocrinol. Metab.* 136, 3444–3451
42. Murthy, K. S., Coy, D. H., and Makhoul, G. (1996) Somatostatin receptor-mediated signaling in smooth muscle. Activation of phospholipase C- β_3 by G $\beta\gamma$ and inhibition of adenylyl cyclase by G α_i and G α_o . *J. Biol. Chem.* 271, 23458–23463
43. Patel, Y. C., Greenwood, M. T., Kent, G., Panetta, R., and Srikant, C. B. (1993) Multiple gene transcripts of the somatostatin receptor SSTR2: tissue selective distribution and cAMP regulation. *Biochem. Biophys. Res. Commun.* 192, 288–294
44. Vidal, C., Raulf, I., Zeggari, M., Delesque, N., Esteve, J.-P., Saint-Laurent, N., Vaysse, N., and Susini, C. (1994) Up-regulation of somatostatin receptors by epidermal growth factor and gastrin in pancreatic cancer cells. *Mol. Pharmacol.* 46, 97–104
45. Bruno, J. F., Xu, Y., and Berelowitz, M. (1994) Somatostatin regulates somatostatin receptor subtype mRNA expression in GH3 cells. *Biochem. Biophys. Res. Commun.* 202, 1738–1743
46. Xu, Y., Berelowitz, M., and Bruno, J. F. (1995) Dexamethasone regulates somatostatin receptor subtype messenger ribonucleic acid in rat pituitary GH4C1 cells. *Endocrinology* 136, 5070–5075
47. Xu, Y., Song, J., Berelowitz, M., and Bruno, J. F. (1996) Estrogen regulates somatostatin receptor subtype 2 messenger ribonucleic acid expression in human breast cancer cells. *Endocrinology* 137, 5634–5640
48. James, R. A., Sarapura, V. D., Bruns, C., Raulf, F., Dowding, J. M., Gordon, D. F., Wood, W. M., and Ridgway, E. C. (1997) Thyroid hormone-induced expression of specific somatostatin receptor subtypes correlates with involution of the TtT-97 murine thyrotrope tumor. *Endocrinology* 138, 719–724
49. Hauser, F., Meyerhof, W., Wulfsen, I., Schonrock, C., and Richter, D. (1994) Sequence analysis of the promoter region of the rat somatostatin receptor subtype 1 gene. *FEBS Lett.* 345, 225–228
50. Greenwood, M. T., Robertson, L.-A., and Patel, Y. C. (1995) Cloning of the gene encoding human somatostatin receptor 2: sequence analysis of the 5'-flanking promoter region. *Gene* 159, 291–292
51. Pscherer, A., Dorflinger, U., Kirfel, J., Gawlas, K., Ruschoff, J., Buettner, R., and Schule, R. (1996) The helix-loop-helix transcription factor SEF-2 regulates the activity of a novel initiator element in the promoter of the human somatostatin receptor II gene. *EMBO J.* 15, 6680–6690
52. Xu, Y., Bruno, J. F., and Berelowitz, M. (1995) Characterization of the proximal promoter region of the rat somatostatin receptor gene, SSTR4. *Biochem. Biophys. Res. Commun.* 206, 935–941
53. Greenwood, M. T., Panetta, R., Robertson, L.-A., Liu, J.-L., and Patel, Y. C. (1994) Sequence analysis of the 5'-flanking promoter region of the human somatostatin receptor 5. *Biochem. Biophys. Res. Commun.* 205, 1883–1890.

Received for publication May 12, 1998.
Revised for publication August 27, 1998.

Agonist-dependent Up-regulation of Human Somatostatin Receptor Type 1 Requires Molecular Signals in the Cytoplasmic C-tail*

(Received for publication, March 19, 1999, and in revised form, May 14, 1999)

Nedim Hukovic‡, Magalie Rocheville§, Ujendra Kumar, Ramakrishnan Sasi, Suvarnalatha Khare, and Yogesh C. Patel¶

From Fraser Laboratories, Departments of Medicine, Neurology and Neurosurgery, and Pharmacology and Therapeutics, McGill University, Royal Victoria Hospital and the Montreal Neurological Institute, Montreal, Quebec H3A 1A1, Canada

We have previously reported that the human somatostatin receptor type 1 (hSSTR1) stably expressed in Chinese hamster ovary-K1 cells does not internalize but instead up-regulates at the membrane during continued agonist treatment (1 μ M somatostatin (SST)-14 \times 22 h). Here we have investigated the molecular basis of hSSTR1 up-regulation. hSSTR1 was up-regulated by SST in a time-, temperature-, and dose-dependent manner to saturable levels, in intact cells but not in membrane preparations. Although hSSTR1 was acutely desensitized to adenylyl cyclase coupling after 1 h SST-14 treatment, continued agonist exposure (22 h) restored functional effector coupling. Up-regulation was unaffected by cycloheximide but blocked by okadaic acid. Confocal fluorescence immunocytochemistry of intact and permeabilized cells showed progressive, time-dependent increase in surface hSSTR1 labeling, associated with depletion of intracellular SSTR1 immunofluorescent vesicles. To investigate the structural domains of hSSTR1 responsible for up-regulation, we constructed C-tail deletion (Δ) mutants and chimeric hSSTR1-hSSTR5 receptors. Human SSTR5 was chosen because it internalizes readily, displays potent C-tail internalization signals, and does not up-regulate. Like wild type hSSTR1, Δ C-tail hSSTR1 did not internalize and additionally lost the ability to up-regulate. Swapping the C-tail of hSSTR1 with that of hSSTR5 induced internalization (27%) but not up-regulation. Substitution of hSSTR5 C-tail with that of hSSTR1 converted the chimeric receptor to one resembling wild type hSSTR1 (poor internalization, 71% up-regulation). These results show that ligand-induced up-regulation of hSSTR1 occurs by a temperature-dependent active process of receptor recruitment from a pre-existing cytoplasmic pool to the plasma membrane. It does not require new protein synthesis or signal transduction, is sensitive to dephosphorylation events, and critically dependent on molecular signals in the receptor C-tail.

Somatostatin (SST),¹ a naturally occurring regulatory peptide with two biologically active forms, SST-14 and SST-28, is produced in neural, endocrine, and immune cells and exerts potent effects on many different tissue targets including the brain, pituitary, pancreas, gut, thyroid, adrenals, and kidneys (1–3). The cellular actions of SST include the inhibition of hormone and exocrine secretion as well as modulation of neurotransmission and cell proliferation and are mediated by G protein-coupled receptors (GPCR) (2, 3). Somatostatin receptors (SSTR) belong to the family of seven transmembrane domain proteins and comprise five distinct subtypes that are encoded by separate genes (2, 3). In the case of the human receptors, four of the isoforms (hSSTR1–4) display weak selectivity for binding to SST-14, whereas hSSTR5 shows preference for SST-28 binding (2). SSTRs are widely expressed in many tissues frequently as multiple subtypes that coexist in the same cell (2–6). The five receptors share common signaling pathways such as the inhibition of adenylyl cyclase, activation of phosphotyrosine phosphatase, or modulation of mitogen-activated protein (MAP) kinase through G protein-dependent mechanisms (2, 3, 7). Some of the subtypes are also coupled to K⁺ and Ca²⁺ ion channels, to phospholipase C, and phospholipase A₂ (2). hSSTR1 activates a Na⁺/H⁺ exchanger via a non-G protein-linked pathway (8).

A common property of most GPCRs is their ability to regulate their responsiveness to continued agonist exposure (9). Such agonist-specific regulation typically involves receptor desensitization due to uncoupling from G proteins, as well as receptor internalization and receptor degradation (9). The underlying molecular mechanisms have been extensively studied in the case of the β -adrenergic and several other GPCRs, and a general model has been proposed that involves phosphorylation of the C-tail and intracellular loops of the agonist-occupied receptor by a second messenger activated or G protein-coupled receptor kinase, resulting in rapid attenuation of receptor signaling. G protein-coupled receptor kinase phosphorylation promotes the binding of β -arrestin, which acts as an adapter molecule linking the receptor to clathrin-mediated endocytosis (9–11). The endocytosed receptor is either sorted to lysosomes for degradation if agonist stimulation is prolonged or recycled back to the cell surface as a result of pH-dependent conformational change and dephosphorylation by a membrane-associated GPCR phosphatase in endosomes (9–11). Another less

* This work was supported in part by the Medical Research Council of Canada Grant MT-10411, National Institutes of Health Grant R01 NS32160-04A1, U. S. Department of Defense Grant DAMD17-96-1-6189, and National Cancer Institute of Canada Grant 7140. The costs of publication of this article were defrayed in part by the payment of page charges. This article must therefore be hereby marked "advertisement" in accordance with 18 U.S.C. Section 1734 solely to indicate this fact.

‡ Supported by a fellowship from the Fonds de la Recherche en Sante du Quebec.

§ Recipient of studentship support from the Royal Victoria Hospital Research Institute and the FRSQ.

¶ Distinguished Scientist of the Canadian Medical Research Council. To whom correspondence should be addressed: Royal Victoria Hospital, Rm. M3-15, 687 Pine Ave. West, Montreal, Quebec H3A 1A1, Canada. Tel.: 514-842-1231 (ext. 5042); Fax: 514-849-3681; E-mail: patel@rvhmed.lan.mcgill.ca.

¹ The abbreviations used are: SST, somatostatin; LTT SST-28, Leu⁸, D-Trp²², Tyr²⁵ SST-28; SSTR, somatostatin receptor; wt hSSTR5, wild type human somatostatin receptor type 5; wt hSSTR1, wild type human somatostatin receptor type 1; β_2 AR, β_2 -adrenergic receptor; D2_LR, long form of dopamine 2 receptor; GPCR, G protein-coupled receptor; C-tail, cytoplasmic C-terminal segment; PCR, polymerase chain reaction; CHO, Chinese hamster ovary; MAP, mitogen-activated protein; GnRH, gonadotropin-releasing hormone.

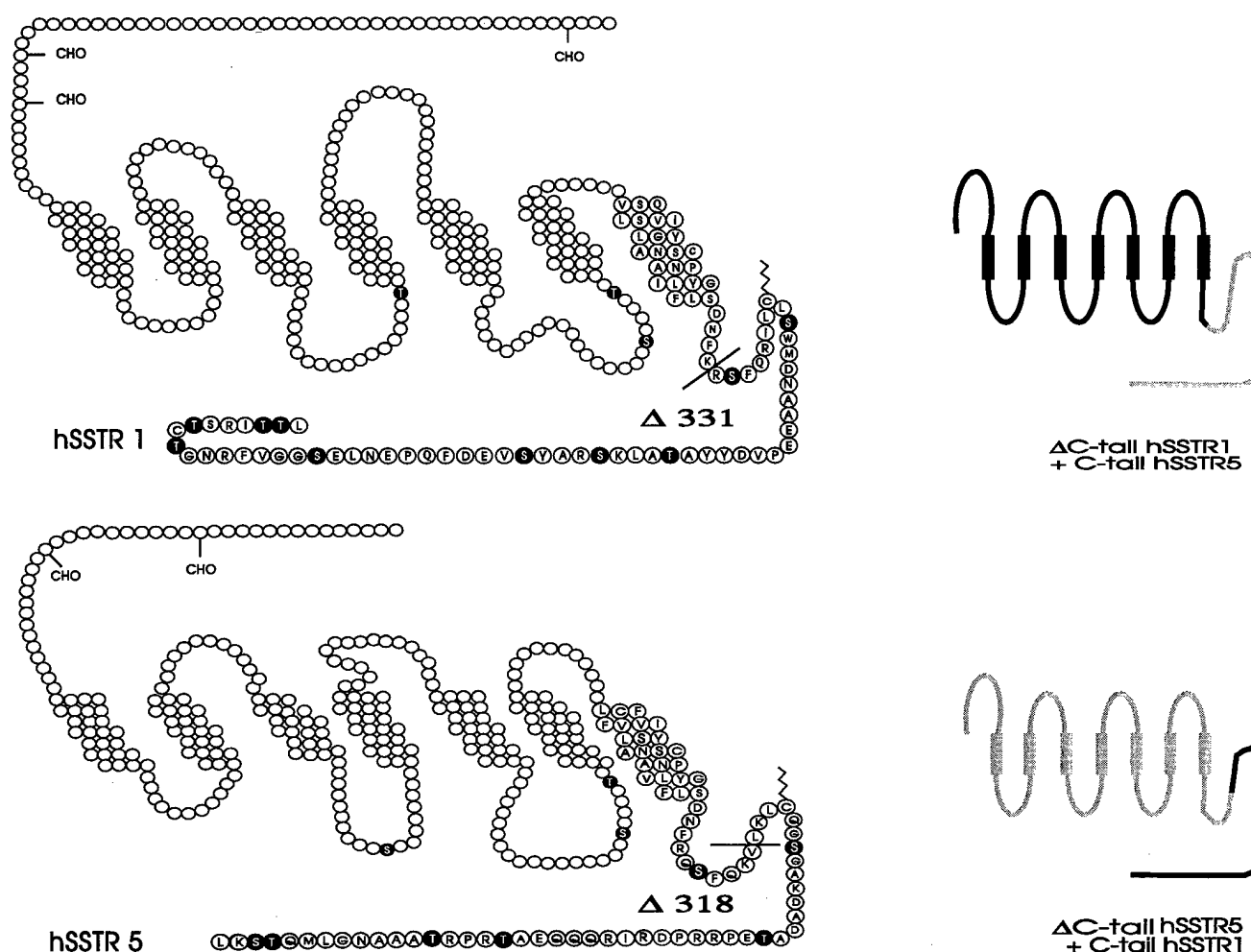


FIG. 1. Schematic depiction of the putative membrane topology of wt hSSTR1 (391 residues) and wt hSSTR5 (363 residues) and of the Δ C-tail hSSTR1 + C-tail hSSTR5 and Δ C-tail hSSTR5 + C-tail hSSTR1 chimeric receptors. Residues in the VIIth transmembrane domain and C-tail of wt hSSTR1 and wt hSSTR5 are marked. Putative phosphorylation sites on serine and threonine residues are highlighted by the dark circles. CHO, putative N-linked glycosylation site, the zig-zag line denotes putative palmitoylation site. C-tail deletion mutants of hSSTR1 and hSSTR5 were created by introducing stop codons after position 331 (hSSTR1) and position 318 (hSSTR5).

well known type of agonist-induced receptor regulation is the property of receptor up-regulation that occurs in response to chronic agonist stimulation of receptors such as the β_3 -adrenergic receptor (β_3 AR) (12), 5HT_{2A} (13, 14), gonadotropin-releasing hormone (GnRH) (15), angiotensin II (16), dopamine 3 (17), the long form of dopamine 2 (D_{2LR}) (18–21), and endogenous SSTRs (22). Since continuous exposure of receptors to agonists is unlikely to occur under normal physiological conditions, this type of response appears to be pharmacological and is observed during long term drug therapy or in disease states. Unlike receptor down-regulation, the underlying molecular mechanisms for up-regulation are poorly understood and thought to involve ligand-induced transcriptional or posttranscriptional induction of receptor synthesis and targeting to the plasma membrane (12–20).

In the case of the SSTR family, we have previously reported that hSSTR5 stably expressed in CHO-K1 cells undergoes rapid agonist-dependent desensitization and internalization, whereas hSSTR1 under the same conditions fails to be internalized and is up-regulated at the plasma membrane following prolonged agonist exposure (23, 24). To identify the underlying molecular signals, we have here created C-tail deletion mutants and hSSTR1/hSSTR5 chimeras, and we have analyzed the ability of these mutant receptors to undergo agonist-dependent internalization or up-regulation as well as G protein-

linked coupling to adenylyl cyclase. We have further investigated membrane and intracellular trafficking of hSSTR1 as well as the relationship between the internalization and up-regulation pathways. We report that the up-regulated receptor is functionally coupled to G proteins and that up-regulation of hSSTR1 is an intrinsic property of the receptor that occurs in the absence of endocytosis or new protein synthesis by an active process of receptor recruitment from the cytoplasm to the cell surface. Furthermore, the receptor C-tail contains molecular signals that specify up-regulation.

EXPERIMENTAL PROCEDURES

Materials—SST-14, SST-28, and Leu⁵, D-Trp²², Tyr²⁵ SST-28 (LTT SST-28) were from Bachem (Marina Del Rey, CA). Cycloheximide, pertussis toxin, okadaic acid, phenylmethylsulfonyl fluoride, and bacitracin were from Sigma. Carrier-free Na¹²⁵I was obtained from Amersham Pharmacia Biotech. Rhodamine-conjugated goat anti-rabbit IgG was from Jackson ImmunoResearch Laboratories (West Grove, PA). Ham's F-12 medium, fetal bovine serum, and G418 were from Life Technologies Inc. Cyclic AMP radioimmunoassay kits were obtained from Diagnostic Products Corp. (Los Angeles, CA). All other reagents were of analytical grade and purchased from various suppliers.

Construction of Wild Type, Mutant, and Chimeric Receptors—cDNA for wild type hSSTR5 was created as a cassette construct in PTEJ8. Wild type (wt) hSSTR1 DNA encoding the complete receptor sequence was generated by PCR amplification using human genomic DNA as template and subcloned into the pDNA3 expression vector. A series of

TABLE I
Comparison of binding, internalization, up-regulation, and adenylyl cyclase coupling of wild type, mutant, and chimeric receptors
Data shown are the mean \pm S.E. of at least three independent experiments.

Receptor	K_d nM	B_{max} fmol/mg protein	Internalization % 60 min	Up-regulation % 22 h	Adenylyl cyclase coupling % inhibition of forskolin-stimulated cAMP
wt hSSTR1	0.62 ± 0.13	229 ± 10	0	110 ± 17	68 ± 4
wt hSSTR5	0.31 ± 0.03	180 ± 28	66 ± 7	0	70 ± 6
Δ C tail hSSTR1	2.3 ± 0.75	113 ± 14	0	0	46 ± 3
Δ C tail hSSTR5	0.89 ± 0.07	262 ± 32	44 ± 5	0	0
Δ C tail hSSTR1 + C tail hSSTR5	0.64 ± 0.11	384 ± 39	27 ± 9	0	30 ± 3
Δ C tail hSSTR5 + C tail hSSTR1	0.34 ± 0.07	220 ± 23	0	71 ± 18	38 ± 4

mutant and chimeric hSSTR1/hSSTR5 receptors were created to investigate the role of the C-tail in the internalization and up-regulation properties of the receptors (Fig. 1). The cytoplasmic tail (C-tail) of wt hSSTR1 contains 65 amino acid residues with 3 tyrosine residues and 11 serine or threonine residues that could serve as putative phosphorylation sites. The wt hSSTR5 C-tail contains 55 amino acid residues with 7 potential serine/threonine phosphorylation sites. C-tail deletions were created at position 318 for hSSTR5 (Δ C-tail hSSTR5) and at position 331 for hSSTR1 (Δ C-tail hSSTR1). Chimeric receptors were constructed by swapping the C-tail of hSSTR5 with the C-tail of hSSTR1 and of the C-tail of hSSTR1 with the C-tail of hSSTR5. Mutations were created by the PCR overlap extension technique (25); for the C-tail-truncated mutants, oligonucleotide primers were used that contain an appropriately placed stop codon after position 331 (hSSTR1) and position 318 (hSSTR5). Chimeric receptors were constructed using oligonucleotide primers designed to allow separate amplification of 5', 3', and internal segments that were subsequently fused by PCR. All primers were designed so as to avoid any change in the reading frame as follows: primer A, 5'-GATCAAGCTTGCCGCCACCAGTGTCCCA-ATGGCACCGCC-3' (R1 forward); primer B, 5'-CAGCCCCGCCGCAC-ACACCACGGAGTAGAT-3' (R1-R5 reverse); primer C, 5'-TGTGCGG-CCGGGCTG-3' (R1-R5 forward); primer D, 5'-GATCGAATTCATTATC-AGACGCTCGTGATCCGG-3' (R5 reverse); primer E, 5'-GACTAAGC-TTCTGCCGCCATGAGAGCCCTG-3' (R5 forward); primer F, 5'-GCG-CTTGAAGTTGTCCGAGAGGAAGC-3' (R5-R1 reverse); primer G, 5'-CTCGGACAACCTCAAGCGCTC-3' (R5-R1 forward); primer H, 5'-GATCGAATTCATTATCAGAGCGTGTGATCCGG-3' (R1 reverse).

To construct the Δ C-tail hSSTR1/C-tail hSSTR5 chimera, primer pairs A and B were used to synthesize the 5' fragment of SSTR1 using SSTR1 cDNA as template for PCR. Primer pairs C and D were used to generate the 3' C-terminal fragment using SSTR5 cDNA as template. PCR was carried out with 50 ng of SSTR cDNA in 100 μ l containing 20 mM Tris-HCl, pH 8.5, 50 mM KCl, 200 μ M dNTPs, 1.5 mM MgCl₂, 7% Me₂SO, and 2.00 units of *Pfu* polymerase (Stratagene). The PCR conditions were as follows: denaturation at 94 °C for 1 min, annealing at 58 °C for 50 s, and extension at 72 °C for 75 s for 25 cycles followed by extension at 72 °C for 10 min. PCR products were separated by agarose gel electrophoresis; the amplified bands were electroeluted and purified. Receptor fragments A—B and C—D were then fused in a third PCR reaction to generate the full-length chimeric receptor in a ligation reaction using flanking primer pairs A and D. The Δ C-tail hSSTR5 + C-tail SSTR1 chimera was generated using primer pairs E—F and G—H to synthesize the 5' and 3' receptor fragments, respectively. The purified amplification products were ligated by PCR using primer pairs E and H. All 5'-flanking primers contained *Hind*III endonuclease restriction sites, Kozak consensus sequences, and initiation codons. All 3'-flanking primers comprised a stop codon followed by an *Eco*RI restriction site. After PCR ligation, the products were digested to completion with *Hind*III and *Eco*RI, and purified fragments were subcloned into the *Hind*III-*Eco*RI multiple cloning sites of pTEJ8. The structure of all mutant and chimeric receptor constructs was confirmed by sequence analysis (University Core DNA Service, University of Calgary, Alberta, Canada). CHO-K1 cells were transfected with cDNAs for wild type or mutant and chimeric hSSTR1/hSSTR5 receptors by the Lipofectin method (Life Technology, Inc.), and stable G418-resistant nonclonally selected cells were propagated for study. wt hSSTR1 was also stably expressed in HEK-293 cells by the same method.

Binding Assays—CHO-K1 cells expressing wild type, mutant, or chimeric receptors were cultured in D75 flasks to ~70% confluency in Ham's F-12 medium containing 10% fetal calf serum and 700 μ g/ml G418. Cells were harvested, homogenized, and membranes prepared by centrifugation. Binding studies were carried out for 30 min at 37 °C with 20–40 μ g of membrane protein and ¹²⁵I-LTT SST-28 radioligand

in 50 mM Hepes, pH 7.5, 2 mM CaCl₂, 5 mM MgCl₂, 0.5% bovine serum albumin, 0.02% phenylmethylsulfonyl fluoride, and 0.02% bacitracin (binding buffer) as described previously (23, 24). Saturation binding experiments were performed with membranes using increasing concentrations of ¹²⁵I-LTT SST-28 (2–2000 pM) under equilibrium binding conditions (24). Incubations were terminated by the addition of 1 ml of ice-cold phosphate-buffered saline containing 0.2% bovine serum albumin, rapid centrifugation, and washing. Radioactivity associated with membrane pellets was quantified in an LKB gamma counter (LKB-Wallach, Turku, Finland). Binding data were analyzed with INPLOT 4.03 (Graph Pad Software, San Diego, CA).

Coupling to Adenylyl Cyclase—Receptor coupling to adenylyl cyclase was tested by incubating cells for 30 min with 1 μ M forskolin and 0.5 mM 3-isobutyl-1-methylxanthine with or without SST (10⁻⁶–10⁻¹⁰ M) at 37 °C as described previously (24). Cells were then scraped in 0.1 N HCl and assayed for cAMP by radioimmunoassay.

Internalization Experiments (Acute Agonist Exposure)—CHO-K1 cells expressing wild type, mutant, and chimeric SSTRs were cultured in 6-well plates and studied at ~90% confluency (1.5 \times 10⁶ cells/well). Cells were equilibrated overnight at 4 °C with ¹²⁵I-LTT SST-28 with or without 100 nM SST-14 (for hSSTR1) or 100 nM SST-28 (for hSSTR5). After washing, cells were warmed to 37 °C for 15, 30, and 60 min to initiate internalization (23, 24). At the end of each incubation, surface-bound radioligand was removed by treatment for 10 min at 37 °C with 1 ml of acid wash (Hanks'-buffered saline acidified to pH 5.0 with 20 mM sodium acetate). Internalized radioligand was measured as acid-resistant counts in 0.1 N NaOH extracts of acid-washed cells.

Up-regulation Experiments (Chronic Agonist Exposure)—CHO-K1 cells expressing wild type, mutant, and chimeric receptors were cultured in 6-well plates in F-12 medium without fetal calf serum with 10⁻⁷ M SST-14 or SST-28 for 4, 9, 13, 16, 19, and 22 h at 37 °C. After acid wash to remove surface-bound SST, whole cell binding assays were performed to determine total and nonspecific binding (24). Residual surface binding was calculated as the difference between control and experimental groups. Dose dependence of up-regulation was studied by incubating cells with 10⁻¹¹–10⁻⁶ M SST-14 for 22 h at 37 °C. The effect of blocking protein synthesis on up-regulation of hSSTR1 was investigated by applying cycloheximide 10 μ g/ml for 30 min to CHO-K1 cells expressing wt hSSTR1 as described previously (22). The effect of pertussis toxin and okadaic acid on SST-induced hSSTR1 up-regulation was determined by continuous treatment with pertussis toxin 100 ng/ml or okadaic acid 200 nM followed by whole cell binding analyses. To investigate the fate of the up-regulated membrane receptor, cells were cultured for 22 h with 10⁻⁷ M SST-14 to induce up-regulation. Cells were then washed gently with 1 ml of 20 mM sodium acetate pH 5.0 for 2 min to remove surface-bound SST-14 and reincubated in culture medium without ligand. Residual surface receptors were analyzed at 12 and 22 h by whole cell binding.

Immunocytochemistry—To analyze surface and cytoplasmic pools of receptors, intact or 0.2% Triton X-100-permeabilized CHO-K1 cells expressing wt hSSTR1 or wt hSSTR5 were processed for confocal fluorescence immunocytochemistry using rabbit polyclonal antipeptide receptor antibodies (4–6, 24). CHO-K1 cells expressing SSTRs were cultured to ~70% confluency and treated with SST for different times. To analyze surface expression of receptors, cells were incubated in serum-free Ham's F-12 medium supplemented with 1% bovine serum albumin in the presence of SSTR primary antibodies for 8–12 h at 4 °C. After washing in 50 mM Tris-HCl, 0.9% NaCl (TBS), pH 7.4, cells were fixed for 30 min at 4 °C in 4% paraformaldehyde. To label the cytoplasmic pool of receptors, cells were permeabilized with 0.2% Triton X-100 in TBS for 5 min at room temperature, washed three times in TBS, and incubated with SSTR primary antibodies for 8–12 h at 4 °C. Antipeptide antibodies directed against the N-terminal segment of hSSTR1

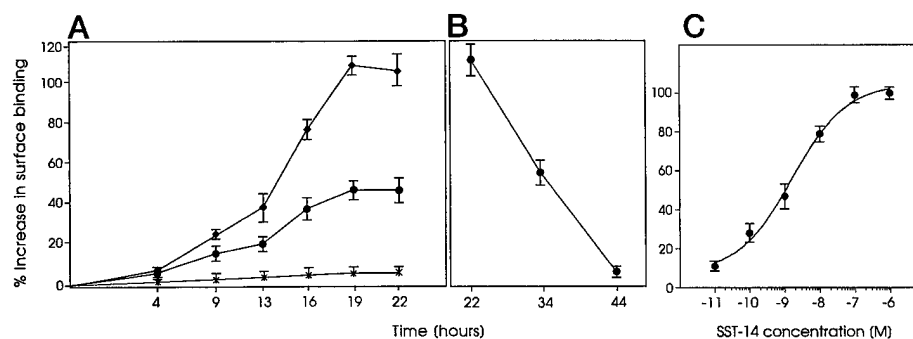


FIG. 2. Effect of time, temperature, and agonist (SST-14) concentration on surface hSSTR1 expression in stable CHO-K1 cells determined by whole cell binding with ^{125}I -LTT-SST-28 ligand. A, 10^{-7} M SST induces surface-receptor expression in a time- and temperature-dependent manner. \blacklozenge , 37 °C; \bullet , 20 °C; $*$, 4 °C. B, removal of SST-14 results in a slow loss of surface hSSTR1-binding sites over 48 h. C, agonist dose-response curve of hSSTR1 up-regulation. (Mean \pm S.E. of three independent experiments in triplicate.)

($^{49}\text{GTLSEGQGS}^{57}$) and hSSTR5 ($^{4}\text{LF(P/S)(A/L)STPS}^{11}$) were produced as described previously and used at a dilution of 1:500 (4). Preimmune serum and antigen-absorbed antibody were used as controls. Cells were then rinsed three times in TBS and incubated for 1 h with rhodamine-conjugated goat anti-rabbit secondary antibody (1:100) at room temperature. After three additional washes, cells were mounted with immunofluor and viewed under a Zeiss LSM 410 confocal microscope. Images were obtained as single optical sections taken through the middle of cells and averaged over 32 scans/frame. They were archived on an Iomega Jaz Disc and printed on a Kodak XLS 8300 high resolution (300 dpi) printer.

RESULTS

Binding Characteristics of C-tail Deletion and Chimeric Receptors—The C-tail deletion and chimeric receptors were correctly targeted to the plasma membrane as determined by binding analysis (Table I). Saturation binding analysis of CHO-K1 cell membranes revealed a comparable level of expression of wt hSSTR1 and wt hSSTR5 (229 ± 10 and 180 ± 28 fmol/mg protein, respectively). The Δ C-tail hSSTR1 mutant displayed a small reduction in B_{max} (113 ± 14 fmol/mg) and binding affinity (K_d 2.3 nM compared with K_d 0.62 nM for wt hSSTR1). As previously reported, the Δ C-tail hSSTR5 mutant displayed high affinity ligand binding (K_d 0.89 nM) which, however, was 3-fold lower than that of the wild type receptor (21). In contrast, the binding parameters of the Δ C-tail hSSTR5 mutant were comparable to those of the wild type receptor. Likewise, the K_d and B_{max} of the two chimeric receptors were comparable to that of wt hSSTR1 and wt hSSTR5.

Agonist-induced Regulation of wt hSSTR1 and wt hSSTR5—As reported previously, ^{125}I -LTT SST-28 when bound to hSSTR5 was rapidly internalized in a time- and temperature-dependent manner with $66 \pm 7\%$ internalization after 60 min at 37 °C, whereas hSSTR1 under comparable incubation conditions showed no internalization (21, 22). Furthermore, long term exposure to SST-14 or SST-28 (10^{-7} M) induced time-dependent up-regulation of hSSTR1 ($110 \pm 17\%$ increase in surface binding after 22 h at 37 °C) with no effect on hSSTR5 (Fig. 2A). Up-regulation of hSSTR1 was temperature-dependent and was reduced to $44 \pm 16\%$ at 20 °C and virtually abolished at 4 °C (Fig. 2A). Up-regulation was also dose-dependent over the concentration range 10^{-11} – 10^{-6} M SST-14 (Fig. 2C). When cells expressing hSSTR1 were first treated with SST-14 (10^{-7} M) for 22 h to up-regulate the receptors, and the SST was then removed, there was a slow loss of surface hSSTR1 expression from 110% at time 0 to $48 \pm 9\%$ at 12 h and $8 \pm 3\%$ at 22 h (Fig. 2B). To determine whether receptor up-regulation was a membrane phenomenon due to aggregation or clustering, membranes rather than whole cells were pre-exposed to SST-14 for 22 h at 37 °C in binding buffer with protease inhibitors (Protease Inhibitor Mixture, 1 tablet/50 ml binding buffer, Roche Molecular Biochemicals). Under these

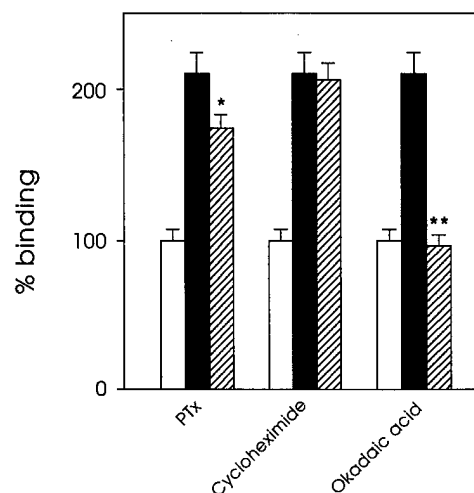


FIG. 3. Effect of pertussis toxin (PTx), cycloheximide, and okadaic acid on hSSTR1 up-regulation by SST-14 (10^{-7} M) treatment for 22 h. Whole cell binding assays were carried out with ^{125}I -LTT-SST-28. SST increases surface binding by 110% which is reduced by 36% by pertussis toxin. Cycloheximide has no effect on hSSTR1 up-regulation, whereas okadaic acid completely abolishes the up-regulation response. \square , control binding; \blacksquare , SST-14; \hatched , SST-14 + test agent shown (mean \pm S.E. of three independent experiments); $*$, $p < 0.05$; $**$, $p < 0.01$.

conditions, receptor concentration (B_{max}) immediately after the preparation of membranes was 229 ± 10 fmol/mg protein and did not change significantly when incubated in binding buffer alone for 22 h at 37 °C indicating stability of the receptor in the membrane preparation. In contrast to whole cells, however, hSSTR1 in membrane preparations showed no up-regulation during 22 h treatment with 10^{-7} M SST-14. This suggests that up-regulation is a temperature-dependent, active process requiring the intact cell. Treatment of hSSTR1 cells with pertussis toxin reduced up-regulation by $36 \pm 8\%$ suggesting that the up-regulation response is only partly mediated by G_i or G_o proteins (Fig. 3). Pretreatment of cells with cycloheximide ($10 \mu\text{g}/\mu\text{l}$ for 30 min) had no effect on hSSTR1 up-regulation (Fig. 3). Okadaic acid (200 nM) completely abolished up-regulation. This suggests that up-regulation of hSSTR1 does not require new protein synthesis but is dependent on dephosphorylation events. To exclude the possibility that up-regulation is a peculiarity of CHO-K1 cell transfection or the level of receptor expression, HEK-293 cells transfected with hSSTR1 were analyzed. These cells expressed 5-fold higher density of hSSTR1 (B_{max} 1.2 ± 0.135 pmol/mg protein); like CHO-K1 cells they failed to internalize ^{125}I -LTT SST-28 and displayed $97 \pm 16\%$ up-regulation of cell surface binding after continuous treatment with SST-14 (10^{-7} M) for 22 h at 37 °C.

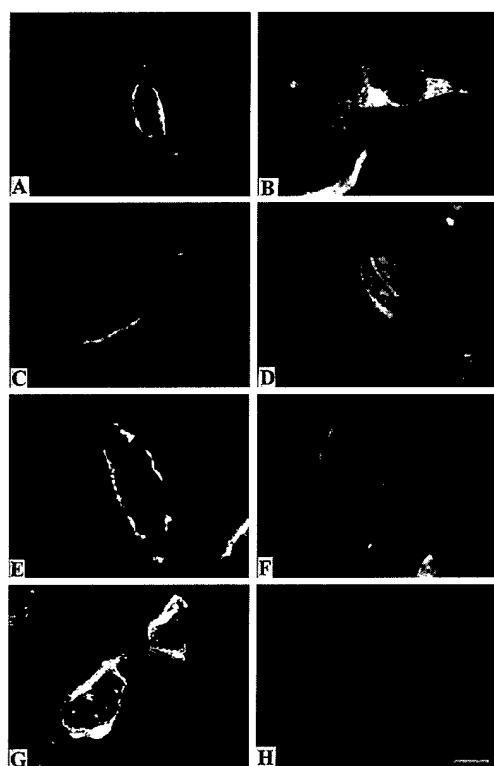


FIG. 4. Immunofluorescence optical sections illustrating fluorescence analysis of hSSTR1 in stably transfected CHO-K1 cells. After treatment with SST-14 for 0, 1, 16, and 22 h, nonpermeabilized cells (A, C, E, and G) and Triton X-100-permeabilized cells (B, D, F, and H) were labeled with rabbit anti-hSSTR1 primary antibody and rhodamine-conjugated goat anti-rabbit secondary antibody. Nonpermeabilized hSSTR1 cells display surface labeling which increases progressively with SST-14 treatment. Permeabilized cells reveal labeling of ill-defined small cytoplasmic vesicular structures at 0 and 1 h which decrease over time with agonist treatment. Scale bar, 25 μ m.

Confocal Fluorescence Immunocytochemistry of hSSTR1 and hSSTR5—In this experiment, we investigated changes in the pattern of expression of hSSTR1 and hSSTR5 proteins in the plasma membrane and intracellular compartments by immunofluorescence with antipeptide receptor antibodies in intact and permeabilized CHO-K1 cells stably expressing hSSTR1 and hSSTR5 (Figs. 4 and 5). After treatment with SST-14 for 0, 1, 16, and 22 h, nonpermeabilized hSSTR1 cells (Fig. 4, A, C, E, and G) displayed surface labeling that increased progressively over time with agonist treatment. Permeabilized cells (Fig. 4, B, D, F, and H) revealed labeling of ill defined small cytoplasmic vesicular structures at 0 and 1 h which decreased after 16 and 22 h treatment with SST-14. Fig. 5 (A, C, E, and G) show surface labeling of hSSTR5 in nonpermeabilized cells. In contrast to hSSTR1, permeabilized hSSTR5 cells (Fig. 5, B, D, F, and H) showed a well defined population of hSSTR5-positive cytoplasmic vesicles. Morphologically, these vesicles were larger than the hSSTR1-positive vesicles, and their cytoplasmic density appeared to be unchanged following agonist stimulation. As expected, surface labeling of both hSSTR1 and hSSTR5 in Figs. 4 and 5 was virtually abolished in the permeabilized cells as a result of Triton X-100 treatment. These results suggest that SSTR1 up-regulation is due to recruitment of receptors from cytoplasmic vesicles to the plasma membrane.

Time Course of Agonist Pretreatment on hSSTR1 Coupling to Adenylyl Cyclase—To determine the effect of continued agonist exposure on the desensitization response, we investigated coupling of hSSTR1 to adenylyl cyclase after 0, 1, and 22 h pretreatment with SST-14 (10^{-7} M). After removal of surface-bound SST-14 by acid wash, the ability of subsequently added

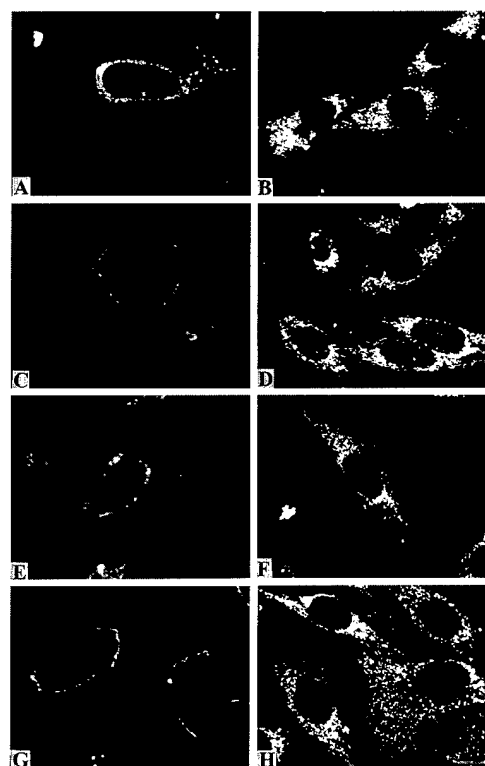


FIG. 5. Immunofluorescence optical sections illustrating immunofluorescence analysis of hSSTR5 in stably transfected CHO-K1 cells. Cells were treated with SST-14 for 0, 1, 16, and 22 h, and receptor immunoreactivity was detected in intact (A, C, E, and G) and permeabilized (B, D, F, and H) cells by immunofluorescence using rabbit anti-hSSTR5 primary antibody and rhodamine-conjugated goat anti-rabbit secondary antibody. Permeabilized hSSTR5 cells show a well defined population of hSSTR5 positive cytoplasmic vesicles which remain the same in density during continued agonist exposure. Scale bar, 25 μ m.

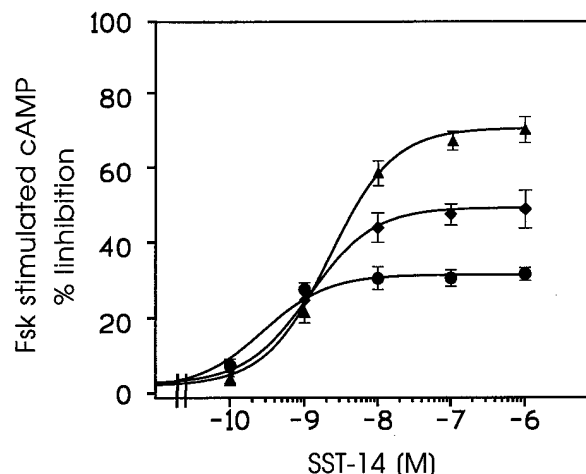


FIG. 6. Time course of agonist pretreatment on hSSTR1 coupling to adenylyl cyclase. Control cells display dose-dependent maximum 68% inhibition of forskolin-stimulated cAMP with 10^{-6} M SST-14 (\blacktriangle) which is reduced to 29% after 1 h pretreatment with SST-14 (10^{-7} M) suggesting receptor uncoupling (\bullet). After 22 h pretreatment with SST-14, receptor coupling to adenylyl cyclase is partially restored (\blacklozenge) suggesting that the up-regulated membrane receptors are not desensitized but are functionally coupled to G protein-linked effector pathways (mean \pm S.E. of three independent experiments in triplicate).

SST-14 to inhibit forskolin-stimulated cAMP accumulation was determined (Fig. 6). Control cells (time 0) displayed dose-dependent maximum $68 \pm 4\%$ inhibition of forskolin-stimulated cAMP with 10^{-6} M SST-14. One hour pretreatment with

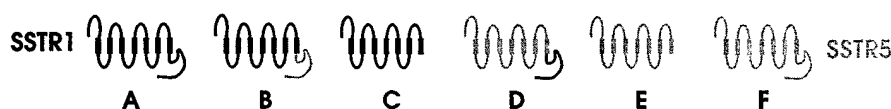
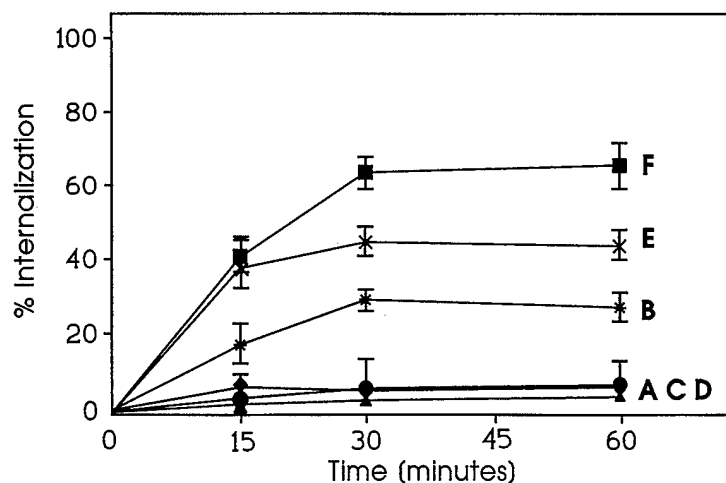


FIG. 7. Time course of internalization of ^{125}I -LTT SST-28 by CHO-K1 cells expressing mutant and hSSTR1-hSSTR5 chimeric receptors. Compared with internalization of wt hSSTR5 of 66% at 60 min (F) truncation of the C-tail reduces internalization to 44% (E). wt hSSTR1 does not internalize (A), and deletion of its C-tail does not induce internalization (C) suggesting that the failure of hSSTR1 to internalize is not due to the presence of negative internalization signals. Replacement of hSSTR1 C-tail with the C-tail of hSSTR5 (B) induces 27% internalization indicating the presence of potent internalization signals in the hSSTR5 C-tail (mean \pm S.E. of three complete experiments).



SST-14 markedly reduced the inhibitory effect of SST-14 on forskolin-stimulated cAMP to a maximum of $29 \pm 3.4\%$ suggesting receptor uncoupling. After 22 h pretreatment with SST-14, absolute cAMP levels increased 2.4-fold. At the same time, the maximum forskolin-stimulated cAMP inhibition by SST-14 increased to $45 \pm 4.1\%$ indicating partial restoration of receptor coupling to adenylyl cyclase. These results suggest that the up-regulated membrane receptors are not desensitized but are functionally coupled to G protein-linked effector pathways.

Internalization of Mutant and hSSTR1-hSSTR5 Chimeric Receptors—Fig. 7 and Table I depict the internalization profiles of ^{125}I -LTT SST-28 incubated over 60 min with CHO-K1 cells expressing C-tail deletion mutants and hSSTR1-hSSTR5 chimeric receptors. Compared with internalization of wt hSSTR5 ($66 \pm 7\%$ at 60 min), truncation of the C-tail reduced internalization to $44 \pm 5\%$. In the case of hSSTR1, both the wild type and C-tail deletion mutants displayed a comparable inability to undergo agonist-promoted endocytosis. Replacement of hSSTR5 C-tail with the C-tail of hSSTR1 completely abolished internalization of the chimeric receptor. This suggests the presence of potent negative internalization signals in the C-tail of hSSTR1 sufficient to block internalization of hSSTR5. The C-tail signals alone, however, cannot explain the inability of hSSTR1 to internalize, since deletion of hSSTR1 C-tail did not induce internalization suggesting the additional involvement of other intracellular domains. Replacement of the hSSTR1 C-tail with the C-tail of hSSTR5 induced $27 \pm 9\%$ internalization confirming the presence of internalization signals in hSSTR5 C-tail (24).

Up-regulation of Mutant and hSSTR1-hSSTR5 Chimeric Receptors—Fig. 8 and Table I illustrate the results of whole cell binding analysis of mutant and chimeric receptors treated with SST-14 for 22 h. Like wt hSSTR5, the Δ C-tail hSSTR5 mutant showed no agonist-dependent increase in cell surface binding. Deletion of the C-tail of hSSTR1, however, completely abolished the ability of this receptor to undergo agonist-dependent up-regulation. The chimeric Δ C-tail hSSTR1 + C-tail hSSTR5 receptor behaved identically to the Δ C-tail hSSTR1 receptor in showing a complete absence of up-regulation. Substitution of hSSTR5 C-tail with that of hSSTR1, however, converted the chimeric receptor to one resembling wt hSSTR1 with $71 \pm 18\%$ up-regulation at the cell surface. This suggests that up-regulation is a functional property of hSSTR1 and is dependent on

molecular signals localized in the receptor C-tail.

Coupling of Mutant and Chimeric hSSTR1-hSSTR5 Receptors to Adenylyl Cyclase—To determine the influence of receptor signaling capability, if any, on the up-regulation process, we determined the ability of mutant and chimeric hSSTR1-hSSTR5 receptors to inhibit forskolin-stimulated cAMP by SST-14 (Fig. 9 and Table I). Deletion of the hSSTR1 C-tail reduced its ability to inhibit forskolin-stimulated cAMP by 23% (from 68 ± 4 to $46 \pm 3\%$). In contrast, as previously shown, deletion of the C-tail of hSSTR5 completely abolished the ability of this receptor to couple to adenylyl cyclase. The two C-tail chimeric constructs maintained some ability to inhibit forskolin-stimulated cAMP; the maximum inhibitory response, however, was reduced to 38 ± 4 and $30 \pm 3\%$ for the Δ C-tail hSSTR1 + C-tail hSSTR5 and Δ C-tail hSSTR5 + C-tail hSSTR1 chimeras, respectively.

DISCUSSION

Although negative regulation by agonists has been established as a fundamental property of most GPCRs (reviewed in Ref. 9), there are only sporadic reports describing the opposite phenomenon of receptor up-regulation by agonists (12–23). This is because unlike acute receptor desensitization, which is clearly a physiological event, receptor up-regulation is elicited only during prolonged agonist stimulation and is consequently less well characterized. Agonist-induced up-regulation has been shown not only for GPCRs but applies to other classes of membrane proteins as well, such as the nicotinic acetylcholine receptor and may, therefore, be a fundamental cellular response (26). Up-regulated receptor function may explain drug tolerance and the ability of receptors such as the $\text{D}_{2\text{L}}$ receptor and SSTRs to maintain normal responsiveness during long term pharmacotherapy (2, 3, 21). Several different mechanisms have been described. In cultured rat pituitary cells, GnRH up-regulates its receptor after a delay of 6 h by a process that is dependent on extracellular Ca^{2+} and new protein synthesis (15). Agonist-mediated up-regulation of 5HT $_2\text{A}$ receptor in cerebellar granule neurons requires transcriptional induction of receptor mRNA by receptor-activated Ca^{2+} influx and activation of calmodulin kinase (13, 14). Likewise, the $\beta_3\text{AR}$ up-regulates after chronic agonist exposure through transcriptional induction of multiple cAMP response elements in the receptor gene secondary to ligand-induced activation of the cAMP signaling pathway (12). Agonist-induced up-regulation

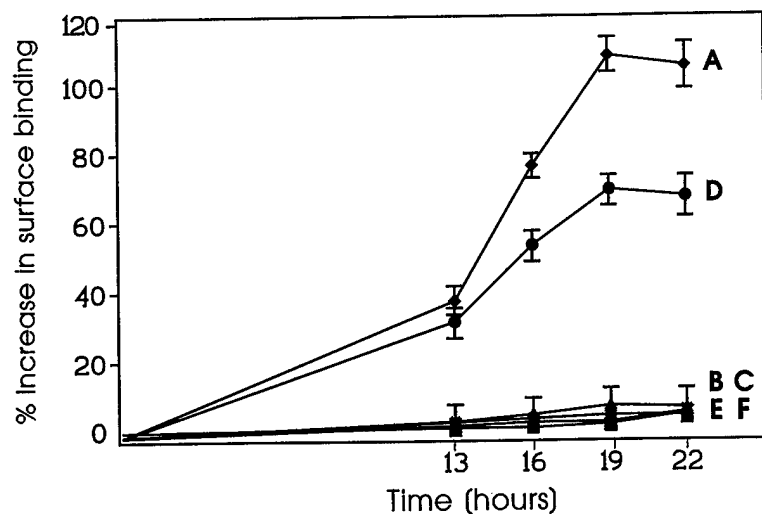
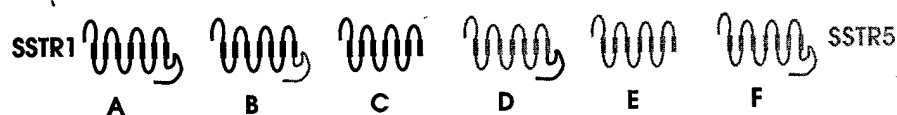


FIG. 8. Up-regulation of mutant and hSSTR1-hSSTR5 chimeric receptors. Whole cell binding analysis of mutant and chimeric receptors in stable CHO-K1 cells treated with SST-14 (10^{-7} M) for 22 h. Up-regulation of hSSTR1 by chronic agonist treatment (A) is completely abolished by truncating the receptor C-tail (C). The hSSTR5 C-tail Δ mutant (E) shows no up-regulation. Substitution of the hSSTR5 C-tail with that of hSSTR1 converts the chimeric receptor to one resembling wt hSSTR1 with 71% up-regulation of surface binding (D) (mean \pm S.E. of three independent experiments).

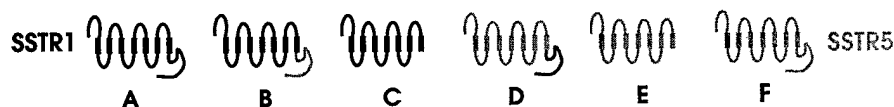
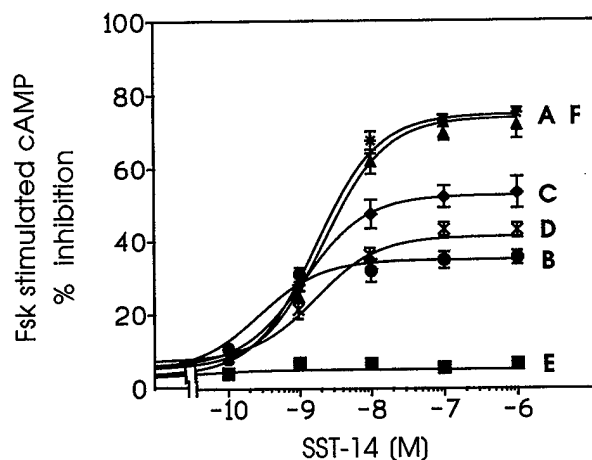


FIG. 9. Coupling of mutant and chimeric hSSTR1-hSSTR5 receptors to adenylyl cyclase. Dose-dependent inhibition by SST-14 of forskolin-stimulated cAMP in CHO-K1 cells stably expressing mutant and chimeric hSSTR1-hSSTR5 receptors (mean \pm S.E. of three independent experiments in triplicate).



has been extensively investigated in the case of the D_2 L_R, either as endogenous receptors in tumor cell lines or as recombinant receptors in various host cells (18–21). These studies have revealed a time- and concentration-dependent induction of surface receptors by 30–300% over 4–20 h by 10^{-9} – 10^{-6} M dopamine in different cells (17–19). The effect of cycloheximide on up-regulation of D_2 L_R is controversial, with some (18) but not all (19–21) studies reporting blockade of up-regulation by the protein synthesis inhibitor, cycloheximide. The kinetics of hSSTR1 up-regulation that we found were comparable to those of the D_2 L_R. Thus hSSTR1 was up-regulated in a time-, temperature-, and dose-dependent manner to saturable levels. Up-regulation did not occur in membrane preparations, required the intact cell, and produced functional G protein-coupled surface receptors. Furthermore, up-regulation was unaffected by cycloheximide suggesting that it is not due to new receptor synthesis but likely represents receptors from a pre-existing pool. This is in agreement with earlier findings that up-regulation of endogenous SSTRs in GH₄C₁ cells (which express

predominantly the SSTR1 subtype) are also insensitive to cycloheximide (22). Overall then, these results suggest that up-regulation of most GPCRs is dependent on transcriptional and posttranscriptional induction of new receptor synthesis, the exception being SSTR1 and probably the D_2 L_R.

Four of the five SSTR isotypes, SSTR2, -3, -4, -5, are readily internalized by ligand binding (23, 24, 27, 28). Internalization of SSTR2, -3, -5 has been shown to be dependent on residues in the C-tail (24, 27, 28), and in the case of hSSTR5 both negative and positive endocytic signals have been identified (24). Like the other SSTRs, the C-tail of hSSTR1 is rich in putative serine and threonine phosphorylation sites, and additionally features three tyrosine residues that could act as potential endocytic signals (Fig. 1). Nonetheless, this receptor was incapable of ligand-induced internalization. We found that the C-tail of hSSTR1 contains negative internalization signals, since substitution of the C-tail of hSSTR5 with that of hSSTR1 blocked internalization of the chimeric receptor. The inability of hSSTR1 to internalize, however, cannot be attributed solely to

negative signals in the C-tail since deletion of the C-tail did not activate internalization suggesting that additional positive signals in the C-tail or on residues located in other intracellular domains are required. Our finding that SSTR1 is refractory to agonist-promoted endocytosis raises the question of whether the increased surface binding over time is simply a reflection of receptor aggregates, such as dimers with altered binding, or membrane accumulation of ligand-stabilized SSTRs that would otherwise have been degraded. Several other receptors that up-regulate, e.g. β_3 AR, D_{2L}R are also resistant to internalization (21, 29–31), whereas others such as the GnRH receptor (15), 5HT₂ receptor (32), and SSTR2 and -4 display both endocytosis and up-regulation (23, 27) suggesting that lack of internalization is not an absolute requirement for up-regulation. Likewise, up-regulation is not an automatic consequence of poor internalization as indicated by the Δ C-tail hSSTR1 mutant in the present study which displayed neither internalization nor up-regulation. We have recently reported that hSSTR1 and hSSTR5 associate as dimers both as homodimers or heterodimers and that dimerization alters the functional properties of the receptor such as ligand binding affinity and agonist regulation (33). Our finding, however, that up-regulation is temperature-dependent and does not occur when membranes are incubated directly with agonist rules out surface aggregation and points toward an active process of receptor recruitment to the plasma membrane. This was directly demonstrated by confocal fluorescence immunocytochemistry that showed a progressive time-dependent increase in surface SSTR labeling associated with a parallel depletion of intracellular SSTR immunofluorescent vesicles suggesting translocation from the cytoplasm to the plasma membrane.

Up-regulation of hSSTR1 was not dependent on receptor signaling as evident from the dissociated effects of the C-tail deletion mutants and chimeric receptors on up-regulation and coupling to adenylyl cyclase. For instance, the Δ C-tail hSSTR1 mutant showed complete loss of up-regulation in the face of only a small decrease in adenylyl cyclase coupling efficiency. Up-regulation was only partially inhibited by pertussis toxin implying that coupling to a second messenger system via pertussis toxin-sensitive G proteins such as G_i or G_o is not required. The involvement of non-G protein-linked pathways such as the Na⁺/H⁺ antiporter to which hSSTR1 is coupled, however, cannot be excluded (8). Dissociation of up-regulation from signaling has also been noted in the case of the D_{2L} receptor that has been shown to up-regulate as efficiently with antagonists as with agonists suggesting that receptor occupancy irrespective of signaling capability is the critical determinant (20). This means that as in the case of the internalization of many GPCRs which can be dissociated from receptor signaling, up-regulation is an intrinsic property of some receptors such as hSSTR1, being triggered by a specific ligand-induced conformational change. The molecular signals that specify hSSTR1 up-regulation are located in the C-tail since deletion of this segment abrogated the up-regulation response. Even more compelling evidence that the C-tail of hSSTR1 harbors up-regulating sequences came from the chimeric receptor studies in which the C-tail of hSSTR1 conferred the property of up-regulation to hSSTR5, a receptor that normally displays agonist-dependent internalization. The nature of the molecular signals in the C-tail of hSSTR1 that mediate up-regulation remains to be determined. As in the case of internalization, phosphorylation of C-tail residues is likely to be important, given our finding that okadaic acid, an inhibitor of serine, threonine phosphatase, completely abolished up-regulation, suggesting that receptor dephosphorylation is a requisite step for up-regulation. But where is the cytoplasmic receptor pool

that interacts with the receptor C-tail and what are the intervening steps? Since the receptor is not internalized, it is likely to be in a nonendosomal compartment, probably in post-Golgi transport vesicles for targeting the receptor to the plasma membrane. This is consistent with our immunocytochemical studies that showed that hSSTR1 is distributed in morphologically distinct cytoplasmic vesicles compared with the endosomal localization of hSSTR5. Recent work with the β -adrenergic receptor has proposed internalization as an obligatory requirement for activation of the mitogenic signaling complex (34). This model assigns a pivotal role to β -arrestin that binds to the ligand-activated, phosphorylated receptor and triggers the assembly of clathrin and the cytoplasmic tyrosine kinase c-src on β -arrestin molecules to initiate internalization of the receptor complex as a necessary step for effecting MAP kinase activation. The finding that SSTR1 can activate MAP kinase (35) without being internalized suggests that there may be alternative non-arrestin-dependent pathways for coupling the receptor to the MAP kinase signaling cascade.

In summary, these results show that hSSTR1 can desensitize rapidly in response to agonist but lacks the ability to be internalized, and thus displays only part of the acute agonist-dependent regulatory response. Continued agonist exposure induces a time- and concentration-dependent up-regulation of functional surface receptors. Up-regulation occurs by a temperature-dependent active process of ligand-induced receptor recruitment from a pre-existing cytoplasmic pool. It does not require new protein synthesis or signal transduction, is sensitive to dephosphorylation events, and is critically dependent on molecular signals in the receptor C-tail. Further studies are required to map the specific regulatory motifs in the C-tail of hSSTR1 and to identify the mediators distal to the C-tail which direct receptor trafficking from the cytoplasm to the plasma membrane.

Acknowledgment—We thank Wei-Yi for technical assistance and M. Correia for secretarial help.

REFERENCES

- Reichlin, S. (1983) *N. Engl. J. Med.* **309**, 1495–1501, 1556–1563
- Patel, Y. C., and Srikant, C. B. (1997) *Trends Endocrinol. Metab.* **8**, 398–405
- Lamberts, S. W. J., Van Der Lely, A. J., and de Herder, W. W. (1996) *N. Engl. J. Med.* **334**, 246–254
- Kumar, U., Laird, D., Srikant, C. B., Escher, E., and Patel, Y. C. (1997) *Endocrinology* **138**, 4473–4476
- Kumar, U., Sasi, R., Suresh, S., Patel, A., Thangaraju, M., Metrakos, P., Patel, S. C., and Patel, Y. C. (1998) *Diabetes* **48**, 77–85
- Khare, S., Kumar, U., Sasi, R., Puebla, L., Calderon, L., Lemstrom, K., Hayry, P., and Patel, Y. C. (1999) *FASEB J.* **13**, 387–394
- Sharma, K., Patel, Y. C., and Srikant, C. B. (1999) *Mol. Endocrinol.* **13**, 82–90
- Hou, C., Gilbert, R. L., and Barber, D. L. (1994) *J. Biol. Chem.* **269**, 10357–10362
- Dohlman, H. G., Thorner, J., Caron, M. G., and Lefkowitz, R. J. (1991) *Annu. Rev. Biochem.* **60**, 653–658
- Goodman, O. B., Jr., Krupnick, J. G., Santini, F., Gurevich, V. V., Penn, R. B., Gagnon, A. W., Keen, J. H., and Benovic, J. L. (1996) *Nature* **383**, 447–450
- Zhang, J., Barak, L. S., Winkler, K. E., Caron, M. G., and Ferguson, S. S. G. (1997) *J. Biol. Chem.* **272**, 27005–27014
- Thomas, R. F., Holt, B. D., Schwinn, D. A., and Liggett, S. B. (1992) *Proc. Natl. Acad. Sci. U. S. A.* **89**, 4490–4494
- Akiyoshi, J., Hough, C., and Chuang, D.-M. (1993) *Mol. Pharmacol.* **43**, 349–355
- Chen, H., Li, H., and Chuang, D.-M. (1995) *J. Pharmacol. Exp. Ther.* **275**, 674–680
- Loumaye, E., and Catt, K. J. (1983) *J. Biol. Chem.* **258**, 12002–12009
- Dudley, D. T., and Summerfelt, R. M. (1993) *Regul. Pept.* **44**, 199–206
- Cov, B. A., Rosser, M. P., Kozlowski, M. R., Duwe, K. M., Neve, R. L., and Neve, K. A. (1995) *Synapse* **21**, 1–9
- Zhang, L. J., Lochowicz, J. E., and Sibley, D. R. (1994) *Mol. Pharmacol.* **45**, 878–889
- Starr, S., Kozell, L. B., and Neve, K. A. (1995) *J. Neurochem.* **65**, 569–577
- Filtz, T. M., Guan, W., Artymyshyn, R. P., Pacheco, M., Ford, C., and Molinoff, P. B. (1994) *J. Pharmacol. Exp. Ther.* **271**, 1574–1582
- Ng, G. Y. K., Varghese, G., Chung, H. T., Trogadis, J., Seeman, P., O'Dowd, B. F., and George, S. R. (1997) *Endocrinology* **138**, 4199–4206
- Presky, D. H., and Schonbrunn, A. (1988) *J. Biol. Chem.* **263**, 714–721
- Hukovic, N., Panetta, R., Kumar, U., and Patel, Y. C. (1996) *Endocrinology* **137**, 4046–4049
- Hukovic, N., Panetta, R., Kumar, U., Rocheville, M., and Patel, Y. C. (1998)

- J. Biol. Chem.* **273**, 21416–21422
25. Ho, S. N., Hunt, H. D., Horton, R. M., Pullen, J. K., and Pease, L. R. (1989) *Gene (Amst.)* **77**, 51–59
26. Whiteaker, P., Sharples, C. G. V., and Wonnacott, S. (1998) *Mol. Pharmacol.* **53**, 950–962
27. Hipkin, R. W., Friedman, J., Clark, R. B., Eppler, C. M., and Schonbrunn, A. (1997) *J. Biol. Chem.* **272**, 13869–13876
28. Roth, A., Kreienkamp, H.-J., Meyerhof, W., and Richter, D. (1997) *J. Biol. Chem.* **272**, 23769–23774
29. Liggett, S. B., Freedman, N. J., Schwinn, D. A., and Lefkowitz, R. J. (1993) *Proc. Natl. Acad. Sci. U. S. A.* **90**, 3665–3669
30. Nantel, F., Bonin, H., Emorine, L. J., Zilberfarb, V., Strosberg, A. D., Bouvier, M., and Marullo, S. (1993) *Mol. Pharmacol.* **43**, 548–555
31. Barton, A. C., Black, L. E., and Sibley, D. R. (1991) *Mol. Pharmacol.* **39**, 650–658
32. Perry, R. C., Unsworth, C. D., and Molinoff, P. B. (1993) *Mol. Pharmacol.* **43**, 726–733
33. Rocheville, M., Sasi, R., and Patel, Y. C. (1999) *Program of the 81st Annual Meeting of the Endocrine Society, San Diego, June 12–15, 1999*, Abstr. P2–459, Endocrine Society, Bethesda, MD
34. Luttrell, L. M., Ferguson, S. S. G., Daaka, Y., Miller, W. E., Maudsley, S. et al. (1999) *Science* **283**, 655–660
35. Florio, T., Yao, H., Carey, K. D., Dillon, T. J. and Stork, P. J. S. (1999) *Mol. Endocrinol.* **13**, 24–37

C-Terminal Region of Human Somatostatin Receptor 5 Is Required for Induction of Rb and G₁ Cell Cycle Arrest

Kamal Sharma, Yogesh C. Patel, and Coimbatore B. Srikant

Fraser Laboratories

Departments of Medicine (K.S., Y.C.P.), Neurology (Y.C.P.), and
Neurosurgery (Y.C.P.)

McGill University and Royal Victoria Hospital
Montreal, Quebec, Canada, H3A 1A1

Ligand-activated somatostatin receptors (SSTRs) initiate cytotoxic or cytostatic antiproliferative signals. We have previously shown that cytotoxicity leading to apoptosis was signaled solely via human (h) SSTR subtype 3, whereas the other four hSSTR subtypes initiated a cytostatic response that led to growth inhibition. In the present study we characterized the antiproliferative signaling mediated by hSSTR subtypes 1, 2, 4, and 5 in CHO-K1 cells. We report here that cytostatic signaling via these subtypes results in induction of the retinoblastoma protein Rb and G₁ cell cycle arrest. Immunoblot analysis revealed an increase in hypophosphorylated form of Rb in agonist-treated cells. The relative efficacy of these receptors to initiate cytostatic signaling was hSSTR5>hSSTR2>hSSTR4~hSSTR1. Cytostatic signaling via hSSTR5 also induced a marginal increase in cyclin-dependent kinase inhibitor p21. hSSTR5-initiated cytostatic signaling was G protein dependent and protein tyrosine phosphatase (PTP) mediated. Octreotide treatment induced a translocation of cytosolic PTP to the membrane, whereas it did not stimulate PTP activity when added directly to the cell membranes. C-tail truncation mutants of hSSTR5 displayed progressive loss of antiproliferative signaling proportional to the length of deletion, as reflected by the marked decrease in the effects of octreotide on membrane translocation of cytosolic PTP, and induction of Rb and G₁ arrest. These data demonstrate that the C-terminal domain of hSSTR5 is required for cytostatic signaling that is PTP dependent and leads to induction of hypophosphorylated Rb and G₁ arrest. (*Molecular Endocrinology* 13: 82-90, 1999)

INTRODUCTION

The antiproliferative actions of somatostatin (SST) signaled via cell surface SST receptors (SSTRs) regulate cellular protein phosphorylation and elicit cytostatic (growth arrest) and cytotoxic (apoptosis) responses in tumor cells. For instance, SST treatment causes apoptosis in MCF-7 and AtT-20 cells, whereas it induces cell cycle arrest in GH₃ cells (1-5). Such discrepant findings may be due to the existence of five distinct SSTR subtypes and their differential expression in these tumor cells (6-10). We have reported that human (h) SSTR3 is the only subtype that is capable of cytotoxic signaling: upon ligand activation, cells transfected with hSSTR3 respond with induction of wild-type (wt) tumor suppressor protein p53, the proapoptotic protein Bax, and an acidic endonuclease and intracellular acidification and undergo apoptosis (11, 12). The antiproliferative action of SST is also signaled via SSTRs 2, 4, and 5. However, neither apoptosis nor changes in any of the above parameters were seen in cell lines stably expressing these subtypes (11, 13). While SST was shown to inhibit cell growth via hSSTRs 2, 4, and 5, such a conclusion was based on measurement of thymidine incorporation or cell number at a single time point during SST treatment (14-17). Thus, the mechanism underlying the antiproliferative signaling mediated by the SSTR subtypes incapable of triggering apoptosis remained unknown. Since these SSTR subtypes do not initiate apoptotic signals, it appeared likely that they may transduce cytostatic signals leading to cell cycle arrest.

Cytostatic events leading to G₁ cell cycle arrest are associated with the induction of two proteins Rb (retinoblastoma tumor suppressor protein) and p21 (cyclin-dependent kinase inhibitor, also called Waf-1/Cip1) (18). Rb is a phosphorylated protein: it remains hyperphosphorylated (ppRb) in S and G₂/M phases and becomes hypophosphorylated (pRb) in G₁. pRb negatively regulates the G₁/S transition and promotes accumulation of cells in the G₁ phase (18, 19). Rapid

phosphorylation of Rb occurs before entry of cells into S phase. While Rb functions independently of p53, p21 mediates p53-dependent G₁ arrest (18, 20). Nevertheless, overexpression of p21 can induce G₁ arrest in the absence of p53 induction (21). To determine whether the antiproliferative signaling via these hSSTRs causes cell cycle arrest and to identify the molecular mediators involved in this process, we evaluated the effect of SST in CHO-K1 cells expressing hSSTRs 1, 2, 4, and 5 on cell cycle progression and induction of Rb and p21. We report here that SST-induced G₁ cell cycle arrest in these cells is due mainly to the induction of Rb. Maximal effect was exerted via hSSTR5 followed by hSSTR 2, 4, and 1. In hSSTR5-expressing cells, a major portion of SST-induced Rb was hypophosphorylated. SST-induced G₁ arrest and induction of Rb were pertussis toxin sensitive, G protein dependent, and protein tyrosine phosphatase (PTP) dependent. In octreotide (OCT)-treated cells there was a redistribution of PTP activity from the cytosol to the membrane. Mutational analysis of the C tail of this receptor revealed that the C tail of the receptor is essential for PTP-dependent cytostatic signaling.

RESULTS

We first compared the effect of SST agonists [OCT (hSSTRs 2, 3, and 5) or D-Trp⁸ SST-14 (hSSTRs 1 and 4)] on cell cycle parameters in CHO-K1 cells expressing individual hSSTRs. Cells were incubated for 24 h in the absence or presence of agonists at a maximal stimulatory concentration of 100 nM. (11). Cell cycle analysis revealed that cells expressing hSSTRs 1, 2, 4, and 5 responded with a decrease in the rate of proliferation. This was evident from the agonist-induced increase in cells in G₁ and a decrease in S (Fig. 1). The greatest cytostatic response was elicited through hSSTR 5 followed by hSSTR2>hSSTR4~hSSTR1. The effect of agonist treatment on cell cycle parameters is shown in Fig. 2. In addition to the changes in G₁ and S phases, a relative increase of cell number in G₂/M was also seen. The absence of oligonucleosomal DNA fragmentation, even after treatment for 48 h, indicated that SST-induced cell cycle arrest via hSSTR5 did not lead to apoptosis (data not shown).

Inhibition of cell cycle progression signaled via hSSTR 5 was associated with induction of Rb. The increase in intensity of fluorescence of immunolabeled Rb counterstained with fluorescein isothiocyanate (FITC)-conjugated second antibody was seen in all phases of the cell cycle after OCT treatment. Dual label analysis of fluorescence emissions of propidium iodide (PI) and immunostained Rb revealed that the majority of cells were in G₀/G₁ phase (Fig. 3A). Immunoblot analysis of cell extracts revealed that the level of Rb was low in untreated cells and was present mainly as ppRb. An OCT-induced increase in Rb was

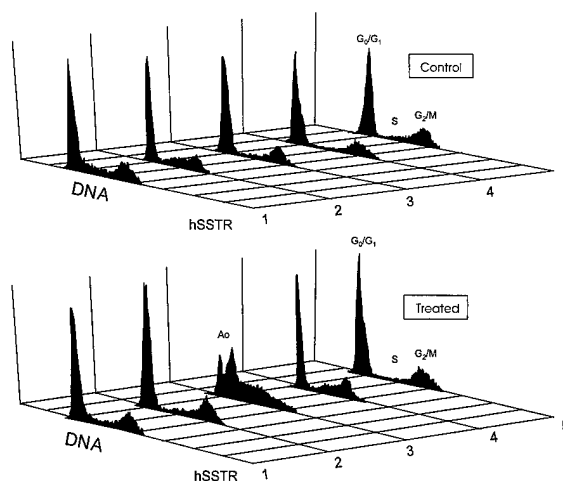


Fig. 1. Effect of Peptide Treatment on Cell Cycle Parameters in CHO-K1 Cells Expressing hSSTR1-5

Representative plots showing the phase distribution of cells incubated for 24 h in the absence (*top panel*) or presence (*bottom panel*) of 100 nM OCT (hSSTRs 2, 3, and 5) or D-Trp⁸ SST-14 (hSSTRs 1 and 4). Cellular DNA was stained with PI and analyzed by flow cytometry. An increase in G₁ peak can be seen in cells expressing four of the five hSSTR subtypes (hSSTR5>hSSTR2>hSSTR4~hSSTR1). This contrasts with the decrease in G₁ peak and the appearance of a hypodiploid peak in the region A₀ after peptide treatment in cells expressing hSSTR3.

reflected in both hyper- and hypophosphorylated (ppRb and pRb) forms detectable by their differential electrophoretic mobility (Fig. 3B). A marked enlargement of the nuclei in hSSTR5-expressing cells was observed in OCT-treated cells (Fig. 3C), a typical characteristic of G₁ arrested cells (22). OCT-induced increase in Rb was time dependent and was detectable by 4 h (2.7 ± 0.9 fold) and was maximal at 24 h (8.1 ± 0.8 fold) (Fig. 4A). Induction of Rb preceded the onset of G₁ arrest since an increase in G₁/S ratio, which is an index of inhibition of cell proliferation, was detectable only by 8 h (Fig. 4B). The ability of OCT to induce Rb during 24 h incubation was dose dependent and occurred over the concentration range 10–100 nM (Fig. 5A). Immunoblot analysis revealed a dose-dependent increase in both ppRb and pRb in OCT-treated cells (Fig. 5B).

OCT-treated hSSTR5 cells also displayed an increase in p21 (3 ± 0.6 fold over basal level) and was of much smaller magnitude compared with that of Rb. OCT-induced increase in Rb and p21 was abolished by pertussis toxin pretreatment (Fig. 6). Sodium orthovanadate, an inhibitor of PTP, also abrogated the inductive effect of OCT on Rb and p21^{Waf1} in these cells. To confirm that PTP activity is involved in the cytostatic signaling via hSSTR5, we measured PTP activity in extracts of cells before and after incubation with SST. In OCT-treated cells there was a 40% increase in membrane-associated PTP while the cytosolic enzyme activity decreased by 20% (Fig. 7). By contrast, when added to the membrane fractions at

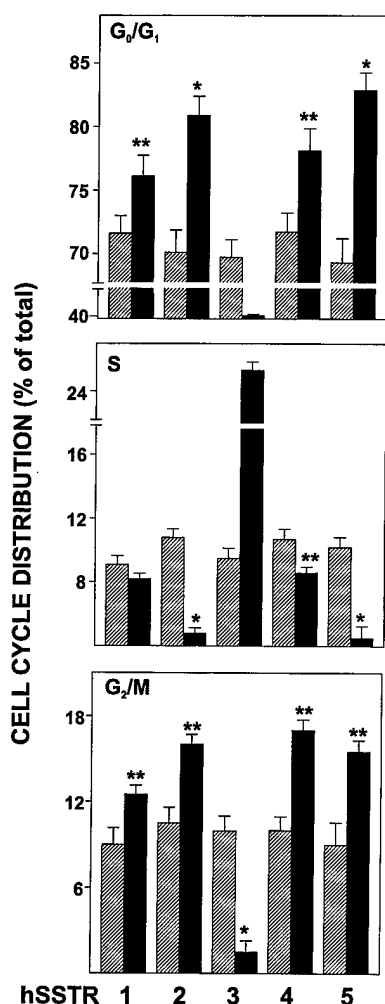


Fig. 2. Effect of Agonist Treatment on Cell Cycle Parameters in CHO-K1 Cells Expressing Individual hSSTR Subtypes

The distribution of cells in G₀/G₁ (top panel), S (middle panel), and G₂/M (bottom panel) were quantitated by analysis of PI-stained cells by flow cytometry. The increase in the number of cells G₀/G₁ was accompanied by a decrease in cell number in S phase. A small increase in G₂/M was also evident in agonist-treated cells (mean ± SE, n = 3). *, P < 0.005; **, P < 0.05.

the time of enzyme assay, OCT failed to stimulate PTP activity (data not shown). While the maximal induction of Rb was hSSTR5 mediated, three other subtypes were also found to initiate cyostatic signals leading to Rb induction (Fig. 8). The rank order potency of these SSTRs for signaling the increase in Rb was hSSTR5 > 2 > 4 > 1, the same as that observed for triggering G₁ arrest (Figs. 1 and 2). By contrast, no increase in Rb occurred in hSSTR3 expressing cells, in agreement with our previously reported finding that OCT does not induce G₁ arrest via this subtype (11, 12).

The C tail of several G protein-coupled receptors has been implicated in G protein interaction and effector coupling (23, 24). To evaluate the importance of the C tail of hSSTR5 in cyostatic signaling, we inves-

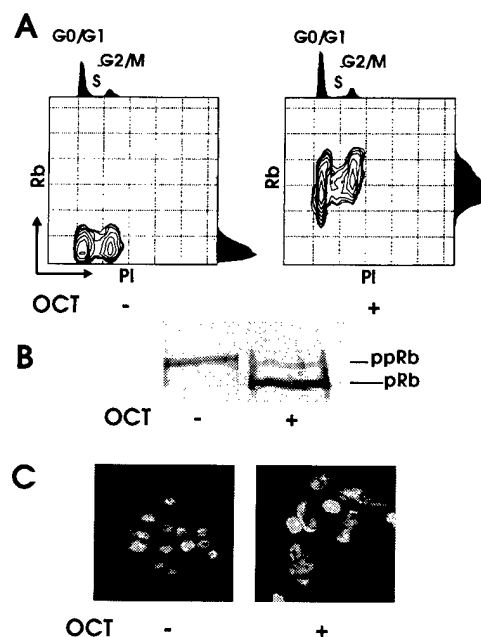


Fig. 3. hSSTR5-Mediated Antiproliferative Signaling in CHO-K1 Cells Causes G₁ Cell Cycle Arrest Associated with Induction of Rb

A, Flow cytometric analysis of hSSTR5 expressing cells incubated in the absence and presence of 100 nM OCT for 24 h. Scattergram represents dual label plot of FITC fluorescence of immunostained Rb measured on a log scale against PI fluorescence measured on a linear scale. In addition, PI fluorescence depicting the cell cycle distribution is shown on the top, and the FITC fluorescence of immunostained Rb is shown on the right of the scattergram. An OCT-induced increase in Rb occurred in all phases of the cell cycle and was associated with an increase in the number of cells in G₁. Data are representative of three separate experiments. B, Western blot analysis of Rb in CHO-K1 cells. In addition to the total increase in Rb in OCT-treated cells, a significant portion was in the hypophosphorylated form (pRb) that could be distinguished from the hyperphosphorylated form (ppRb) on the basis of differential electrophoretic mobility. C, Nuclear morphology of PI-stained cells revealed nuclear enlargement, a feature that is characteristic of G₁ arrested cells.

tigated the effect of mutant hSSTR5 receptors with progressive truncation of the C tail (Fig. 9). These mutants have been previously reported to display binding characteristics and G protein coupling comparable to wild-type hSSTR5 (25). Progressive truncation of the C tail of hSSTR5 was associated with an impaired ability of OCT to signal activation of Rb and induce G₁. Compared with the wild-type receptor, which triggered 8.1 ± 0.8 fold increase in Rb in response to OCT, the Δ347 mutant displayed only a 6.1 ± 0.4 fold increase in Rb (Fig. 10). The Δ338, Δ328, and Δ318 mutants displayed more marked loss in the ability to activate Rb in response to OCT (3.0 ± 0.9 fold for Δ338, 2.1 ± 0.7 fold for Δ328, and 1.3 ± 0.2 fold for Δ318). To determine whether progressive loss of ability to induce Rb parallels the decrease in membrane-associated PTP, we compared PTP activity in cytosol-

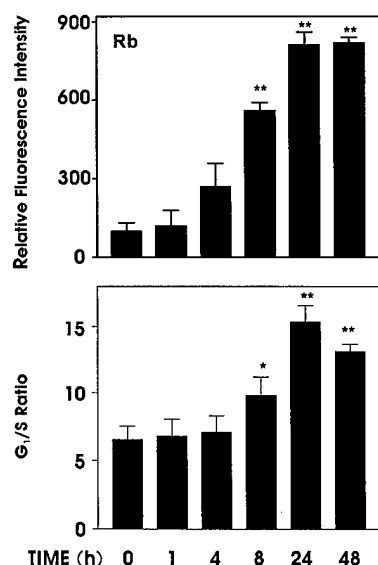


Fig. 4. Time Dependency of hSSTR5-Mediated Induction of Rb and Inhibition of Cell Cycle Progression

After incubation in the presence of 100 nM OCT for the indicated time, Rb and DNA were quantitated in the same cell populations by dual label flow cytometry (mean \pm SE, $n = 3$; *, $P < 0.05$; **, $P < 0.005$). A, Rb was quantitated by flow cytometry after immunolabeling. Values represent as percent change in fluorescence intensity measured on a log scale and compared with that in untreated cells taken as 100% (mean \pm SE, $n = 3$). B, Inhibition of cell proliferation by OCT is reflected in the increase in the ratio of cells in G₁ and S phases is evident by 8 h and was maximal at 24 h.

lic and membrane fractions in cells incubated in the absence and presence of OCT. In contrast to the more than 2-fold increase induced by OCT pretreatment in cells expressing hSSTR5, only ~25% increase occurred with the mutant $\Delta 347$, and no change was seen with the shorter hSSTR5 mutants (Fig. 11). Interestingly, the basal membrane-associated PTP activity was higher in untreated cells expressing each of the mutant receptors compared with wild-type hSSTR5.

DISCUSSION

The present study establishes that SSTR-mediated antiproliferative signaling elicits subtype-selective cytostatic effect via hSSTRs 1, 2, 4, and 5. In CHO-K1 cells expressing each of these four hSSTR subtypes, there was decreased proliferation due, in part, to a G₁ cell cycle arrest associated with an increase in Rb. The extent of Rb induction and inhibition of cell cycle progression was the greatest in CHO-K1 cells expressing hSSTR5, followed by hSSTR2>hSSTR4~hSSTR1. A significant proportion of Rb induced via hSSTR5 was present in a hypophosphorylated form as evident from its greater electrophoretic mobility. We show that OCT treatment caused nuclear enlargement in hSSTR5-expressing cells, a feature that is characteristic of cells in

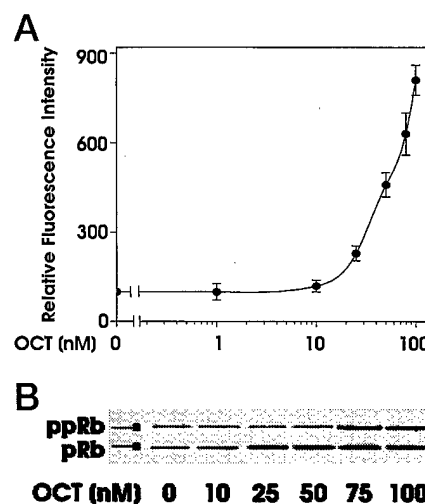


Fig. 5. Dose-Dependent Induction of Rb by OCT via hSSTR5

A, Rb was measured by flow cytometry after immunolabeling in cells incubated with the indicated concentrations of the peptide for 24 h. Values represent percent change in fluorescence intensity measured on a log scale and compared with that in untreated cells taken as 100% (mean \pm SE, $n = 3$). B, Immunoblot demonstrating that OCT-induced augmentation in Rb is associated with a dose-dependent increase in hypophosphorylated form of Rb (pRb).

G₁ arrest (22). Additionally, hSSTR5-mediated cytostatic signaling did not lead to apoptosis. While the cytostatic action exerted through hSSTR5 by OCT was dose- and time dependent, such an effect occurred with a relatively slow time course and could be seen only at concentrations greater than 10 nM. This is in contrast to the greater sensitivity of hSSTR3-mediated induction of wild-type p53, which was clearly discernible within minutes and could be elicited at less than 10 nM concentration of OCT (11).

Pretreatment of cells with PTx abolished the induction of Rb, p21, and G₁ arrest, indicating that the cytostatic signaling by hSSTRs 1, 2, 4, and 5 is G protein dependent. Likewise, our finding that orthovanadate abolishes the effects of SST suggests a mediatory role for PTP in the cytostatic signaling initiated via hSSTRs 1, 2, and 4 as well. PTP-mediated antimitogenic effect of SST has previously been reported to be signaled through hSSTR1, mouse and human SSTR2, human and mouse SSTR3, and rat SSTR4 (11, 15, 16, 26-28). By contrast, rat SSTR5-initiated antiproliferative signaling was found to be PTP independent (14, 17). The present findings suggest that the antiproliferative signaling via hSSTR 5 leading to growth inhibition is also PTP dependent and contradicts the reported inability of the rat homolog of SSTR5 to regulate PTP (14). Such a difference between the rat and human SSTR5 receptors is surprising given the high degree of C-terminal sequence identity between the two receptors. It remains to be seen whether structural differences in other regions of

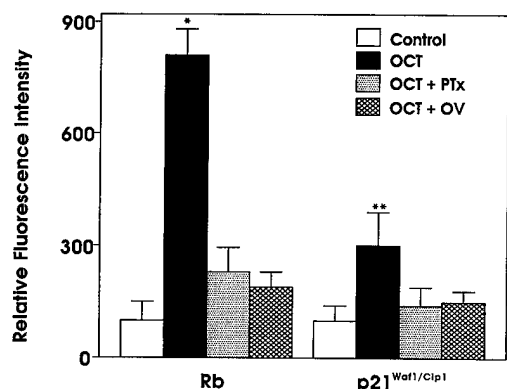


Fig. 6. hSSTR5-Mediated Cytostatic Signaling Is Pertussis Toxin Sensitive, G Protein Mediated, and PTP Dependent

OCT-treated cells displayed an increase in p21 in addition to Rb. Fluorescence intensity of antibody-labeled Rb and p21 was quantitated by flow cytometry after immunolabeling. Values represent percent change in fluorescence intensity in OCT-treated cells measured on a log scale and compared with that in untreated cells taken as 100%. The increase in p21 in cells incubated with 100 nM OCT was less than that of Rb (3.0 ± 0.8 vs. 8.1 ± 0.8 fold, respectively). hSSTR5-signaled induction of these proteins was abolished by pretreatment of the cells with 100 ng pertussis toxin for 18 h before incubation with the peptide. Na orthovanadate (10 mg/ml) present during the incubation with the peptide also inhibited the action of OCT (mean \pm SE, $n = 3$, *, $P < 0.005$; **, $P < 0.05$).

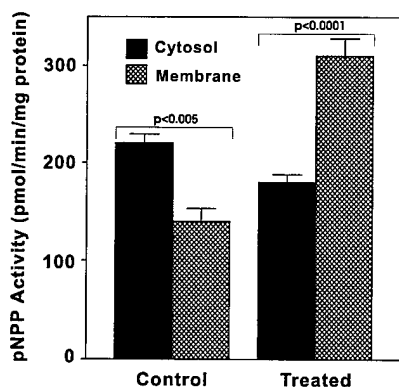


Fig. 7. Effect of OCT on PTP Activity in CHO-K1 Cells Expressing hSSTR5

PTP activity was measured in membrane and cytosolic fractions prepared from cells incubated in the absence or presence of 100 nM OCT for 24 h. The enzyme activity was measured using pNPP as the substrate (mean \pm SE, $n = 3$). By contrast, OCT did not stimulate PTP activity of the membrane fractions when added at the time of enzyme assay (not shown).

rat and human SSTR5 contribute to their divergent behavior.

The mechanism involved in SST induction of hypophosphorylated Rb remains to be elucidated. The concomitant, albeit smaller, induction of p21 raises the possibility that it may inhibit cyclin-dependent kinase-

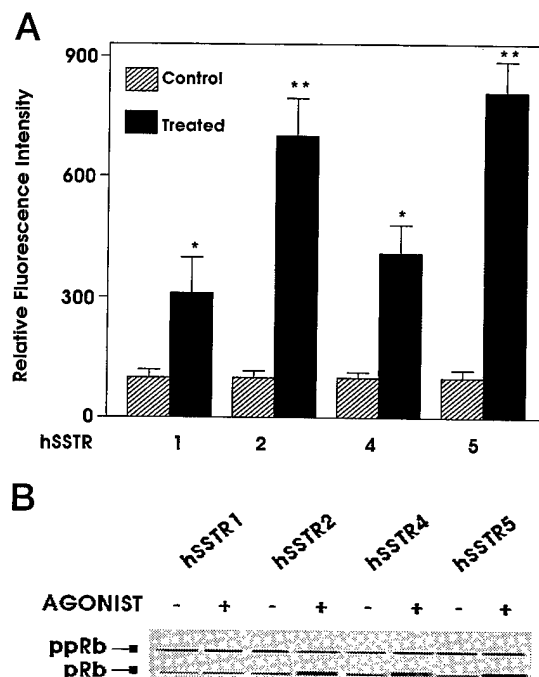


Fig. 8. hSSTR Subtype Selectivity for Induction of Rb

Maximum induction of Rb was seen in cells expressing hSSTR5, followed by hSSTR2>hSSTR4>hSSTR1. The fluorescence intensity of immunostained Rb was measured in cells incubated with 100 nM OCT (hSSTRs 2, 3, and 5) or D-Trp⁸ SST-14 (hSSTRs 1 and 4) for 24 h. Induction of Rb by agonists was quantitated by flow cytometry after immunolabeling. Values represent percent change in fluorescence intensity measured on a log scale and compared with that in untreated cells taken as 100% (mean \pm SE, $n = 3$; *, $P < 0.05$; **, $P < 0.005$).

mediated phosphorylation of Rb that is required for the cells to exit G₁. Alternatively, SST may activate phosphatase(s) that may dephosphorylate hyperphosphorylated Rb. Evidence for the existence of such a phosphatase comes from studies using anticancer drugs that promote p53-independent G₁ arrest in the absence of p21 induction (29). It remains to be tested whether hSSTR5-mediated increase in hypophosphorylated Rb is due to activation of Rb phosphatase alone or in conjunction with p21-mediated inhibition of Rb phosphorylation. Another possibility is that SST may inhibit Ca²⁺/calmodulin-mediated hyperphosphorylation of Rb (30, 31). Cross-talk between SST-induced PTP and mitogenic signaling pathways involving mitogen-activated protein (MAP) kinase may also contribute to the regulation of serine phosphorylation in Rb as well as cell cycle progression. It has been shown that cell cycle progression due to induction of cyclin-dependent kinase and phosphorylation of Rb can occur after MAP kinase activation (32). It is likely that inhibition of MAP kinase activity by SST may be an additional factor involved in its cytostatic signaling. SSTR regulation of MAP kinase activation is complex and involves inhibition by SSTR2 and SSTR5,

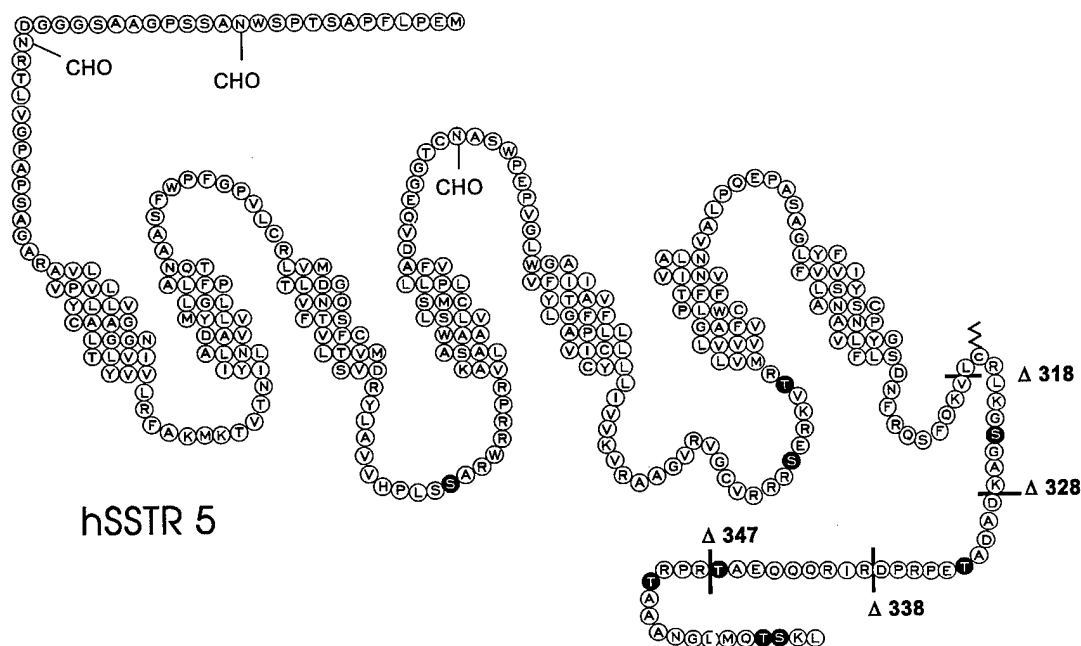


Fig. 9. Topographical Arrangement of Primary Amino Acid Sequence of hSSTR5 Showing the N-glycosylation Sites (CHO), S/T Phosphorylation Sites (●), and Palmitoylation Site (wavy line)

C tail truncation mutants of this receptor were generated by inserting stop codons at sites indicated by solid lines.

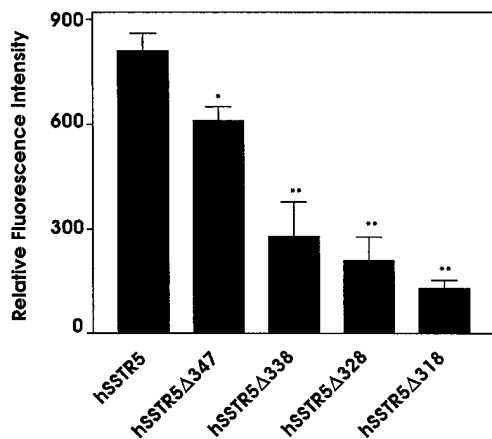


Fig. 10. Effect of C Tail Deletion Mutations on hSSTR5-Initiated Rb Induction

Induction of Rb by agonists was quantitated by flow cytometry after immunolabeling. Values represent percent change in fluorescence intensity measured on a log scale and compared with that in untreated cells taken as 100% (mean \pm SE, $n = 3$, *, $P < 0.01$; **, $P < 0.0001$).

stimulation through SSTR4, or a transient increase followed by subsequent decrease elicited by (murine) SSTR3 (33). $G_{\beta\gamma}$ -subunit-mediated activation of Ras is implicated in the induction of MAP kinase (34, 35). On the other hand, PTP-dependent regulation of serine/threonine phosphorylation inactivates Raf-1, which functions downstream of Ras in the mitogenic signaling cascade (27, 36–39). Thus, regulation of MAP kinase cascade by SST may occur at two levels: acti-

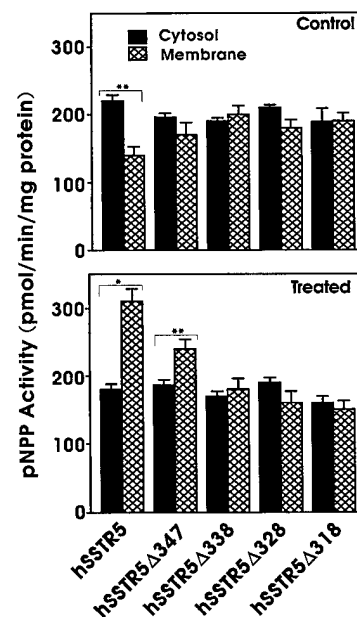


Fig. 11. Effect of C Tail Truncation on hSSTR5-Signaled Change in Cellular Distribution of PTP Activity in CHO-K1 Cells

PTP activity was measured using pNPP as the substrate in membrane and cytosolic fractions of cells incubated for 2 h in the absence and presence of 100 nM OCT (mean \pm SE, $n = 3$; *, $P < 0.0001$; **, $P < 0.005$).

vation of Ras by $\beta\gamma$ -subunits of G protein and tyrosine phosphorylation-dependent inactivation of MAP kinase. Thus, it is plausible that activation of different

phosphorylation/dephosphorylation mechanisms by SST elicited in a receptor subtype-specific or cell-specific manner may exert dual effects on cell growth and proliferation (40, 41). A direct correlation between subtype-selective change(s) in MAP kinase and cell cycle arrest or apoptosis remains to be established.

Of the five hSSTRs, only hSSTR3 induces cytotoxicity, the other four subtypes being cytostatic (Refs. 11 and 13 and the present study). We have previously reported that the $\Delta 347$, $\Delta 338$, $\Delta 328$, and $\Delta 318$ hSSTR5 mutants show progressive loss of the ability to inhibit forskolin-stimulated cAMP and variable impairment of agonist-dependent desensitization and internalization responses (25). This suggests a multifunctional role of the C tail of hSSTR5 in mediating effector coupling, desensitization, and internalization (25). Here we have extended an analysis of these mutants to their ability to regulate membrane-associated tyrosine phosphatase activity and to determine whether decreased potency to recruit cytosolic PTP to the membrane may account for their inability to initiate cytosolic signaling. After OCT treatment, only a 25% increase in PTP activity in the membrane fraction was seen in cells expressing hSSTR5 $\Delta 347$, in contrast to the 100% increase detected in cells expressing the wild-type receptor. Membrane-associated PTP activity did not increase in response to OCT in cells expressing $\Delta 338$, $\Delta 328$, and $\Delta 318$ mutants. Surprisingly, however, the enzyme activity was 20–35% higher in the membrane fraction of these cells under basal conditions than in hSSTR5-expressing cells. We do not know the reason for this, but this observation raises the intriguing possibility that, in the absence of ligand activation, the C tail of the wild-type receptor may inhibit the association of PTP with the membrane. Such a phenomenon has not previously been described. However, chronic association of the tyrosine phosphatase SHP-1 to the killer cell-inhibitory receptor in natural killer cells has been reported to tonically inhibit the function of the receptor in the inactivated state; dissociation of SHP-1 upon receptor ligation restores its function (42). Despite its inability to recruit cytosolic PTP to the membrane in cells expressing these mutants, OCT was still capable of inducing Rb, albeit with progressively less efficiency paralleling the length of C tail deletion. While this raises the possibility that OCT may be able to elicit cytostatic signaling through the PTP already present at the membrane, alternate, PTP-independent mechanisms may also contribute to hSSTR5-initiated antiproliferative signaling. For instance, hSSTR5 can decrease intracellular Ca^{2+} , thereby inhibiting cell growth (14, 43). While the nature of SST-induced, Ca^{2+} -sensitive growth inhibition was not established in these studies, it may invoke hypophosphorylation of Rb. Indeed, Ca^{2+} /calmodulin-dependent Rb hyperphosphorylation occurs during cell proliferation (30, 31).

In summary, the present findings demonstrate that SST peptides exert a cytostatic action via SSTR 1, 2, 4, and 5. Such subtype-specific cytostatic signals

target Rb and p21, leading to G_1 cell cycle arrest (hSSTR5>hSSTR2 >hSSTR4~hSSTR1). These effects are pertussis toxin- and G protein dependent and are PTP mediated. The marked decrease in the ability of C tail mutants of hSSTR5 to induce Rb and G_1 cell cycle arrest suggests that the C-terminal domain of hSSTR5 is involved in cytosolic antiproliferative signaling.

MATERIALS AND METHODS

Materials

The SST analog SMS 201–995 (octreotide, OCT) was obtained from Sandoz Pharmaceutical Co. (Basel, Switzerland). (PI) was purchased from Sigma Chemical Co. (St. Louis, MO). Rabbit polyclonal antibodies against p21 (C-19) and Rb (C-15) were purchased from Santa Cruz Biotechnology (Santa Cruz, CA). FITC-conjugated goat antimouse and antirabbit IgG antibodies were supplied by Zymed Laboratories (San Francisco, CA). All other reagents were obtained from local commercial sources and were of analytical quality.

CHO-K1 Cells Stably Expressing hSSTR1–5 and Mutant hSSTR5

Genomic fragments of hSSTR 2, 3, and 5 or cDNA clones for hSSTR 1 and 2A containing the entire coding sequences were subcloned into the polylinker region of the mammalian expression vector pRc/CMV (Invitrogen, San Diego, CA). Mutant hSSTR5 receptors with progressive truncation of the C tail ($\Delta 347$, $\Delta 338$, $\Delta 328$, and $\Delta 318$) were created by introducing stop codons at positions 347, 338, 328, and 318 of a cassette cDNA construct using the PCR overlap extension technique (25); the mutant cDNAs were cloned into the mammalian expression vector PTEJ8 (25). Wild-type hSSTRs and the mutant hSSTR5 receptors were stably transfected in CHO-K1 cells maintained under G418 selection (11, 44, 45). The binding characteristics of the different hSSTRs and the hSSTR5 C tail deletion mutants are compared in Tables 1 and 2. These values were estimated from saturation binding analysis using [125 I]-LTT[SST-28 as the radioligand as previously described (25, 44, 45). Cells were grown in T75 flasks in Hams F-12 medium containing 5% FCS (Life Technologies, Grand Island, NY) and 400 U/ml G-418 and cultured for 3–5 days at 37°C in a humidified atmosphere with 5% CO_2 . When the cells had reached 60–70% confluency, medium was replaced with fresh medium containing 100 nM of either OCT (hSSTRs 2, 3, and 5) or D-Trp⁸ SST-14 (hSSTR 1 and 4 subtypes to which OCT does not bind) (11, 44). To investigate the G protein dependency of hSSTR5-mediated cytostatic

Table 1. Binding Characteristics of hSSTR Subtypes Expressed in CHO-K1 Cells

Receptor	K_d (nM)	B_{max} (fmol/mg)
hSSTR1	1.23 ± 0.40	174 ± 40
hSSTR2	1.11 ± 0.32	260 ± 61
hSSTR3	1.88 ± 0.27	294 ± 44
hSSTR4	0.93 ± 0.09	256 ± 37
hSSTR5	0.31 ± 0.01	162 ± 42

Receptor binding capacity was quantitated using [125 I]-LTT[SST-28 as the radioligand in saturation binding assays (mean \pm SE, $n = 3$).

Table 2. Binding Characteristics of Wild-Type and Mutant hSSTR5 Receptor

	K _d (nM)	B _{max} (fmol/mg)
wt hSSTR5	0.31 ± 0.01	162 ± 42
Δ 318 hSSTR5	0.89 ± 0.07	262 ± 71
Δ 328 hSSTR5	0.47 ± 0.16	298 ± 99
Δ 338 hSSTR5	0.41 ± 0.18	247 ± 40
Δ 347 hSSTR5	0.21 ± 0.07	352 ± 96

Receptor binding capacity was quantitated using [¹²⁵I]-LTTJST-28 as the radioligand in saturation binding assays (mean ± SE, n = 3) (25).

signaling, cells were preincubated for 18 h with pertussis toxin. To determine whether such action was PTP mediated, the effect of OCT was compared in the absence and presence of the tyrosine phosphatase inhibitor Na orthovanadate. The pertussis toxin and Na orthovanadate were used at optimal concentrations of 100 ng/ml and 10 mg/ml, as determined in earlier studies (11, 46). After 24 h incubation, the cells were washed in PBS, scraped, and fixed sequentially in 1% paraformaldehyde and 70% ethanol. Cellular DNA was labeled with the intercalating dye PI (50 mg/ml) in PBS and incubated at 37°C for 5 min in the presence of RNase A (50 mg/ml). Rb and p21 were immunolabeled with their respective antibodies, followed by counterstaining with FITC-conjugated secondary antibodies as previously described (11).

Flow Cytometry

Flow cytometry was carried out in an EPICS 750 series flow cytometer (Coulter Electronics, Hialeah, FL). Fluorescence was excited by a 5-watt argon laser generating light at 351–363 nm. PI emission was detected through a 610-nm long pass filter, and FITC fluorescence was detected with a 560-nm short pass dichroic filter. At least 10,000 gated events were recorded for each sample, and the data were analyzed by Winlist software (Verity Software House).

Analysis of Nuclear Morphology

Aliquots of cells stained with PI for analysis by flow cytometry were cytospun onto microscope slides, mounted using Immunomount (Shandon, Pittsburgh, PA), viewed, and photographed through a Reichert Polyvar 2 fluorescence microscope (original magnification × 400).

Western Blot Analysis

Cells were lysed in Tris-HCl buffer (100 mM, pH 7.2) containing 300 mM NaCl, 2% Nonidet P-40, 20% glycerol, 2 mM ZnCl₂, 10 mg/ml pepstatin, and 0.2 mM pefabloc (Boehringer Mannheim, Canada). Protein measurement was performed using the Bio-Rad protein assay kit (Bio-Rad Laboratories, Hercules, CA). Aliquots (30 µg) were electrophoresed in 10% SDS-polyacrylamide gel in running buffer (50 mM Tris-HCl, 60 mM boric acid, 1 mM EDTA, 0.1% SDS) and transferred onto Protran plus membranes electrophoretically in a buffer containing 25 mM Tris, 192 mM glycine, and 15% methanol. Blots were probed with anti-RB antibody (Pharmingen, San Diego, CA) and visualized with alkaline phosphatase conjugate detection kit (Bio-Rad). Molecular size was determined using 10 kDa protein ladder (Life Technologies) and staining with Pon- ceau S (46).

Measurement of PTP Activity

Phosphatase activity in whole-cell extracts or membrane and cytosolic fractions was determined using pNPP as the substrate as described previously (47).

Acknowledgments

We thank Ms. J. Cai for technical assistance with cell culture, Dr. N. Hukovic for binding studies with hSSTR5 mutants, and Ms. S. Schiller and Dr. Halwani for assistance with flow cytometry.

Received May 8, 1998. Re-revision received September 22, 1998. Accepted September 28, 1998.

Address requests for reprints to: Dr. C. B. Srikant, M3.15, Royal Victoria Hospital, 687 Pine Avenue West, Montreal, Quebec, Canada, H3A 1A1. E-mail: mdcs@musica.mcgill.ca.

This work was supported by grants from the Medical Research Council of Canada (MT 12603 and MT 10411) and the US Department of Defense. K.S. is a recipient of a student-ship award of the Fonds de la Recherche en Sante du Quebec.

REFERENCES

- Cheung NW, Boyages SC 1995 Somatostatin-14 and its analog octreotide exert a cytostatic effect on GH3 rat pituitary tumor cell proliferation via a transient G0/G1 cell cycle block. *Endocrinology* 136:4174–4181
- Candi E, Melino G, De Laurenzi V, Piacentini M, Guerreri P, Spinedi A, Knight RA 1995 Tamoxifen and somatostatin affect tumors by inducing apoptosis. *Cancer Lett* 96:141–145
- Pagliacci MC, Tognellini R, Grignani F, Nicoletti I 1991 Inhibition of human breast cancer cell (MCF-7) growth *in vitro* by the somatostatin analog SMS 201–995: effects on cell cycle parameters and apoptotic cell death. *Endocrinology* 129:2555–2562
- Sharma K, Srikant CB 1998 Induction of a novel type p53, Bax and a cation-insensitive acidic endonuclease during somatostatin signaled apoptosis in MCF-7 human breast cancer cells. *Int J Cancer* 76:259–266
- Srikant CB 1995 Cell cycle dependent induction of apoptosis by somatostatin analog SMS 201–995 in AtT-20 mouse pituitary cells. *Biochem Biophys Res Commun* 209:400–406
- Patel YC, Greenwood MT, Panetta R, Demchishyn L, Niznik H, Srikant CB 1995 The somatostatin receptor family. *Life Sci* 57:1249–1265
- Patel YC, Greenwood M, Panetta R, Hukovic N, Grigorakis S, Robertson LA, Srikant CB 1996 Molecular biology of somatostatin receptor subtypes. *Metabolism* 45:31–38
- Bruno JF, Xu Y, Berelowitz M 1994 Somatostatin regulates somatostatin receptor subtype mRNA expression in GH3 cells. *Biochem Biophys Res Commun* 202:1738–1743
- Patel YC, Panetta R, Escher E, Greenwood M, Srikant CB 1994 Expression of multiple somatostatin receptor genes in AtT-20 cells. Evidence for a novel somatostatin-28 selective receptor subtype. *J Biol Chem* 269:1506–1509
- Xu Y, Song J, Berelowitz M, Bruno JF 1996 Estrogen regulates somatostatin receptor subtype 2 messenger ribonucleic acid expression in human breast cancer cells. *Endocrinology* 137:5634–5640
- Sharma K, Patel YC, Srikant CB 1996 Subtype-selective induction of wild-type p53 and apoptosis, but not cell cycle arrest, by human somatostatin receptor 3. *Mol*

- Endocrinol 10:1688-1696
12. Sharma K, Srikant CB 1998 G protein-coupled receptor signaled apoptosis is associated with induction of a cation-insensitive acidic endonuclease and intracellular acidification. *Biochem Biophys Res Commun* 242:134-140
13. Sharma K, Patel YC, Srikant CB, Subtype selective human somatostatin receptor (h SSTR) mediated cytostatic and cytotoxic actions involve different signaling mechanisms. Program of the 77th Annual Meeting of The Endocrine Society, Minneapolis, MN, 1997, p 172 (Abstract P-152)
14. Buscail L, Esteve JP, Saint-Laurent N, Bertrand V, Reisine T, O'Carroll AM, Bell GI, Schally AV, Vaysse N, Susini C 1995 Inhibition of cell proliferation by the somatostatin analogue RC-160 is mediated by somatostatin receptor subtypes SSTR2 and SSTR5 through different mechanisms. *Proc Natl Acad Sci USA* 92:1580-1584
15. Buscail L, Delesque N, Esteve JP, Saint-Laurent N, Prats H, Clerc P, Robberecht P, Bell GI, Liebow C, Schally AV, Vaysse N, Susini C 1994 Stimulation of tyrosine phosphatase and inhibition of cell proliferation by somatostatin analogues: mediation by human somatostatin receptor subtypes SSTR1 and SSTR2. *Proc Natl Acad Sci USA* 91:2315-2319
16. Florio T, Scorizello A, Fattore M, VDA, Salzano S, Rossi G, Berlingieri MT, Fusco A, Schettini G 1996 Somatostatin inhibits PC C13 thyroid cell proliferation through the modulation of phosphotyrosine activity. Impairment of the somatostatinergic effects by stable expression of E1A viral oncogene. *J Biol Chem* 271:6129-6136
17. Lopez F, Esteve JP, Buscail L, Delesque N, Saint-Laurent N, Vaysse N, Susini C 1996 Molecular mechanisms of antiproliferative effect of somatostatin: involvement of a tyrosine phosphatase. *Metabolism* 45:14-16
18. Weinberg RA 1995 The retinoblastoma protein and cell cycle control. *Cell* 81:323-330
19. Sherr CJ 1993 Mammalian G1 cyclins. *Cell* 73:1059-1065
20. Hermeeking H, Funk JO, Reichert M, Ellwart JW, Eick D 1995 Abrogation of p53-induced cell cycle arrest by c-Myc. Evidence for an inhibitor of p21(WAF1/CIP1/SDI1). *Oncogene* 11:1409-1415
21. Michieli P, Chedid M, Lin D, Pierce JH, Mercer We, Givol D 1994 Induction of WAF1/CIP1 by a p53-independent pathway. *Cancer Res* 54:3391-3395
22. Ookawa K, Tsuchida S, Adachi J, Yokota J 1997 Differentiation induced by RB expression and apoptosis induced by p53 expression in an osteosarcoma cell line. *Oncogene* 14:1389-1396
23. Baldwin JM 1994 Structure and function of receptors coupled to G proteins. *Curr Opin Cell Biol* 6:180-190
24. Dohlman HG, Thorne J, Caron MG, Lefkowitz RJ 1991 Model systems for the study of seven-transmembrane-segment receptors. *Annu Rev Biochem* 60:653-688
25. Hukovic N, Panetta R, Kumar U, Rocheville M, Patel YC 1998 The cytoplasmic tail of the human somatostatin receptor type 5 is crucial for interaction with adenylyl cyclase, and in mediating desensitization and internalization. *J Biol Chem* 273:21416-21422
26. Yoshitomi Y, Fujii Y, Miyazaki M, Nakajima N, Inagaki N, Seino S 1997 Involvement of MAP kinase and c-fos signaling in the inhibition of cell growth by somatostatin. *Am J Physiol* 272:E769-E774
27. Reardon DB, Wood SL, Brautigan DL, Bell GI, Dent P, Sturgill TW 1996 Activation of a protein tyrosine phosphatase and inactivation of Raf-1 by somatostatin. *Biochem J* 314:401-404
28. Lopez F, Esteve JP, Buscail L, Delesque N, Saint-Laurent N, Theveniau M, Nahmias C, Vaysse N, Susini C 1997 The tyrosine phosphatase SHP-1 associates with the sst2 somatostatin receptor and is an essential component of sst2-mediated inhibitory growth signaling. *J Biol Chem* 272:24448-24454
29. Dou QP, An B, Will PL 1995 Induction of a retinoblastoma phosphatase activity by anticancer drugs accompanies p53-independent G1 arrest and apoptosis. *Proc Natl Acad Sci USA* 92:9019-9023
30. Nie L, Oishi Y, Doi I, Shibata H, Kojima I 1997 Inhibition of proliferation of MCF-7 breast cancer cells by a blocker of Ca^{2+} -permeable channel. *Cell Calcium* 22:75-82
31. Takuwa N, Zhou W, Kumada M, Takuwa Y 1993 Ca^{2+} -dependent stimulation of retinoblastoma gene product phosphorylation and p34cdc2 kinase activation in serum-stimulated human fibroblasts. *J Biol Chem* 268:138-145
32. Yatsunami J, Komori A, Ohta T, Suganuma M, Fujiki H 1993 Hyperphosphorylation of retinoblastoma protein and p53 by okadaic acid, a tumor promoter. *Cancer Res* 53:239-241
33. Cordelier P, Esteve JP, Bousquet C, Delesque N, O'Carroll AM, Schally AV, Vaysse N, Susini C, Buscail L 1997 Characterization of the antiproliferative signal mediated by the somatostatin receptor subtype sst5. *Proc Natl Acad Sci USA* 94:9343-9348
34. Crespo P, Xu N, Simonds WF, Gutkind JS 1994 Ras-dependent activation of MAP kinase pathway is mediated by G protein $\beta\gamma$ subunits. *Nature* 369:418-420
35. Koch WJ, Hawes BE, Allen LF, Lefkowitz RJ 1994 Direct evidence that Gi-coupled receptor stimulation of mitogen-activated protein kinase is mediated by $G\beta\gamma$ activation of p21^{ras}. *Proc Natl Acad Sci USA* 91:12706-12710
36. Marshall CJ 1994 MAP kinase kinase kinase, MAP kinase and MAP kinase. *Curr Opin Gene Dev* 4:82-89
37. Dent P, Reardon DB, Wood SL, Lindorfer MA, Graber SG, Garrison JC, Brautigan DL, Sturgill TW 1996 Inactivation of raf-1 by a protein-tyrosine phosphatase stimulated by GTP and reconstituted by Galphai/o subunits. *J Biol Chem* 271:3119-3123
38. Dent P, Reardon DB, Morrison DK, Sturgill TW 1995 Regulation of Raf-1 and raf-1 mutants by Ras-dependent and Ras-independent mechanisms *in vitro*. *Mol Cell Biol* 15:4125-4135
39. Yao B, Zhang Y, Delikat S, Mathais S, Basu S, Kolesnick R 1995 Phosphorylation of Raf by ceramide-activated protein kinase. *Nature* 378:307-310
40. Cattaneo MG, Amoroso D, Gussoni G, Sanguini AM, Vicentini LM 1996 A somatostatin analogue inhibits MAP kinase activation and cell proliferation in human neuroblastoma and in human small cell lung carcinoma cell lines. *FEBS Lett* 397:164-168
41. Ruiz-Torres P, Lucio FJ, Gonzalez-Rubio M, Rodriguez-Puyol M, Rodriguez-Puyol D 1993 A dual effect of somatostatin on the proliferation of cultured rat mesangial cells. *Biochem Biophys Res Commun* 195:1057-1062
42. David M, Chen HE, Goelz S, Lerner AC, Neel BG 1995 Differential regulation of the alpha/beta interferon-stimulated Jak/Stat pathway by the SH2 domain-containing tyrosine phosphatase SHPTP1. *Mol Cell Biol* 15:7050-7058
43. Wilkinson GF, Thurlow RJ, Sellers LA, Coote JE, Fenuik W, Humphrey PP 1996 Potent antagonism by BIM-23056 at the human recombinant somatostatin sst5 receptor. *Br J Pharmacol* 118:445-447
44. Patel YC, Srikant CB 1994 Subtype selectivity of peptide analogs for all five cloned human somatostatin receptors (hsstr1-5). *Endocrinology* 135:2814-2817
45. Patel YC, Greenwood MT, Warszynska A, Panetta RP, Srikant CB 1994 All five cloned human somatostatin receptors (hSSTR1-5) are functionally coupled to adenylyl cyclase. *Biochem Biophys Res Commun* 198:605-612
46. Srikant CB, Shen SH 1996 Octapeptide somatostatin analog SMS 201-995 induces translocation of intracellular PTP1C to membranes in MCF-7 human breast adenocarcinoma cells. *Endocrinology* 137:3461-3468
47. Zhao Z, Bouchard P, Diltz CD, Shen SH, Fischer EH 1993 Purification and characterization of a protein tyrosine phosphatase containing SH2 domains. *J Biol Chem* 268:2816-2820

CASPASE-8-MEDIATED INTRACELLULAR ACIDIFICATION PRECEDES MITOCHONDRIAL DYSFUNCTION IN SOMATOSTATIN-INDUCED APOPTOSIS

Danni Liu[@], Giovanni Martino[@], Muthusamy Thangaraju^{@1}, Monika Sharma[@], Fawaz Halwani[†], Shi-Hsiang Shen[‡], Yogesh C. Patel[@] and Coimbatore B. Srikant^{@*}

[@]Fraser Laboratories, Department of Medicine, [†]Department of Pathology, McGill University and Royal Victoria Hospital, Montreal, Quebec, H3A 1A1 and [‡]Pharmaceutical Sector, N.R.C. Biotechnology Research Institute, Montreal, Quebec, H4P 2R2, Canada

*Address correspondence to
Dr. C.B. Srikant
M3.15, Royal Victoria Hospital
687, Pine Avenue West
Montreal, Quebec, H3A 1A1
Canada
Tel: 514 842 1231 ext. 5359
Fax: 514 849 3681
Email: mdcs@musica.mcgill.ca

Running Title: Caspase-8-mediated acidification precedes mitochondrial dysfunction

[†]Abbreviations used: cyt c, cytochrome c; $\Delta\psi_m$, mitochondrial membrane potential; DiOC₆(3), 3,3'-dihexyloxacarbocyanine iodide; NHE, Na⁺/H⁺ exchanger; pH_i, intracellular pH; SST, somatostatin.

¹ Present address: Department of , Mayo Clinic and Foundation, Rochester, MN

Activation of initiator and effector caspases, mitochondrial changes involving a reduction in its membrane potential and release of cytochrome c (cyt c) into the cytosol are characteristic features of apoptosis. These changes are accompanied by cell acidification in some models of apoptosis. The hierarchical relationship between these events has, however, not been deciphered. We have shown that somatostatin (SST), acting via the src homology 2 bearing tyrosine phosphatase SHP-1, exerts cytotoxic action in MCF-7 cells and triggers cell acidification and apoptosis. We investigated the temporal sequence of apoptotic events linking caspase activation, acidification and mitochondrial dysfunction in this system and report here that (i) SHP-1-mediated caspase-8 activation is required for SST-induced decrease in pH_i , (ii) effector caspases are induced only when there is concomitant acidification. (iii) decrease in pH_i is necessary to induce reduction in mitochondrial membrane potential, cytochrome c release and caspase-9 activation and (iv) depletion of ATP ablates SST-induced cyt c release and caspase-9 activation, but not its ability to induce apoptosis. These data reveal that SHP-1-/ caspase-8--mediated acidification occurs at a site other than the mitochondrion and that SST-induced apoptosis is not dependent on disruption of mitochondrial function and caspase-9 activation.

Apoptosis is a physiological process of cell death indispensable for the maintenance of multicellular organisms. This process drives the cell into self-destruction via a common execution pathway. The cellular machinery utilized for this process creates distinct apoptotic features of cell shrinkage, cytoplasmic and nuclear condensation, membrane blebbing, chromatin compaction and fragmentation of chromosomal DNA into 180 base pair multimers. A central event in the process of apoptosis is the activation of cysteine aspartate proteases (caspases) (1). Active caspases consist of dimeric complexes of ~20 and 10 kDa fragments derived from the procaspases that exist as inactive zymogens by internal proteolytic cleavage at cysteine-aspartate sites (2). Mammalian caspases can be divided into initiator (e.g., caspases 2,8,9,10) and effector (caspases 3,4,5,6,7,11,12,13) enzymes. A feature of apoptosis that impinges on caspases is altered mitochondrial function characterized by a reduction in the electrochemical gradient across the mitochondrial membrane ($\Delta\psi_m$)² and release of mitochondrial cytochrome c (cyt c) into the cytoplasm (3-15). Cyt c is necessary for caspase-9 activation (16, 17). Caspase-9 can function as an initiator caspase when mitochondrial dysfunction is the primary event in apoptosis, but it can amplify the apoptotic signaling of other initiator caspases under conditions in which disruption of mitochondria is a late event (16, 17, 18, 19)

In some models of apoptosis activation of caspases is associated with intracellular acidification (20-23). The question of whether intracellular acidification is necessary for inducing caspases or occurs merely as a consequence of caspase activation has been an issue of debate (24-32). Likewise, it is not known whether mitochondrial dysfunction is necessary for acidification to occur during pH-dependent apoptosis or is induced by the decrease in intracellular pH (pH_i). For

² * Abbreviations used: (see page 1)

instance, contradictory reports suggest that the pan-caspase inhibitor z-VAD-fmk prevents decrease in pH_i whereas acidification per se was found to activate z-VAD-fmk-sensitive caspases (27, 32). Since z-VAD-fmk inhibits both initiator and effector caspases, its use does not allow differentiation between caspases that may be activated in a pH_i -sensitive and -insensitive manner during apoptosis associated with acidification.

We recently reported that somatostatin (SST) receptor (SSTR)-mediated cytotoxic signaling triggers acidification (33-35). SST induces acidification-dependent apoptosis in MCF-7 and T47D breast cancer cells: prevention of acidification by pH clamping inhibited its ability to induce apoptosis (34). In the present study we undertook to delineate the temporal sequence of activation of different caspases in relation to cellular acidification and mitochondrial dysfunction during SST-induced apoptosis in MCF-7 cells. Here we present evidence demonstrating that caspase 8 activation is necessary for intracellular acidification to occur during SST-induced apoptosis and that the effector caspases are induced only as a consequence of the decrease in pH_i . Moreover, the reduction in $\Delta\psi_m$ and release of cyt c into the cytosol from the mitochondria also occur distal to acidification. Depletion of ATP prevented the activation of caspase-9 but only partially inhibited its ability to activate the terminal caspases and induce apoptosis. Thus, while caspase-9 can amplify SST-induced, acidification-dependent, cytotoxic signaling it is not essential for pH-dependent apoptosis.

MATERIALS AND METHODS

MCF-7 cells (clone HTB22) was obtained from ATCC. Special reagents were obtained from the following sources: D-Trp⁸ SST-14 (Bachem, Torrance, CA); agonistic Anti-Fas (CD95/APO-1) antibody and annexin-V labeling kit (Roche Diagnostics, Montreal, CA);

Doxorubicin and nigericin (ICN, Costa Mesa, CA). Carboxy-SNARF-1 acetoxymethyl ester and 3,3'-dihexyloxacarbocyanine iodide [$\text{DiOC}_6(3)$] (Molecular Probes, Eugene, OR). Aminomethylcoumarin derivatives (caspase substrates) and aldehyde derivatives (caspase inhibitors) of tetrapeptide sequences that are recognized by distinct caspases - IETD (caspase-8), LEHD (caspase-9) and DEVD (caspases -3/-7) (BioMol Research Laboratories, Plymouth Meeting, PA). Antibodies against the different caspases and cyt c were purchased from Pharmingen (San Diego, CA). All other reagents used were of analytical grade and were obtained from regular commercial sources.

Cell Culture and Incubation Conditions:

Cells were plated in 75 cm^2 culture flasks and grown in minimal essential medium containing non-essential amino acids and supplemented with 10% fetal bovine serum. Cells were incubated in the presence or absence of 100 nM D-Trp⁸ SST-14 or 20 ng/ml for different time periods as indicated. To examine the effect of direct acidification, cells were incubated in medium supplemented with 140 mM K^+ and 10 nM nigericin. Caspase inhibitors were dissolved in DMSO and used at 1:1000 dilution to yield a final concentration of 50 $\mu\text{g/ml}$. Depletion of intracellular ATP was achieved in glucose deprived cells by inhibiting F0/F1 ATPase with oligomycin (36). Briefly, cells were incubated with 10 μM oligomycin in glucose-free DMEM (Canadian Life Technologies, Guelph, Ontario) supplemented with 50 mM malic acid, 2 mM glutamate, 1 mM sodium pyruvate, 10 mM HEPES/ Na^+ (pH 7.4), 0.05 mM β -mercaptoethanol, and 10% dialyzed fetal bovine serum as described by Eguchi et al., prior to peptide treatment (37). Cellular ATP was measured using a commercial luciferase luminescence assay kit (Sigma, St. Louis,

MO). The ATP concentration decreased by $>83 \pm 6\%$ ($n=4$) following oligomycin treatment (data not shown).

Detection of apoptosis:

Apoptosis was determined by annexin-V positivity using the annexin-V-FLUOS kit (Roche Diagnostics, Montreal, Canada) or by the presence of oligonucleosomal DNA fragments as previously described (34, 35, 38). Cells labeled with FITC conjugated annexin-V and propidium iodide were analyzed by flow cytometry in a Becton Dickinson Vantage Plus flow cytometer. A 5W argon laser generating light at 351-363 nm was used as the excitation source and FITC fluorescence was detected with a 560 nm short pass dichroic filter while propidium iodide fluorescence was detected using a 610 nm long pass filter. At least 10,000 gated events were recorded for each sample and the data analyzed by Winlist software (Verity Software House, ME). To assess DNA fragmentation, cellular DNA was extracted twice with phenol/chloroform and once with chloroform from cells incubated in lysis buffer (500 mM Tris-HCl (pH 9) containing 2 mM EDTA, 10 mM NaCl, 1% SDS and 1 mg/ml proteinase K) at 48° C for 30 h. DNA extracts were incubated with 300 µg/ml bovine pancreatic RNase A at 37° C for 1 h and 10 µg aliquots of DNA samples containing 10 µg/ml ethidium bromide were subjected to electrophoresis on 1.2% (w/v) agarose gels using the Hoefer SwitchbackTM pulse controller and visualized under UV light.

Measurement of intracellular pH

For measuring intracellular pH, cells were loaded with 10 µM acetoxymethylester derivative of SNARF-1 for during the final hour of incubation in the absence or presence of 100 nM D-Trp⁸ SST-14 at 37° C (38). The cells were then scraped, washed and maintained at 37° C. Intracellu-

lar carboxy SNARF-1 was excited at 488 nm and emission was recorded at both 580 and 640 nm with 5 nm band pass filters with linear amplifiers in a Becton-Dickinson FACStar Vantage cytometer. The ratio of the emissions at these wavelengths was electronically calculated and used as a parameter indicative of pH_i . The intracellular pH values in control and treated cells were estimated by comparison of the mean ratios of the samples to a calibration curve of intracellular pH generated by incubation of carboxy-SNARF-1 loaded cells in buffers ranging in pH from 8.0 to 6.25 and containing the proton ionophore nigericin (33). Cells with fluorescence of <50 units were excluded in the calculation of the ratio of the emissions at 580 nm and 640 nm.

Measurement of Mitochondrial Membrane Potential:

$\text{DiOC}_6(3)$ (final concentration 50 nM) was added to the cells 15 min prior to the completion of incubation. The cells were then washed to remove excess fluorochrome, scraped and maintained at 37°C. $\text{DiOC}_6(3)$ fluorescence was measured in a EPICS 750 series Flow Cytometer (Coulter Electronics, Hialeah, FL) with the excitation and emission wavelengths set at 488 and 520 nm respectively. At least 10,000 events were recorded for each sample and the data analysed by WinList Program (Verity Software House, Topsham, ME).

Subcellular fractionation and Western blotting

Cells were washed in phosphate buffered saline and resuspended in 500 μl of a buffer containing 25 mM Hepes-KOH buffer (pH 7.4) containing 10 mM KCl, 1.5 mM MgCl_2 , 5 mM EDTA, 1 mM EGTA, 2 mM DTT, 250 mM sucrose, 0.2% Triton-X-100 and protease inhibitor cocktail (Roche Canada, Montreal, CA). The cells were homogenized in a Pyrex homogenizer using a type B pestle. Cell debris and nuclei were removed by centrifugation at 1000 x g for 10 min at 4°C.

Mitochondrial fraction was then pelleted by centrifugation at 10,000 x g for 20 min. The supernatant obtained at this stage was recentrifuged at 40,000 x g for 1 h to obtain cytosolic fraction.

Thirty micrograms of cytosolic fractions prepared from cells incubated under different experimental conditions were subjected to SDS-polyacrylamide gel electrophoresis. The separated proteins were blotted on to nitrocellulose membranes and subjected to immunoblot analysis for cyt c, or caspases -8, -9, -3 and -7.

Measurement of caspase activity

Activities of caspases were measured in the lysates measuring the *in vitro* hydrolysis of DEVD-AMC (caspases -3 and -7), IETD-AMC (caspase-8) and LEHD-AMC (caspase-9) (39, 40). The fluorescence of the aminomethylcoumarin released from the substrates was measured in a Perkin-Elmer spectrofluorimeter with the excitation and emission wavelengths set at 380 and 460 nm respectively. Enzyme activity was quantitated against a standard fluorescence curve generated using aminomethylcoumarin over a concentration range of 0-1000 nM.

RESULTS

In order to determine the hierarchy of caspase activation during acidification-dependent apoptosis we measured the time course of D-Trp⁸ SST-14-induced changes in enzyme activities using substrates that display specificity for initiator and effector caspases *in vitro*: IETD-AMC (caspase-8), and DEVD-AMC (caspases -3/-7) respectively. In cells incubated with 100 nM D-Trp⁸ SST-14 at which concentration it induces maximal apoptosis (35, 38), the IETD-AMC hydrolysing activity was maximal by 3 h (6-fold increase over the basal value of 0.5 nmol/mg protein, fig 1), but had fallen to basal levels by 24 h. By contrast, DEVD-specific caspase activity increased by <3-fold during SST treatment but continued to increase and remained elevated even

at 24 h ($1.21 \pm$ and 3.61 ± 0.7 respectively, compared to 0.45 ± 0.05 nmol/mg protein in untreated control cells). When acidification was prevented by pH clamping by the inclusion of the proton ionophore nigericin, SST-induced increase in IETD-ase was unaffected whereas its ability to induce DEVD-ase activity was completely inhibited (fig. 2). We next examined the effect of selective inhibitors of these caspases on SST-induced acidification and apoptosis. IETD-CHO (the tetrapeptide aldehyde inhibitor of caspase-8) prevented the decrease pH_i in SST treated cells whereas DEVD-CHO (the caspase 3/7 inhibitor) was without effect (fig. 3A). By contrast, the ability of SST to induce apoptosis was suppressed by both inhibitors as confirmed by DNA fragmentation analysis (fig. 3B) and by annexin-V positivity (not shown). The temporal sequence of activation of the different caspases during D-Trp⁸ SST-14-induced apoptosis was confirmed by measuring the effect of each of the caspase inhibitors on the activities of other caspases (fig. 4). IETD-specific caspase activation by SST was unaffected by DEVD-CHO (fig. 4A) but the inductive effect of SST on DEVD-specific caspase activity was totally inhibited by IETD-CHO (fig. 4B).

Mitochondrial dysfunction characterized by a reduction in its transmembrane potential ($\Delta\Psi_m$) and release of cyt c into the cytosol, are characteristic features of apoptosis (6, 9, 10, 41, 42). An important arm of apoptotic signaling involves cyt c dependent activation of caspase-9. Cyt c released from the mitochondria complexes with APAF-1 (the mammalian homolog of the pro-apoptotic protein CED-4 of *C. elegans*) and procaspase-9. Such activation of caspase-9 has been reported to be necessary for the full expression of nuclear apoptotic events (43). To determine whether mitochondrial dysfunction precedes or follows acidification, we compared the effects of pH clamping and different caspase inhibitors on $\Delta\Psi_m$, cyt c release and caspase-9 acti-

vation in SST treated cells. SST induced a decrease in $\Delta\psi_m$ in MCF-7 cells (fig. 5A). Inhibition of acidification by pH clamping totally abrogated the ability of SST to decrease $\Delta\psi_m$. Maximal effect was seen at 6 h when 48 ± 7 % of SST treated cells displayed a significant reduction in $\Delta\psi_m$ compared to the untreated control (fig. 5B). Additionally, loss of $\Delta\psi_m$ during SST treatment was prevented almost completely by IETD-CHO but was decreased only by 23 ± 3 % by DEVD-CHO (fig. 5B). A marked increase in in cytosolic cyt c content was seen in SST treated cells (fig. 6). Such an increase did not occur when acidification was prevented by pH clamping. SST-induced increase in cytosolic cyt c was completely suppressed by IETD-CHO but was not inhibited by inhibition of effector caspases by DEVD-CHO. We measured the caspase-9 activity in extracts of cells incubated with SST using the tetrapeptide substrate LEHD-AMC, a substrate with reported caspase-9 selectivity (40). LEHD-specific caspase activity was induced by SST in MCF-7 cells in an acidification-dependent manner (fig. 7). Inhibition of caspase-9 activity with LEHD-CHO did not affect SST-induced loss of $\Delta\psi_m$ or the release of cyt c into the cytosol (not shown).

Cyt c- and APAF-1-mediated activation of caspase-9 is an energy-dependent process requiring ATP (44). In order to establish to what extent SST-signaled apoptosis is mediated via ATP-dependent caspase-9 activation, we tested the effect of depleting intracellular ATP on the cytotoxic signaling of SST. In ATP-depleted cells, SST failed to activate LEHD-ase (fig. 8A). Additionally, SST-induced increase in DEVD-ase activity was 40% less than that seen in control cells (2.2 ± 0.5 vs 3.61 ± 0.7 nmol/mg protein, fig. 8B). ATP depletion also inhibited SST-induced increase in cytosolic cyt c (fig. 8C). ATP-depletion also decreased the extent of apopto-

sis by 27 % ($8.8 \pm 1\%$ vs $12.1 \pm 1.2\%$ in control) during 6 h treatment with SST (fig. 8D). We could not assess the effect of SST for longer periods due to the presence of necrosis caused by prolonged ATP depletion.

Immunoblot analysis confirmed the pH-independent generation of active caspase-8 (IETD-AMC-specific) by the formation of the 20 kDa caspase-8 fragment from the 50 kDa procaspase-8 in D-Trp⁸ SST-14 treated cells. Inhibition of acidification by pH clamping did not prevent activation of caspase-8 (Fig. 9). By contrast, generation of the 20 kDa fragments of caspase-3 and caspase-7 (DEVD-AMC-specific proteases) from procaspase-3 (32 kDa) and procaspase-7 (35 kDa) and of caspase-9 (LEHD-AMC-specific) from procaspase-9 (48 kDa) occurred only if acidification was present.

We have previously reported that SST-induced cell acidification is SHP-1-mediated (34, 35). Moreover, the resting pH_i of MCF-7 cells was lower in presence of overexpressed SHP-1 ($\text{pH}_i = 7.07$ vs. 7.25 in untransfected cells) whereas dominant negative suppression of SHP-1 raised the resting pH_i (7.41) (35). SST-induced redistribution of SHP-1 resulting in its accumulation at the membrane was not prevented by IETD-CHO (not shown) indicating that activation of caspase-8 is SHP-1-dependent. This coupled with the observation that caspase-8 mediates SST-induced acidification prompted us to assess caspase-8 activity in MCF-7 cells overexpressing SHP-1 or its mutant SHP-1C455S. Basal caspase-8 activity was higher in SHP-1 overexpressing cells compared to MCF-7 cells (0.85 ± 0.2 vs. 0.5 ± 0.12 nmol/mg protein, Table 1). SST induced activation of caspase-8 was also higher in SHP-1 expressing cells (3.7 ± 0.5 vs. 3.1 ± 0.4 nmol/mg protein). The mutant SHP-1 suppressed the ability of SST to activate caspase-8.

DISCUSSION

In this study we demonstrated that the cytotoxic signaling of SST in MCF-7 cells activates multiple caspases and that caspase-8 is induced early and precedes the decrease in pH_i , whereas acidification is necessary for the induction of the effector caspases. In accordance with this was the finding that inhibition of SST-induced acidification by pH-clamping with nigericin did not affect SST-induced activation of caspase 8 while completely abrogating the induction of other caspases. Likewise, inhibition of caspase-8 by IETD-CHO prevented SST-induced acidification and activation of terminal caspases. By contrast, LEHD-CHO and DEVD-CHO did not prevent SST-induced increase in caspase 8 activity and the decrease in pH_i . Moreover, SST-induced increase in caspase 8 activity peaked by 3 hours and declined thereafter paralleling the previously reported time course of acidification (35). The distal caspases, in contrast, displayed sustained increase in activity. These data demonstrate for the first time that caspase 8 activation is required for SST-induced acidification and, additionally, that its activity cannot be sustained in cells with acidic pH_i . This is supported by the finding that the 20 kDa fragment derived from procaspase-8 was present in cells with acidic pH_i during SST treatment. By contrast, the generation of caspases -9, -3 and -7 from the respective procaspases occurred only when there was acidification. The detection of caspase 3 in the HTB22 clone of MCF-7 cells used in the present study contrasts to its reported absence in other clones of this cell line due to a 47 base pair deletion within the exon 3 of the caspase 3 gene (45, 46)³. We found that acidification *per se* was sufficient to activate the effector caspases in the absence of detectable increase in caspase-8 activity. We do not know if acidification induces direct activation of the effector caspases directly.

³ Janicke, personal communication

However the possibility that transient activation of caspase-8 during rapid acidification may suffice to induce these caspases cannot be ruled out.

Caspase-8 can activate caspases -3 and -7 directly and/or through induction of caspase-9 (17, 18, 44, 47). Caspase-9 activation as a consequence complexing with Apaf-1, a mammalian CED-4 homolog, in presence of cyt c released from the mitochondria is an energy dependent process requiring ATP (44, 48). In order to assess the relative importance of caspase-9 in the cytotoxic signaling of SST, we compared the effect of SST in control and ATP-depleted MCF-7 cells. SST was unable to activate caspase-9 in ATP-depleted cells, but was still capable of activating DEVD-ase and inducing apoptosis. Thus, SST-induced apoptosis in MCF-7 cells involves caspase-8-mediated direct activation of terminal caspases as well as an amplifying effect mediated through mitochondrial dysfunction and consequent activation of caspase-9. These data support the concept that caspase-8 can activate apoptotic pathways involving effector caspases through both mitochondria-dependent and -independent pathways (17, 43, 49-53). The extent of SST-induced apoptosis was 34 ± 5 % lower in ATP-depleted cells, an effect that could be accounted for by the loss of caspase-9-mediated activation of the terminal caspases and/or the loss of effector caspase mediated activation of caspase-9. We found that DEVD-CHO only partially suppressed the effect of SST on $\Delta\psi_m$ and cyt c release suggesting that mitochondrial dysfunction may be caused to a some extent by the action of the effector caspases as demonstrated previously in an *in vitro* model (10).

We showed that intracellular acidification precedes the onset of reduction in $\Delta\psi_m$ in MCF-7 cells exposed to the cytotoxic action of SST. This is in contrast to the report that mitochondrial permeability transition causes acidification during valinomycin-induced apoptosis in

hematopoietic cells (54). It is possible that the cause and effect relationship between mitochondrial dysfunction and cell acidification may be cell type-dependent. Indeed the existence of two cell types in which caspase-8 can trigger apoptosis without invoking mitochondrial dysfunction (type I cells) and those in which apoptosis is induced predominantly in a mitochondria-dependent manner (type II cells) has been described (50).

The mechanism of SHP-1-/caspase-8-mediated inhibition of pH homeostasis remains to be elucidated. We have previously shown that amiloride and bafilomycin-1, which inhibit Na^+/H^+ exchanger (NHE) and H^+ ATPase respectively, trigger acidification and apoptosis in MCF-7 cells. Inhibition of NHE lowered the pH_i to a greater extent than inhibition of H^+ ATPase. (34). This raises the possibility that SHP-1 and caspase-8 mediated signaling may generate or unmask molecule(s) that may disrupt proton extrusion pathways involving these channels. The finding that SST-induced acidification does not occur at the mitochondria suggests that it inhibits the regulation of proton transport through NHE and H^+ ATPase either at the cell membrane or some other subcellular locus. The existence of multiple NHE isoforms and their differential localization at the cell membrane (e.g., NHE-1 and NHE-2) or at the endoplasmic reticulum-nuclear envelope and endosomes (e.g., NHE-3) raises the possibility that SST may inhibit some or all of the NHEs. Studies are in progress to gain insight into the subcellular sites at which SHP-1- and caspase-8-mediated disruption of pH homeostasis and the the proton extrusion pathway(s) involved are in progress.

In summary, these findings define the temporal sequence of events that link the initiator and effector caspases with inhibition of pH homeostasis and mitochondrial dysfunction in acidification-dependent apoptosis. The data presented herein demonstrate that (i) SHP-1-dependent ac-

tivation of caspase-8 is required for SST-induced decrease in pH_i and (ii) mitochondrial dysfunction and activation of effector caspases occur distal to acidification and (iii) caspase-9 is not essential for SST-induced apoptosis to occur but, when induced, can amplify the cytotoxic signaling of SST.

Acknowledgements

This study was supported by grants from the Canadian Medical Research Council (MT-12603) and a U.S. Department of Defense Breast cancer initiative grant. We thank Dr. J.J. Lebrun for the use of the luminometer.

TABLE 1

SHP-1-dependency of activation of caspase-8 by D-Trp⁸ SST-14

<u>CELL</u>	<u>IETD-ase Activity</u> (nmol/mg protein)	
	<u>Basal</u>	<u>Stimulated</u>
MCF-7	0.51 ± 0.06	3.10 ± 0.42*
MCF-7-SHP-1	0.85 ± 0.11**	3.75 ± 0.46*
MCF-7-SHP-1C455S	0.49 ± 0.02	0.50 ± 0.03

MCF-7 cells stably overexpressing wild type SHP-1 or the inactive mutant SHP-1C455S were established as previously described (ref. 34,35). Caspase-8 activity was measured in extracts of control and peptide treated cells using IETD-AMC as the substrate (mean ± SEM, n=6). * p < 0.005 basal vs. stimulated; ** p < 0.05 basal values, MCF-7 vs. MCF-7-SHP-1

FIGURE LEGENDS

Figure 1.

D-Trp⁸ SST-14-induced activation of caspase-8 (IETD-ase) precedes that caspases -3/-7 (DEVD-ase) in MCF-7 cells. Enzyme activities were measured using the aminomethylcoumarin derivatives of the tetrapeptide substrates in extracts of cells incubated with 100 nM peptide at the indicated times. IETD-ase activity was maximal at 3 h, and declined to basal level by 24 h (top panel). By contrast, DEVD-ase activity was maximal at 24 h (bottom panel). Values represent nmol of aminomethylcoumarin liberated from the substrates during 30 min incubation with cell extracts *in vitro* and was quantitated against the fluorescence readings of serially diluted aminomethylcoumarin as described under Methods (mean \pm SEM, n=6).

Figure 2

Effect of pH clamping on caspase activation. D-Trp⁸ SST-14 induced increase in caspase-8 (IETD-ase) activity was not affected by the prevention of acidification by nigiericin (top panel) whereas pH clamping prevented the increase in caspase-3/-7 (DEVD-ase) activity (bottom panel). Enzyme activities were measured after 4 h treatment (IETD-ase) or 24 h (DEVD-ase) (mean \pm SEM, n=6).

Figure 3

Differential effects of caspase-inhibitors on D-Trp⁸ SST-14-induced acidification, but not on apoptosis in MCF-7 cells. A. The decrease in pHi in cells incubated with 100 nM peptide for 24 h was prevented by the caspase-8 inhibitor IETD-CHO, but not by the caspase-3/-7 inhibitor-DEVD-CHO (mean \pm SEM, n=6). B. Oligonucleosomal DNA fragmentation in peptide treated

cells was completely inhibited by both IETD-CHO and DEVD-CHO (figure representative of 4 different experiments)..

Figure 4

Inhibition of DEVD-ase does not prevent D-Trp⁸ SST-14-induced activation of IETD-ase whereas inhibition of IETD-ase abrogates induction of DEVD-ase. A. Extracts of cells incubated with 100 nM peptide \pm DEVD-CHO for 4 h were assayed for IETD-ase activity or for 24 h \pm IETD-CHO for DEVD-ase assay (mean \pm SEM, n=6).

Figure 5

D-Trp⁸ SST-14-induced reduction in $\Delta\psi_m$ is acidification-dependent. A. Cells were incubated in the absence (panel 1) or presence of 100 nM peptide (panel 2) in regular medium or with the peptide in nigericin containing medium (panel 3), labeled with DiOC6(3) and analysed by flow cytometry. Representative recordings of six separate measurements are shown. The reduction in $\Delta\psi_m$ in peptide treated cells is evident from the decrease in the number of cells with the resting potential as well as from the appearance of distinct peak of cells with lower DiOC6(3) fluorescence (panel 2). Inhibition of acidification prevented the ability of D-Trp⁸ SST-14 to decrease $\Delta\psi_m$ (compare panels 3 and 1). B. Quantitation of the effect of pH clamping, IETD-CHO and DEVD-CHO on D-Trp⁸-induced reduction in $\Delta\psi_m$ (mean \pm SEM, n=6). The effect of the peptide was only partially inhibited by DEVD-CHO whereas it was completely abolished in presence of IETD-CHO similar to that seen in cells clamped at physiological pH in presence of nigericin. *, p < 0.001; **, p < 0.01.

Figure 6

D-Trp⁸ SST-14-induced increase in cytosolic cyt c precedes the activation of DEVD-ase. 30 ug protein aliquots from cytosolic extracts of cells incubated in the absence and presence of 100 nM D-Trp⁸ SST-14 alone or with the indicated inhibitors were subjected to immunoblot analysis following electrophoresis and membrane-transfer. Nigericin and IETD-CHO, but not DEVD-CHO, prevented D-Trp⁸ SST-14-induced increase in cyt c.

Figure 7

Activation of caspase 9 (LEHD-ase) by D-Trp⁸ SST-14 is attenuated by inhibition of acidification. Cells were incubated as described in the legend for fig.2B (mean \pm SEM, n=6).

Figure 8

Effect of ATP depletion on D-Trp⁸ SST-14-induced cytotoxic signaling. ATP-depleted cells were prepared by incubating with oligomycin in glucose-free medium for 1 h. Control and ATP-depleted cells were incubated for 6 h in the absence (lanes 1 and 3) or presence of 100 nM peptide (lanes 2 and 4). A. Induction of LEHD-ase induced by the peptide in control cells was completely abolished by ATP-depletion. B. The increase in DEVD-ase activity was only partially inhibited by ATP-depletion. C. Peptide-induced increase in cyt c was inhibited by ATP depletion. D. ATP-depletion inhibits D-Trp⁸ SST-14-induced apoptosis by $34 \pm 5\%$. Annexin V positive cells following 6 h treatment averaged $8.4 \pm 1.5\%$ in ATP-depleted cells compared to $12.8 \pm 1.8\%$ in control cells. Values in panels A,B and D represent mean \pm SEM (n=6).

Figure 9

Immunoblot analysis demonstrating differential pH sensitivity of caspase activation. Formation of the 20 kDa active caspase from the inactive procaspase-8 induced by D-Trp⁸ SST-14-mediated cytotoxic signaling was pH-independent. By contrast, the formation of the 20 kDa fragments

from procaspases -9, -7 and -3 in peptide treated cells was prevented by inhibition of acidification by nigericin (data representative of 4 independent experiments)..

REFERENCES

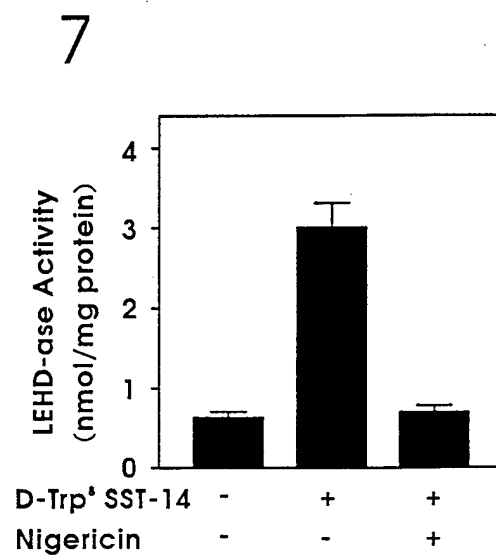
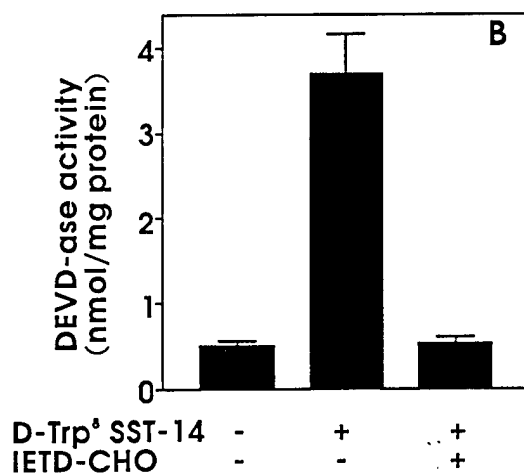
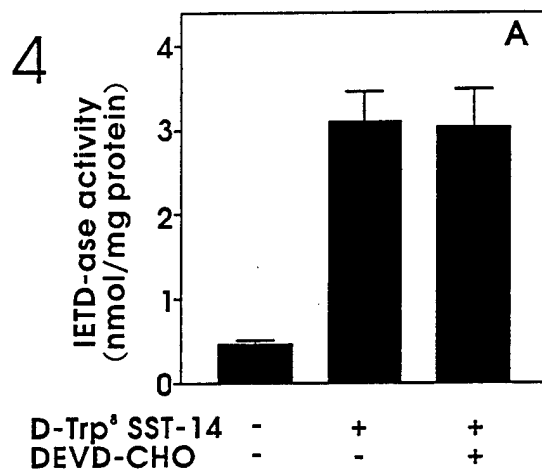
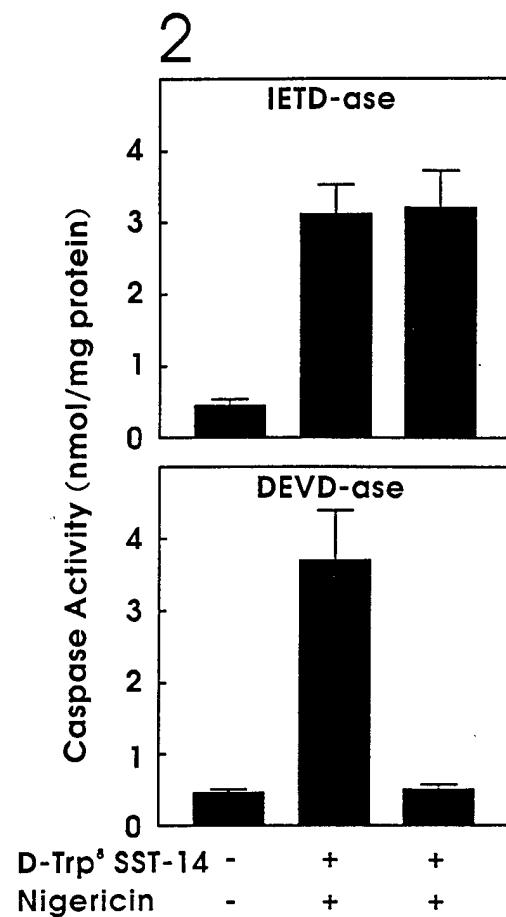
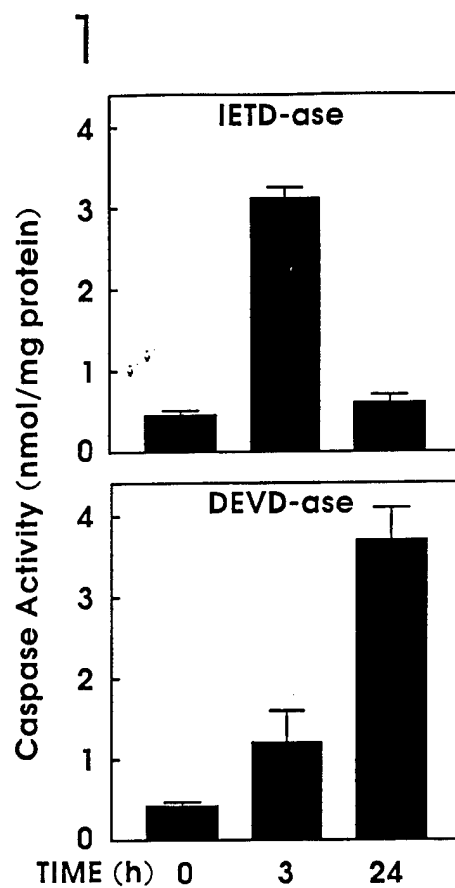
1. Cohen, G.M., (1997) *Biochem.J.* **326**: 1-16.
2. Walker, N.P., Talanian, R.V., Brady, K.D., Dang, L.C., Bump, N.J., Ferenz, C.R., Franklin, S., Ghayur, T., Hackett, M.C., Hammill, L.D., and et al., (1994) *Cell* **78**: 343-352.
3. Vayssiere, J.L., Petit, P.X., Risler, Y., and Mignotte, B., (1994) *Proc Natl Acad Sci U S A* **91**: 11752-11756.
4. Kroemer, G., Petit, P.X., Zamzami, N., Vayssiere, J.-L., and Mignotte, B., (1995) *Faseb.J.* **9**: 1277-1287.
5. Zamzami, N., Marchetti, P., Castedo, M., Zanin, C., Vayssiere, J.-L., Petit, P.X., and Kroemer, G., (1995) *J. Exp. Med.* **181**: 1661-1672.
6. Petit, P.X., Lecoœur, H., Zorn, E., Dauguet, C., Mignotte, B., and Gougeon, M.L., (1995) *J Cell Biol* **130**: 157-167.
7. Kroemer, G., Zamzami, N., and Susin, S.A., (1997) *Immunol Today* **18**: 44-51.
8. Kroemer, G., (1997) *Nat Med* **3**: 614-620.
9. Susin, S.A., Zamzami, N., and Kroemer, G., (1998) *Biochim Biophys Acta* **1366**: 151-165.
10. Bossy-Witzel, E., Newmeyer, D.W., and Green, D.G., (1998) *EMBO J.* **17**: 37-49.
11. Rosse, T., Olivier, R., Monney, L., Rager, M., Conus, S., Fellay, I., Jansen, B., and Borner, C., (1998) *Nature* **391**: 496-499.
12. Hirsch, T., Marzo, I., and Kroemer, G., (1997) *Biosci Rep* **17**: 67-76.
13. Marchetti, P., Hirsch, T., Zamzami, N., Castedo, M., Decaudin, D., Susin, S.A., Masse, B., and Kroemer, G., (1996) *J Immunol* **157**: 4830-4836.

14. Marchetti, P., Castedo, M., Susin, S.A., Zamzami, N., Hirsch, T., Macho, A., Haeffner, A., Hirsch, F., Geuskens, M., and Kroemer, G., (1996) *J Exp Med* **184**: 1155-1160.
15. Marzo, I., Brenner, C., and Kroemer, G., (1998) *Biomed Pharmacother* **52**: 248-251.
16. Fraser, A. and Evan, G., (1996) *Cell* **85**: 781-784.
17. Gross, A., Yin, X.M., Wang, K., Wei, M.C., Jockel, J., Milliman, C., Erdjument-Bromage, H., Tempst, P., and Korsmeyer, S.J., (1999) *J Biol Chem* **274**: 1156-1163.
18. Fernandes-Alnemri, T., Armstrong, R.C., Krebs, J., Srinivasula, S.M., Wang, L., Bullrich, F., Fritz, L.C., Trapani, J.A., Tomaselli, K.J., Litwack, G., and Alnemri, E.S., (1996) *Proc Natl Acad Sci U S A* **93**: 7464-7469.
19. Muzio, M., Salvesen, G.S., and Dixit, V.M., (1997) *J Biol Chem* **272**: 2952-2956.
20. Kakutani, T., Ebara, Y., Kanja, K., Hidaka, M., Matsumoto, Y., Nagano, A., and Wataya, Y., (1998) *Biochem Biophys Res Commun* **247**: 773-779.
21. Zanke, B.W., Lee, C., Arab, S., and Tannock, I.F., (1998) *Cancer Res* **58**: 2801-2008.
22. Liu, D., Thangaraju, M., Shen, S.-H., and Srikant, C.B. (1999) *Program of the Annual Meeting of the Endocrine Society*. San Diego, CA.
23. Wolf, C.M. and Eastman, A., (1999) *Biochem Biophys Res Commun* **254**: 821-827.
24. Park, H.J., Makepeace, C.M., Lyons, J.C., and Song, C.W., (1996) *Eur J Cancer* **32A**: 540-546.
25. Newell, K., Wood, P., Stratford, I., and Tannock, I., (1992) *Br J Cancer* **66**: 311-317.
26. Maidorn, R.P., Cragoe, E.J., Jr., and Tannock, I.F., (1993) *Br J Cancer* **67**: 297-303.
27. Furlong, I., Ascaso, R., Rivas, A., and Collins, M., (1997) *J Cell Sci* **110**: 653-661.

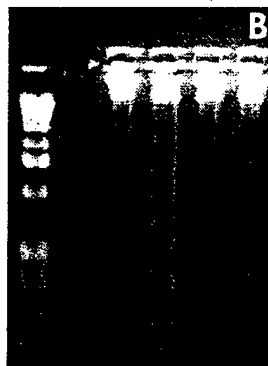
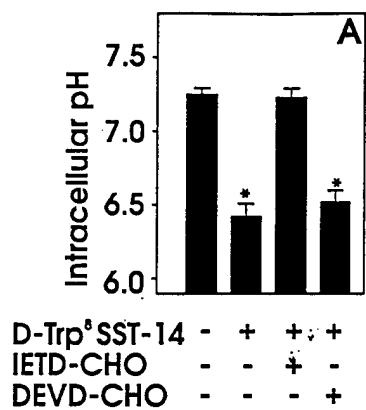
28. Angoli, D., Delia, D., and Wanke, E., (1996) *Biochem Biophys Res Commun* **229**: 681-685.
29. Gottlieb, R.A., Giesing, H.A., Zhu, J.Y., Engler, R.L., and Babior, B.M., (1995) *Proc Natl Acad Sci U S A* **92**: 5965-5968.
30. Gottlieb, R.A., Nordberg, J., Skowronski, E., and Babior, B.M., (1996) *Proc Natl Acad Sci U S A* **93**: 654-658.
31. Meisenholder, G.W., Martin, S.J., Green, D.R., Nordberg, J., Babior, B.M., and Gottlieb, R.A., (1996) *J Biol Chem* **271**: 16260-16262.
32. Wolf, C.M., Reynolds, J.E., Morana, S.J., and Eastman, A., (1997) *Exp Cell Res* **230**: 22-27.
33. Sharma, K. and Srikant, C.B., (1998) *Biochem Biophys Res Commun* **242**: 134-140.
34. Thangaraju, M., Sharma, K., Liu, D., Shen, S.H., and Srikant, C.B., (1999) *Cancer Res* **59**: 1649-1654.
35. Thangaraju, M., Sharma, K., Leber, B., Andrews, D.W., Shen, S.-H., and Srikant, C.B., (1999) *J. Biol. Chem.* **274**: in press.
36. Lee, C. and Ernster, L., (1966) *Biochem Biophys Res Commun* **23**: 176-181.
37. Eguchi, Y., Shimizu, S., and Tsujimoto, Y., (1997) *Cancer Res* **57**: 1835-1840.
38. Sharma, K. and Srikant, C.B., (1998) *Int. J. Canc.* **76**: 259-266.
39. Thornberry, N.A., (1994) *Methods Enzymol* **244**: 615-631.
40. Thornberry, N.A., Rano, T.A., Peterson, E.P., Rasper, D.M., Timkey, T., Garcia-Calvo, M., Houtzager, V.M., Nordstrom, P.A., Roy, S., Vaillancourt, J.P., Chapman, K.T., and Nicholson, D.W., (1997) *J Biol Chem* **272**: 17907-17911.

41. Kluck, R.M., Bossy-Wetzel, E., Green, D.R., and Newmeyer, D.D., (1997) *Science* **275**: 1132-1136.
42. Cai, J., Yang, J., and Jones, D.P., (1998) *Biochim Biophys Acta* **1366**: 139-149.
43. Kuwana, T., Smith, J.J., Muzio, M., Dixit, V., Newmeyer, D.D., and Kornbluth, S., (1998) *J Biol Chem* **273**: 16589-16594.
44. Li, P., Nijhawan, D., Budihardjo, I., Srinivasula, S.M., Ahmad, M., Alnemri, E.S., and Wang, X., (1997) *Cell* **91**: 479-489.
45. Janicke, R.U., Sprengart, M.L., Wati, M.R., and Porter, A.G., (1998) *J Biol Chem* **273**: 9357-9360.
46. Kurokawa, H., Nishio, K., Fukumoto, H., Tomonari, A., Suzuki, T., and Saijo, N., (1999) *Oncol Rep* **6**: 33-37.
47. Srinivasula, S.M., Ahmad, M., Otilie, S., Bullrich, F., Banks, S., Wang, Y., Fernandes-Alnemri, T., Croce, C.M., Litwack, G., Tomaselli, K.J., Armstrong, R.C., and Alnemri, E.S., (1997) *J Biol Chem* **272**: 18542-18545.
48. Zou, H., Henzel, W.J., Lui, X., Lutschg, A., and Wang, X., (1997) *Cell* **90**: 405-413.
49. Chauhan, D., Pandey, P., Ogata, A., Teoh, G., Krett, N., Halgren, R., Rosen, S., Kufe, D., Kharbanda, S., and Anderson, K., (1997) *J Biol Chem* **272**: 29995-29997.
50. Scaffidi, C., Fulda, S., Srinivasan, A., Friesen, C., Li, F., Tomaselli, K.J., Debatin, K.M., Krammer, P.H., and Peter, M.E., (1998) *Embo J* **17**: 1675-1687.
51. Li, H., Zhu, H., Xu, C.J., and Yuan, J., (1998) *Cell* **94**: 491-501.
52. Ferrari, D., Stepczynska, A., Los, M., Wesselborg, S., and Schulze-Osthoff, K., (1998) *J Exp Med* **188**: 979-984.

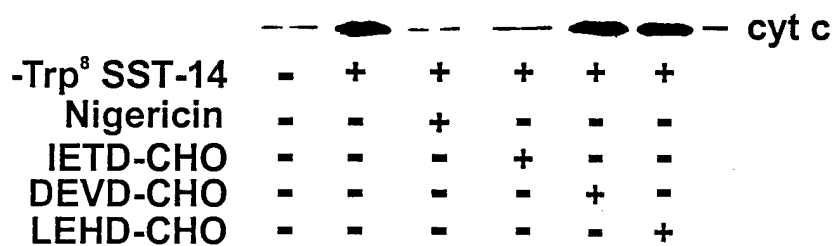
53. Vier, J., Linsinger, G., and Hacker, G., (1999) *Biochem Biophys Res Commun* **261**: 71-78.
54. Furlong, I.J., Lopez Mediavilla, C., Ascaso, R., Lopez Rivas, A., and Collins, M.K., (1998) *Cell Death Differ* **5**: 214-221.



3

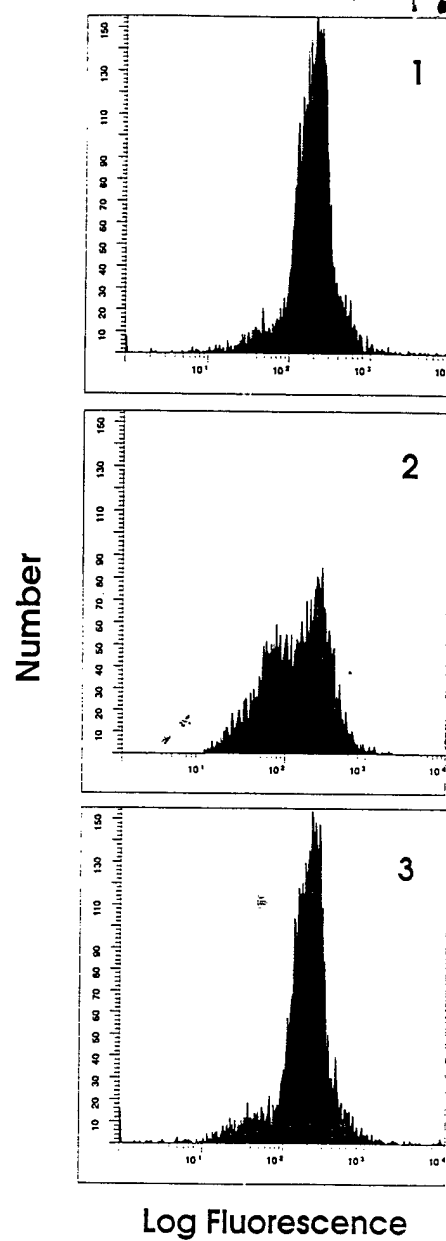


6



5

A



B

